INFORMATION TO USERS

This manuscript has been reproduced from the microfilm master. UMI films the text directly from the original or copy submitted. Thus, some thesis and dissertation copies are in typewriter face, while others may be from any type of computer printer.

The quality of this reproduction is dependent upon the quality of the copy submitted. Broken or indistinct print, colored or poor quality illustrations and photographs, print bleedthrough, substandard margins, and improper alignment can adversely affect reproduction.

In the unlikely event that the author did not send UMI a complete manuscript and there are missing pages, these will be noted. Also, if unauthorized copyright material had to be removed, a note will indicate the deletion.

Oversize materials (e.g., maps, drawings, charts) are reproduced by sectioning the original, beginning at the upper left-hand corner and continuing from left to right in equal sections with small overlaps.

Photographs included in the original manuscript have been reproduced xerographically in this copy. Higher quality 6" x 9" black and white photographic prints are available for any photographs or illustrations appearing in this copy for an additional charge. Contact UMI directly to order.

Bell & Howell Information and Learning
300 North Zeeb Road, Ann Arbor, MI 48106-1346 USA
800-521-0600

Université d'Ottawa · University of Ottawa

Lake Level Variations and Global Hydrological Change: A Spatio-Temporal Analysis

By

André E. Viau

A Thesis Submitted to the School of Graduate Studies and Research in Partial Fulfilment of the Requirements for the Degree of Master of Arts, Geography

Department of Geography
University of Ottawa
165 Waller St.
Ottawa, ON
K1N 6N5

Lake Level Variations and Global Hydrological Change: A Spatio-Temporal Analysis

André E. Viau

Abstract

Variations in the global hydrological cycle occur at many time and space scales. An important source of evidence about past variations in the hydrological balance are records of lake level fluctuations. The spatial extent and depth of a lake varies in response to changes in the water balance over its surface and catchment. These variations may result from local factors or climate change. However, spatial climatically-induced patterns can be identified when most lakes in a region change in a similar way. These regional patterns can be used to reconstruct sub-continental to global variations in the hydrological cycle and can be interpreted as shifts in atmospheric circulation patterns. However, in previous studies, these regional patterns have been identified in a qualitative, or semi-quantitative way at best.

A global lake-level database was constructed from three previously developed databases, and used to investigate large-scale patterns present in the lake-level data during the Holocene. Using the geostatistical approach, regional patterns were objectively identified by examining the spatial correlation between sites and gridded using ordinary and indicator kriging at 3,000 year intervals. These maps were produced using two assumptions. First, the data were used under the assumption that climate is continuous in space, and hence, the data were treated as spatial continuous interval data. Then, the data were used under the assumption that the data is spatial categorical and that the classes are mutually exclusive.

The two griding methodologies show overall similar estimated regional patterns, thus suggesting robust estimations of the patterns of lake-level variations for four periods of the past 12,000 ka years. Comparisons were made with four Atmospheric General Circulation models (AGCMs) at 0 ka and 6 ka, in order to objectively study their agreements. While CCM1and CCM0 show overall better results in the data-model comparison, these models are coarser resolution, thus capture the broader-scale patterns in lake status change. The high resolution CCCMA experiments show some similarities spatially, however, they do not seem to capture the broad-scale patterns in lake status change.

Les Variations des Niveaux Lacustres et le Cycle Hydrologique Panétaire: Une Analyse Spatio-Temporelle.

André E. Viau

Résumé

Les variations du cycle hydrologique planétaire se manifestent à plusieurs échelles de temps et espace. Une source importante qui renseigne sur les variations de l'équilibre hydrologique sont les fluctuations des niveaux de lacs. L'extension spatiale et la profondeur d'un lac varie selon les changements dans l'équilibre hydrologique au-dessus de sa surface et de son bassin versant. Ces variations résultent de facteurs locaux ou de changements climatiques. Cependant, lorsque la majorité des lacs d'une region démontrent les mêmes variations, ceci ne peut-être qu' une réponse à un changement climatique. Ces patrons régionales peuvent être utilisés pour reconstruire les variations du cycle hydrologique sub-continentale et planétaire, et aider dans l'interprétation des variations au niveau de la circulation atmosphérique générale. Cependant, les études passées révèlent ques ces patrons régionales n'ont jamais été quantifiés, l'interprétation demeurant plus ou moins qualitative ou semi-quantitative.

Une base de données planétaire a été assemblée et utilisée afin d'identifier les patrons spatials à grande échelle présente dans les données des niveaux de lacs durant l'Holocène. L'approche géostatistique a permis d'identifier les patrons spatials en examinant l'autocorrelation spatial à échelle local et de les cartographier objectivement en utilisant le krigeage ordinaire et le krigeage par indicateurs à 3,000 ans d'intervalles. Deux prémisses sont utilisées afin de produire les cartes finales. Premièrement, les données sont utilisées sous la premisse que le climat est continu dans l'espace, et donc, les données sont traitées comme spatialement continues par intervalles. Par suite, les données sont traitées comme étant spatiales et catégoriques, dont les classes sont mutuellement exclusives.

Les deux méthodes de krigeage démontrent des similarités générales qui suggère une estimation rigoureuse des patrons régionales au niveau des variations de niveau lacustres pour quatre périodes durant l' Holocène. Des comparaisons avec des modèles de circulation atmosphérique générale (AGCMs) ont été entreprit pour les périodes de 0 ka et 6 ka, afin d'étudier leurs similarités. Les modèles CCM0 et CCM1 démontrent les meilleurs résultats, par contre, ces modèles ont une faible résolution, et donc, capture les patrons à grande échelles dans les variations des niveaux lacustres. Les simulations à haute résolutions du CCCMA révèlent certaines similarités spatiales. Cependant, ces modèles ne capture pas les patrons à grandes échelles.

To my children, Marc, Shawn and Vincent, for the inspiration that made this research a reality.

Aknowledgements

I would like to thank those whose support was fundamental to the success of this thesis. With highest respect, Dr. Konrad Gajewski, my thesis supervisor, whom guided me through many encountered problems and financially supported my research through the CSHD Collaborative Research Grant Network. His acute scientific knowledge and skills aided me in developing analytical and methodological skills needed to become a competent researcher. My thesis committee members, Dr. Daniel Lagarec for his numerous and precious discussions that helped me apply rigour and critique to my research and Professor David Douglas for his references and support. The Laboratory for Paleoclimatology and Climatology - LPC members of the department of Geography of the University of Ottawa for their helpful comments and support, with a special thanks to Michael C. Sawada for his specialized computer skills. A very special thanks goes to Dr. Peter G. Johnson of the University of Ottawa for his support and understanding in difficult times while in Kluane National Park, Yukon, Canada, in the summer of 1997.

This thesis could not have been possible without the continuous love and support of my parents, Mr.and Mrs. Ernest Viau. A special mention of thanks also goes to my uncle Mr. Fernand Viau for his understanding and support. A special thanks to Lisa, Philip and Donna-Maria Dolan for believing in me and Mr. James Becker and Mr. Daniel Lefebvre for their everlasting respect and friendship.

Lastly, but most important, I thank my children, Marc, Shawn and Vincent. They were instrumental in my capacity to continue even in times of troubled waters.

André E. Viau - 1999

Table of contents

List of Figures

List of Tables

Chapter 1

Introduction

"From the time when written records began, and doubtless long before that, thoughtful men have had two preoccupations: the past and the future. It is this impelling sense of time and process that distinguishes such individuals from the 'practical man', absorbed as he is in the immediate present. Although we still have with us this divergence of attention and emphasis, the birth of modern science has been, in a curious way, the result of their fusion. For man has, at length, learnt that the key to past and future lies in the scrutiny of evidence that is before his eyes, here and now...."

Sears,1964.

This thesis presents the results of a spatial analysis of lake-level data which is a proxy for precipitation and temperature. The data is global in extent and covers the past 12,000 years. This data has been extensively used by the scientific community for paleoclimate studies. In this study, the spatial autocorrelation is analysed in order to more objectively identify spatial patterns in lake-level data.

Lake level data have been extensively used in paleoclimate reconstructions (Street and Grove,1976, 1979; Street-Perrott and Harrison,1984; Harrison and Metcalfe,1985a,b; Harrison,1989; Guiot *et al.*,1993; Yu and Harrison,1995 a,b; Prentice *et al.*,1996; Cheddadi *et al.*,1997) for describing the climate of various periods in the past. Some attempts have been made to validate General Circulation Models (GCMs) using this data (COHMAP, 1988; Harrison and Dodson, 1992; Kutzbach, 1993; Yu and Harrison, 1996; Qin *et al.*,1998). However, these paleoclimate reconstructions and comparisons with GCMs have remained qualitative due to the nature of the data, as will be discussed below. With the exception of a multidimensional scaling analysis that identified spatial clusters in North America (Harrison *et al.*, 1988), little has been done to quantitatively determine the spatial continuity within the data.

The purpose of this thesis is to model the geographical patterns in the lake-level data in order to objectively study the spatio-temporal variability of the data. It is assumed that large-scale patterns are associated with climate changes, and that this can be found by identifying the spatial autocorrelation.

Spatial autocorrelation looks at the degree of similarity between localities in space. In climate research, the lack of spatial autocorrelation would be difficult to conceive since this implies that every location on the earth's surface would be independent and there would be no spatial pattern of natural phenomenon (Goodchild,1987). Spatial information is not explicitly taken into account by most classical statistical methods (Isaaks and Srivastava, 1989). Geostatistics offers a method through which to describe the spatial continuity present in most earth science datasets. Spatial continuity analysis is undeniably necessary for the spatial modelling of data and avoiding this step can lead to serious errors in estimation and interpretation (Getis and Ord, 1992).

The questions raised in this thesis are: Do lake-level data exhibit spatial autocorrelation? If so, can it be modelled? What are the limitations of these models imposed on the data and what are the implications of imposing these models on the data? Can these modelled patterns be used in paleoclimate reconstructions and in the validation of global climate model (GCMs) simulations? This thesis will investigate these fundamental questions in an objective way. The spatial continuity of lake-level data will be examined on a sub-continental to global scale for the Holocene period. Using different geostatistical techniques, global maps will be constructed at 3,000 year interval spanning the last 12,000 years. The limitations associated with these estimations are also discussed. Finally, the maps produced in this thesis are compared with climate model outputs in

order to give insight into the nature and mechanisms of global hydrological change.

Hypothesis

The hypothesis underlying this research is that changes in closed basin as well as temperate lake-levels exhibit spatial autocorrelation that is primarily controlled by large-scale climate patterns.

The plan of this thesis is as follows. Chapter 1 reviews the literature on lake-level variations and global hydrological change. Chapter 2 discusses the history and organisation of the global database used in this study. Three databases, the Oxford lake-level (Street-Perrott *et al.*, 1989), the European lake-level (Harrison and Yu, 1995) and the former Soviet Union and Mongolia lake-level (Tarasov *et al.*, 1996), were merged into one global database in order to maximize spatial coverage of the world. Chapter 3 discusses exploratory data analysis of the lake-level data. Summary statistics and frequency histograms are used to describe the distribution of lake-levels sites through time. Maps enable a thorough description of the spatial organisation of the data and provide insight into sampling errors as well as the identification of problematic locations. This chapter also investigates the fine-scale variability using an example of two sites that are separated by very short distances, yet exhibit dissimilar sequences. Chapter 4 presents a spatial continuity analysis and the modelling of the data at 3,000 year intervals covering the last 12,000 years at a global scale. Different spatial autocorrelation measurements such as the variogram, correlogram (Moran I) and local indicator spatial autocorrelation (LISA) are used. Chapter 5 addresses the estimation process and demonstrates two interpolation methods used on the data. The first method applied is ordinary kriging, which is based on the assumption that the data is continuous in climate space. The second method is indicator kriging, in which the raw data is transformed into a binary

vector. This method is commonly used for categorical data (Isaaks and Srivastava, 1989; Deutsch and Journel, 1992; Goovearts, 1997). The resulting maps are then compared in order to find similarities in the results of the two kriging methods. Chapter 6 is presented in the form of an article to be submitted for publication and includes a summary of the methods and results which were presented in Chapters 1 through 5, and a comparison with GCM climate model outputs. Finally, Chapter 7 offers a summary of the spatio-temporal analysis of lake-level data and gives insight into future research with lake-level data.

1.1 Literature review

The terrestrial climate has varied significantly and continuously on time scales ranging from years to glacial periods to the age of the earth. This climatic variability is caused in part by forcings (Peixoto and Oort, 1992), comprising, among others, the Milankovitch astronomical parameters (eccentricity of the orbit, axial precession and obliquity of the ecliptic), the intensity of solar irradiance, the composition of the atmosphere, oceanic circulation and temperature, the presence of ice sheets and long-term changes in tectonic factors (ie. continental drift, mountain building). Understanding the relative importance of these, or other factors, on the climate of any scale is the fundamental goal of paleoclimate research.

The Milankovitch astronomical parameters have been established as the main forcing mechanism of long term climate variations such as the glacial and interglacial cycle (10^4 yr). In addition, Kutzbach (1981) demonstrated that the Milankovitch insolation variations could also explain major climate changes at the Holocene time-scale (10^3 yr). This hypothesis was tested using numerical models which demonstrated the hypothesized climatic responses at the scale of 10^3 year

(Kutzbach,1981; Kutzbach and Guetter,1986). The simulations were compared to maps of paleoclimate fields derived from proxy climate data. Thus, the interpretation of past climates from proxy data provide validation for data-model comparisons.

Numerous time periods throughout the Earth's history have been simulated using GCMs however the Quaternary has received the most attention because the boundary conditions are better known, and because there are large amounts of data available for this period for validation. Some example of modelling experiment studies are CLIMAP project (1976), Kutzbach(1981), Boer *et al.* (1984), Kutzbach and Guetter (1986), COHMAP members (1988), Rind *et al.* (1989), Schultz *et al.* (1992), Marshall *et al.* (1997), Hewitt and Mitchell (1997), Texier *et al.* (1997), and Vettoretti *et al.* (1998). These modelling experiments are used to simulate particular climate processes, or to test hypotheses of forcing mechanisms. Output from these models need to be tested against data. Data-model comparisons can thus make significant contributions to paleoclimate research in that they determine to what extent the global climate models (GCMs) accurately represent the data and which of these various models are the best estimators of the climate. However, to properly test the model output, the paleoclimate data needs to be (a) spatial, and cover as large a part of the globe as possible and (b) objectively derived independently of the model output.

Lake-level data have been used extensively in paleoclimate research and thus provide an important source for validation of climate models. Examples of lake-level mapping and syntheses include Street and Grove (1976, 1979), Street-Perrott and Harrison (1984), Harrison and Metcalfe (1985 a, b), Harrison (1989), Guiot *et al.* (1993), Yu and Harrison (1995 a, b), Prentice *et al.* (1996), and Cheddadi *et al.* (1997).

For more than 250 years, lake level fluctuations have been recognised to be a response to changes in climate (Halley, 1715; In: Street-Perrott and Harrison, 1985). However, it was not until 1833 that the study of lake-level fluctuations was placed on a solid scientific foundation with the publication of Jackson's book *Observations on Lakes* (Street-Perrott and Harrison, 1985). Subsequent studies on lake-level fluctuations around the world gave rise to a large number of relatively well dated stratigraphic records. Tricart (1956, In: Street and Grove, 1979) suggested that lake-level fluctuations exhibited a geographic pattern. Although the precise paleoclimatic significance of lake-level had been disputed (Galloway, 1965, 1970; Brackenridge, 1978; In: Street and Grove, 1979), Tricart's hypothesis prompted Street and Grove (1976) to initially analyse the water-level fluctuations in African closed-basin lakes. They found clearly defined spatial variations in lake-levels on a subcontinental scale which seemed to reflect changes in atmospheric circulations. Street and Grove (1979) constructed global maps of lake-level fluctuations for the last 30,000 years. This study confirmed their previous work and responded to objections of the paleoclimatic significance by demonstrating the consistency of the evidence for the late Quaternary period.

Water-level fluctuations in closed-basin lakes thus provide evidence of climatic changes on a Quaternary time scale (Smith and Street-Perrott, 1983; Street-Perrott and Harrison, 1985; COHMAP Members, 1993). Most sensitive are closed basin lakes, which lack surface outlets. Fluctuations in closed lakes are particularly sensitive to changes in the balance between precipitation and evaporation, and provide a detailed record of variations in the regional and continental mean annual water budget (Smith and Street-Perrott, 1983; Street-Perrott and Harrison, 1985).

The mean annual water balance of any lake is given by equation (1) (from Street-Perrott and Harrison, 1985) :

$$\Delta V = A_L (P_L - E_L) + (R - D) + (G_I - G_O) \qquad (1)$$

where ΔV = net change in volume of the lake; A_L = area of the lake; P_L = precipitation on the lake; E_L = evaporation from the lake (P_L and E_L are expressed as a depth of water); R = runoff from the catchment and, D = surface discharge from the lake; G_I and G_O = groundwater flows into, and out of, the lake.

For a closed basin lake, D is zero and assuming groundwater transfers are negligible under equilibrium conditions, equation (1) becomes

$$R = A_L (E_L - P_L) \qquad (2)$$

If it is further assumed that the runoff from the drainage basin is represented by

$$R = A_b (P_b - E_b) \qquad (3)$$

where A_b = area of the catchment; P_b = precipitation over the catchment; E_b = evapotranspiration over the catchment.

then,

$$z = \frac{A_L}{A_b} = \frac{P_b - E_b}{E_L - P_L} \qquad (4)$$

where z = lake area/catchment area ratio.

Equation 4 suggests that the equilibrium area of a closed lake under natural conditions is dependent on the precipitation and evaporation over its catchment and water surface (Street-Perrott and Harrison, 1985).

Changes in the size of a lake can be reconstructed from several kinds of geological evidence, such as raised shoreline features, from lake-side archaeological sites, and the stratigraphic record of sediments, including macrofossils. These provide information on changes in the local hydrological balance which reflect changes in climate or local factors. It is difficult to separate the different factors from the analysis of one site. However, when most lakes in a given region change in a similar way, then the pattern can only be a response to climatic change (Harrison, 1988; Harrison *et al.*, 1993). Lake-level fluctuations alone cannot differentiate between changes in specific climatic variables that control the hydrological balance, but water and energy balance models have been used to estimate the change in water-balance parameters necessary to maintain a closed lake in equilibrium (Street-Perrott and Harrison, 1985, Harrison, 1988, Harrison *et al.*, 1993).

Lake-level changes have been used to reconstruct geographic patterns of change in the hydrologic balance and thus to infer paleoclimatic changes at a continental scale (Street and Grove, 1976,1979; Street-Perrott and Roberts, 1983; Street-Perrott and Harrison, 1984,1985, Harrison *et al.*, 1993, Yu and Harrison, 1995 b). This was originally applied to subtropical areas and only more recently in temperate regions, because many temperate lakes are overflowing today. The existence of an outlet moderates the response to hydrologic change. Furthermore, most temperate lakes are near their highest levels at present, which makes evidence of water-level changes harder to detect. These conditions, however, do not mean that temperate lakes are insensitive or unsuitable for paleoclimatic reconstructions, as is well documented in Harrison and Metcalfe (1985 a,b), Street-Perrott and Harrison (1985), Gaillard (1985), Street-Perrott (1986), Winkler *et al.* (1986), Harrison (1989); Harrison *et al.* (1991), Harrison and Digerfeldt (1991), Harrison *et al.* (1993), Harrison *et al.* (1995b).

Compilations of lake-level histories at a sub-continental to global scale can be used to investigate the spatial patterns of climatic change and to infer changes in continental-scale circulation patterns. Distinct, spatially coherent patterns in lake behaviour in North America have been identified by the use of multidimensional scaling (Harrison, 1987). Inferences about climatic changes from regional lake-level changes can be confirmed by comparisons with independent climatic reconstructions, for example, those based on the analysis of fossil pollen assemblages. In addition, the changing patterns can be compared with simulations made with general circulation models (GCMs) in order to test hypotheses about the mechanisms of climatic change (COHMAP, 1988; Harrison and Dodson, 1992, Kutzbach, 1993; Yu and Harrison, 1996; Qin *et al.*, 1998).

The next chapter introduces the lake-level data used in this study. The history of the three lake-level databases are discussed as well as the merging procedure used to create a global lake-level database.

Chapter 2

History of the Data

"Familiarity with the data is an asset in any statistical study. When trying to sort out inconsistencies in the data, it often helps to understand how the data set came to be in its current form ... "

Isaaks and Srivastava, 1989.

Three lake-level datasets have been merged to create a global database. The Oxford Lake Level Data Bank (Street-Perrott *et al.*, 1989), the European Lake Level database (Yu and Harrison,1995) and the Former Soviet Union (FSU) and Mongolia Lake level database (Tarasov *et al.*, 1994) were downloaded via the Internet through anonymous FTP access by the World Data Center - A for Paleoclimatology in Boulder, Colorado, USA. Because of its unusual format, the Oxford Lake level Data Bank was first reformatted into speadsheet format using a SAS program (Appendix A). The European and FSU and Mongolia databases were downloaded in EXCEL 5.0 format so that no further manipulation was required. Each of the datasets were verified for consistency according to the documentation available. One inconsistency that was found is that the Oxford Lake Level Data Bank was coded in opposite (ie: 1-High, 2-Intermediate, 3-Low) to the other two databases (1-Low, 2-Intermediate and 3-High) and the data were recoded. A second problem was duplicate sites with the same coordinates. These were verified for coding consistency and only one was included in the global database for that location. A third manipulation was performed in order to render the three datasets compatible where lake status was extracted by 1,000 year intervals ranging from present to 30,000 years ka. Sites that had no data for a particular time frame were given a 0 code for "no status". The merging of the three datasets was performed in EXCEL 7.0 and then imported in Microsoft Access 5.0. This enable quick access to the data via SQL statements. The global lake

level database is available from the Laboratory of Paleoclimatolgy and Climatology (LPC) of the Department of Geography of the University of Ottawa, Ottawa, Ontario, Canada. The LPC web page address is http://aix1.uottawa.ca/academic/arts/geographie/lpcweb/.

2.1 The Oxford Lake Level Data Bank

The Oxford Lake-Level Data Bank comprises records of lake status, a measure of relative water depth, for lake basins which have been closed for part, or all, of their Late Quaternary history. The database is global in extent, although geographical coverage is unequal.

Lake status was originally determined at 1,000 year intervals between 30 ka BP and present day. The sampling scheme used has the effect of suppressing short-term variations, which may reflect regional climatic and hydrological perturbations, and emphasizing longer-term global hydrological variations (Street-Perrott and Harrison, 1985). A standardizing procedure was applied in order to render all basins comparable, regardless of size. The total range of fluctuation experienced by each basin during the past 30,000 years was divided into three lake-status categories (Butzer *et al.*, 1972) with a similar overall frequency of occurrence in the data set (Street and Grove, 1976, 1979): Low status was given to 0-15% of the total altitudinal range of fluctuation, including dry lakes; intermediate status to 15-70% of the total range and high status to 70-100% of the total range of fluctuation, including overflowing lakes.

Interpretation of the record for each site is based on multiple lines of evidence, including sediment lithology, aquatic pollen, and other biostratigraphic indicators. Chronologies are provided either by ^{14}C dating or pollen correlation with a well established ^{14}C-dated regional pollen stratigraphy. Basins

with records that appear to have been influenced by tectonism, changes in the course of a river, changes in the threshold of the lake overflow, or glacier fluctuations are excluded from the data base. There are 358 sites available for the time period that is used in this study (Appendix A), although the geographical coverage decreases through time (Figure 2.1).

2.2 The European Lake-Level database

The European lake-level database (Yu and Harrison, 1995) contains records from 118 sites across Europe spanning 55,000 years (Appendix B). Each site is fully documented and coded based on information in lake status changes from different lithological and biostratigraphic evidence. The coding is consistent with the standards established for the Oxford lake-level database. Most of the sites have continuous records for the Holocene period. Sites where water depth appears to have been influenced by non-climatic factors, such as tectonism or human impact, or by indirect climatic influence such as sea-level changes, glacier fluctuations or fluvial influence, have been excluded from the database (Yu and Harrison, 1995). The sites included in the database have been screened to meet the standards of dating control and consistency as the Oxford Lake Level Data Bank (Yu and Harrison, 1995). This dataset increases significantly the number of sites in Europe in comparison to the Oxford Lake Level Data Bank (Figure 2.2).

2.3 Lake Status Records from the Former Soviet Union and Mongolia

The FSU and Mongolia database (Tarasov *et al.*, 1996) consists of 98 basins from the FSU and 5 basins from Mongolia for the period of 15,000 ka BP to present (Appendix C). As in the case of the Oxford Lake Level Data Bank and the European Lake Level Database, each site is fully

documented and coded consistently with the standards established for the Oxford lake-level database. Most of the sites have continuous records for the Holocene period. The exclusion of sites were based on the same scheme as the previous datasets. There is a heavy representation in western Russia while most of the Siberian territory has no data (Figure 2.3).

2.4 The Global Lake Level Database

The three datasets were merged into one global database. Each site includes the following information: identification number, name of basin, latitude, longitude, altitude and collapsed status fields spanning 30,000 years at 1,000 year intervals. Where no status was recorded, a 0 was coded.

North America, Europe and Africa are well represented while South America, most of Eastern Russia, China, and Australasia exhibit poor representation (Figure 2.4). Major gaps appear in Canada, the American midwest, northern Mexico and the African equatorial rain forest region. Although some data exists for parts of Canada, it is not available due to the closure of the paleoclimate database project at the Geological Survey of Canada. In addition, the Chinese lake status database (Fang, 1991) was not included due to accessibility problems. Finally, the number of sites decreases through time.

The next chapter will focus on the spatial organisation of the global lake level database.

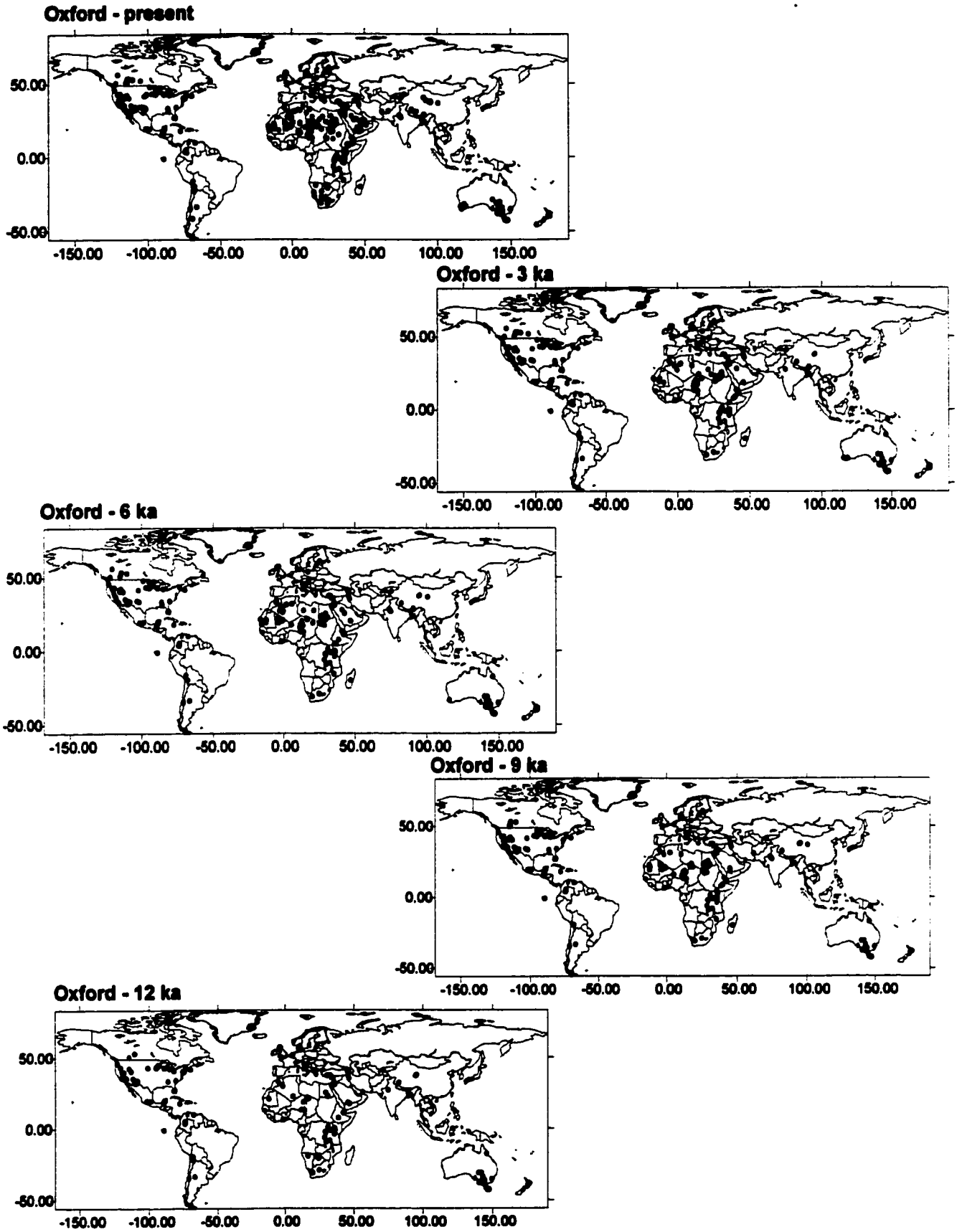

Figure 2.1: Distribution of sites for the Oxford Lake Level Database at present, 3 ka, 6 ka, 9 ka and 12 ka.

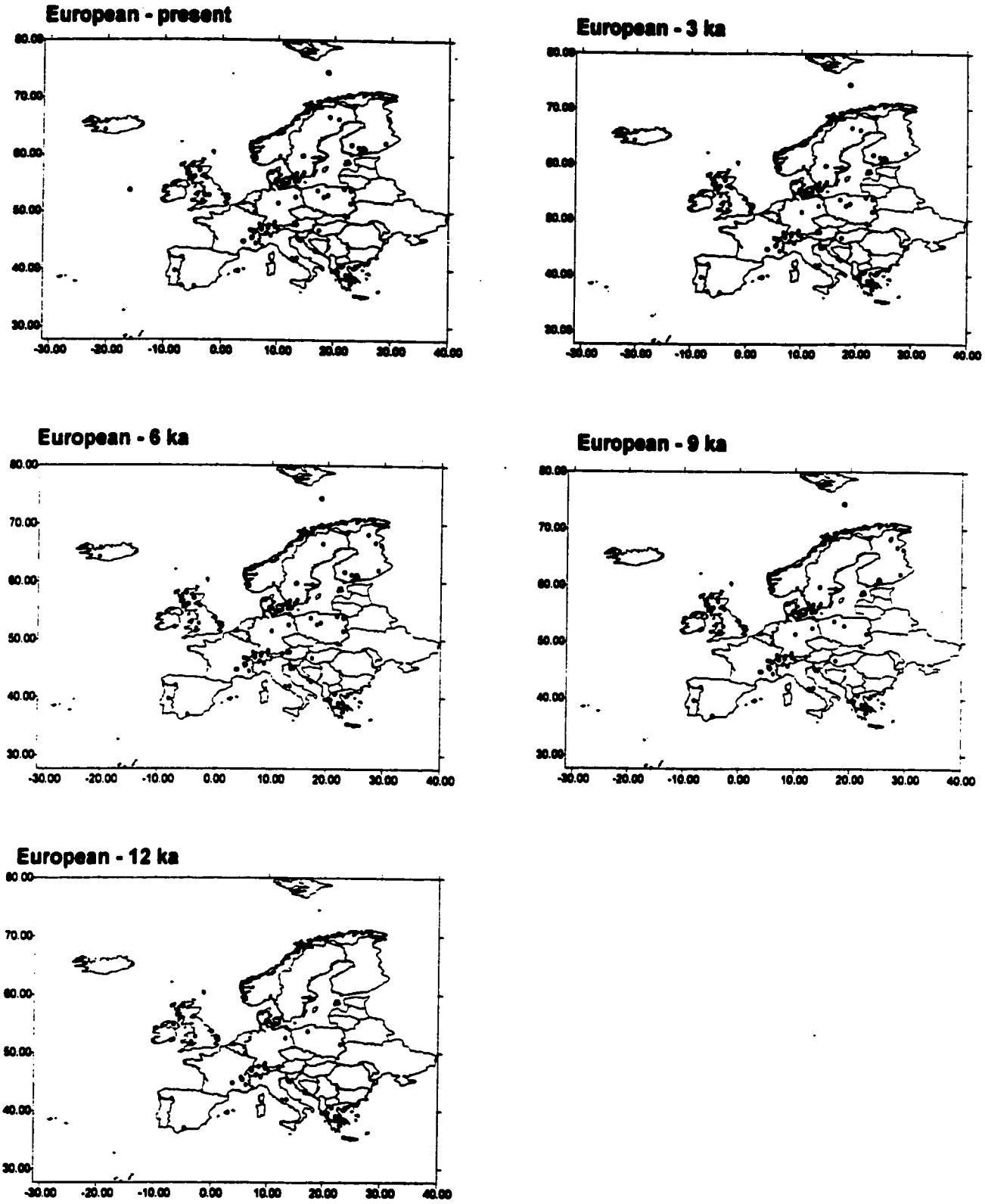

Figure 2.2: Distribution of sites in the European Lake Level Database at present, 3 ka, 6 ka, 9 ka and 12 ka.

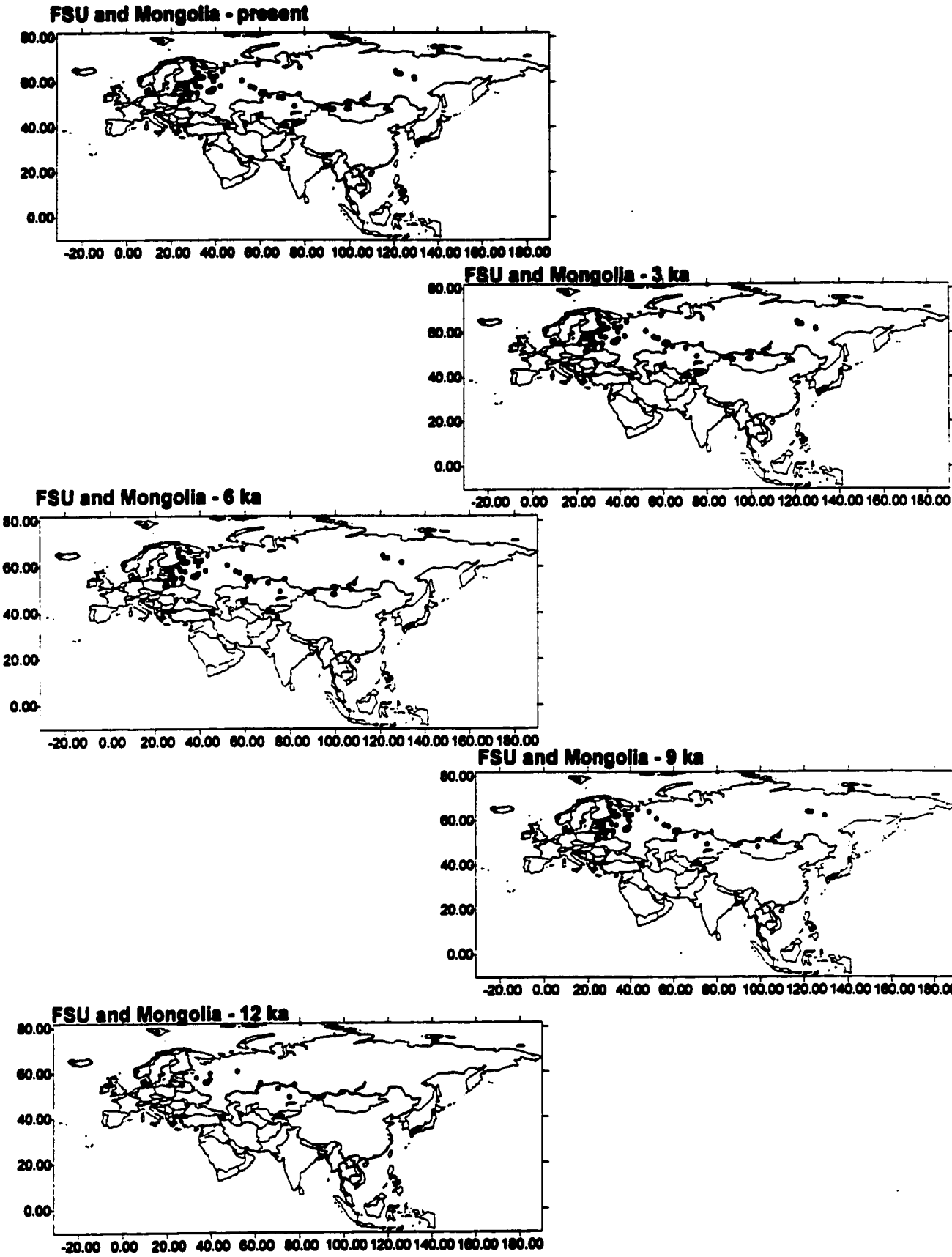

Figure 2.3: Distribution of sites in the Former Soviet Union and Mongolia Lake Level Database at present, 3 ka, 6 ka ,9 ka and 12 ka.

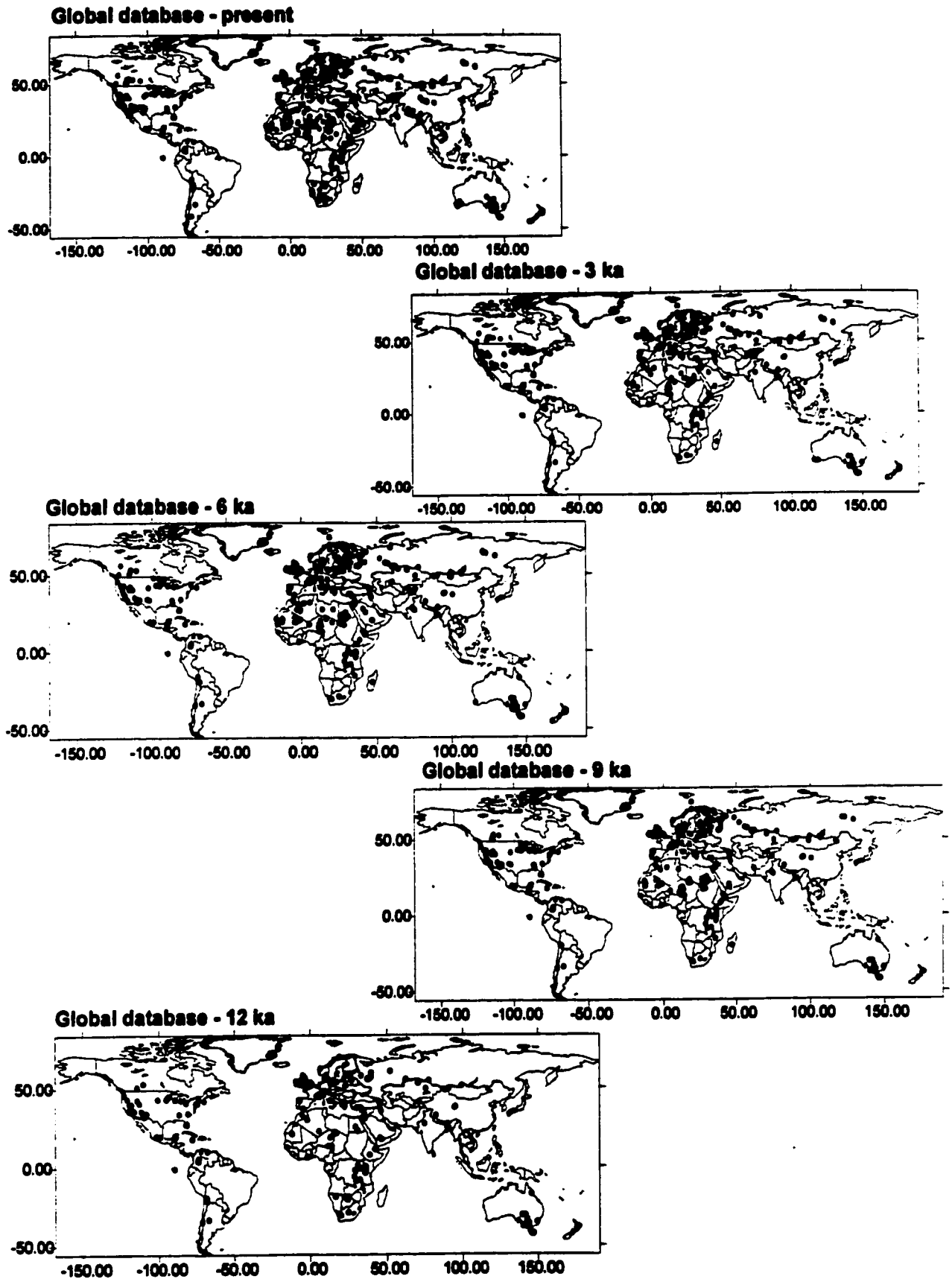

Figure 2.4: Distribution of sites in the Global Lake Level Database at present, 3 ka, 6 ka, 9 ka and 12 ka.

Chapter 3

Exploratory Data Analysis

"One of the things that distinguishes earth science datasets from others is that the data belong to some location in space. In some cases, establishing boundaries are visible, however, in a lot of cases, such boundaries are difficult to establish because of small scale intermingling of values... "

Isaaks and Srivastava, 1989.

The goal of this chapter is a four-part description of the distribution of the data. First is a univariate description of the data, followed by a spatial description. The third part is an example investigation into error checking, and finally, some summary statistics of the spatial organization of the data will be presented.

The initial step in any statistical study is becoming familiar with the data. As with any statistical study, problems with the data can lead to erroneous results (Isaaks and Srivastava, 1989). Exploratory data analysis enables the investigation and understanding of important features in the data. Although some of the features identified in exploratory data analysis may prove unimportant, it is at this stage that key features of the organisation of the data may be revealed. In most studies, the sample statistics are all that we have to tells us about the entire population (Isaaks and Srivastava, 1989).

3.1 Summary of the lake-level status

Lake level data are qualitatively coded as high, intermediate and low status. The variable is discrete and ordinal for each observation and has only three possible values. The only univariate description of a dichotomous variable is a cumulative frequency table or histogram (Isaaks and Srivastava, 1989). Additional summary statistics provide no further information.

Figure 3.1 shows the frequency histograms for the five time frames under study. The histogram for lake-level status at present shows that more than 50% of lakes are low. The 3 ka histogram reveals a decrease of low status in favour of an intermediate or transitional status suggesting a transition period at 3 ka. A sharp increase in the frequency of high lake-level status marks the 6 ka histogram, which indicates increased humidity or decreased evaporation at the sites in question. The 9 ka histogram shows an increase in low status while the intermediate status decreases, suggesting a period of increase evaporation at specific sites. The 12 ka histogram reveals a dominant high lake status suggesting a slight increase in humidity at a number of sites.

Although these summary statistics provide little information on the spatial distribution of the lake-level statuses, they do provide insight on the variations of the global hydrological cycle through time. In general, they show a gradual change in the global hydrological cycle through the Holocene. However, these results are based on different sample distributions (Figure 3.2) and a conclusion about the global hydrological cycle may not be warranted. The next section discusses the spatial distribution of lake levels in order to describe these variations of the global hydrological cycle through space and time.

3.2 Spatial distribution of lake status

Spatial features of the lake-level data, such as the location of extreme values, the overall trend and the degree of spatial continuity are of significant interest (Isaaks and Srivastava, 1989). The univariate description tools discussed above do not capture the spatial variations in the high, intermediate and low status. Knowing their location is important in that distinct spatial patterns can be established. However, in a lot of cases, the patterns are difficult to distinguish because of fine-scale variability present in the data (Isaaks and Srivastava,1989).

The simplest visual tool for spatial description is a map on which each data location is plotted with its corresponding data value (Isaaks and Srivastava, 1989; Deutsch and Journel, 1992). The advantages, among others, of these maps is that they reveal potential errors in the data location (ie: lone high values surrounded by low values merit investigating), and also give insight into finer-scale variability (ie. some sites may demonstrate local changes in the hydrological balance while others reflect regional climate changes). In irregularly spaced data, a symbol map gives insight to how the data was collected (ie: poorly represented areas versus densely sampled ones). The use of the symbol map consists of plotting each location and replacing its value by a symbol (or number) that indicates a certain class of values (ie. in this case, different symbols represent each individual lake status) (Isaaks and Srivastava,1989). Another way to visualize lake level status is a breakdown of the data into its components and plotting each lake status individually, which provides a detailed spatial description of each lake status category (Isaaks and Srivastava, 1989; Goovearts, 1997).

Variability in space is often of interest and it is common to find that the data values in some regions exhibit more fine-scale variability than others. The presence of such variability is termed

heteroscedasticity (Isaaks and Srivastava, 1989). Irregularities in the local variability will have an impact on the accuracy of estimates where *"the estimates from any reasonable method will always benefit from low variability and suffer from high variability"* (Isaaks and Srivastava, 1989). In cases where local variability is roughly constant, then estimates in any particular area will be as good as estimates elsewhere. The local variability is related to the local average in some way, therefore somewhat predictable. It is useful, therefore, to establish in the initial data analysis if such anomalies in the variability does exist.

Figures 3.3 a-e to 3.4 a-e illustrate the maps of the lake status during the Holocene. First, all three lake statuses are posted to give insight into the distribution of lake statuses, as well as indicate local variability (Figures 3.3 a-e). Next, figures 3.4 a-e present the breakdown of lake status to give insight into the spatial distribution of each lake status individually and, also helps to identify distinct spatial patterns that are obvious in the data.

Lake Level Status - present

The present-day distribution of available sites is irregularly spaced (Fig. 3.3 a). In North America lake status is fairly-well represented for the most part of the United States except for the Midwest. There are few sites in Canada outside the southern prairies. Mexico and Central America have very few sites. There are also few sites for South America except in the northern and southwestern coast region. Europe is well represented while the border region of eastern Europe and Asia show a substantial decrease in the number of sites. There are many sites in northern and eastern Africa whereas the equatorial rain forest and southwestern coastal areas have no sites. There are no data available for Indonesia. Australia reveals a cluster of sites in the southeast.

The present-day lake status of the combined datasets reveal distinct spatial patterns (Fig. 3.4 a). In North America, high lake levels are predominant in the Midwest, northeastern coast and Florida. The lakes are primarily intermediate status along the southern Great Lakes region, the western interior cordilleran region, and in the proximity of the Gulf of Mexico. Lakes along the southwestern cordilleran region and west of the Gulf of Mexico are low at present. Central America has few sites and these range from intermediate status in Mexico to high status in mid-central America. South America is divided into a northeastern region of high lake-level status and a southwestern region of low lake-level status stretching south along the Cordilleran into Argentina. Lake status in Europe is more variable compared to the Americas. High lake-level status is dominant in the western region while intermediate status are generally confined to the eastern interior and southern regions. Low lake-level status exhibits a south to north direction predominantly east of the intermediate lake-level status with some fine-scale variability. The extreme southern Mediterranean region also has predominantly low lake-level status. The majority of North African lakes record low levels and this extends to the Middle East. There is some fine-scale variability in the southeastern coastal region while the extreme southern tip of Africa has dominantly low status. Although there are few sites, Asia exhibits evidence of latitudinal spatial continuity where the general trend is high status in the northern regions, intermediate status across mid-Asia and low status in the south. Finally, Australia reveals considerable fine-scale variability similar to that of Europe. Interior sites are dominantly low status, followed by intermediate status closer to the southern coast and finally high status in the vicinity of the coast. In the southwest, all lakes are low.

In spite of differences in fine-scale variability in different regions of the world, distinct spatial patterns are present in this dataset. There are many regions where both high and low lake-levels are found in close proximity. For example, the southern prairies of North America shows that the majority of

lakes are high status while two lakes show low and intermediate status.

Lake Level Status - 3 ka

At 3 ka, there are already fewer available sites (Fig. 3.3 b). The main difference in coverage is a significant decrease in the number of sites in north Africa.

Lake level status at 3 ka reveal distinct spatial patterns (Fig. 3.4 b). The primary differences are as follows. The lakes of North America are similar to the present. The lakes are mainly intermediate status along the southwestern Great Lakes region, although some low status sites are now present. Lakes along the southwestern cordilleran region and west of the Gulf of Mexico remains predominantly low, however there is evidence of heightened fine-scale variability. The lakes of the northwestern coastal region of Europe are predominantly high while intermediate status remains generally confined in the eastern interior and southern regions. The evidence of low lake status running in a north-south direction east of the intermediate status is not as noticeable at 3 ka because of increased fine-scale variability. Africa at 3 ka shows fine-scale variability in most parts of the north, as well as the southeastern coastal region.

Due to the heightened fine-scale variability that characterises most of the regions of the world, the patterns are not as obvious as 0 ka. Moreover, certain regions , for example Northern Africa, have declined significantly in the number of available sites.

Lake Level Status - 6 ka

The number of available sites at 6 ka is similar to 3 ka (Fig. 3.3 c). The main differences are in Europe which has fewer available sites in the north; however there is a significant increase in sites for Northern Africa.

The majority of the lakes of North America are low (Figure 3.4 c). The lakes in intermediate status are confined to the Florida region while high lake-levels are found in a northwest-southeastern direction. The American Midwest seems to be a transitional area between the pockets of low status. Unfortunately, this area is not well represented. There are fewer sites with a predominantly intermediate status along the Cordilleran region of South America. Lakes in Europe continue to be more variable than the Americas, however the spatial patterns of lake status remain similar to 3 ka and 0 ka. Lakes with low status lie predominantly east of the intermediate lake status sites. North Africa no longer shows fine-scale variability in the north, rather, the majority of the lake in the north are high. This decrease in fine-scale variability is also present in the southeastern coastal region where most lakes are also high status. The extreme southern tip of Africa exhibits fine-scale variability, however, there is a substantial decrease in the number of available sites. Although there are fewer sites, Asia shows little change (high lake status is dominant in the northern regions, intermediate status across mid-Asia and low status in the south). However, lakes in the extreme southwest of China and northern India are primarily high.

Contrary to 3 ka, lake-level status at 6 ka exhibit more coherent spatial patterns. Fine-scale variability across most of the regions is still present but to a lesser extent than at 3 ka. There remain many regions where both high and low lake-levels are found in close proximity.

Lake Level Status - 9 ka

At 9 ka, the number of available sites has decreased slightly to 334 sites (Figure 3.3 d), the primary differences being a visible decrease in the number of sites in Northern Europe and Northern Africa.

In North America, low lake-levels are predominant along the cordilleran region and eastern coast while intermediate status is primarily in the southwest of the Great Lakes region (Figure 3.4 d). The heightened fine-scale variability obscures spatial patterns of high lake records. There are few sites in Central and South America which makes spatial patterns difficult to observe. In Europe, the low lake status lie east of the predominant intermediate lake status while high lake-levels occupy the western coastal region and are clustered around the northwest region. The majority of African lakes reveal little change from 6 ka. However, fine-scale variability between intermediate and high status are apparent in the north. Although few sites remain in the extreme southern tip of Africa, fine-scale variability is also visible. There a few sites remaining in Asia, where high lake status is predominant in the northern regions, intermediate lake-levels across mid-Asia and low status in the south.

The variability present at 9 ka is comparable to 3 ka, which suggests a possible transition phase in the global hydrological cycle. Africa is the only region that exhibits low variability.

Lake Level Status - 12 ka

There is a significant decrease in the number of available sites at 12 ka (171 sites) (Figure 3.3 e). The main differences are in the decreased number of available sites in Europe, leaving the north unrepresented; a significant decrease is also visible in northern Africa (Figure 3.4 e).

High lake levels are dominant over much of North America except for the southwest desert regions. The few sites in Central America are primarily low. High lake status is predominant in the southwestern region of France. Fine-scale variability characterises the north and eastern coastal regions of Africa. Although still decreasing in number of available sites, Asia continues to show little change except in the extreme southwest of China and northern India where fine-scale variability has increased. There are few sites in Australia and most are low.

Lake-level status at 12 ka display a significant decrease in fine-scale variability in most regions of the world due in part to the decreased coverage, although there are exceptions such as in Europe and Africa.

The periods of 0 ka, 6 ka, and 12 ka exhibits more distinct spatial patterns while 3 ka and 9 ka tend to exhibit more fine-scale variability throughout all regions of the world. Furthermore, Europe consistently shows fine-scale variability throughout all time periods. This suggests that the lake-level database entries contain potential errors and/or sites that are primarily influenced by other factors such as local hydrological factors. This will inevitably cause problems in estimating spatial autocorrelation. Further investigation is needed in order to validate sites within regions of high variability. This study of global hydrological change assumes that large-scale climate patterns are the primary control of closed basin and temperate lake-level fluctuations. The identification of potential errors and sites influenced primarily by other more local factors is inevitable in the estimation and modelling of this data. The next section looks at potential errors in the coding in high variability areas and is termed error checking.

3.3 Investigation into fine-scale variability

One of the more time-consuming tasks in a geostatistical study is error checking. The study of the densely sampled areas can give insight into the consistency of the data. When attempting to sort out inconsistencies in the data, it is important to understand how the dataset came about. Some questions to ask include: Were all of the data collected in one program? Is the sampling procedure consistent from one program to the other? Were different people involved in the sampling? If so, were their sampling scheme or procedures different? And most importantly, how was the data treated? (Isaaks and Srivastava, 1989). The coding of the samples may reveal differences in sampling. Changes in the precision of the data values may be the result of switching to different methods of measuring the values. All these can lead to inconsistencies and should be investigated before the statistical analysis proceeds. Some helpful error checking procedures include: lone high values surrounded by low values or vice-versa, these are worth rechecking to establish their validity, quality dating control of the sample and suspicious isolated values (Isaaks and Srivastava, 1989).

The Oxford Lake-Level database originated in a study of closed basin lake-level variations in Africa (Street and Grove, 1976, 1979). The development of a global lake status database is an ongoing research program. Yu and Harrison (1995) established the European lake level database using consistent standards of coding and dating control of the Oxford Lake Level database. However, the inclusion of temperate and overflowing lakes as indicators of climate change is one major difference between the Oxford Lake Level database and the European Lake Level database. Tarasov *et al.* (1994) constructed the FSU and Mongolia Lake Level Database with the same sampling scheme and coding standards as the Oxford Lake Level Database. This database also contains temperate and overflowing lakes.

Given that coding standards are consistent between all three datasets and potential errors and/or fine-scale variability seem to be present in most regions of the world, we can investigate other possible sources of errors. Such possibilities include quality dating control and stratigraphic sampling schemes. Figure 3.5 illustrates an example of fine-scale variability in one region. This example was randomly chosen and we are interested in the lone high value surrounded by low values at close proximity.

Lac de Chalain(Fig. 3.5; id:21) (46°40'30"N, 5°46'E, 488 m above sea level) lies within a blind valley cut into the western edge of the calcareous plateau which forms the western margin of the Ain Valley (Magny et *al.*, 1988: from Yu and Harrison, 1995). It is fed by a karst spring and has a natural outlet. A number of drowned archaeological sites around the lake (Bourdier, 1962; Duret and Martini, 1965; Lambert et *al.*, 1983; from Yu and Harrison, 1995) indicate that the lake was lower than present *ca.* 5600 and 3600 yr B.P. Artefacts have been radiocarbon dated between 4170 and 5850 yr B.P. (Hassko *et al.*,1974; Evin *et al.*, 1973,1983; Delibrias *et al.*,1986; from Yu and Harrison, 1995). A transect of six cores were taken by Magny *et al.*, 1988 and stratigraphic and palynological analyses were made. However, the chronology is based on a single radiocarbon date from Core 4 (Magny *et al.*,1988, from Yu and Harrison,1995). Nine radiocarbon dates (mostly from archaeological fragments) were used for coding where the closest radiocarbon date to 3000 yr B.P. is 4170 yr B.P. The coding was established for the time period under study as high from 3600 to 2290 yr B.P. based on the evidence.

The lacs Clairvaux (46°34'N, 5°45'E, 526 m above sea level) are two closely-connected lakes lying in the same valley as lac de Chalain (Yu and Harrison, 1995). These lakes are also fed by karst springs, and there are also drowned archeological sites along the shores. These also indicate lake

levels lower than the present between 5600 and 3600 yr B.P. (Lambert *et al.*,1983, from Yu and Harrison, 1995). However, Lambert *et al.*(1983) argue that the abandonment of the sites may not have been synchronous or caused by an increase in water level since a pollen core showed an hiatus in sedimentation between 3300 and 3000 yr B.P. which in turn suggests that low lake level persisted after the archeological sites were abandoned. Further evidence of lake-level changes are provided by a transect of three cores which were taken for stratigraphic and aquatic pollen analyses (Magny *et al.*,1988; from Yu and Harrison, 1995). The coding, on a five-level scale from very low to high, of the lake-level fluctuation was based on 28 radiocarbon dates from the cores and archeological fragments. The status at ca. 3000 yr B.P. was coded low.

Thus, although Lac de Chalain and Lacs de Clairvaux lie in the same valley, are close in proximity, are fed by karst springs and have archeological sites dating back at the same time period, they exhibit totally different lake-levels ca. 3000 yr B.P. Moreover, most other lakes around Lac de Chalain exhibit low status during the period around 3000 yr B.P. The relatively poor radiocarbon dating of Lake de Chalain compared to a high quality radiocarbon dating of the Lacs de Clairvaux suggests a possible error in interpretation of lake-level at Lac de Chalain ca. 3000 yr B.P. Furthermore, the suggestion of Lambert *et al.*, (1983) that the archeological sites may have been abandoned prior to the rising of the lake levels also suggest that the Lac de Chalain could be interpreted as low status 3000 yr B.P., as most of the other lakes in that area show.

Lake Paludru, also in this area, is coded intermediate and is also surrounded by low lake levels. The documentation reveals confusion with 4800 to 1000 yr B.P. being coded low status and between 3900 and 1300 yr. B.P. having an intermediate status. Therefore, Lake Paludru could be interpreted as low or intermediate around 3000 yr B.P. The raw data gives a priority code of intermediate and

secondary code of low (Figure 3.5).

These examples illustrate the potential errors in interpretation and accuracy of the data. In the case of Lac de Chalain, it seem that poor radiocarbon dating and stratigraphic analysis would be the cause of an apparent fine-scale variability over very short distances. Therefore, by excluding these two problematic lakes, the fine-scale variability is no longer present in this area.

Although this investigation illustrated potential errors in developing a large database, some investigations into fine-scale variability may confirm the validity of the coding. Two lakes in close proximity could presumably exhibit very different lake status due to local factors influencing the hydrological balance. Since this study deals with a large amount of sites, one can conclude that checking every site for validity in coding would require an enormous amount of time and may prove to be a futile effort. In this case, the analysis clearly points to poor temporal control, but in other areas, it may not be as clear. Even if all sites could be checked, there would still be ambiguous interpretations.

In Chapter 4, we will illustrate a way of dealing with potential errors and fine-scale variability using Local Indicators of Spatial Autocorrelation (LISA) (Anselin, 1995). This procedure identifies sites that are spatially autocorrelated at specified distances. The procedure allows the identification of local instabilities, potential errors and homogenous regions within a specified distance scale. LISA is not a substitute for error checking but serves as a depiction of spatially autocorrelated sites at specific distance scales when dealing with large datasets.

3.4 Summary statistics of the spatial organization of the data

Table 3.1 lists the mean distance between sites, the maximum and minimum distances, the medians and quartiles which will be of important use for the next chapter which deals with spatial continuity analysis and modelling. The data were projected to Hammer-Aitoff equal area projection in which the units are kilometres (Appendix D). The reprojection was needed to facilitate computational requirements since the original data were in degrees (Plate Carré projection).

Time (ka yr.)	Minimum distance (km)	First quartile distance (km)	Median distance (km)	Mean distance (km)	Third quartile distance (km)	Maximum distance (km)
Present	0.7368	32.65	75.93	149.2	178.4	1939.0
3 ka	0.9914	28.61	89.87	177.9	212.7	1965.0
6 ka	0.9914	26.36	80.71	176.1	213.8	1939.0
9 ka	0.9914	33.64	92.5	196.7	214.1	2307.0
12 ka	1.4	66.78	161.9	269.3	337.1	2175.0

Table 3.1: Table of the spatial summary statistics for present, 3 ka, 6 ka, 9 ka and 12 ka.

There is a significant difference between the median and mean distances for all time periods. This is a positive skewness in the distribution of distances between sites. However, the oceans are an important factor influencing greatly the mean. Furthermore, the maximum distances are significantly greater than the third quartile distances. Therefore, the median distance is more representative of the true measure of central tendency. Moreover, the minimum distances between sites are very short (around 1 km). These short distances between sites is another way of analysing fine-scale variability as will be discussed in Chapter 4. Note that at 12 ka, the distances between sites are substantially greater due to a decrease in geographical coverage or number of sites.

Although these statistics do not provide sufficient insight into choosing a proper distance scale, it serves as a starting point in determining the distance scale at which spatial continuity analysis can proceed in the next chapter.

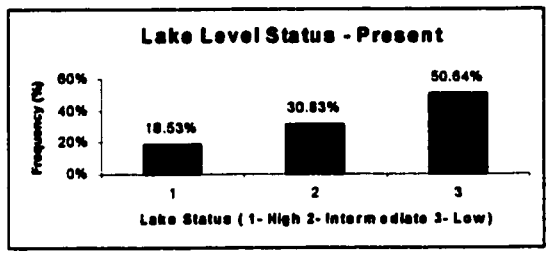

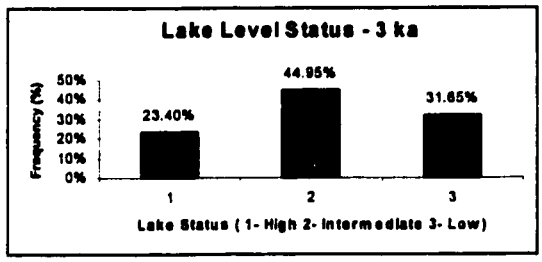

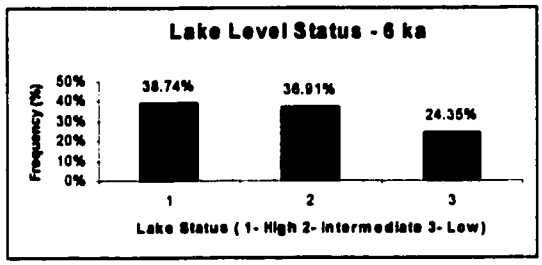

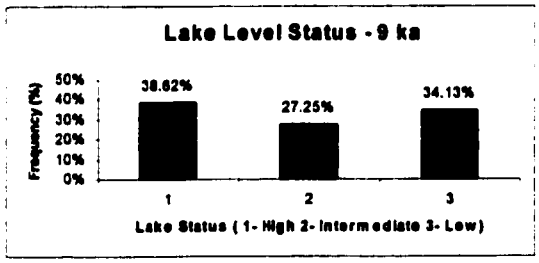

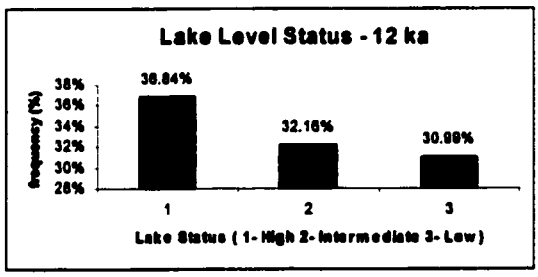

Figure 3.1: Frequency histograms of lake status at present, 3 ka, 6 ka, 9 ka and 12 ka.

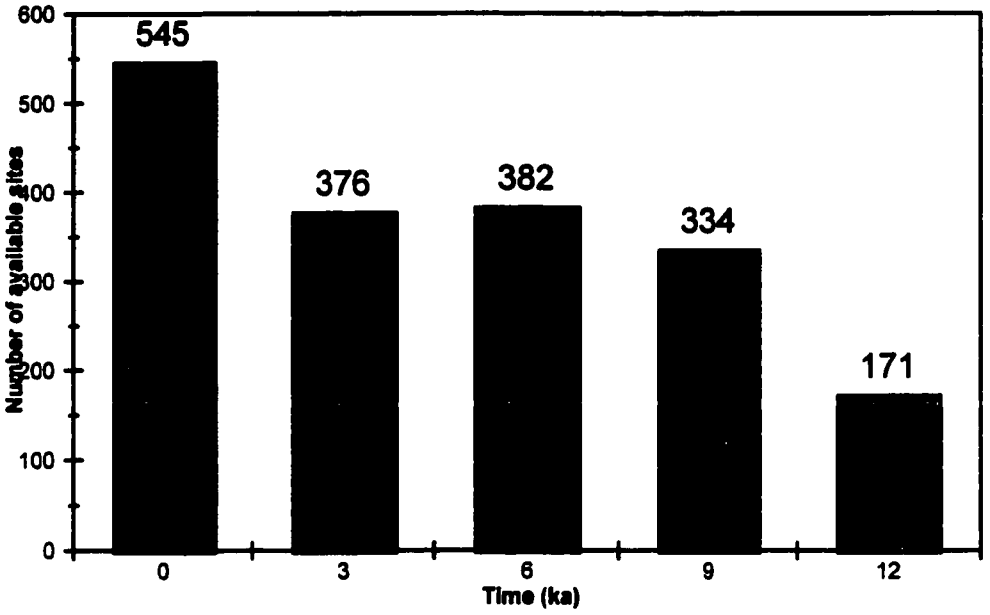

Figure 3.2: Number of available lake-level sites through the Holocene.

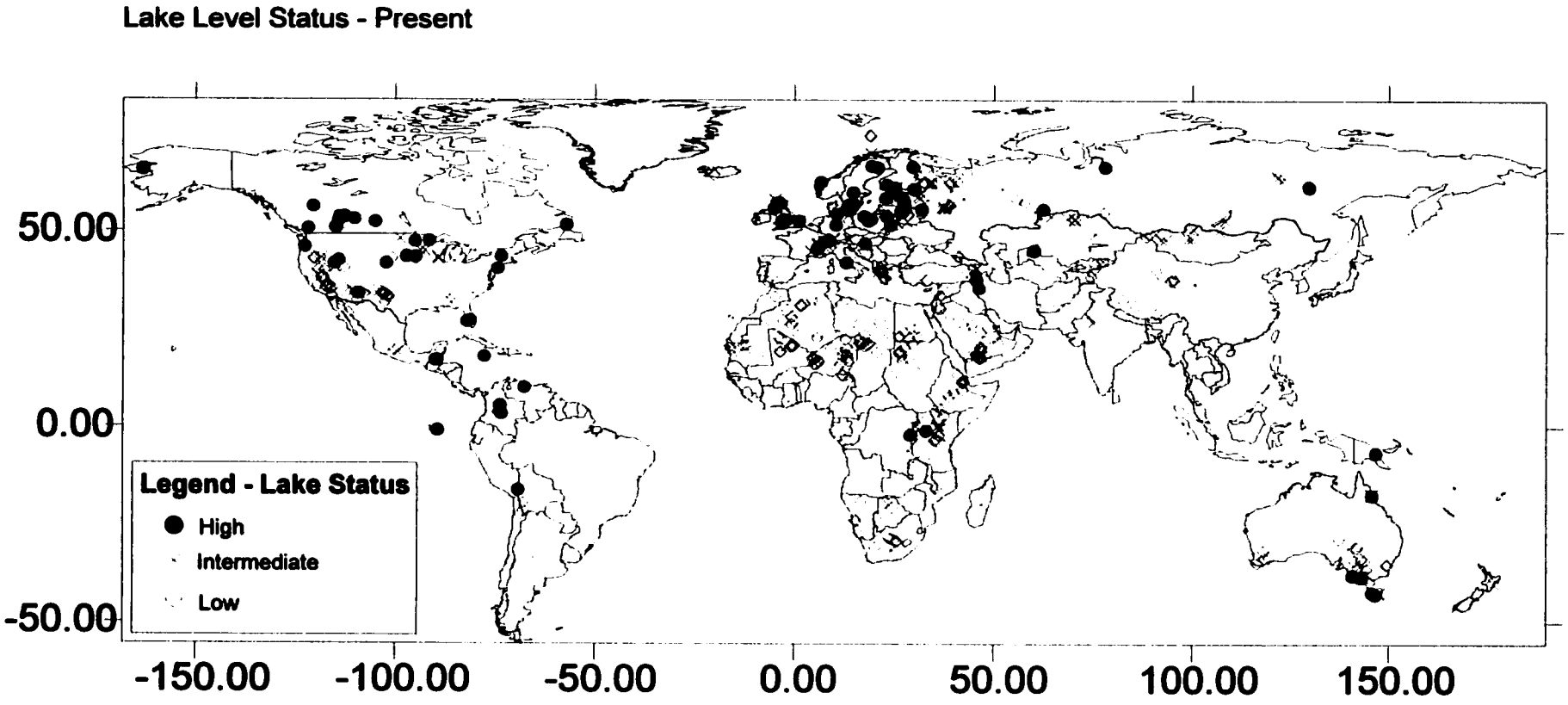

Figure 3.3 a: Lake status at present.

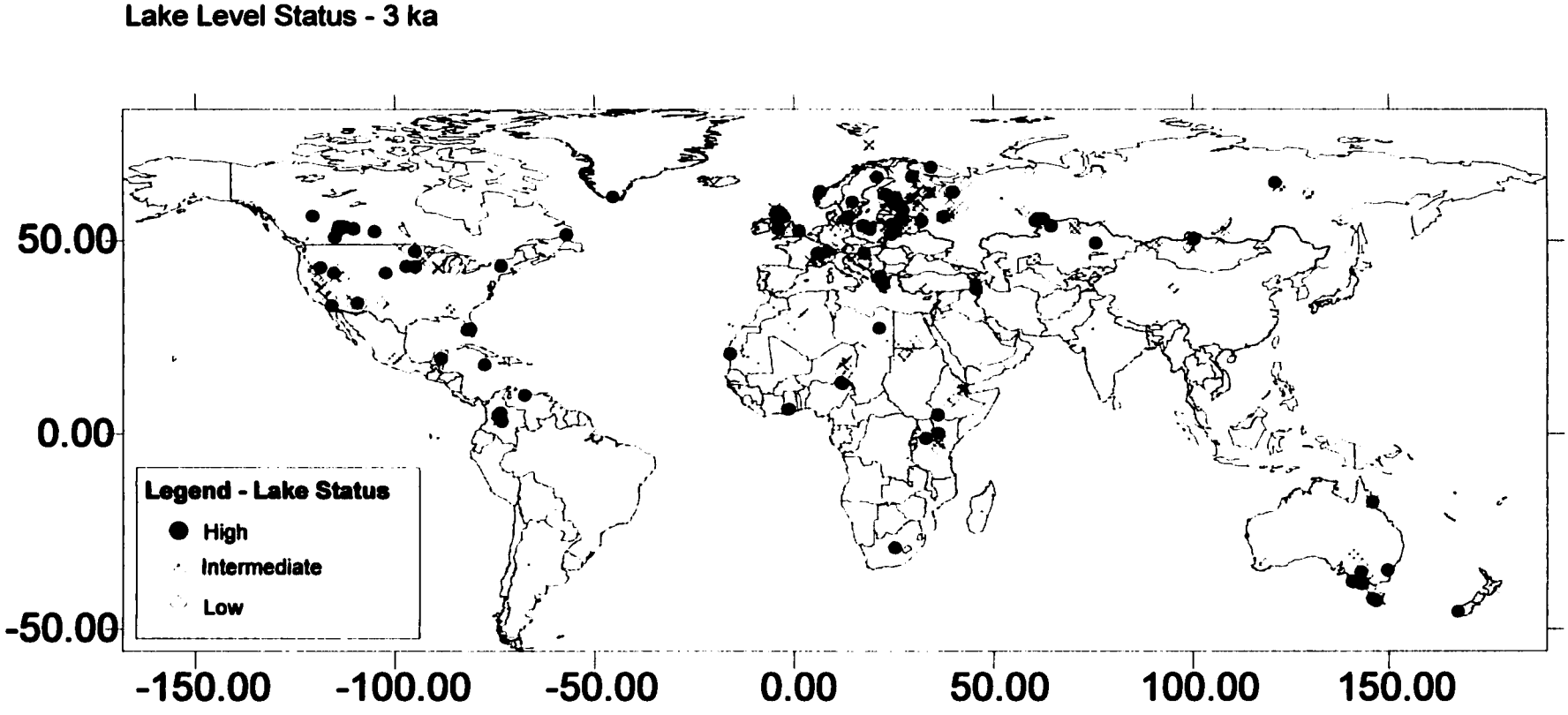

Figure 3.3 b: Lake status at 3 ka.

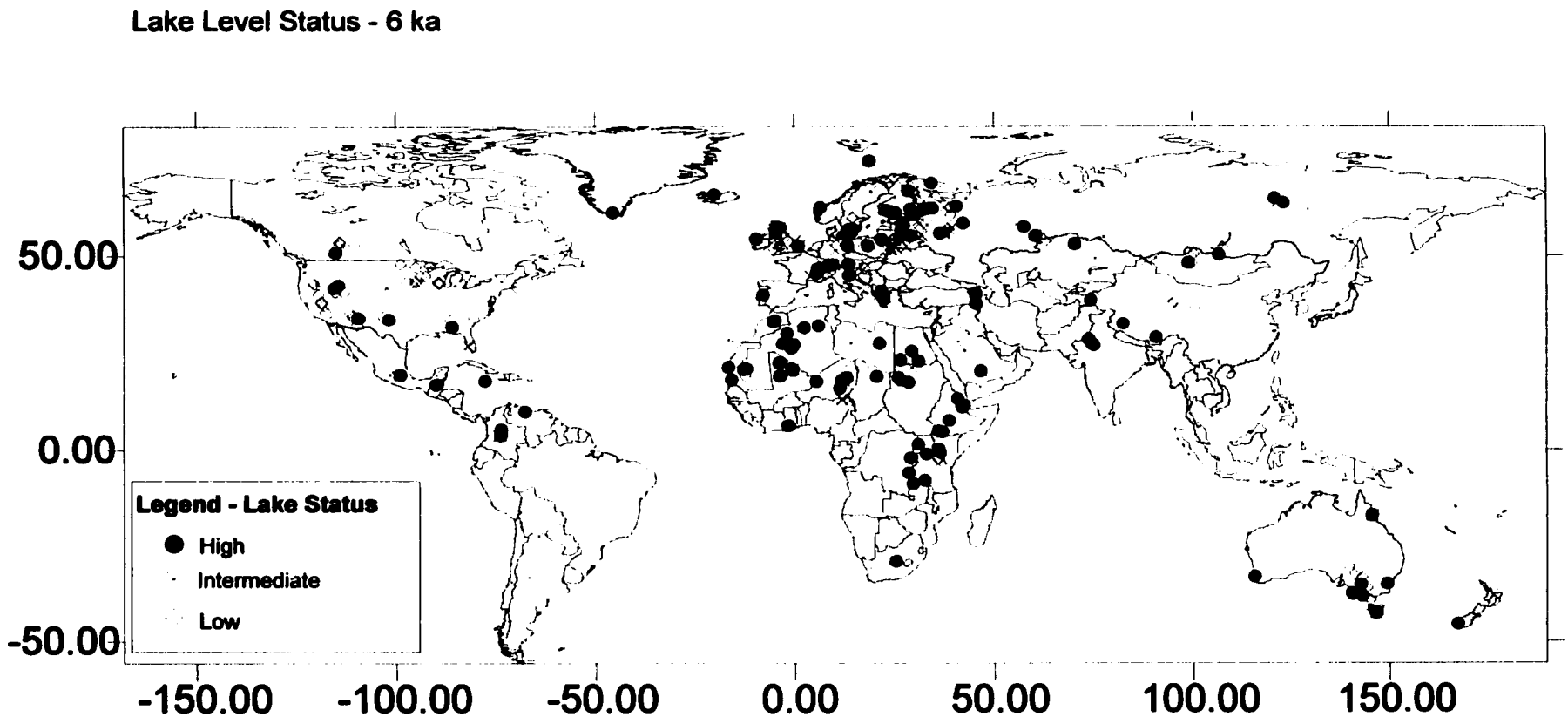

Figure 3.3 c: Lake status at 6 ka.

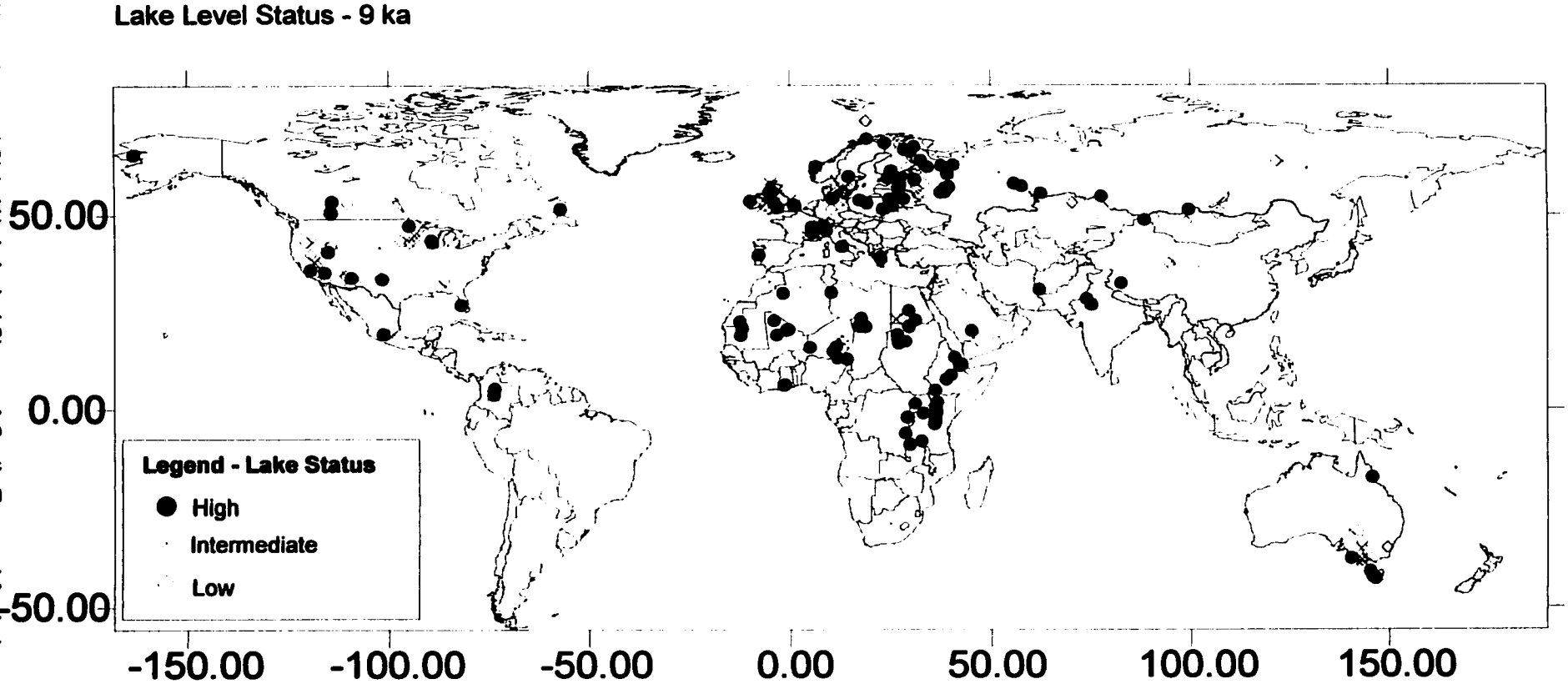

Figure 3.3 d: Lake status at 9 ka.

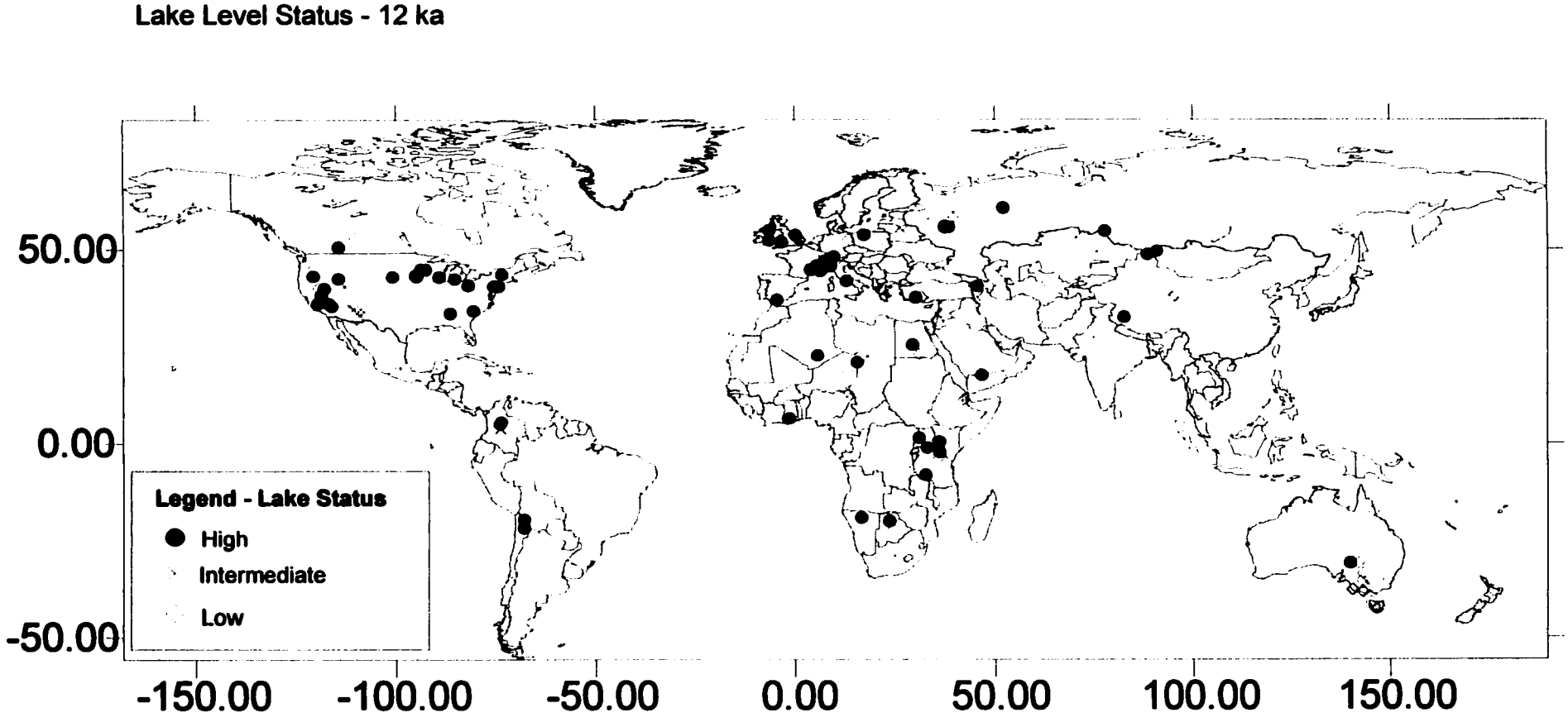

Figure 3.3 e: Lake status at 12 ka.

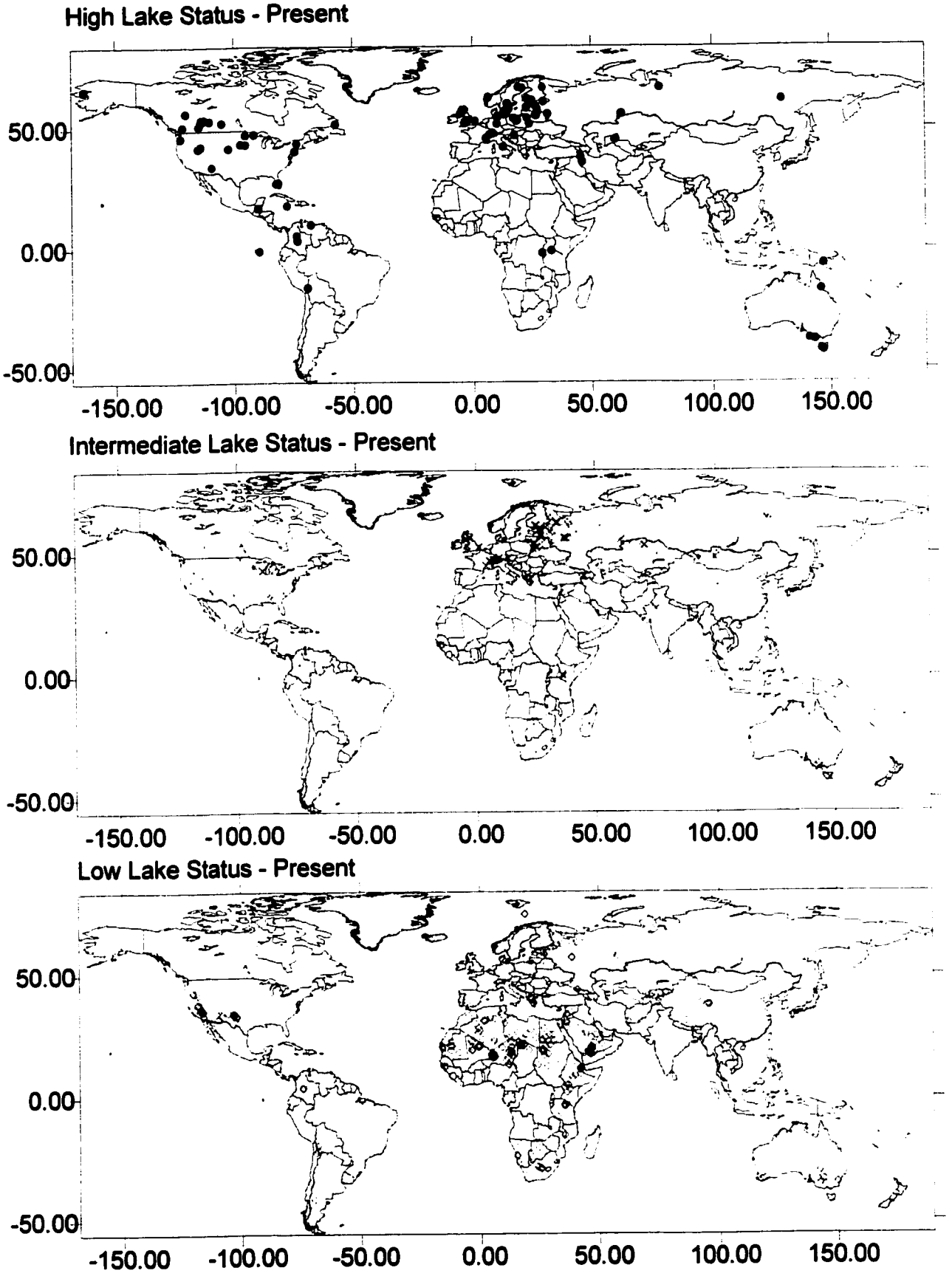

Figure 3.4 a: Breakdown of lake status at present.

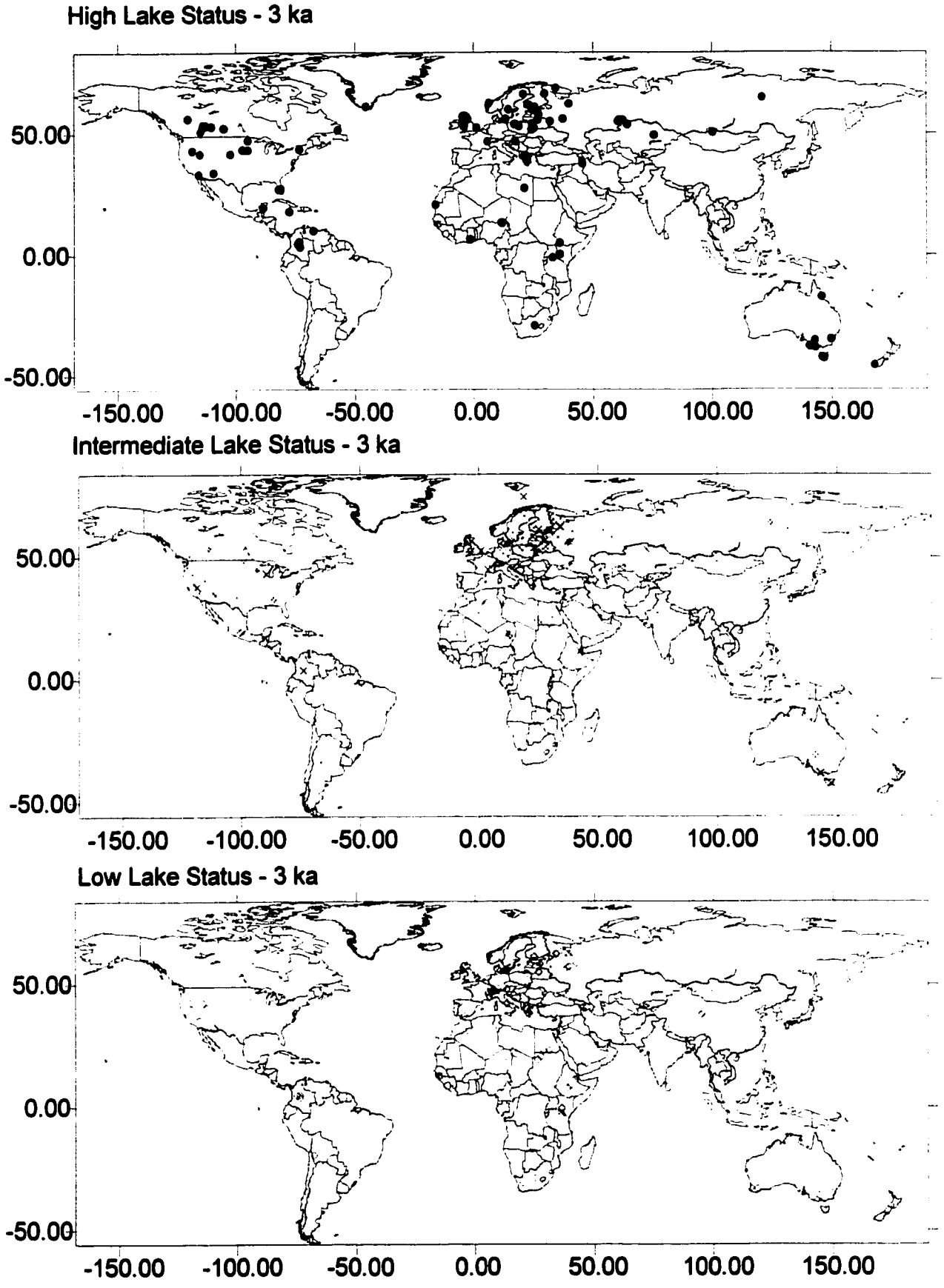

Figure 3.4 b: Breakdown of lake status at 3 ka.

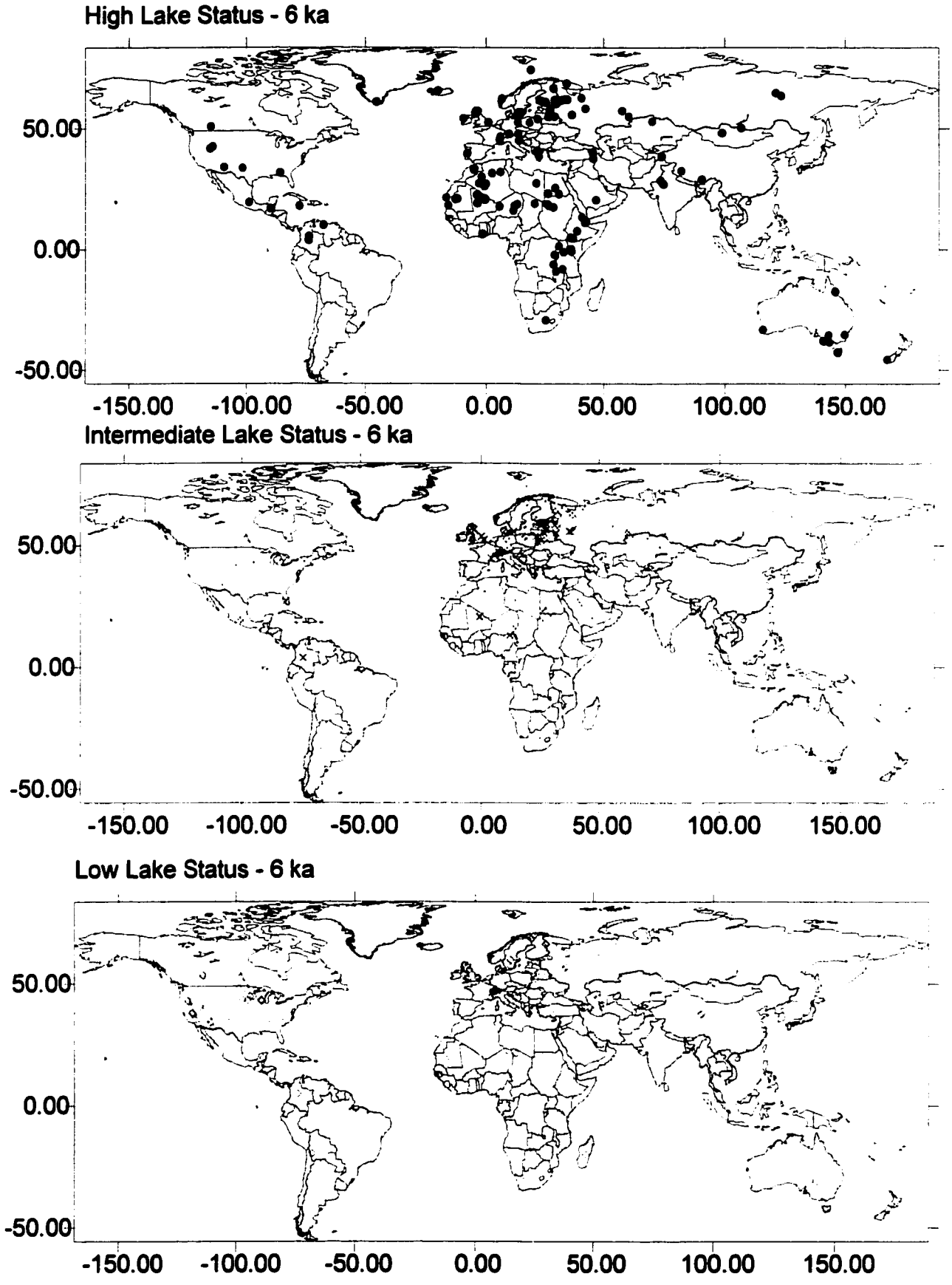

Figure 3.4 c: Breakdown of lake status at 6 ka.

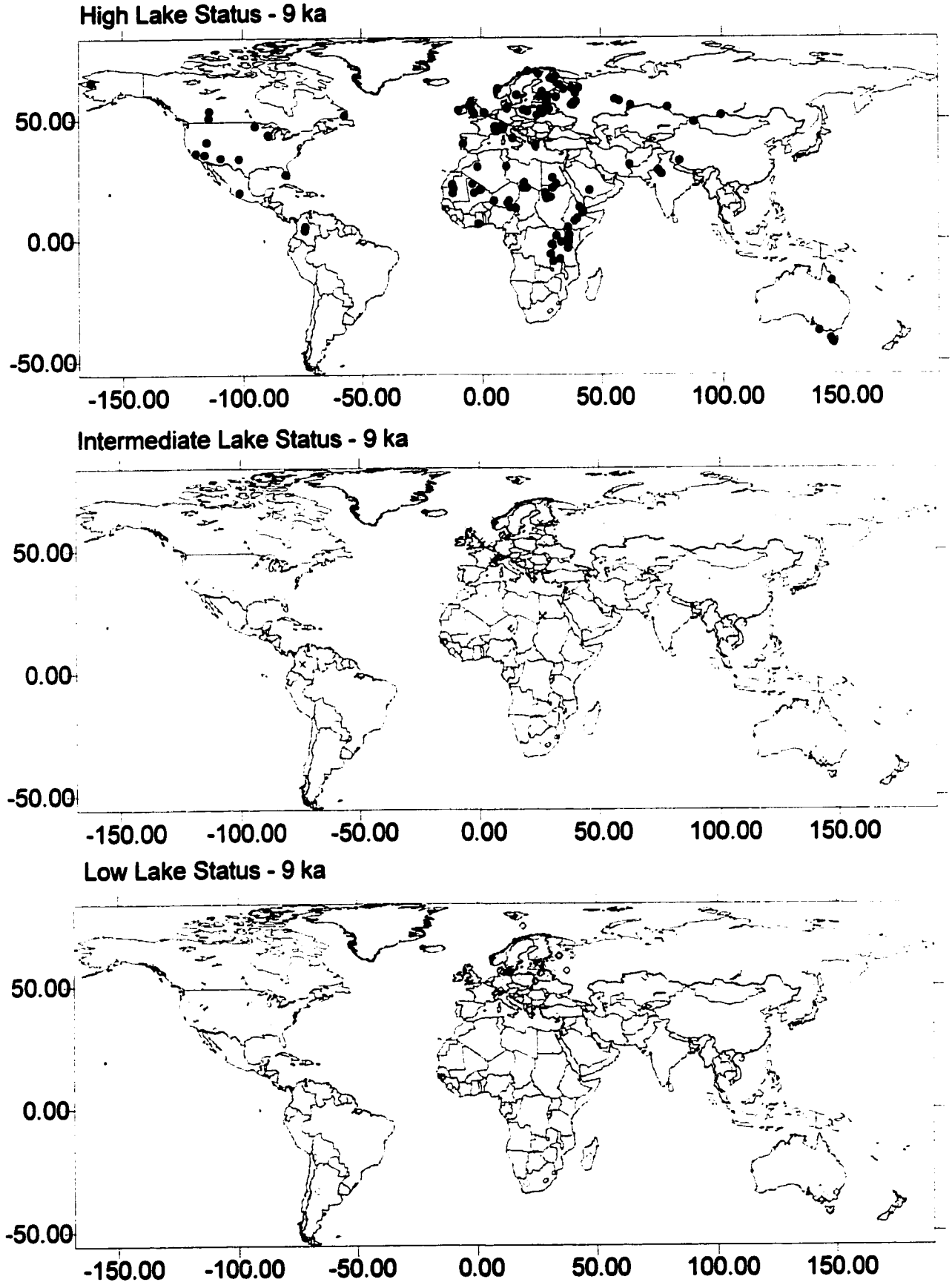

Figure 3.4 d: Breakdown of lake status at 9 ka.

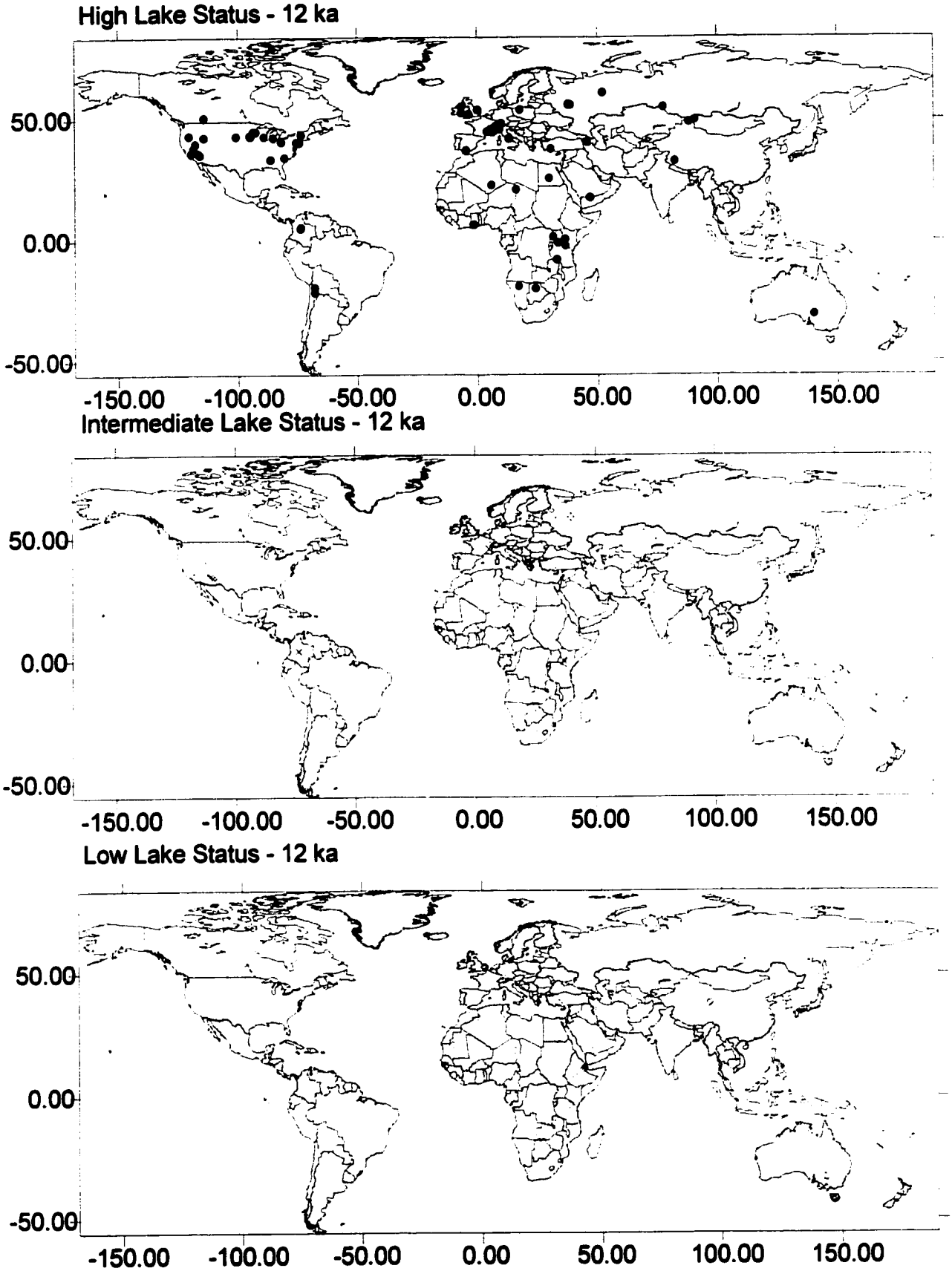

Figure 3.4 e: Breakdown of lake status at 12 ka.

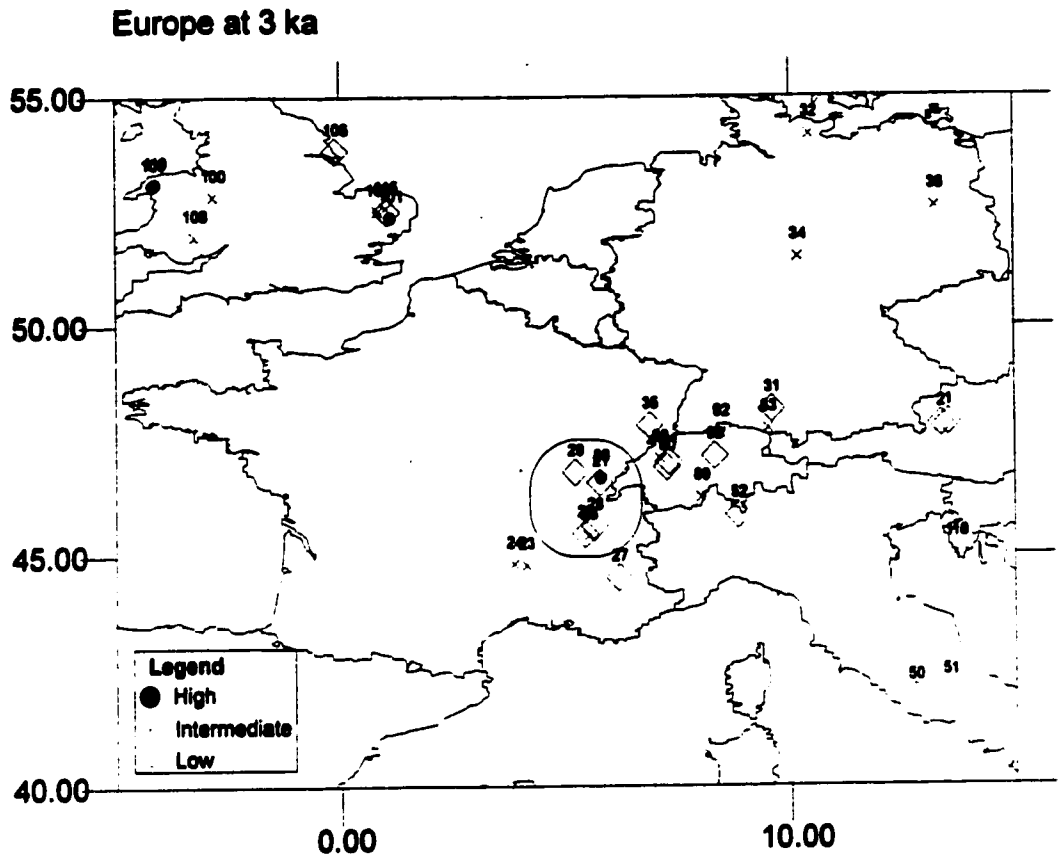

Table of sites information

Legend	Status
1	High
2	Intermediate
3	Low

Id	Basin	Longitude	Latitude	Altitude(m)	3 ka	Documentation
20	Chalain	5.77	46.68	488	1	1
21	Clairvaux	5.75	46.57	526	3	3
25	Le Grand Lemps	5.42	45.47	456	3	3
26	Paladru	5.5	45.42	492	2	2 or 3
28	Pluvis	5.63	45.63	215	3	3 or 1
29	Rousses	5.2	46.8	1058	3	3

Figure 3.5: Investigation into error checking.

Chapter 4

Spatial Continuity Analysis

"Information extracted from a data set or any inference made about the population from which the data originate can only be as good as the original data. Most often researchers face a major data-cleaning exercise before the statistical analysis can proceed ... "

Isaaks and Srivastava, 1989.

The discussion of lake level status presented in Chapter 3 illustrates the spatial patterns present in the data. As we have also seen, the data displays a considerable amount of fine-scale variability which may be partly due to errors in coding or interpretation. This chapter will further analyse the spatial patterns by quantifying the spatial dependence of the data by examining the spatial autocorrelation.

This chapter first describes spatial continuity in the original data using variogram and correlogram functions. Next, a geostatistical technique known as "local indicators of spatial autocorrelation" (LISA), will be used as an exploratory spatial data analysis (ESDA) tool. In essence, the results of LISA will be used to filter the data to include only the large-scale signal. This will permit the identification of large-scale patterns present in the data and used as an alternative to point-by-point error checking which is, in any case, impossible in large datasets. Then, using only sites that exhibit large-scale spatial autocorrelation, the spatial continuity will be re-examined using the variogram and correlogram functions. The autocorrelation will be examined using two approaches. First, the data will be examined for spatial continuity using the original ordinal scale under the assumption of a climate continuum. That is, we can assume that the transition from a region of high lake status to a low lake status region occurs through an intermediate lake status region. Next, the data will be

transformed to a binary vector under the assumption that the three lake statuses are mutually exclusive. The modelling of the spatial continuity presented in this chapter will enable estimation to proceed in Chapter 5.

4.1 Spatial Continuity Analysis

The spatial continuity analysis will emphasize the spatial extent or range of autocorrelation present in the data. The correlogram and the variogram functions describe the spatial continuity as a function of distance (Isaaks and Srivastava, 1989). The variogram is the traditional approach, however, the correlogram is equally useful and can be used to confirm the results obtained from the variogram.

Some of the terminology used to describe the important features of the variogram are as follows (from Isaaks and Srivastava, 1989):

RANGE: As the separation between pairs increase, the corresponding variogram value will also increase. Eventually, however, an increase in the separation distances no longer causes a increase in the average squared difference between pairs of values and the variogram reaches a plateau. The distance at which the variogram reaches this plateau is referred to as the range.

SILL: The plateau that the variogram reaches at the range is called the sill.

NUGGET EFFECT: Though the value of the variogram for H (distance) = 0 is strictly 0, several factors, such as sampling errors and short scale variability, may cause sample values separated by extremely small distances to be quite dissimilar and this leads to a discontinuity at the origin of the

variogram. The vertical jump from 0 is called the nugget effect. The *relative nugget effect* is the ratio of the nugget effect to the sill and is usually quoted in %.

There are two distance parameters that need to be chosen for spatial continuity analysis. One is the distance between successive separation distances or *lag spacing*; the other is the tolerance that we will allow on the distance or *lag tolerance*. With irregularly spaced data the average spacing between neighbouring samples can be used as the initial distance (Isaaks and Srivastava, 1989, Deutsch and Journel, 1992). The most common choice for lag tolerance is half the lag spacing (Isaaks and Srivastava,1989, Deutsch and Journel, 1992, Pannetier, 1994). Although this can result in some pairs not being used in the calculations, it can also make the variogram structure clearer (Isaaks and Srivastava, 1989).

The omnidirectional or isotropic variogram is the typical starting point in spatial continuity analysis where the directional tolerance is large enough such that the direction of any particular separation vector becomes unimportant (Isaaks and Srivastava, 1989). With all possible directions combined, only the magnitude of the distance vector is important. The omnidirectional variogram can be seen as the average of the various directional variograms (Deutsch and Journel, 1992, Isaaks and Srivastava, 1989). However, it does not imply that the spatial continuity is the same in all directions. Since direction does not play a role in the omnidirectional variogram, one can concentrate on finding the distance parameters that produce the clearest structure (Isaaks and Srivastava, 1989).

The omnidirectional variogram, because it contains more pairs, is more likely to show a clearly interpretable structure. "*If the omnidirectional variogram does not show a clear structure, one should not expect much success with the study under investigation. If it is messy, then one should try to find out the reasons for this erractiness. This may involve removing entirely certain samples from*

the dataset" (Isaaks and Srivastava, 1989). For example, removing the most erratic pairs from each particular lag may result in the loss of a significant number of samples, but can make the variogram structure clearer (Isaaks and Srivastava, 1989).

Another way to summarize spatial continuity is the correlogram. It is common to see the correlogram decrease with increasing distance. As described above, the variogram also summarizes spatial continuity where half of the average squared difference between the x and y coordinates of each pair of points is used. Unlike the correlogram, variogram values increase with distance.

These two statistics for summarizing spatial continuity are all sensitive to outliers (Isaaks and Srivastava, 1989) and this is true for any statistic. An outlier or influential point can have a significant impact on the correlation coefficient $\rho(H)$ and variogram value $\gamma(H)$, therefore the question of outliers must be dealt with. One approach is to remove outliers from the data. However, this is often arbitrary, as some values may have been representative of the spatial continuity of the phenomenon under investigation. Alternatively, the statistic can be estimated using all points, hoping that the underlying structure will still be appropriately estimated. Unfortunately, this may not be possible if the outlier data are too influential. In this chapter, we will describe the variogram fitting and how these problems were addressed.

This first section describes the spatial continuity of the lake-level status using all the data for the five different time periods under study. Anisotropy or the tendency for spatial correlation to favour a particular direction (ie. for example high lake status may favour a north-south direction) will not be explored. The reason for using an isotropic or omnidirectional approach is based on the global scale under study where different regional spatial anisotropies can co-exist. For example, high lake status

could favour a north-south direction in Europe while favouring an east-west direction in North America and therefore an anisotropic analysis is inappropriate at this scale.

Spatial continuity description

The following discussion is one example of the many attempts at describing the spatial continuity using all of the original data. A variogram and correlogram were fitted to the data using GS+ (Geostatistics for the Environmental Sciences, Professional Edition v. 3.10.2)

For 0 ka, the variogram displays a continuous increase in semivariance as separation distances increase with little fluctuation over a 5000 km active lag (Figure 4.1 a-i). The corresponding correlogram also confirms the spatial continuity in this dataset with values decreasing as separation distances increase (Figure 4.1 a-iii). However, there is fine-scale variability at lower lags with some sample pairs exhibiting high variance (Figure 4.1 a-iv,v,vi) thus resulting in a relatively high nugget effect. These variance cloud diagrams illustrate the contribution to the variance for each pair of sample sites for lags 1,2 and 3 as a function of distance. There can only be values of 0,1 and 4 (0, 1^2 and 2^2) due to the qualitative nature of the data. An exponential model fitted to the variogram yielded an r2 of 0.88 (Figure 4.1 a-ii).

At 3 ka, both the variogram and correlogram do not show clear structures which suggests no spatial autocorrelation (Figure 4.1 b-i,iii). These structures suggest that the data contains a high amount of fine-scale variability at lower lags. This is confirmed by the large number of sample pairs that exhibit high variance of 4 (Figure 4.1 b-iv,v,vi). These results also confirm the previous investigations of 3 ka, where lake-levels indicated an increase in fine-scale variability and/or potential errors. As expected, the exponential model fitted to the variogram is poor with an r2 of only

0.068 (Figure 4.1 b-ii).

For the lake-level data at 6 and 9 ka, the variograms reveals much the same results as 3 ka and suggest no spatial autocorrelation (Figures 4.1 c-i and 4.1 d-i). Again, the correlograms indicate that spatial continuity is more or less absent at these time periods (Figures 4.1 c-iii and 4.1 d-iii). There are large numbers of sample pairs exhibiting high variance at lower lags which contribute significantly to these results (Figures 4.1 c-iv,v,vi and 4.1 d-iv,v,vi). The exponential models fitted to the variograms confirm the fine-scale variability at lower lags with an r2 of 0.498 for 6 ka and an r2 of 0.02 at 9 ka (Figures 4.1 c-ii and 4.1d-ii).

Compared to 6 and 9 ka, the 12 ka variogram and correlogram (Figure 4.1 e-i,iii) show significant improvement in the lower lags, thus giving a clearer structure than the three previous time periods (Figure 4.1 e-v,vi,vii). In this case, the decrease in coverage reduced the number of pairs used for the calculations and can be one of the reasons for these results. The exponential model fitted to the variogram yielded an r2 of 0.75, thus confirming the improvement at the lower lags (Figure 4.1 e-ii).

In general, spatial continuity or autocorrelation is present at 0 ka and to a lesser extent at 12 ka. However, the periods of 3, 6 and 9 ka show no spatial autocorrelation at all lag distances investigated. The large number of sample pairs exhibiting high variance at the lower lags suggest a high ratio of fine-scale variability and/or potential errors present in these datasets. *One conclusion of this study is therefore that the lake-level data contain significant numbers of samples that may not necessarily reflect large-scale climate patterns.* This conclusion is reached by multiple evidence including the visual description, the investigation into error checking of Chapter 3, and the results of the spatial autocorrelation presentation of this section. It is therefore important, at this stage of the study, to separate sample sites that reflect large-scale patterns from samples that display fine-

scale variability and/or potential errors in coding. By doing so, it will enable the extraction of the large-scale patterns present in the data and allow for the statistical analysis to proceed.

4.2 Exploratory Spatial Data Analysis (ESDA)

If we hypothesize that only large-scale patterns are climatically meaningful, then a climatically-caused spatial scale can be objectively determined from the data. Spatial autocorrelation tests whether one site is independent of neighbouring localities. In general, if high values at one locality are associated with high values in their neighbours, it is positively spatially autocorrelated while if the values alternate from high to low in an area, it is negatively spatially autocorrelated (Sokal and Oden, 1978 a,b). In spatial data analysis, the dependence structure and heteroscedasticity must be taken into account, moreover, the effects of spatial scale must also be considered (Getis and Ord, 1992).

In exploratory spatial data analysis, the most common approach to assess the degree of spatial autocorrelation is Moran's I or Geary's C, which are global statistics. However, these approaches ignore the potential local areas of weakness or outliers in the data that may influence the global statistic (Anselin, 1995). Getis and Ord (1992) suggested that a more appropriate approach would be to focus on local patterns of spatial autocorrelation. In this study, local indicators of spatial autocorrelation (LISA) are used to investigate local spatial autocorrelation and to quantify the fine-scale variability and/or potential errors present in the lake-level data at different distances using the summary spatial statistics presented in section 3.4 of Chapter 3.

LISA (Anselin, 1995) decompose global indicators, such as the Moran's I, into the contribution of each individual observation. LISA has two important uses: the identification of local correlated

spatial patterns and, the identification of local areas which display fine-scale variability or outlier sample sites at specific distances (Anselin,1995).

In this thesis, LISA is used to optimize the spatial scale of this study. We need to maximize global coverage while also retaining maximum spatial resolution. This will result in identifying a consistent and globally homogeneous spatial scale of study. As a consequence, we will remove sample sites that do not reflect spatially correlated patterns below a certain threshold identified by LISA. Sample sites exhibiting negative spatial autocorrelation can thus be objectively eliminated. This will result in more clearly interpretable variograms, retain the original structures of the variograms and allow the modelling of the variograms.

This approach to data-cleaning is used in this thesis in preference to alternative ones. First, error checking of all individual data in the database can be a very long and complicated task. Reviewing the literature may prove to be futile as the results are frequently ambiguous or subjective, or necessary information may not be available. Even after reviewing the original literature, scattered over many journals and several languages, it may not be clear if a sample is poorly coded. Another method is to arbitrarily remove outlier samples from each lag (Isaaks and Srivastava, 1989). It should also be noted that previous users of the lake data have also removed samples, for example, by including only sites with continuous records (Harrison, 1989, Harrison et *al.*, 1993), quality ^{14}C dating control schemes (Guiot *et al.*, 1993; Harrison *et al.*, 1993; Cheddadi *et al.*, 1997 and Qin *et al.*, 1998) and qualitative exclusion (Street-Perrott and Harrison, 1984, Harrison and Metcalfe 1985 a,b). These resulted in analyses using only a fraction of the sites. This study differs only in that the exclusion is done objectively by deciding on the scale of study.

LISA Results

The methodology for maximizing global coverage while retaining maximum resolution consists of the calculation of local spatial autocorrelation (Moran's I) within different search radii distances of each sample site in the five time period datasets. The investigation into the extent of fine-scale variability and/or potential errors in coding present in the lake data will be analysed using the summary inter-site distance statistics of Chapter 3, section 3.4. This will enable the investigation over different search distances for all time periods. Tables 4.1 to 4.5 illustrate the results of the LISA analysis for all time periods expressed as a percentage of the overall number of available sites that exhibit positive and negative spatial autocorrelation at specific lag distances. In addition, the percentage of sites without neighbours means that LISA cannot be measured due to lack of neighbouring samples. This is used as an indicator of achieving maximum world coverage in order to objectively identify the spatial-scale of study.

The LISA statistics indicate maximum geographical coverage can be obtained at 500 km distances with less than 10 % of sites left with no neighbours in all time frames except for 12 ka (14.1%) (Tables 4.1 - 4.5). In this study, the 500 km distance was chosen as the maximum resolution because the ratio between negative and positive spatial autocorrelation increases with distance. With this distance, most time periods show less than 10% of sites with no neighbours.

The ratio between positive and negative spatial autocorrelation is high for most time periods and at all lag distances examined. These results provide further evidence of the conclusion of the previous section in which large amounts of samples exhibited fine-scale variability, especially at lower lag distances.

Lag distance (km)	Positive spatial autocorrelation (%)	Sites with no neighbours (%)	Negative spatial autocorrelation (%)
5	3.9	95.7	0.4
10	8.6	89.9	1.5
25	18.3	77.9	3.7
33	21.1	74.8	4.1
76	42.1	49.9	8.0
150	57.9	31.0	11.0
200	65.8	21.5	12.7
300	73.5	12.5	14.0
400	79.1	6.2	14.8
500	80.6	3.9	15.5

Table 4.1: Summary of local indicators of spatial autocorrelation at present (535 sites).

The present-day lake-level data (Table 4.1) shows positive spatial autocorrelation occurring at 81 % of the sites at 500 km distances. However, we notice that even at small distances, such as 5 km, there are some sites that exhibit finer-scale variability between their coded attributes. Although 15.5 % of sites exhibit negative spatial autocorrelation at 500 km distances, and are excluded from this study, overall good coverage of the world is achieved (Figure 4.2 a).

Lag distance (km)	Positive spatial autocorrelation (%)	Sites with no neighbours (%)	Negative spatial autocorrelation (%)
5	3.3	95.6	1.1
10	5.7	90.7	3.6
29	16.4	74.9	8.7
90	27.6	50.0	22.4
179	39.6	30.9	29.5
213	44.3	24.6	31.1
300	49.2	15.8	35.0
400	51.6	9.8	38.5
500	53.3	6.8	39.9

Table 4.2 : Summary of local indicators of spatial autocorrelation at 3 ka (366 sites).

At 3 ka, the lake-level data reveals positive spatial autocorrelation between lake sites at 500 km distances at 53 % of the sites while negative spatial autocorrelation occurs at 40 % of the sites (Table 4.2). These results confirm previous findings in Chapter 3 and the last section that this time period contains a significant amount of fine-scale variability and/or potential errors in coding. Indeed, negative spatial autocorrrelation is evident at all lag distances in a much higher ratio than at present. Even though almost 40 % of sites are problematic at 500 km distances, and dismissed from this study, overall good coverage of the world remains (Figure 4.2 a).

Lag distance (km)	Positive spatial autocorrelation (%)	Sites with no neighbours (%)	Negative spatial autocorrelation (%)
5	2.7	95.7	1.6
10	6.4	90.1	3.5
27	17.9	74.7	7.5
81	33.6	49.9	16.5
176	44.5	30.4	25.1
213	46.4	25.6	28.0
300	52.8	16.5	30.7
400	57.9	9.9	32.3
500	60.0	6.9	33.1

Table 4.3 : Summary of local indicators of spatial autocorrelation at 6 ka (375 sites).

Lake level data at 6 ka shows an increase in positive spatial autocorrelation with 60 % of lake sites exhibiting positive spatial autocorrelation at 500 km distances (Table 4.3). Negative spatial autocorrelation is present at all lag distances studied, inferring once again finer-scale variability and/or potential errors present at all lag distances. With 33 % of sites exhibiting negative spatial autocorrelation at 500 km distances, and excluded, a relatively good geographical coverage of the world remains (Figure 4.2 a).

An increase in negative spatial autocorrelation (41.8 %) is evident at 500 km distances for the period of 9 ka (Table 4.4). As was also seen above, there is considerable variability in this dataset. More than 50 % of sites exhibit positive spatial autocorrelation at 500 km distances and these sites are sufficient for a good geographical coverage of the world for 9 ka (Figure 4.2 b).

Lag distance (km)	Positive spatial autocorrelation (%)	Sites with no neighbours (%)	Negative spatial autocorrelation(%)
5	3.0	96.3	0.6
10	5.2	91.8	3.0
34	16.2	74.4	9.5
93	28.4	49.7	22.0
200	37.5	27.1	35.4
300	44.2	17.4	38.4
400	50.0	11.6	38.4
500	50.3	7.9	41.8

Table 4.4 : Summary of local indicators of spatial autocorrelation at 9 ka (328 sites).

The lake-level data at 12 ka is characterized by an improvement in the ratio between positive and negative spatial autocorrelation at small distances (Table 4.5). Moreover, none of the sites at 5 and 10 km distances exhibit negative spatial autocorrelation which confirms the results of the previous section displaying a clearer structure at lower lags. However, this time frame contains fewer sites than other time periods, and hence the number of negatively correlated sites, as seen in the last section. At 500 km distances, 50 % of sites exhibit positive spatial autocorrelation, while nearly 36 % show negative spatial autocorrelation. Although 36 % of sites are excluded from this study, major clusters of spatially correlated lake sites are left at 12 ka giving possible insight into the global hydrological cycle for 12 ka (Figure 4.2 b).

Lag distance (km)	Positive spatial autocorrelation (%)	Sites with no neighbours (%)	Negative spatial autocorrelation (%)
5	2.9	97.1	0.0
10	5.3	94.7	0.0
67	17.1	74.7	8.2
162	31.8	50.0	18.2
200	34.1	43.5	22.4
300	47.1	32.4	20.6
400	50.0	20.6	29.4
500	50.0	14.1	35.9

Table 4.5 : Summary of local indicators of spatial autocorrelation at 12 ka (170 sites).

In this study, 500 km was chosen as the spatial-scale of study in order to maximize world geographical coverage, maximize spatial resolution, investigate large-scale patterns present in the lake-level datasets and enable the spatial modelling of the patterns. However, this approach is an alternative, and more properly used in conjunction with a detailed analysis of the data. It is not a substitute to error checking and fine-scale variability analysis, where some sites may have been excluded without investigation into their validity (Appendix E). *Another conclusion of this study is that the data needs further spatial and temporal analysis by returning to the original lake-level data by examining the spatial and temporal correlation on a site-by-site basis, especially at small distances.* It is interesting to note that the application of the LISA technique identified Lac de Chalain and Lac Paladru at 3 ka as negatively autocorrelated, as was determined above. The approach illustrated here can be applied to any area of study in order to maximize spatial resolution and geographical coverage when dealing with large datasets. The next section will re-examine the spatial continuity using the lake-level data after ESDA.

Spatial continuity analysis (original coding)

The assumption underlying the spatial continuity analysis using the original coding is that climate is continuous. The transition of a region of high lake level status to a low lake level status region occurs through a transitional or intermediate status region.

For 0 ka, the variogram shows a smooth curve with few fluctuations over a 5000 km active lag (Figure 4.3 a). As expected, the variogram displays a continuous increase in semivariance as separation distances increase. The corresponding correlogram also confirms the spatial continuity in this dataset with values decreasing as separation distances increase. It is important to notice that the initial variogram structure was retained from the original data (see Figure 4.1 a-i), the only difference being a lowered nugget effect caused by removing negatively correlated data below the 500 km threshold.

At 3, 6 and 9 ka, the variograms are now more clearly interpretable. The variograms and correlograms indicate spatial continuity, especially in lower lag distances (Figure 4.3 b,c,d). The ESDA exercise was successful in making the variograms and correlograms structures much clearer and interpretable (see Figures 4.1 b-i,iii, c-i,iii, d-i,iii). However, the range of spatial continuity is much smaller than at 0 ka. This confirms previous investigations for these time periods where lake-levels exhibited more variability and that this spatial feature remains intact after the ESDA exercise.

At 12 ka, the variogram and correlogram do not reveal generally clear structures (Figure 4.3 e). As expected, the decrease in the number of pairs of data and clusters that remain in the data coverage after ESDA are the main reasons for these results. However, as in the case of the previous time periods, the initial spatial structure was retained (see Figure 4.1 e-l). Nonetheless, this does not

mean that it cannot be modelled with some success.

In summary, spatial continuity is present for all time periods under study using the data after ESDA. The variograms of 3, 6 and 9 ka now show clearer interpretable structures suggesting that the identification of fine-scale variability and/or potential errors in coding was to a certain degree successful. In spite of different ranges of spatial continuity present and at different lag distances, the variogram results will enable spatial modelling to proceed. It is important to notice that the original spatial structures were retained from the original data, especially for 0 and 12 ka (see figures 4.1 a,e), thus suggesting that the data-cleaning exercise kept the initial spatial features present in the data, while permitting the estimation of the correlation structures.

Spatial continuity analysis (indicators)

In this section, the data are assumed to be spatial categorical with mutually exclusive classes, where one lake status region is independent of other regions. This requires that the data be transformed into binary indicators of presence and absence (Deutsch and Journel, 1992; Goovearts, 1997). Since the data has three mutually exclusive values, a vector of three indicator variables (High, Intermediate and Low) was constructed for each observation (Deutsch and Journel, 1992; Goovearts, pers. comm.) where 1 was given to the category of the sample sites and 0 was given to the other categories (ie: in the case of a high lake status, the vector was coded (1,0,0)). After transformation of the data (Appendix F), each lake status category was fitted with a model that capture the spatial continuity proper to each of the categories independently.

For 0 ka, spatial continuity is present in all three lake status categories (Figure 4.4 a). Although high and intermediate status present spatial continuity over smaller ranges than does the low status, this

is due in part to the overwhelmingly homogenous low lake status area over Africa. Nonetheless, all three indicators variograms do not reveal major structural flaws, where the semivariance increases with distance with no major fluctuations.

The variograms at 3 ka also reveal spatial continuity (Figure 4.4 b). However, spatial continuity for the high lake status was established with a 1000 km lag distance which suggests isolated local patterns of this status separated by long distances. The intermediate and low status variograms exhibit spatial continuity at much smaller lag distances (200 km). In spite of the differences in lag distances and ranges between the three lake status variograms, the spatial continuity proper to each lake status is present.

The three lake status indicator variograms for 6 ka reveal relatively acceptable spatial continuity (Figure 4.4 c). The low lake status variogram has a greater lag distance than the intermediate and high lake status variograms. However, all three indicator variograms reveal clear structures. At 9 ka, the three lake status indicator variograms again reveal spatial continuity at different lag distances (Figure 4.4 d). The intermediate lake status variogram shows spatial continuity at very small distances (50 km) over an active lag of 500 km. In spite of these differences, spatial continuity is present and clear enough for modelling each of the lake status independently.

For the 12 ka period, the indicator variograms for the three lake status categories reveal some fluctuations in their structures (Figure 4.4 e). As in the case of the variogram description under the first assumption, the resulting indicator variograms are due in part by a significant decrease in the number of pairs of data and by the clustering of the data.

In summary, spatial continuity was found in all lake categories for all time periods. Each lake status category reveals a variogram structure that captures its independent spatial features inherent in the data. These results enable the modelling of the variograms under both assumptions.

4.3 Modelling Spatial Continuity

Although the sample variograms provide a descriptive summary of the spatial continuity present in the datasets, these will probably not provide all the variogram values needed by the interpolation or estimation process (Isaaks and Srivastava, 1989). To interpolate requires a variogram value for any possible separation vector (Isaaks and Srivastava, 1989).

There are numerous models available for spatial modelling and this thesis will limit itself to describing the four most commonly used in modelling. The spherical model is the most commonly used. It has a linear behaviour at small distances but flattens out at larger distances as it reaches the sill. The exponential model reaches the sill asymptotically, however it rises more steeply and then flattens out more gradually. The Gaussian model is a transitional model used to model very continuous data. Like the exponential model, it reaches the sill asymptotically, but has a parabolic behaviour near the origin. The linear model does not reach a sill, but increases linearly with distance (Isaaks and Srivastava,1989, Deutsch and Journel, 1992, Pannetier, 1996).

This section presents the models that best fit the variograms. Three statistics aid in the interpretation of the model output. The first statistic is C/(Co+C) which provides a measure of the proportion of sample variance (Co+C) that is explained by spatially structured variance C. Next a regression coefficient (r2) provides an indication of how well the model fits the variogram data. However, this value is not as robust as the RSS or reduced sum of squares which provides an exact

measure of how well the model fits the data. The lower the reduced sum of squares (RSS), the better the model fits. Emphasis was given to the greatest range of autocorrelation in cases where two models gave similar results.

Modelling spatial continuity (original coding)

A spherical model was chosen for the 0 ka variogram based on the best fit statistics (r2 = 0.93; RSS = 0.15) (Figure 4.5 a). The model contains a nugget effect of 0.01 and reaches its sill at 0.81 while exhibiting an 4890 km range. The proportion of sample variance (Co+C) that is explained by spatially structured variance C is quite high at 0.99. As expected, 0 ka shows high spatial autocorrelation.

The spherical model imposed to the 3 ka variogram also shows the best fit of the 4 potential models (Figure 4.5 b). There is a significant decrease in range (1536 km) compared to 0 ka which confirms previous analyses of increased variability at 3 ka. Although the variogram of 6 ka is more variable, the spherical model again shows the best fit (Figure 4.5 c). The range of spatial autocorrelation shows a further decrease in range to 1007 km. However, the nugget effect is very low at 0.03.

A spherical model was also chosen for the 9 ka variogram where the best-fit statistics reveal an r2 of 0.93 and RSS of 0.01 (Figure 4.5 d). Note that the range (828 km) of spatial continuity reflects the higher variability at 9 ka as indicated previously. Although the variogram for 12 ka is more variable, due in part to the reduction in the data coverage, acceptable results are obtained using an exponential model (Figure 4.5 e). The statistics show an r2 of 0.66 and an RSS of 0.22. The fact that no nugget effect is registered confirms the observations made in the previous sections where all sites exhibit positive spatial autocorrelation over small distances. In addition, no nugget effect

means an exact interpolation which, will be discussed in Chapter 5. The model reveals a range of 2196 km where this increase can be interpreted as spatial continuity between the remaining clusters.

In summary, models could be fitted to the variograms for all time periods with r2' s above 0.80 and RSS's below zero. Although the poorest result is for the 12 ka period, it is still an acceptable result. Finally, the range of spatial continuity decreases in time, except for 12 ka, where it reflects the decrease in spatial coverage.

Modelling spatial continuity (indicators)

The models fitted to the three lake status categories at 0 ka show generally good results (Figure 4.6 a). Although the high and intermediate lake status categories were fitted with an exponential model, the range of spatial continuity differ somewhat between these two. The best-fit to the low lake status variogram was a spherical model and reveal a range of 5500 km. This is due to the overwhelmingly low lake status area over North Africa.

Although the high lake status of 3 ka is somewhat problematic, it was possible to fit a model to all three lake status variograms with success (Figure 4.6 b). The high lake status variogram was fitted with an spherical model having a range of 833 km. Basically, a linear model could have served equally given the problematic nature of the high lake status. Although different models are used to fit the variograms at 3 ka, this has the advantage of extracting the spatial features inherent in each lake status independently.

At 6 ka, overall acceptable results are achieved for all three lake status variograms (Figure 4.6 c). The high and intermediate lake status variograms show a best-fit with a spherical model with a similar range of spatial continuity. However, the best-fit for the low lake status variogram was an exponential model which yielded the poorest results (r2 = 0.661 and RSS = 0.0002). The range of the low lake status model has decrease to 555 km.

Although the model fitted to the intermediate lake status variogram shows poorer fit than the others at 9 ka, it was possible to fit models to the three lake status variograms (Figure 4.6 d). A spherical model was found to be the best-fit for the high lake status variogram. The model shows a range of 930 km. The intermediate lake status variogram was fitted with an exponential model since the variogram exhibits a steep increase at the origin which can be interpreted as low spatial continuity for this lake status. Indeed, the fitted model is for a 500 km active lag only. However, the model shows an r2 of 0.52 and RSS of 0.002. An exponential model was also found to be the best-fit for the low lake status variogram associated with a range of 1161 km. The decreasing ranges confirm the previous findings that 9 ka is a more variable time period.

Although the 12 ka lake status variograms are more variable, models were fitted to the three lake status categories (Figure 4.6 e). A spherical model showed the best-fit results for the high and intermediate lake status variograms with ranges of spatial continuity of 1640 km and 2052 km respectively. A spherical model was also found to be the best-fit for the low lake status variogram with a range of 3920 km. In spite of the variability in the variograms at 12 ka, overall acceptable results were obtained in modelling the underlying spatial features of all three lake status variograms.

In summary, the fitted models of the three lake status categories reveal generally good-fits for all time periods and enables the estimation process to proceed. These models were imposed on the

transformed data in order to model each lake status independently. The advantages of this approach lies in capturing the spatial features inherent in each lake status category independently. This will have an impact on how the weights are distributed during estimation. Moreover, some of the models fitted showed small spatial continuity ranges where this too will impact the distribution of weight during estimation.

Finally, the results of both approaches reveal that spatial continuity present in the data for all time periods can be modelled with some success. In spite of different models used under both approaches, the estimation process is safe to proceed objectively in order to grid the regional lake-level pattern at the global scale. The next chapter deals with estimation where these models will be used to estimate unsampled locations objectively.

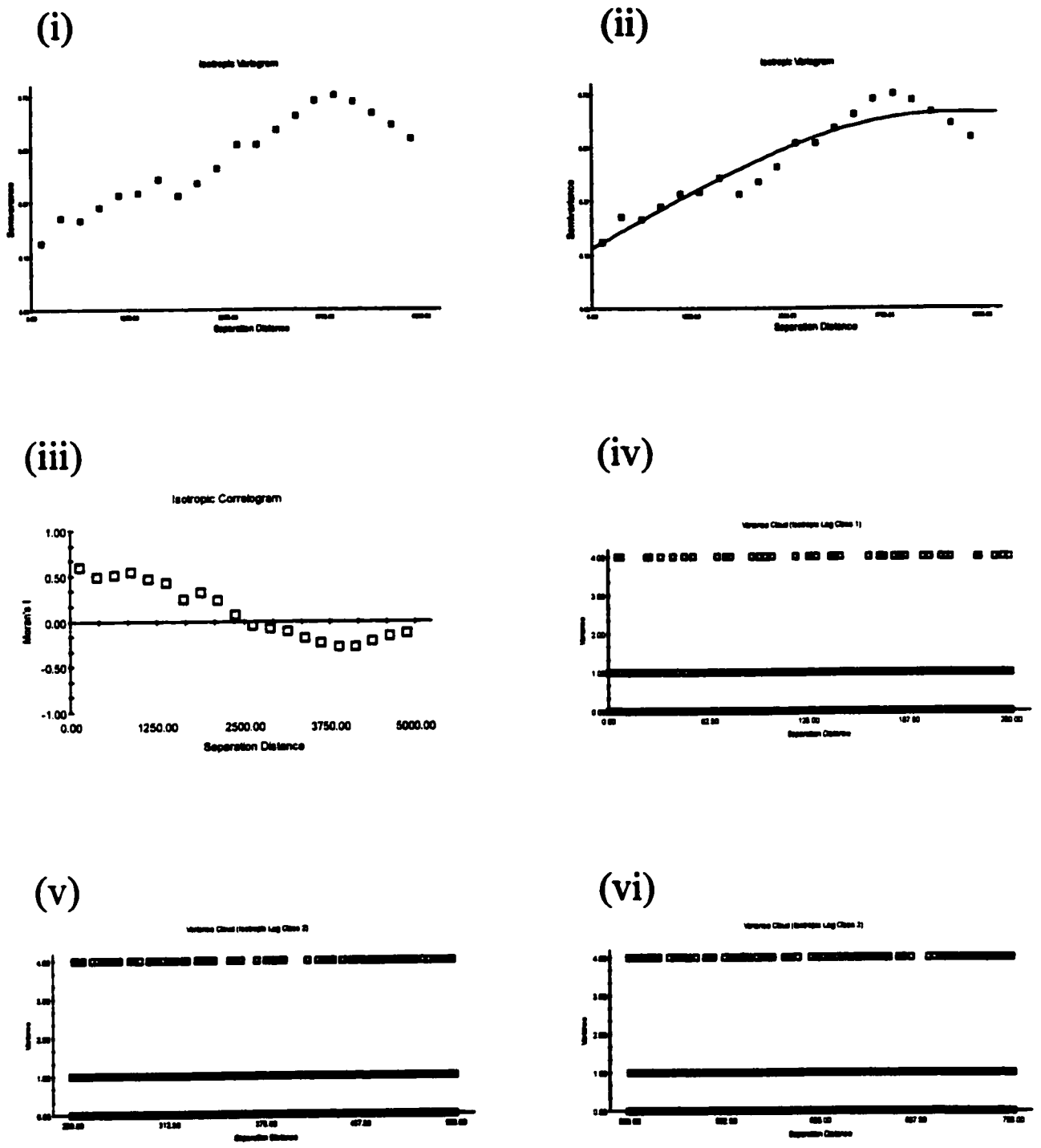

Figure 4.1 a: Summary spatial continuity analysis for 0 ka.

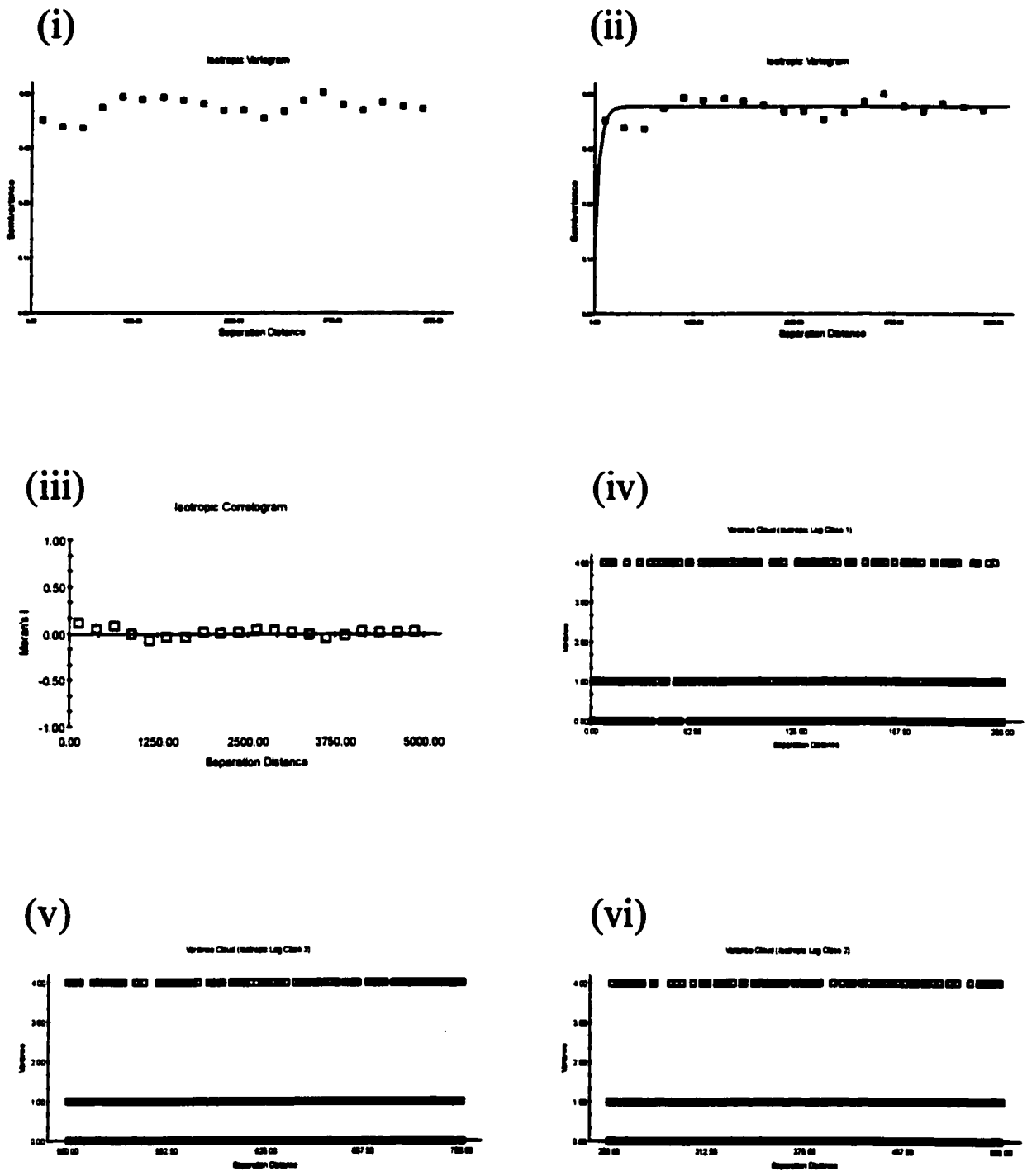

Figure 4.1 b: Summary spatial continuity analysis for 3 ka.

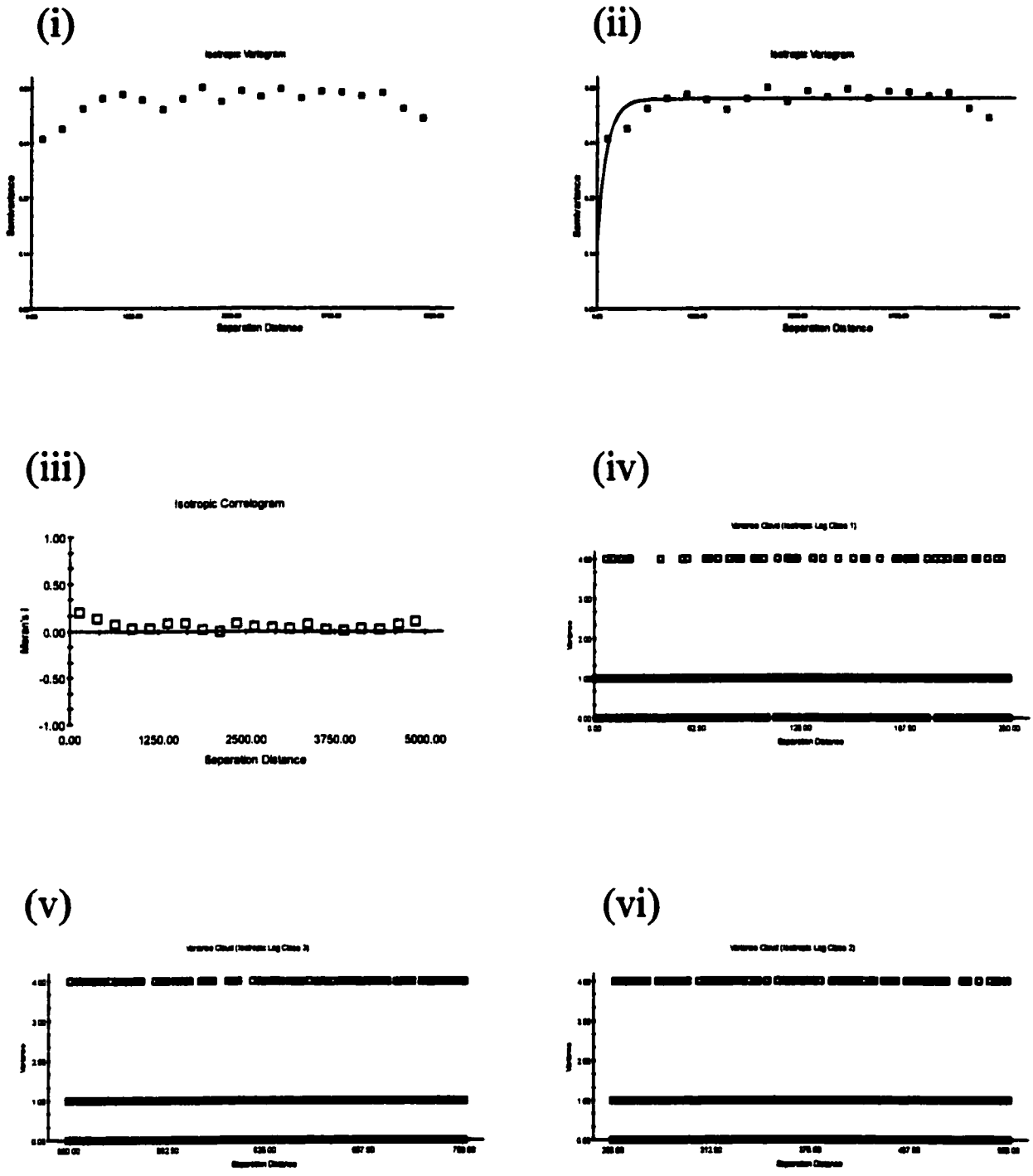

Figure 4.1 c: Summary spatial continuity analysis for 6 ka.

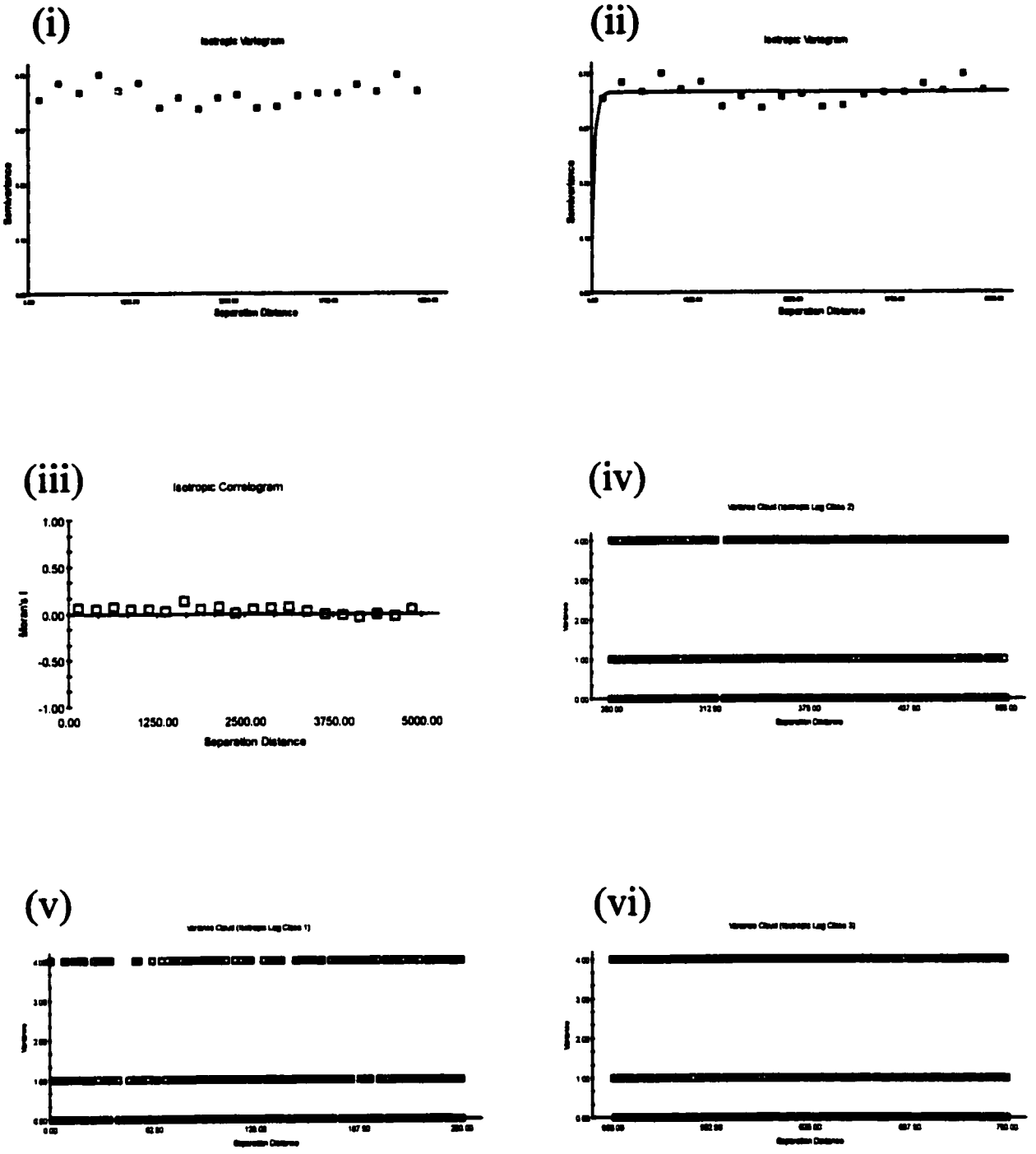

Figure 4.1 d: Summary spatial continuity analysis for 9 ka.

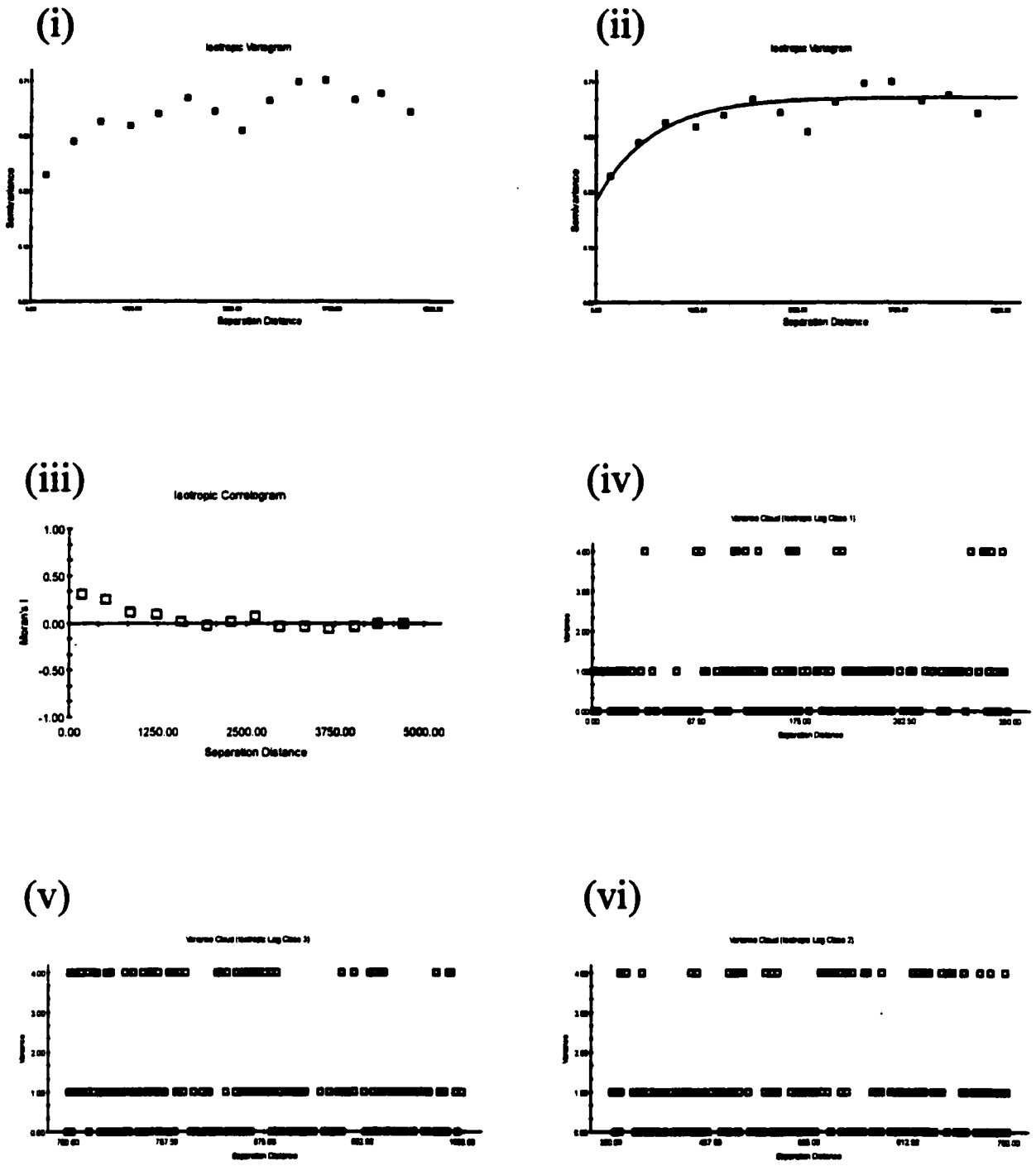

Figure 4.1 e: Summary spatial continuity analysis for 12 ka.

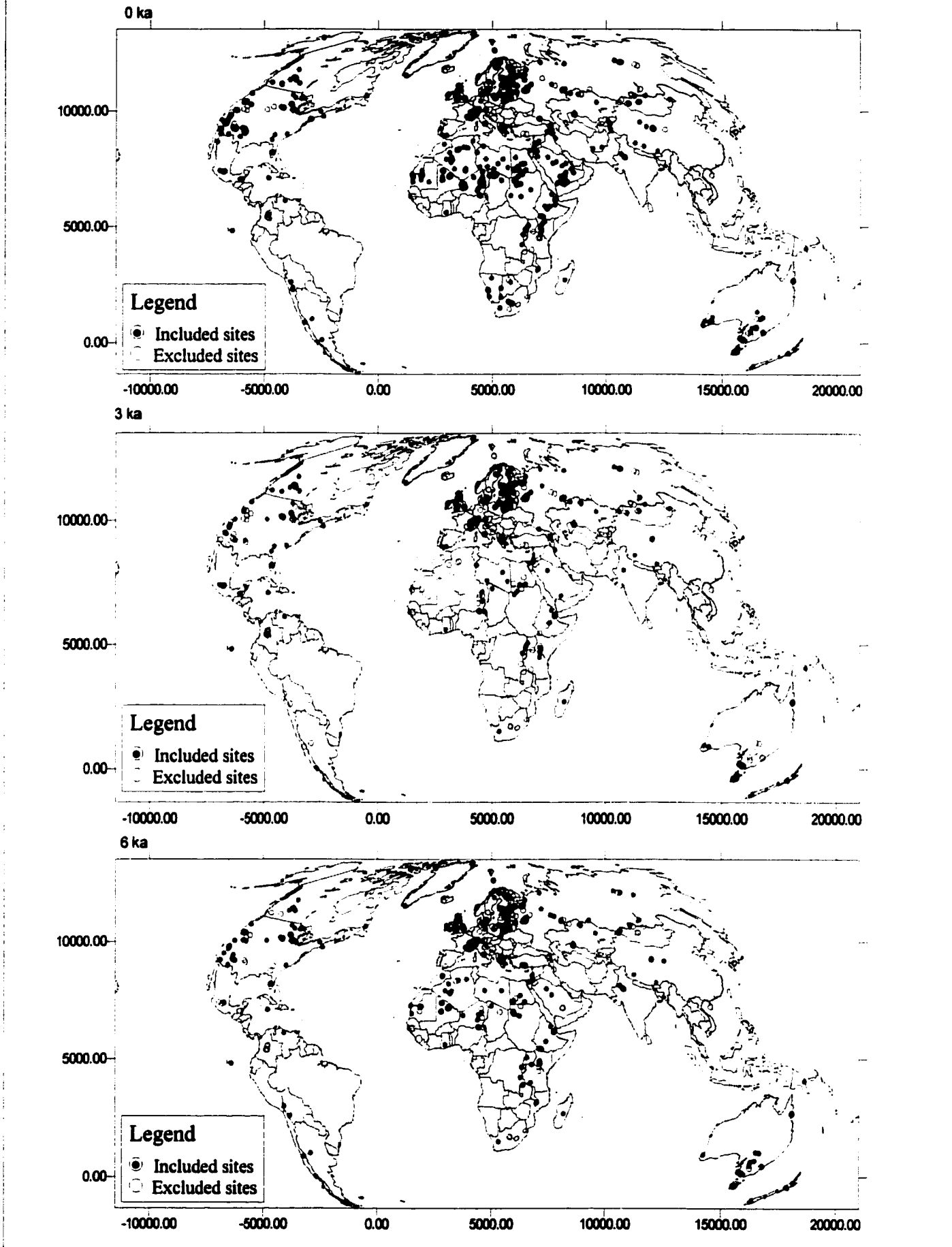

Figure 4.2 a: Maps showing the distribution of included sites and excluded sites after ESDA for 0 ka, 3 ka and 6 ka.

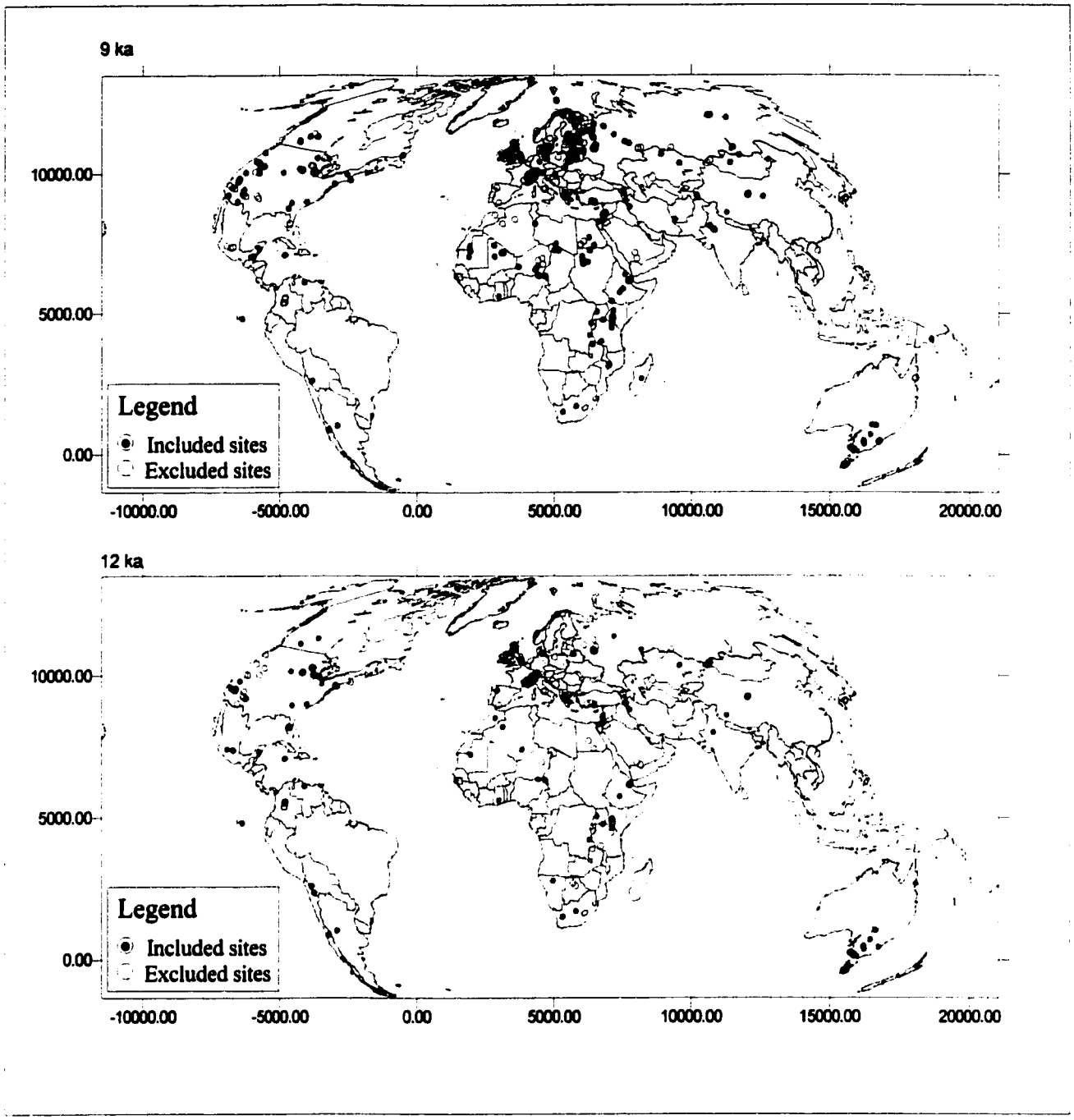

Figure 4.2 b: Maps showing the distribution of included and excluded sites after ESDA for 9 ka and 12 ka.

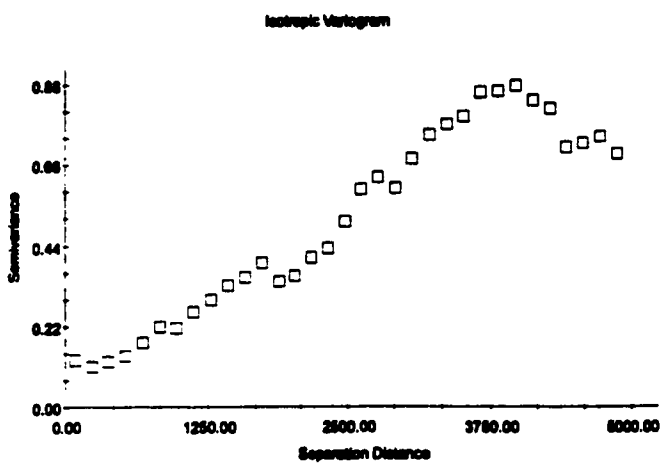

Lake Status - present (Semivariance Data for Status)			
Lag Class	Average Distance	Average Semivariance	Pairs
1	78.61	0.13	494
2	228.49	0.11	570
3	378.09	0.13	735
4	526.16	0.14	740
5	677.33	0.16	978
6	825.32	0.22	1040
7	972.69	0.21	1149
8	1125.94	0.26	979
9	1276.52	0.29	1189
10	1434.16	0.33	1110
11	1578.64	0.38	1082
12	1728.31	0.4	1176
13	1878.68	0.34	1332
14	2024.37	0.38	1339
15	2175.33	0.41	1347
16	2323.28	0.43	1249
17	2473.85	0.51	1199
18	2623.1	0.5	1250
19	2775.03	0.63	1297
20	2928.88	0.6	1370
21	3078.08	0.66	1427
22	3224.34	0.74	1400
23	3377.44	0.77	1432
24	3523.13	0.8	1426
25	3675.17	0.88	1430
26	3824.08	0.88	1387
27	3974.89	0.89	1703
28	4124.82	0.84	1669
29	4275.89	0.82	1613
30	4422.44	0.71	1566
31	4576.16	0.72	1551
32	4726.05	0.74	1497
33	4875.41	0.7	1567

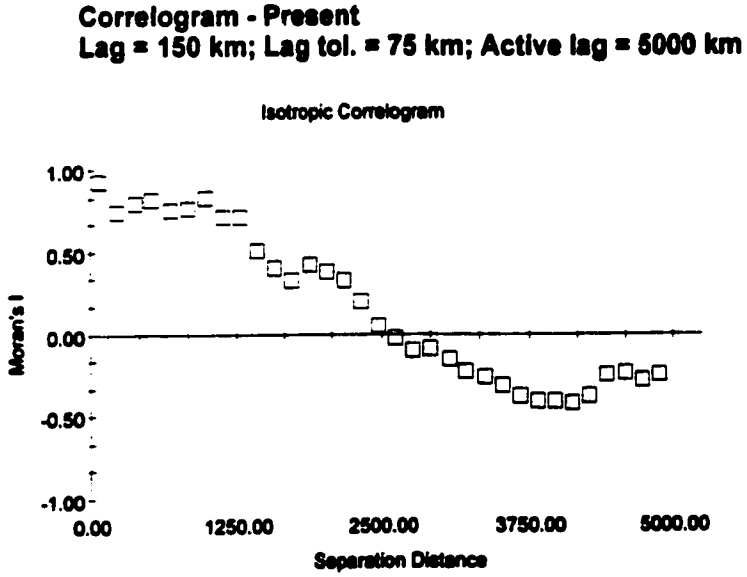

Lake status - present (correlogram)			
Lag Class	Average Distance	Moran's I	Pairs
1	78.61	0.93	494
2	228.49	0.74	570
3	378.09	0.6	735
4	526.16	0.62	740
5	677.33	0.76	978
6	825.32	0.78	1040
7	972.69	0.83	1149
8	1125.94	0.71	979
9	1276.52	0.72	1189
10	1434.16	0.51	1110
11	1578.64	0.4	1082
12	1728.31	0.32	1176
13	1878.68	0.42	1332
14	2024.37	0.38	1339
15	2175.33	0.32	1347
16	2323.28	0.19	1249
17	2473.85	0.05	1199
18	2623.1	-0.03	1250
19	2775.03	-0.11	1297
20	2928.88	-0.09	1370
21	3078.08	-0.15	1427
22	3224.34	-0.23	1400
23	3377.44	-0.27	1432
24	3523.13	-0.31	1426
25	3675.17	-0.36	1430
26	3824.08	-0.41	1387
27	3974.89	-0.41	1703
28	4124.82	-0.42	1669
29	4275.89	-0.36	1613
30	4422.44	-0.25	1566
31	4576.16	-0.24	1551
32	4726.05	-0.28	1497
33	4875.41	-0.25	1567

Figure 4.3 a: Spatial continuity description at present.

Variogram - 3 ka
Lag 150 km; Lag tol. = 75 km; Active lag = 2000 km

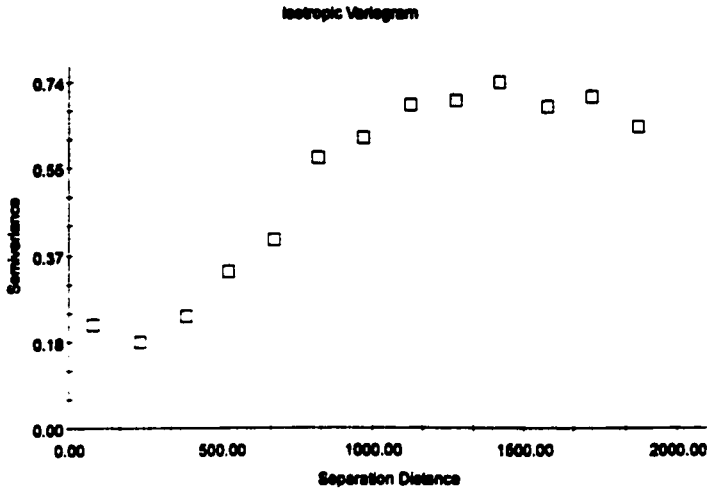

Lake Status - 3 ka (Semivariance Data for Status)			
Lag Class	Average Distance	Average Semivariance	Pairs
1	78.33	0.22	161
2	234.65	0.18	199
3	383	0.24	232
4	525.79	0.33	258
5	676.97	0.4	332
6	822.43	0.57	288
7	974.39	0.62	335
8	1128.97	0.69	316
9	1275.62	0.7	353
10	1421.28	0.74	339
11	1578.97	0.69	294
12	1728.35	0.71	348
13	1873.28	0.64	360

Correlogram - 3 ka
Lag = 150 km; Lag tol. = 75 km; Active lag = 2000 km

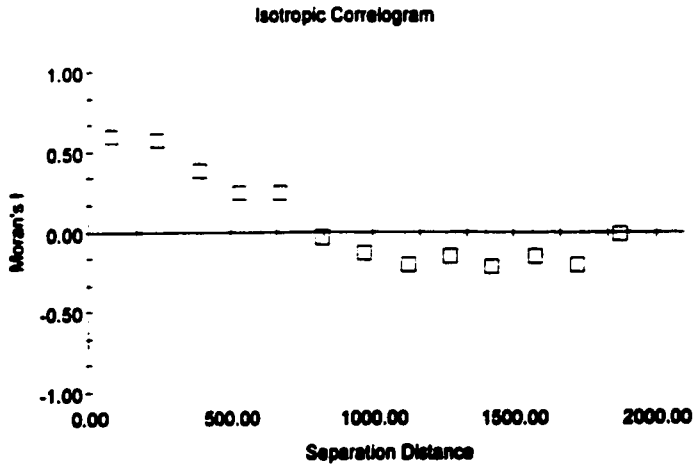

Lake Status - 3 ka (correlogram)			
Lag Class	Average Distance	Moran's I	Pairs
1	78.33	0.6	161
2	234.65	0.58	199
3	383	0.38	232
4	525.79	0.24	258
5	676.97	0.24	332
6	822.43	-0.04	288
7	974.39	-0.14	335
8	1128.97	-0.21	316
9	1275.62	-0.16	353
10	1421.28	-0.22	339
11	1578.97	-0.15	294
12	1728.35	-0.21	348
13	1873.28	-0.02	360

Figure 4.3 b: Spatial continuity description at 3 ka.

Variogram - 6 ka
Lag = 175, Lag tol. = 87.5; Active lag = 2000 km

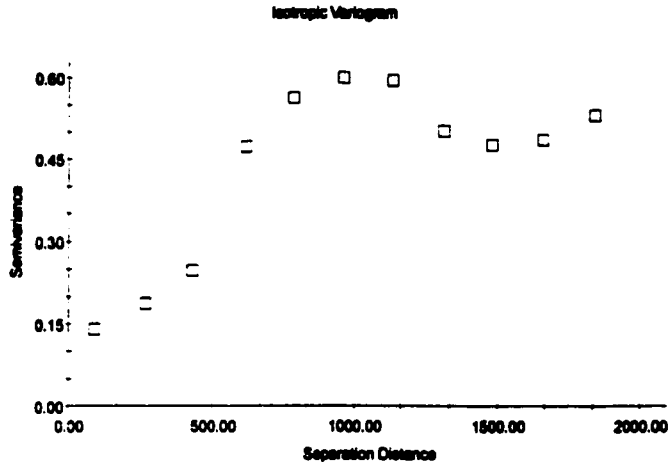

Lake Status - 6 ka (Semivariance Data for Status)			
Lag Class	Average Distance	Average Semivariance	Pairs
1	86.96	0.14	222
2	266.96	0.19	237
3	431.71	0.24	330
4	616.17	0.47	346
5	784.07	0.56	460
6	962	0.6	502
7	1136.67	0.59	479
8	1316.54	0.5	455
9	1481.19	0.48	403
10	1662.26	0.49	482
11	1840.86	0.53	501

Correlogram - 6 ka
Lag = 175 km; Lag tol. = 87.5 km; Active lag = 2000 km

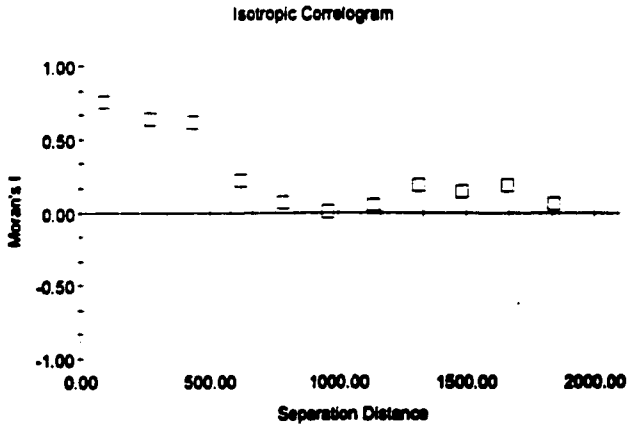

Lake Status - 6 ka (correlogram)			
Lag Class	Average Distance	Moran's I	Pairs
1	86.96	0.75	222
2	266.96	0.64	237
3	431.71	0.61	330
4	616.17	0.22	346
5	784.07	0.07	460
6	962	0	502
7	1136.67	0.05	479
8	1316.54	0.18	455
9	1481.19	0.15	403
10	1662.26	0.19	482
11	1840.86	0.06	501

Figure 4.3 c: Spatial continuity description at 6 ka.

Variogram - 9 ka
Lag = 200 km; Lag tol. = 100 km; Active lag = 1600 km

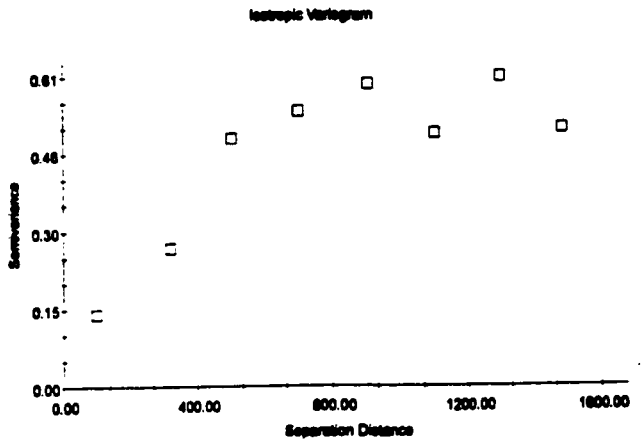

Lake Staus - 9 ka (Semivariance Data for Status)			
Lag Class	Average Distance	Average Semivariance	Pairs
1	97.43	0.14	123
2	316.73	0.27	144
3	503.77	0.49	193
4	703.05	0.54	199
5	906.3	0.59	288
6	1099.68	0.5	272
7	1296.22	0.61	255
8	1484.52	0.51	222

Correlogram - 9 ka
Lag = 200 km; Lag tol. = 100 km; Active lag = 1600 km

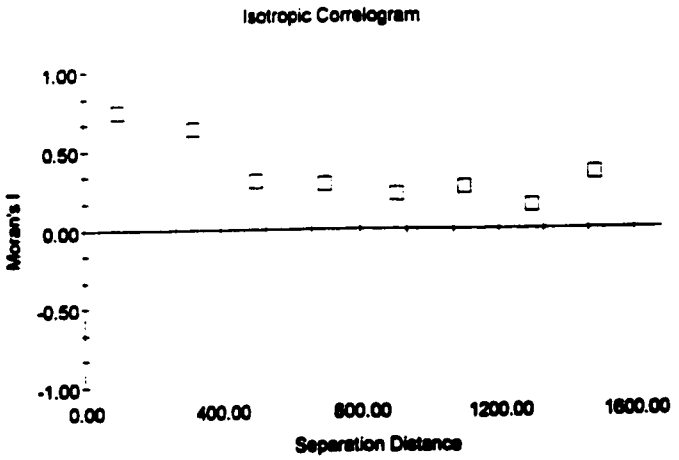

Lake Status - 9 ka (correlogram)			
Lag Class	Average Distance	Moran's I	Pairs
1	97.43	0.74	123
2	316.73	0.63	144
3	503.77	0.31	193
4	703.05	0.29	199
5	906.3	0.22	288
6	1099.68	0.26	272
7	1296.22	0.14	255
8	1484.52	0.35	222

Figure 4.3 d: Spatial continuity description at 9 ka.

Variogram - 12 ka
Lag = 250 km; Lag tol. = 125 km; Active lag = 2500 km

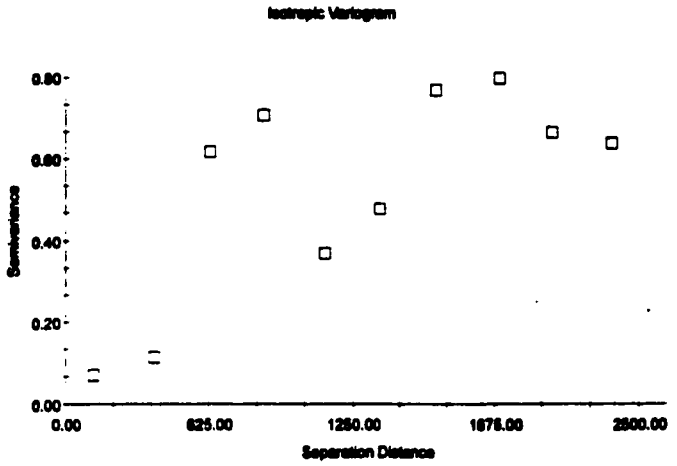

Lake Status - 12 ka (Semivariance Data for Status)			
Lag Class	Average Distance	Average Semivariance	Pairs
1	122.45	0.07	64
2	384.85	0.11	61
3	628.7	0.62	67
4	884.4	0.71	66
5	1128.93	0.37	81
6	1385.42	0.48	73
7	1616.89	0.77	64
8	1888.94	0.8	79
9	2130.6	0.67	91
10	2388.11	0.64	121

Correlogram - 12 ka
Lag = 250 km; Lag tol. 125 km; Active lag = 2500 km

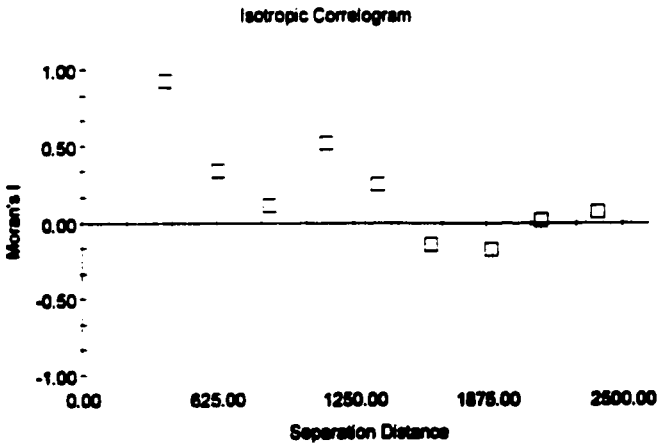

Lake Status - 12 ka (correlogram)			
Lag Class	Average Distance	Moran's I	Pairs
1	122.45	1.02	64
2	384.85	0.92	61
3	628.7	0.34	67
4	884.4	0.11	66
5	1128.93	0.52	81
6	1385.42	0.25	73
7	1616.89	-0.15	64
8	1888.94	-0.18	79
9	2130.6	0.02	91
10	2388.11	0.07	121

Figure 4.3 e: Spatial continuity description at 12 ka.

Variogram - High Status - Present
Lag = 150km; Lag tol. = 75 km; Active lag = 1500 km

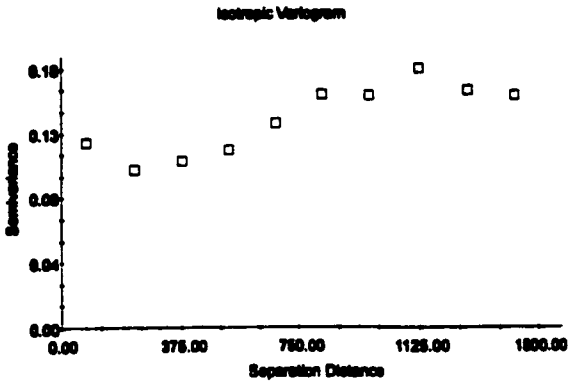

Lake Status - Present (Semivariance Data for High)			
Lag Class	Average Distance	Average Semivariance	Pairs
1	78.61	0.13	484
2	229.46	0.11	570
3	379.09	0.11	735
4	528.16	0.12	740
5	677.33	0.14	978
6	825.32	0.16	1040
7	972.69	0.16	1149
8	1125.94	0.18	979
9	1276.52	0.16	1189
10	1424.16	0.16	1110

Variogram - Intermediate Status - Present
Lag = 150 km; Lag tol. = 75 km; Active lag = 1500 km

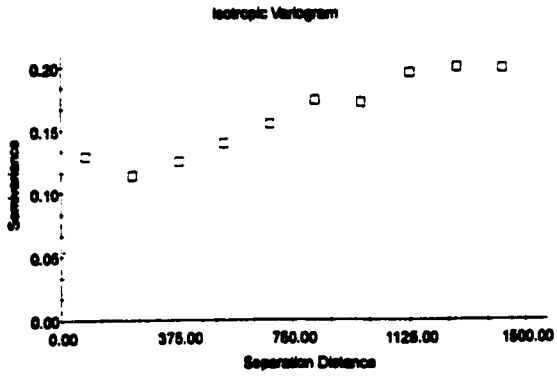

Lake Status - Present (Semivariance Data for Intermediate)			
Lag Class	Average Distance	Average Semivariance	Pairs
1	78.61	0.13	484
2	229.46	0.11	570
3	379.09	0.12	735
4	528.16	0.14	740
5	677.33	0.15	978
6	825.32	0.17	1040
7	972.69	0.17	1149
8	1125.94	0.19	979
9	1276.52	0.2	1189
10	1424.16	0.19	1110

Variogram - Low Status - Present
Lag = 150 km; Lag tol. = 75 km; Active lag = 5500 km

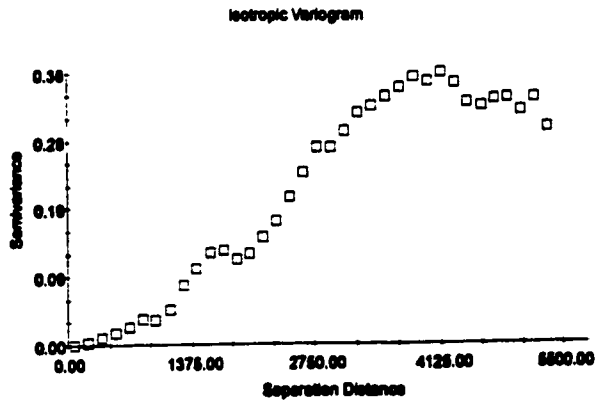

Lake Status - Present (Semivariance Data for Low)			
Lag Class	Average Distance	Average Semivariance	Pairs
1	78.61	0	484
2	229.46	0	570
3	379.09	0.01	735
4	528.16	0.02	740
5	677.33	0.02	978
6	825.32	0.04	1040
7	972.69	0.05	1149
8	1125.94	0.05	979
9	1276.52	0.05	1189
10	1424.16	0.1	1110
11	1578.94	0.13	1052
12	1728.31	0.13	1178
13	1878.68	0.12	1352
14	2024.37	0.13	1289
15	2176.39	0.16	1347
16	2328.28	0.17	1249
17	2472.66	0.2	1189
18	2623.1	0.24	1290
19	2776.68	0.27	1297
20	2928.56	0.27	1378
21	3078.69	0.3	1497
22	3224.34	0.32	1400
23	3377.44	0.33	1452
24	3528.13	0.35	1488
25	3678.17	0.35	1480
26	3824.68	0.37	1397
27	3974.69	0.37	1789
28	4124.82	0.38	1699
29	4276.69	0.38	1613
30	4422.44	0.34	1688
31	4576.16	0.35	1651
32	4726.65	0.34	1497
33	4876.41	0.34	1697
34	5026.04	0.35	1480
35	5176.61	0.34	1341
36	5326.01	0.3	1188

Figure 4.4 a: Spatial continuity description at present (indicators).

Variogram - High Status - 3 ka
Lag = 1000 km; Lag tol. = 500 km; Active lag = 3000 km

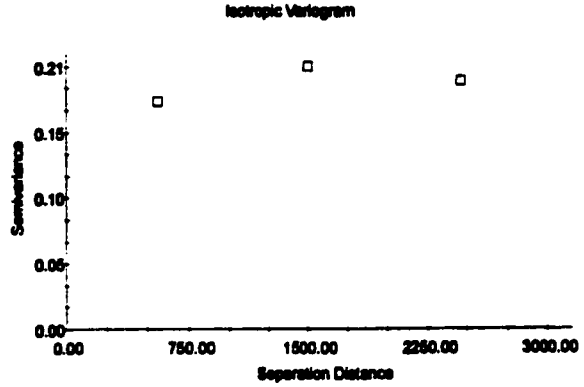

Lake Status - 3 ka (Semivariance Data for High)			
Lag Class	Average Distance	Average Semivariance	Pairs
1	883.81	0.16	1667
2	1806.84	0.21	2345
3	2488.25	0.19	2388

Variogram - Intermediate Status - 3 ka
Lag = 200 km; Lag tol. = 100 km; Active lag = 1600 km

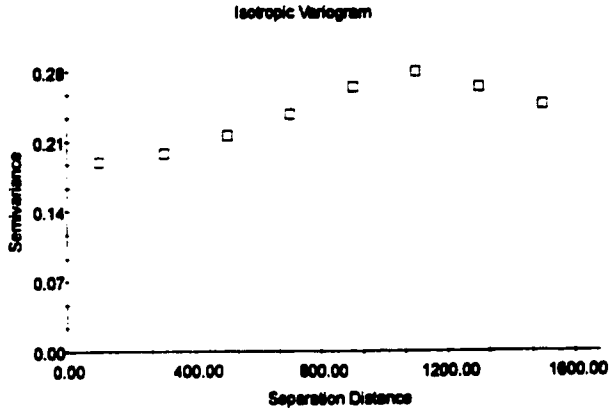

Lake Status - 3 ka (Semivariance Data for Intermediate)			
Lag Class	Average Distance	Average Semivariance	Pairs
1	103.71	0.19	213
2	302.19	0.2	284
3	498.77	0.22	353
4	701.88	0.24	440
5	902.65	0.27	397
6	1100.51	0.28	434
7	1301.3	0.27	477
8	1496.69	0.25	400

Variogram - Low Status - 3 ka
Lag = 200 km; Lag tol. = 100 km; Active lag = 2000 km

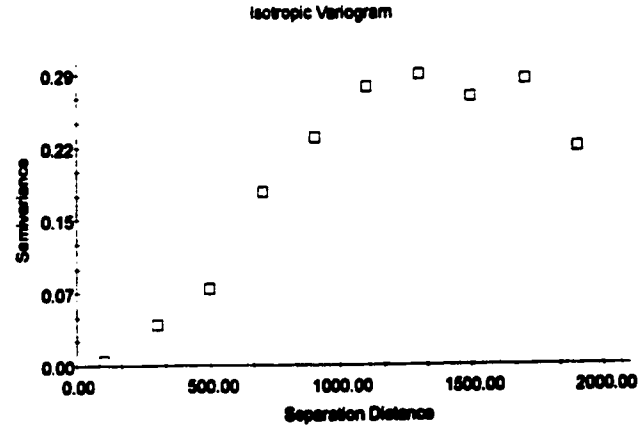

Lake Status - 3 ka (Semivariance Data for Low)			
Lag Class	Average Distance	Average Semivariance	Pairs
1	103.71	0	213
2	302.19	0.04	284
3	498.77	0.08	353
4	701.88	0.17	440
5	902.65	0.23	397
6	1100.51	0.28	434
7	1301.3	0.29	477
8	1496.69	0.27	400
9	1702.75	0.29	456
10	1898.2	0.22	479

Figure 4.4 b: Spatial continuity description at 3 ka (indicators).

Variogram - High Status - 6 ka
Lag = 250 km; Lag tol. = 125 km; Active lag = 2500 km

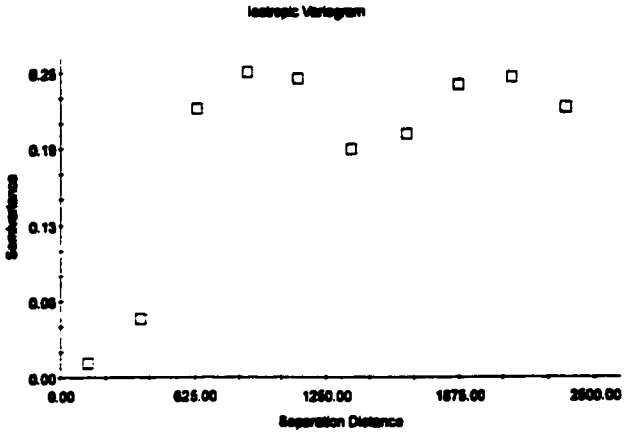

Lake Status - 6 ka (Semivariance Data for High)			
Lag Class	Average Distance	Average Semivariance	Pairs
1	126.86	0.01	316
2	375.79	0.05	418
3	635.35	0.22	548
4	879.76	0.25	678
5	1122.81	0.24	676
6	1375.07	0.19	647
7	1632.47	0.2	633
8	1875.68	0.24	706
9	2128.14	0.25	784
10	2375.61	0.22	847

Variogram - Intermediate Status - 6 ka
Lag = 225 km; Lag tol. = 112.5 km; Active lag = 2500 km

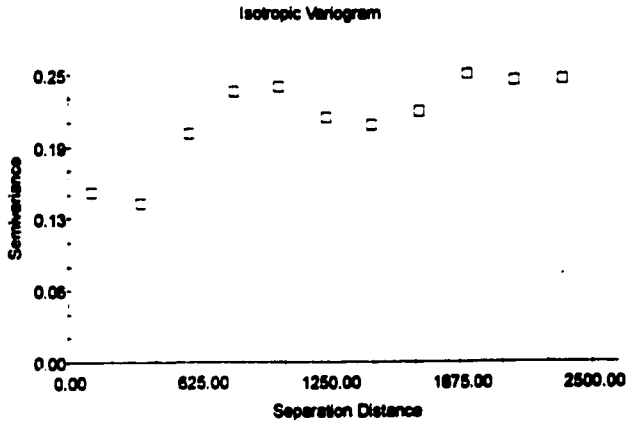

Lake Status - 6 ka (Semivariance Data for Intermediate)			
Lag Class	Average Distance	Average Semivariance	Pairs
1	109.61	0.15	272
2	343.85	0.14	395
3	571.23	0.2	417
4	787.61	0.24	578
5	1010.17	0.24	644
6	1237.85	0.21	585
7	1453.29	0.21	543
8	1686.27	0.22	616
9	1910.31	0.25	631
10	2137.46	0.25	735
11	2363.71	0.25	766

Variogram - Low Status - 6 ka
Lag = 500 km; Lag tol. = 250 km; Active lag = 2000 km

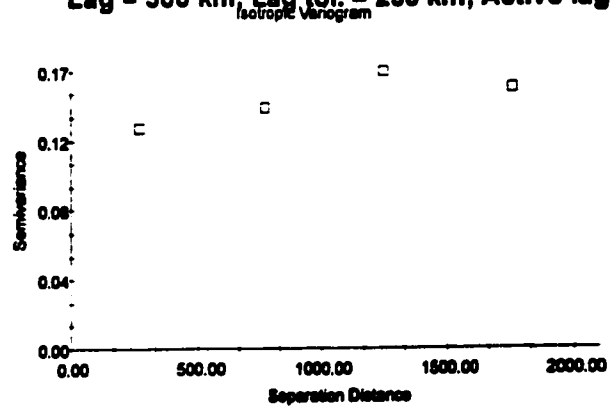

Lake Status - 6 ka (Semivariance Data for Low)			
Lag Class	Average Distance	Average Semivariance	Pairs
1	288.67	0.13	734
2	770.51	0.14	1226
3	1246.17	0.17	1323
4	1760.71	0.16	1339

Figure 4.4 c: Spatial continuity description at 6 ka (indicators).

Variogram - High Status - 9 ka
Lag = 300 km; Lag tol. = 150 km; Active lag = 2500 km

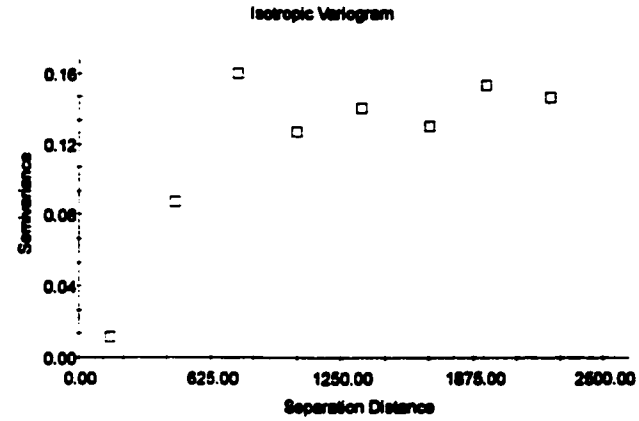

Lake Status - 9 ka (Semivariance Data for High)			
Lag Class	Average Distance	Average Semivariance	Pairs
1	148.44	0.01	179
2	466.41	0.09	281
3	780.89	0.16	324
4	1042.54	0.12	435
5	1350.89	0.14	395
6	1670.53	0.13	379
7	1941.04	0.15	346
8	2248.54	0.14	383

Variogram - Intermediate Status - 9 ka
Lag = 100 km; Lag tol. = 50 km; Active lag = 500 km

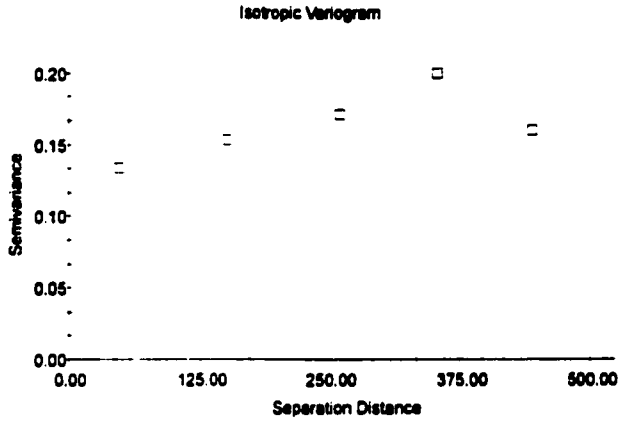

Lake Status - 9 ka (Semivariance Data for Intermediate)			
Lag Class	Average Distance	Average Semivariance	Pairs
1	48.02	0.13	64
2	151.02	0.15	59
3	260.47	0.17	56
4	352.54	0.2	88
5	444.66	0.16	85

Variogram - Low Status - 9 ka
Lag = 200 km; Lag tol. = 100 km; Active lag = 1500 km

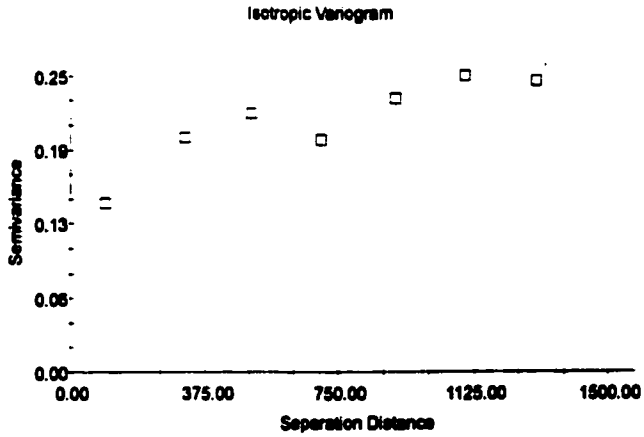

Lake Status - 9 ka (Semivariance Data for Low)			
Lag Class	Average Distance	Average Semivariance	Pairs
1	97.43	0.14	123
2	316.73	0.2	144
3	503.77	0.22	193
4	703.05	0.2	199
5	906.3	0.23	268
6	1099.68	0.25	272
7	1298.22	0.25	255

Figure 4.4 d: Spatial continuity description at 9 ka (indicators).

Variogram - High Status - 12 ka
Laf = 500 km; Lag tol. =250 km; Active lag = 3000 km

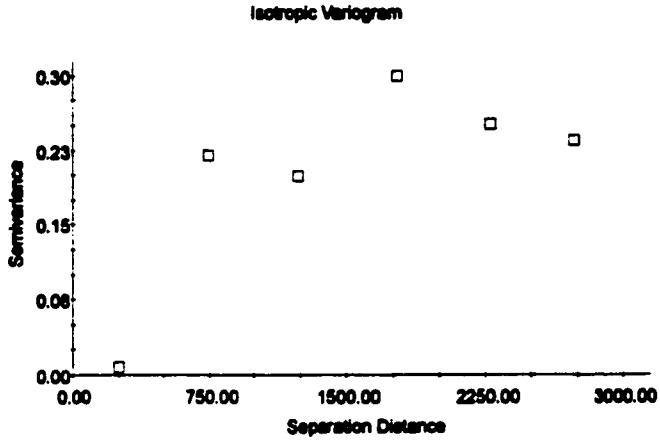

Lake Status - 12 ka (Semivariance Data for High)			
Lag Class	Average Distance	Average Semivariance	Pairs
1	250.5	0.01	125
2	745.66	0.22	133
3	1239.96	0.2	154
4	1772.71	0.3	143
5	2277.57	0.25	212
6	2731.4	0.24	202

Variogram - Intermediate Status - 12 ka
Lag = 250 km; Lag tol. = 125 km; Active lag = 2500 km

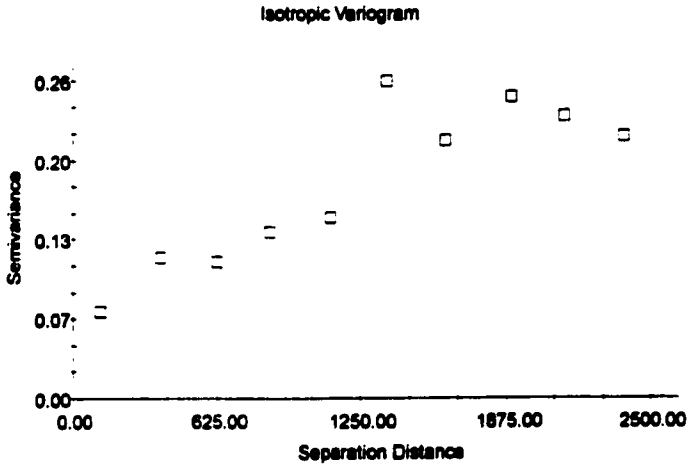

Lake Status - 12 ka (Semivariance Data for Intermediate)			
Lag Class	Average Distance	Average Semivariance	Pairs
1	122.45	0.07	64
2	384.85	0.11	61
3	628.7	0.11	67
4	864.4	0.14	66
5	1126.93	0.15	81
6	1365.42	0.26	73
7	1616.89	0.21	64
8	1866.94	0.25	79
9	2130.6	0.23	91
10	2368.11	0.21	121

Variogram - Low Status - 12 ka
Lag = 600 km; Lag tol. = 300 km; Active lag = 5000 km

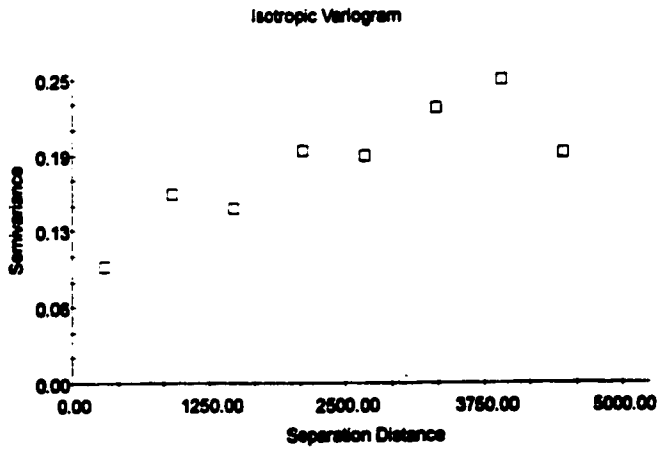

Lake Status - 12 ka (Semivariance Data for Low)			
Lag Class	Average Distance	Average Semivariance	Pairs
1	300.03	0.1	150
2	912.38	0.16	175
3	1472.89	0.15	158
4	2116.33	0.19	226
5	2668.66	0.19	260
6	3308.14	0.23	209
7	3908.17	0.25	195
8	4459.26	0.19	174

Figure 4.4 e: Spatial continuity description at 12 ka (indicators).

Lake Status - Present
Fitted model

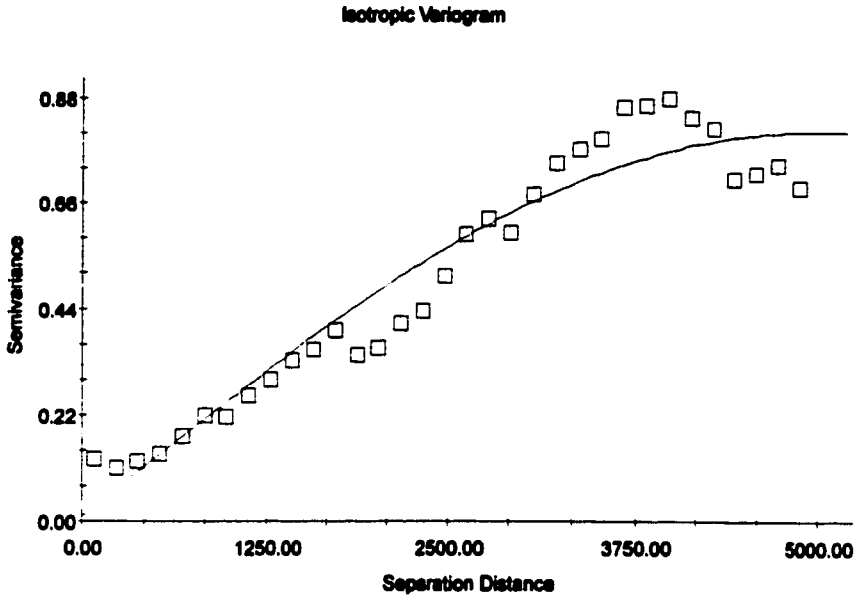

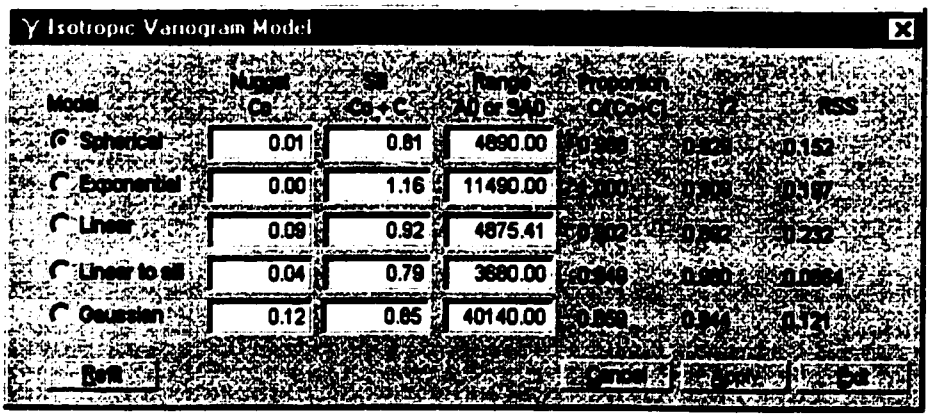

Figure 4.5 a: Spatial continuity modeling at present.

Lake Status - 3 ka
Fitted Model

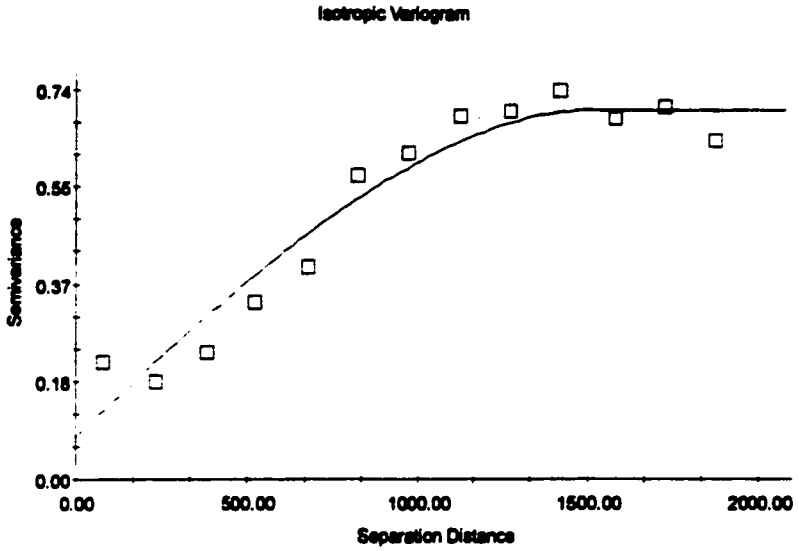

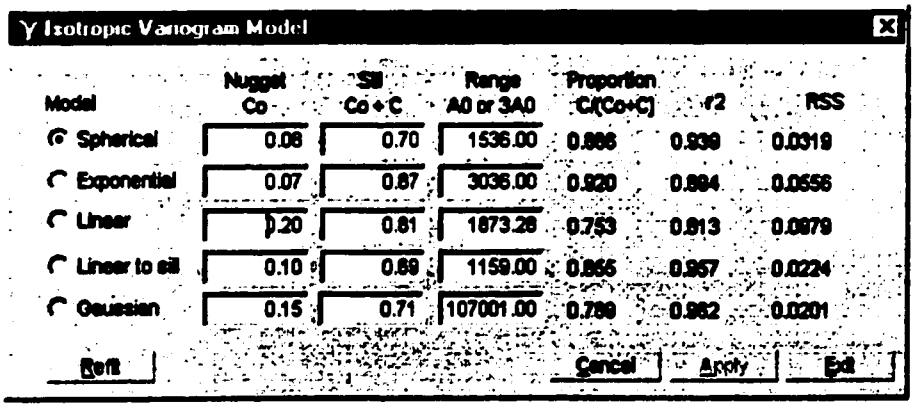

Figure 4.5 b: Spatial continuity modelling at 3 ka.

Lake Status - 6 ka
Fitted Model

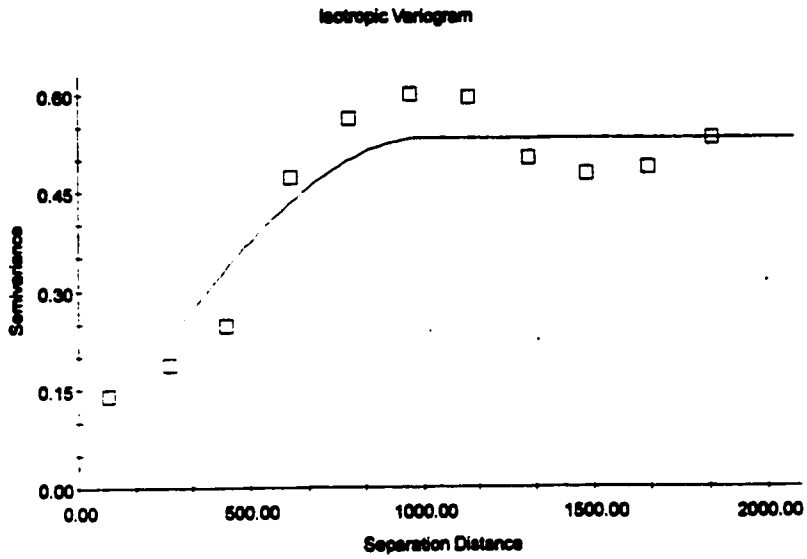

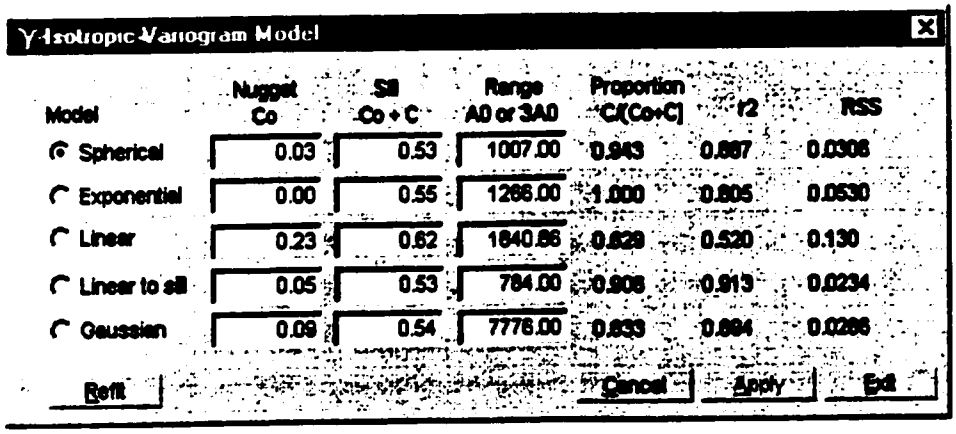

Figure 4.5 c: Spatial continuity modelling at 6 ka.

Lake Status - 9 ka
Fitted Model

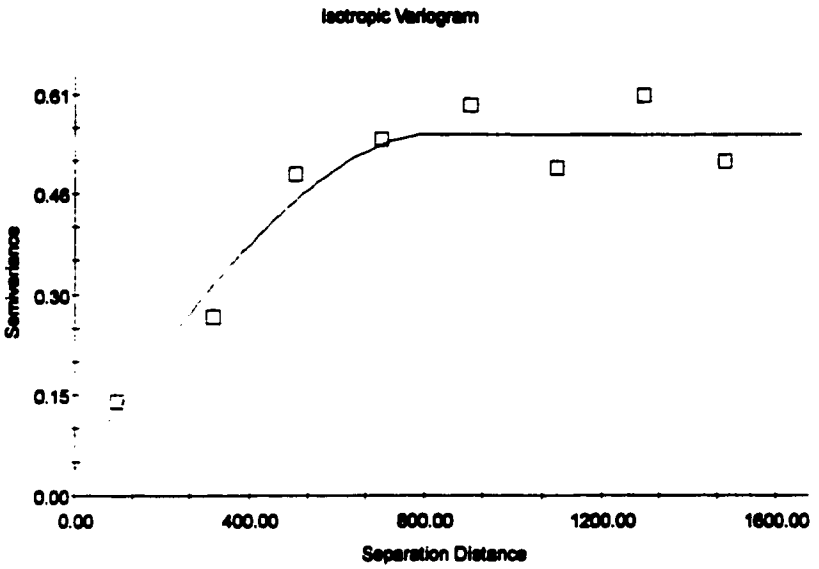

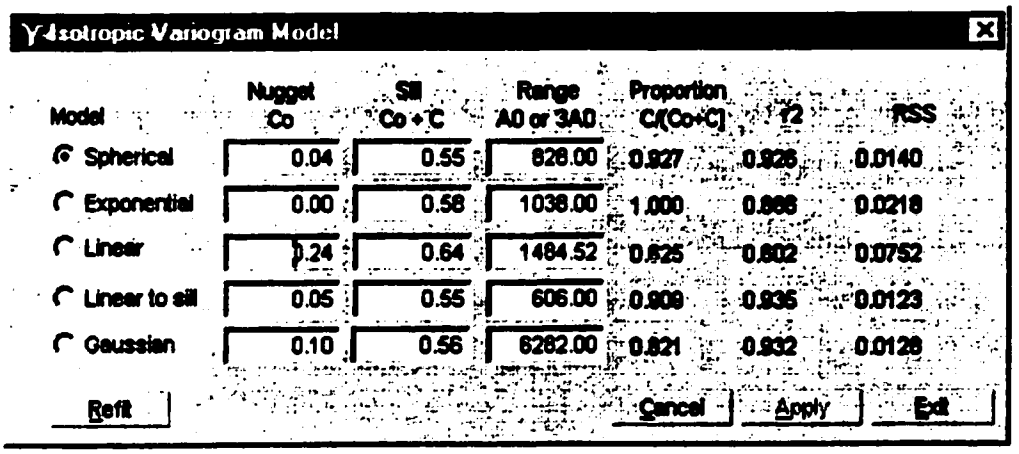

Figure 4.5 d: Spatial continuity modelling at 9 ka.

Lake Status - 12 ka
Fitted Model

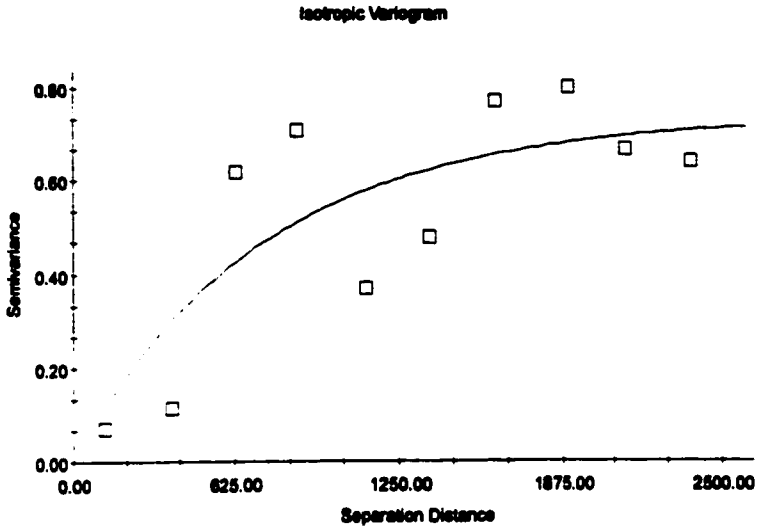

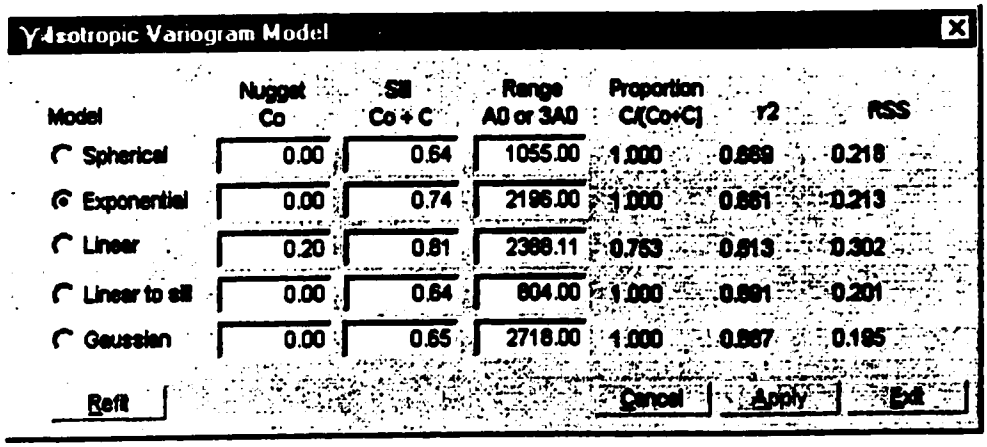

Figure 4.5 e: Spatial continuity modelling at 12 ka.

High Lake Status - Present
Fitted Model

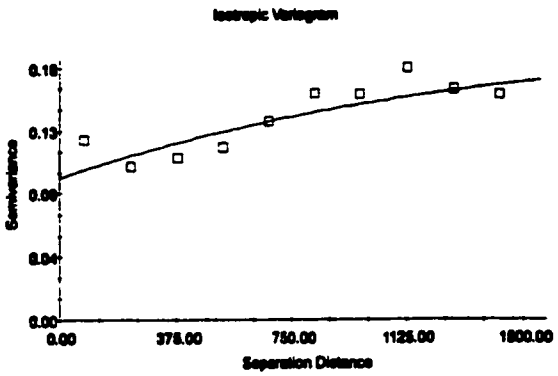

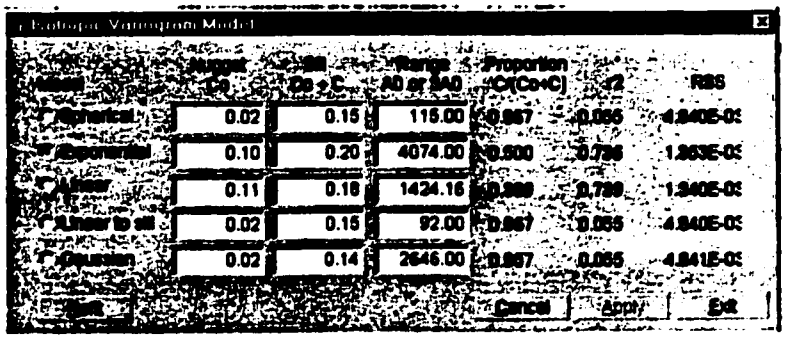

Intermediate Lake Status - Present
Fitted Model

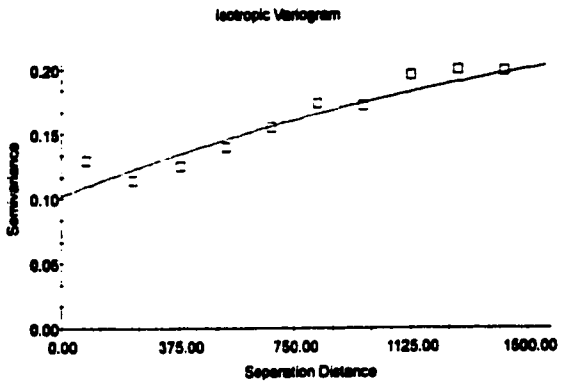

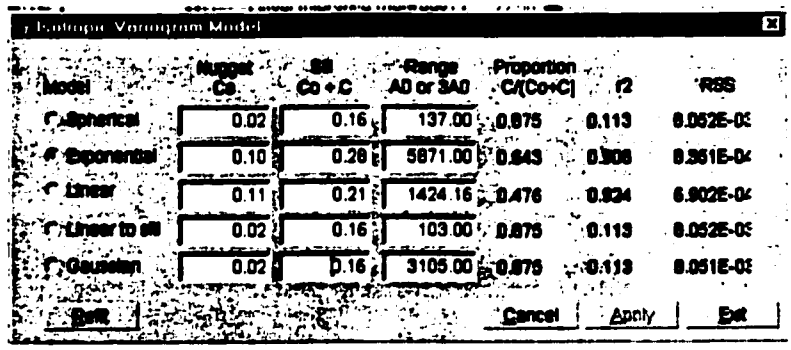

Low Lake Status - Present
Fitted Model

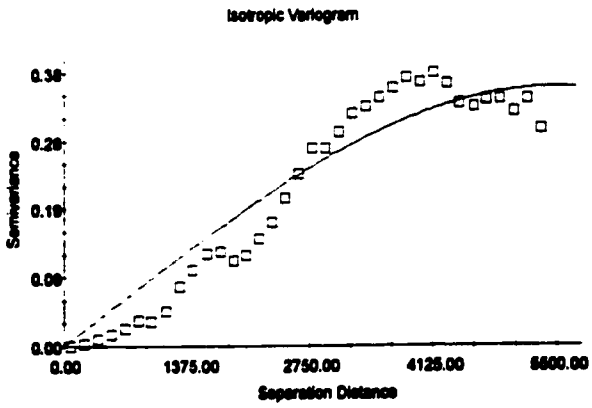

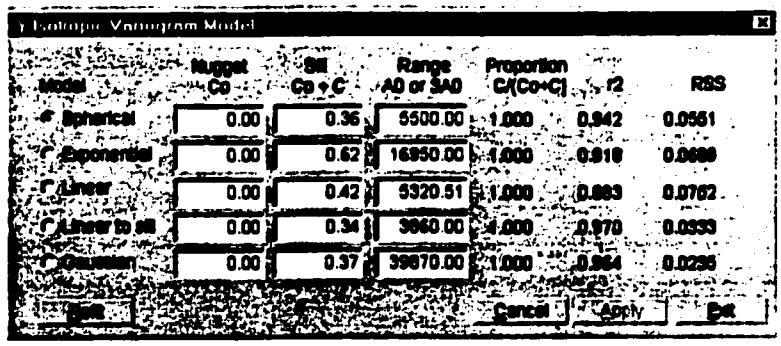

Figure 4.6 a: Spatial continuity modelling at present (indicators).

High Lake Status - 3 ka
Fitted Model

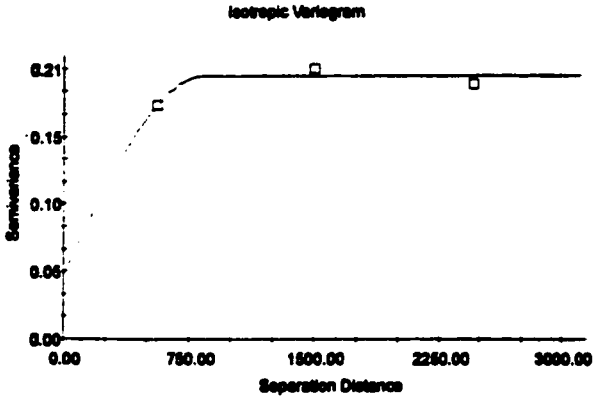

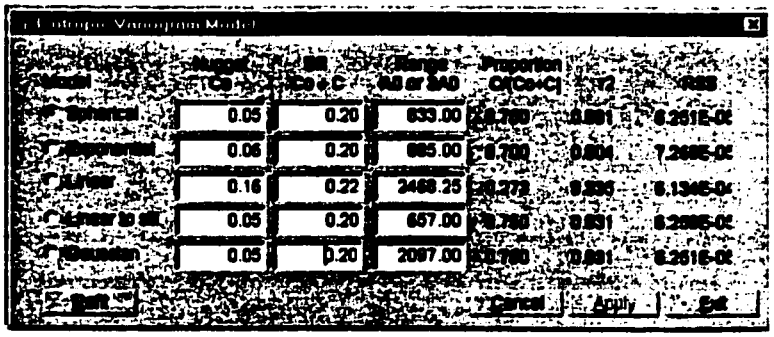

Intermediate Lake Status - 3 ka
Fitted Model

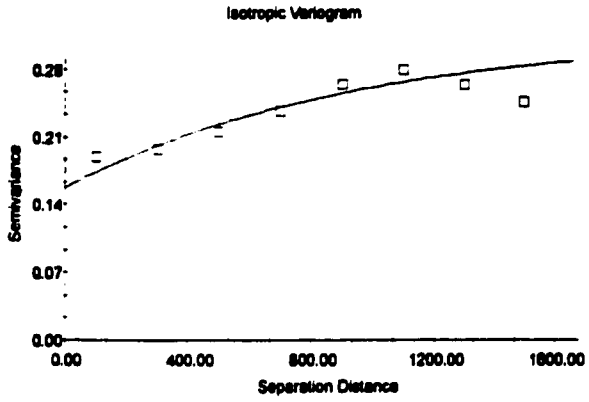

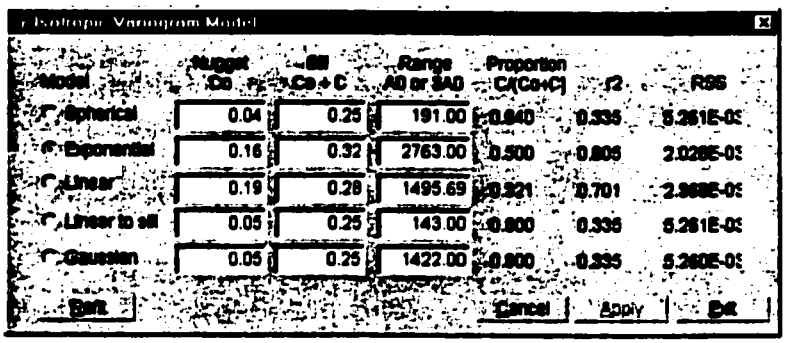

Low Lake Status - 3 ka
Fitted Model

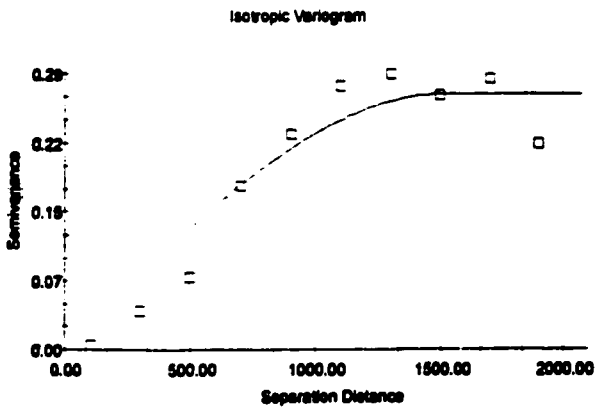

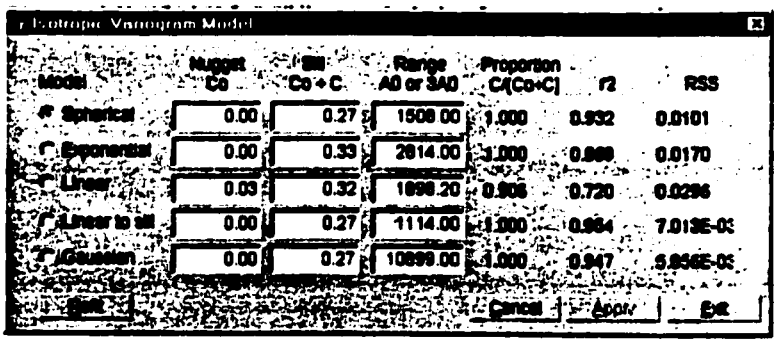

Figure 4.6 b: Spatial continuity modelling at 3 ka (indicators).

High Lake Status - 6 ka
Fitted Model

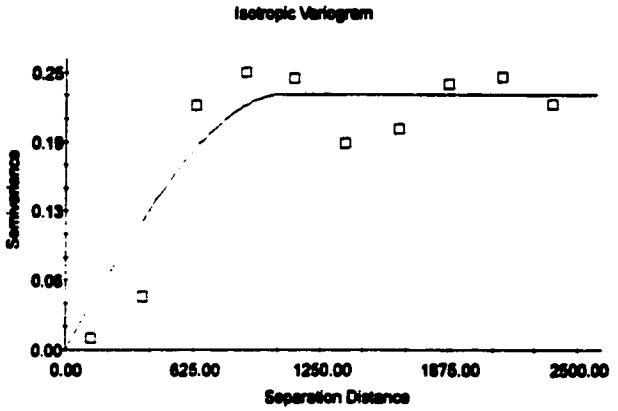

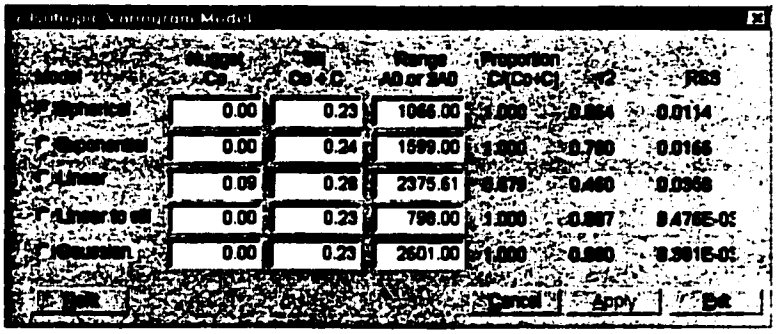

Intermediate Lake Status - 6 ka
Fitted Model

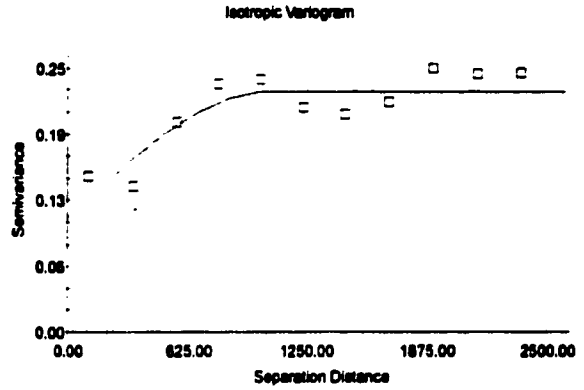

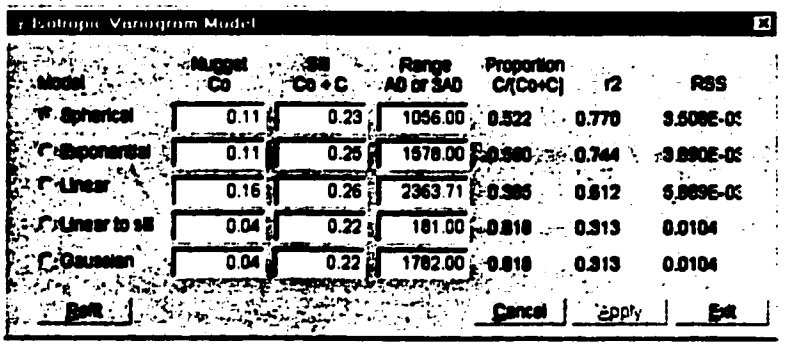

Low Lake Status - 6 ka
Fitted Model

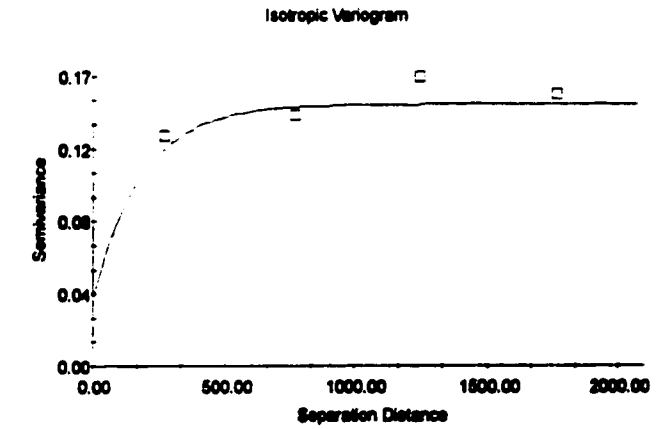

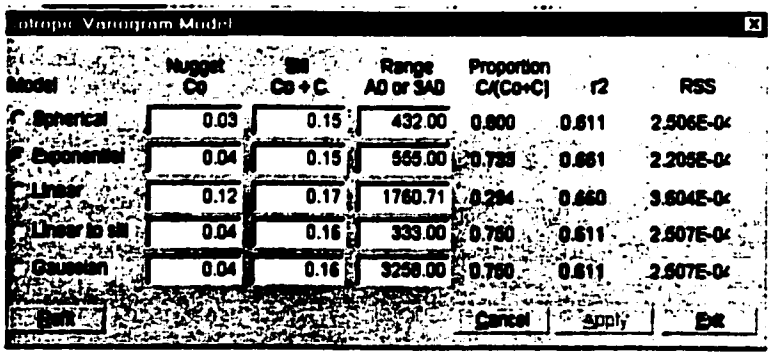

Figure 4.6 c: Spatial continuity modelling at 6 ka (indicators).

High Lake Status - 9 ka
Fitted Model

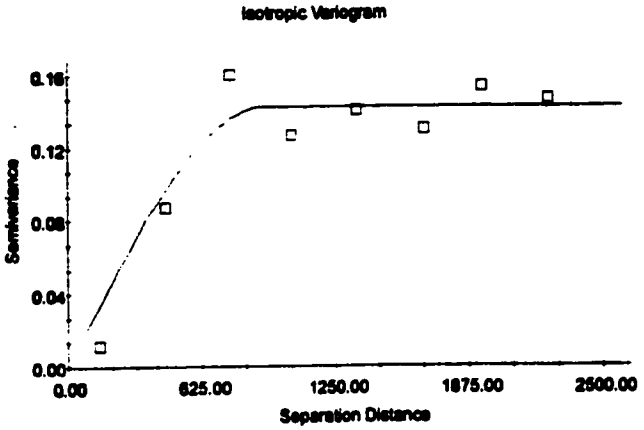

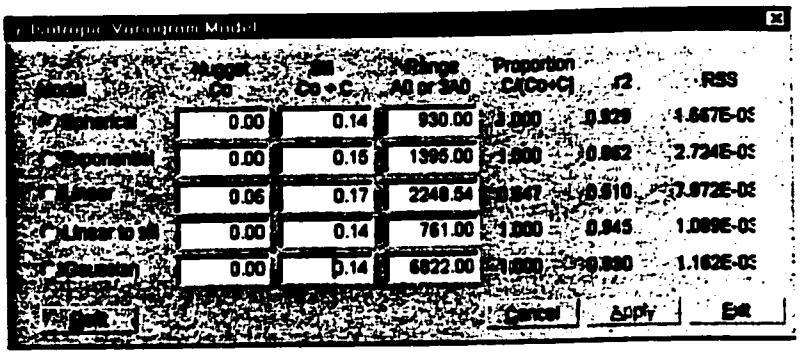

Intermediate Lake Status - 9 ka
Fitted Model

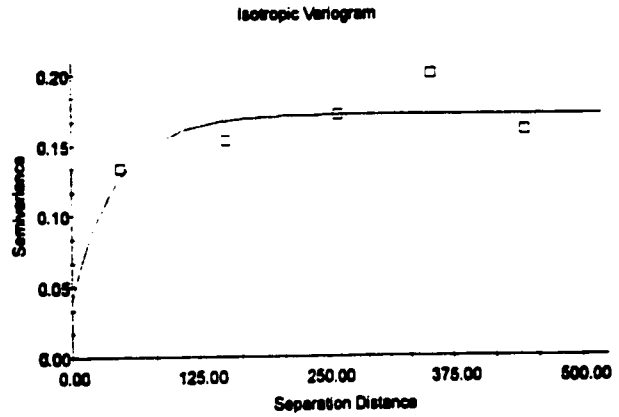

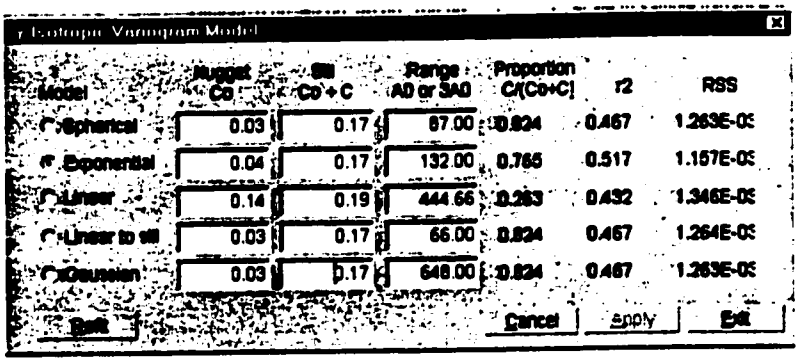

Low Lake Status - 9 ka
Fitted Model

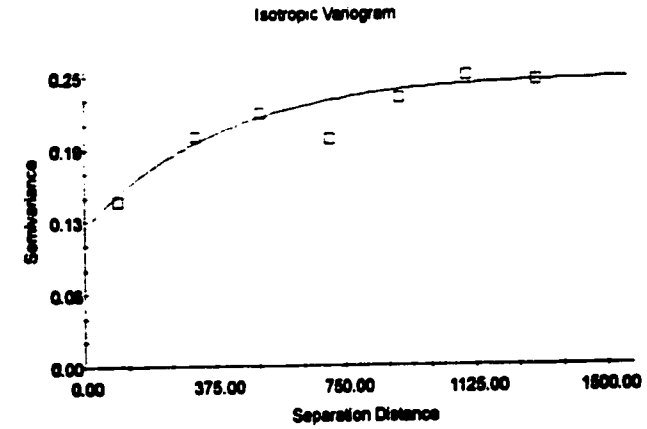

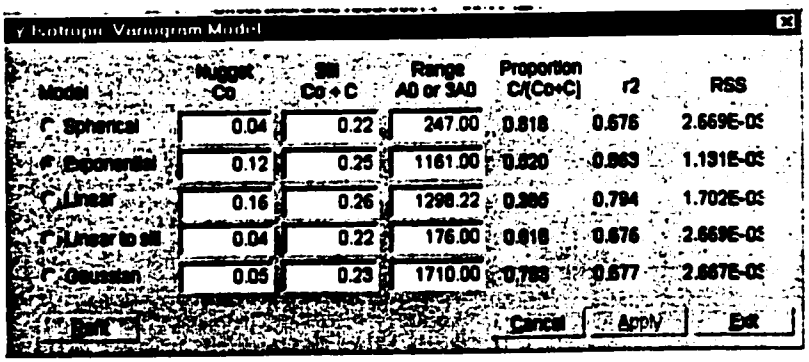

Figure 4.6 d: Spatial continuity modelling at 9 ka (indicators).

High Lake Status - 12 ka

Fitted Model

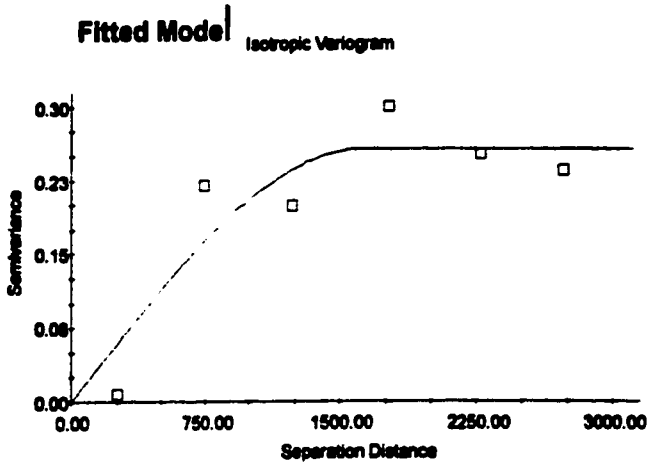

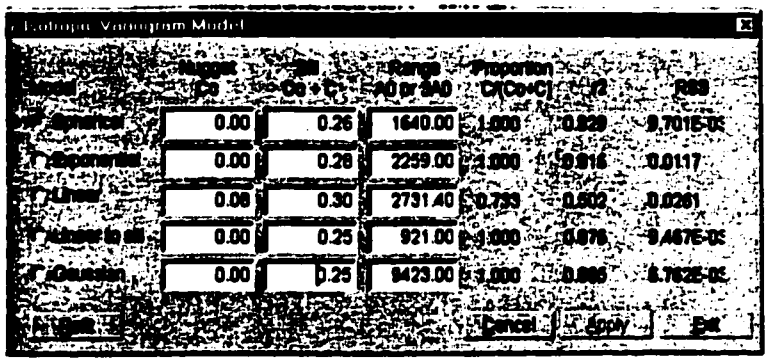

Intermediate Lake Status - 12 ka
Fitted Model

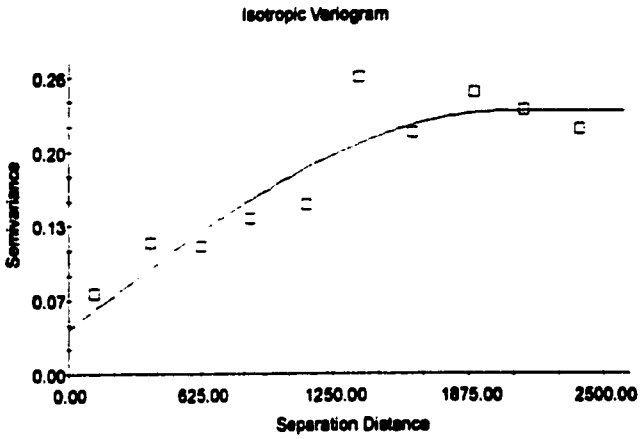

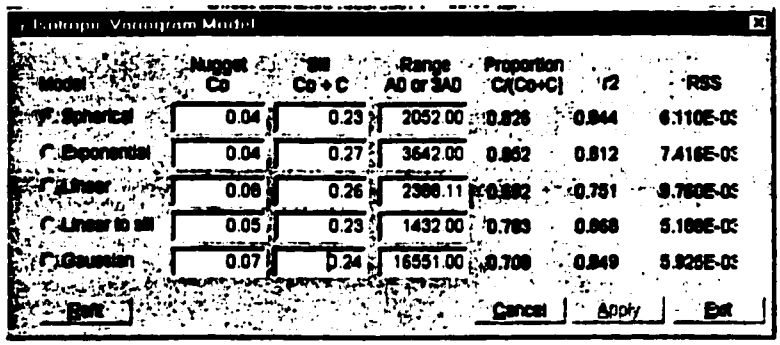

Low Lake Status - 12 ka
Fitted Model

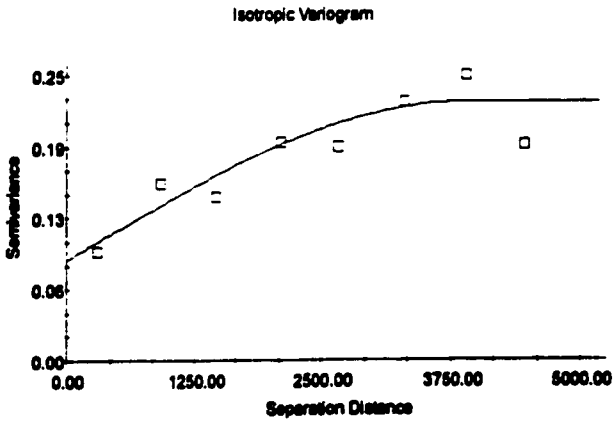

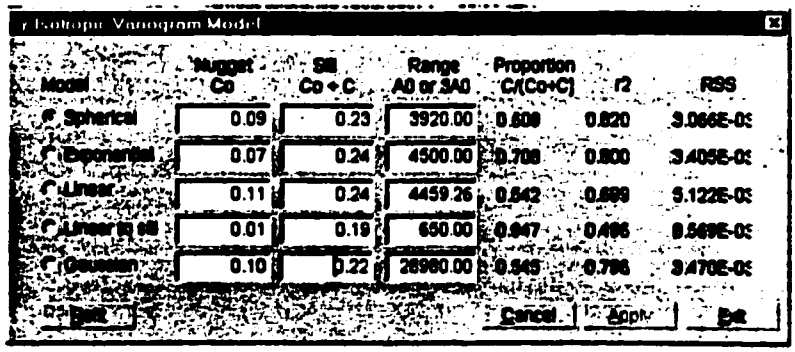

Figure 4.6 e: Spatial continuity modelling at 12 ka (indicators).

Chapter 5

Estimation

"Ordinary kriging is a method that is often associated with the acronym B.L.U.E. for "best linear unbiased estimator". The distinguishing feature of ordinary kriging is its aim of minimizing error variance. The choice of a search strategy that controls the samples that are included in the estimation procedure is an important consideration in any approach to local estimation"

Isaaks and Srivastava, 1989.

In the previous chapter, sample variograms were successfully modelled. In this chapter, the sample variogram models are used to predict values in areas that have not been sampled. Here, we will focus on two different methods of estimation. First, ordinary kriging will be illustrated using the modelled sample variograms under the assumption of climate continuum. Next, indicator kriging will be used to estimate the transformed binary data under the assumption of mutual exclusivity of the categorical data. A reclassification procedure will be applied to the back transformation of all three lake status categories based on the maximum probability vector (Goovearts, 1997). This, in turn, will allow the production of maps at 3,000 year intervals covering the last 12,000 years under both assumptions. Lastly, the patterns derived from both approaches will be compared.

Estimation requires a model of how the phenomenon behaves at locations where it has not been sampled (Isaaks and Srivastava, 1989). Without a model, no inferences can be made about unknown locations that were not sampled. One of the advantages of geostatistical estimation techniques lies with a clearly stated model on which the estimates are based (Isaaks and Srivastava, 1989). Although, the most desirable model would be an deterministic model, very few earth science processes are understood well enough to permit the application of such models.

Therefore, for the vast majority of these processes, there is some uncertainty about how the phenomenon behaves between sample location (Isaaks and Srivastava, 1989). For this reason, the geostatistical approach to estimation is based on a probabilistic model. The random function models recognize the uncertainties and provide tools for estimating values at unsampled locations.

In this study, we use local estimation rather than global estimation. Estimation over a large area in which we have many samples is called a *global estimation*. In *local estimation*, we are considering a smaller area in which there are few samples. In this case, we use nearby samples located outside the area being estimated (Isaaks and Srivastava, 1989). Global estimation is commonly used at a very early stage of analysis to obtain some characteristics of the distribution of data values over the whole area (Isaaks and Srivastava, 1989). In the case of lake level data, the data is sometimes clustered and may not be representative of the whole area.

Both methods discussed below involve weighted linear combinations of the data where the estimate $v = \sum w_i * v_i$; where $v_1..v_n$ are the n available data values and w_i is a weight assigned to the value v_i. These weights are often standardized to sum to one (Isaaks and Srivastava, 1989). Local estimation need to account for the distance from the point (s) being estimated to the individual sample locations. Some samples may be closer to each other and more weight should be given to these points. Local estimation is also affected by sample clusters where a group of closely located sample sites would likely contain redundant data. Therefore, the weights assigned by local estimation should account for both the distance and for possible redundancy between samples (Isaaks and Srivastava, 1989). As the weight for a particular value increases, the influence of that particular value on the estimate also increases. Conversely, data values with small weights have little influence on the estimate. (Isaaks and Srivastava, 1989).

The choice of a search strategy that restricts the samples included in the estimation procedure is important in local estimation (Isaaks and Srivastava, 1989). Adopting a global search neighbourhood (ie: all samples) would require knowledge of the covariance for the largest separation distances (Deustch and Journel, 1992). A major reason for limiting the search neighbourhood is to allow local rescaling as in the case of heteroscedasticity present in the data, and this is true for the lake level data (Deutsch and Journel, 1992). A fundamental question to ask of irregularly distributed data is: are there nearby samples ?. As we have seen in Chapter 4, section 4.2, the maximum spatial coverage was obtained at 500 km for all time frames under study. In addition, sites exhibiting negative spatial autocorrelation were excluded at this scale thus resulting in a consistent scale for the whole world. Furthermore, all of the sites at this distance have nearby samples, except for a small percentage of sites with distances greater than 500 km. Therefore, given that the sites are positively spatially correlated at this distance and have nearby samples, a search strategy of a 500 km radius was established for local point estimation so that only those data falling within this search radius centered at the location being estimated are used.

5.1 Ordinary Kriging

Ordinary kriging is the most commonly used method and is often termed a "best linear unbiased estimator" (Isaaks and Srivastava, 1989). It is "linear" because its estimates are weighted linear combinations of the available data; it is "unbiased" since it aims to have the mean residual or error equal to 0; it is "best" because it aims at minimizing the variance of the errors (Isaaks and Srivastava, 1989). The model parameters described in the previous chapter are now used for estimation in which the principal parameters are the nugget effect, the sill and range. Again, the search neighbourhood is set to 500 km in order to estimate only unsampled locations that contain

nearby samples. As stated above, a small percentage of sites with distance greater than 500 km are also part of the estimation, however, they have no neighbours within the 500 km search radius. These estimations are less reliable, however, they are kept to give insight into possible mechanisms of global hydrological change in isolated regions of the world.

Lake-level status under climate continuum assumption

Under the assumption that the data are continuous in climate space, the mapped estimates can vary between 1 to 3 or from high to low lake status. At 0 ka, high lake status conditions prevail in most of the mid latitudes of North America stretching from the east to west (Figure 5.1 a). The southwestern United States is distinctly low while the eastern coast region is predominantly intermediate. There is a transition from low to high lake status in Mexico. As described in the Chapter 3, South America can be divided into three zones where high lake status is dominant in the northeast, intermediate status in the northwest and low lake status in the southwestern Cordilleran region. In Europe, lake status is high in the northern coastal region, intermediate to the east and south and low in the southern region of Spain and in the western region of Russia. Lake status in Africa is low, except for a small area to the east of the Equatorial Rainforest. Although there are few data in Asia, the results indicate high lake status conditions in the north and low lake-level status in the southwest. Lake-levels in Australia are high to intermediate to the southeast and low in the southwest. In general, the estimation process captured the spatial patterns described in the initial description of the original data. However, the spatial organisation of lake-levels in Europe is much clearer. Whereas in the original data, it is difficult to see clear patterns due to the large inter-site variability, the interpolated results presented here bring out the large-scale patterns.

The 3 ka map shows little difference in lake status from 0 ka in North America (Figure 5.1 a). However, we can observe a shift towards higher latitudes of the low lake-level conditions in the southwest region of North America leaving a region of intermediate lake status conditions in the extreme southwest. Europe also shows low lake status penetrating as far as Germany in the south while a north south band of low status region of the eastern interior is significantly larger in spatial extent compared to 0 ka. Although coverage in Africa is significantly less, the north central region shows high to intermediate lake-level conditions which is surrounded by low lake status. As described above, the western region of Asia has dominantly low lake-levels with higher lake-levels in the north central region. Southwestern China and northern India show an increase towards higher lake-level conditions. In summary, 3 ka shows some regions that have significantly changed, such as Northern Africa and the western region of Russia.

The 6 ka map indicates significant changes in lake status conditions (Figure 5.1 a). Most of North America exhibits low lake-levels. In Europe, high lake-levels are centered around the Baltic Region, and intermediate lake status conditions in eastern Europe penetrate deeper into Russia than at 3 ka. The band of low lake-levels has shifted eastward into Russian territory. One of the most significant changes at 6 ka is the dominant high lake-level conditions in North Africa and its eastern coastal region. These wetter conditions are also present in Arabia, which has intermediate lake-levels. The southern tip of Africa is the only region that remains unchanged with low lake-levels. Asia shows little change from north to south with the exception of higher lake-levels in northern India. The major changes occurring at 6 ka in Australia is high lake-levels in the southwestern region. In general, 6 ka suggest major differences in climate conditions compared to 0 ka, especially in North America and Africa.

The 9 ka map also shows a change in the hydrological cycle from 6 ka (Figure 5.1 b). Low lake-level conditions remain dominant in most regions of North America except for the south and southwest Great Lakes region where intermediate to high lake status are apparent. Central America displays lowered lake-level conditions. The southwestern Cordilleran region of South America indicates low lake-levels, but there are few data available. In Europe, there is a banded pattern of low-high low-high from southeast to northwest. Northern and central Africa remain high, while central Asia has lower lake-levels, except for northern India with high lake-levels. The southeastern coastal region of Australia has predominantly low lake-levels. In summary, the spatial patterns of lake level behaviour at 9 ka show major differences from 0 ka in Asia, Eastern Europe and Australia. The spatial patterns after estimation are also clearer for this time period.

Although there are fewer data at 12 ka, the large-scale patterns can still be inferred from these clusters (Figure 5.1 b). One of the most dramatic changes in lake behaviour is in North America, which has predominantly high lake-levels, except for the southern Canadian prairie region. Low lake-levels are dominant in southwest Mexico and Central America. In South America, high lake-levels are found in the northwest and southwestern Cordilleran region and low lake status in the northeast. The areas estimated in Europe show low lake-levels in the central part and intermediate lake-levels at the peripheries. Although few data are left in Africa, lower lake-level conditions are apparent in the northwestern region and high lake-levels are dominant along the eastern coastal region. The few sites in Asia indicate higher lake-level conditions. In general, the 12 ka map may be useful in the interpretation of global hydrological changes in certain regions, for example, in North America.

Although difficult to validate these models, cross-validation can give insight on how well estimation

has proceeded (Figure 5.2). All results show a high r2, thus suggesting a good estimation process. 0 ka and 12 ka yielded the best results with an r2 of 0.86. Although the 3 and 9 ka time periods come out with poorer results, all of the explained variances of the cross-validations are significant. The resulting maps show that the fundamental spatial features described in previous chapters were retained, thus suggesting a successful modelling and estimation process.

5.2 Indicator Kriging

Ordinary kriging requires a model of the variogram of the variable being estimated. In the case of indicators, spatial continuity of the each individual indicator is required (Isaaks and Srivastava,1989, Goovearts, 1997). With indicator kriging, the unsampled value or its indicator transform provides a value of uncertainty or probability of occurrence rather than an estimate of the value (Deutsch and Journel, 1992, Goovearts, 1997). The ability to customize the estimation procedure to the patterns of spatial continuity appropriate for each class (ie. lake statuses) makes ordinary kriging a more powerful technique for the estimation of indicators than other local estimation procedures (Isaaks and Srivastava, 1989).

Each of the three lake categories was estimated using its own model of spatial continuity to provide a probability of occurrence at unsampled locations using the same search neighbourhood distance of 500 km for consistency reasons between the two procedures.

Only the largest-scale patterns will be here discussed. At 0 ka, high lake status is probable in most of the mid latitudes of North America (Figure 5.3 a) and centered on the Baltic Region of Europe. Intermediate status has a high probability of occurrence along the eastern north American coast and

west of the Great Lakes region. In Europe, intermediate status is likely dominant east of the high lake status sites and penetrating into the western Russian regions. Low lake-level conditions are highly probable in the southwestern United States, southwestern Chile and Argentina and in Europe west of the intermediate status in Russia in a north-south band pattern. As expected, low lake-level conditions are highly probable in northern and eastern Africa and its southern tip region. The band of high probability of low status continues eastward through Arabia, northern India and China.

High lake-level conditions are probable in the Great Lakes and in Canadian prairies in North America at 3 ka (Figure 5.3 b). In Europe, high lake-level conditions are less pronounced than at 0 ka. The north-central region of Africa shows a high probability of occurrence of high lake status. Intermediate lake-level conditions are most probable along the northwestern Cordilleran region and southeast of the Great Lakes in North America. The southern tip of Mexico also indicate intermediate lake status conditions to be highly probable. Intermediate lake-levels are most likely to occur over much of Europe, except in a region west of the Urals which are most likely low status. Low lake-level conditions are most probable in the southwestern United States. There is evidence of an increase in local or isolated lake-level conditions prevailing in certain regions of the world at 3 ka, notably northern Africa.

At 6 ka, the results show low lake-levels in North America most probable in the southwest, the Canadian prairies and southwest of the Great lakes region (Figure 5.3 c). In Europe, high lake-level conditions are most likely to occur in the Baltic Region and evidence suggest lower lake-levels more probable to the east. Northern and eastern Africa shows a large region of high lake-levels as most probable. The lake-level patterns for 6 ka shows large differences from the present in Northern Africa and northern North America; only the southwest of North America remains low in both time

periods. At 6 ka, the pattern of probabilities of occurrence is less clear in Europe than at present.

At 9 ka, western and eastern North American lakes are most probably low status (Figure 5.3 d). In Europe, high lake level status is most probable in the northern regions and southwestern Russia with low lake-levels most probable to the south and northeast. There is less areal coverage in Africa, except the Sahel and eastern Africa, and these are most probably high lake-levels. In general, some fine-scale variability is apparent in central Europe and western Russia.

At 12 ka, North American lake-levels are most probably high in the southwest, east and across the prairies to the border of the United States and Canada. However, just to the north, in Manitoba and Saskatchewan, there is a zone where low lake-levels are probable. In Europe, the patterns are smaller scale but there is evidence of less area of low lake-levels. The few sites available make it difficult to estimate lake-levels over large areas as small regions of high, intermediate and low are seen around the globe.

Cross-validation is inappropriate for the indicator approach since the values are not estimates of the variable under study, but rather probabilities of occurrence for a given category in its binary form.

Lake-level status using the indicator approach

Using a reclassification scheme, the results of the indicator kriging calculations were used to produce maps showing the high, intermediate and low lake-levels status for the time periods under study. The methodology of the reclassification consists of two distinct steps. First, the indicator

kriging results of the three lake status categories were merged into one dataset consisting of a vector of probability of occurrence for each lake status for each grid node estimated. Next, a reclassification routine was performed in order to assign a lake status category for each estimated grid node based on the maximum probability of occurrence (Appendix H). The resulting matrix contains the transformation of the binary data into their respective lake status classes (ie. 1,2 or 3).

The resulting maps using the indicator kriging approach (Figures 5.4 a,b) are virtually identical to those presented under the ordinary kriging assumption of climate continuum (see Figures 5.1 a,b). Only small areas are different and this varies in degree (ie. high lake status under the first assumption as been categorized into intermediate lake status under the second assumption.

In conclusion, spatial patterns are evident in most regions of the world and at all time periods under study. There are significant similarities between the spatial patterns under both assumptions. The next section will investigate the agreements between both sets of maps in order to locate the discrepancies in an objective way.

5.3 Comparative analysis

This section will discuss the results of both approaches from the mapped output perspective. Difference maps were constructed to aid in the comparative analysis in order to quantify the similarity between the grids, locate discrepancies, and interpret the results. These difference maps were produced between the maps under the climate continuum assumption and the maps under the indicator kriging approach. Since the estimates under the indicator approach have only three possible values (1,2,3), differences were computed as *indicator estimate - continuous estimate*, and

therefore the signs are arbitrary. The resulting maps consist of the continuous estimates in the background and the discrepancies between both approaches are in symbol form.

Time/Difference	-3 to -0.5 units	-0.5 to 0.5 units	0.5 to 3 units
Present	1.0 % (34 nodes)	98.6 % (3366 nodes)	0.4 % (14 nodes)
3 ka	0.5 % (17 nodes)	95.6 % (3195 nodes)	3.9 % (131 nodes)
6 ka	0.9 % (30 nodes)	98.8 % (3388 nodes)	0.3 % (10 nodes)
9 ka	0.8 % (27 nodes)	98.6 % (3346 nodes)	0.6 % (19 nodes)
12 ka	0.4 % (14 nodes)	99.5 % (3300 nodes)	0.1 % (4 nodes)

Table 5.1: Summary of the difference analysis between both grids.

All time periods yielded good results with less than 4.5 % of over and underestimations. A plus or minus 0.50 units was allocated in order to take into account the continuous character of the estimates of the grid files which would probably fall close to the target indicator estimate of the data file. At 0 ka, the results are excellent where the main patterns are similar (Figure 5.5 a). Furthermore, the difference maps show that over and underestimation occur mostly in and around distinct boundaries. For example, the southern region of the Great Lakes in North America shows two overestimations of the continuous estimates at the extreme boundary of that region. This is most probably due to the continuous estimate being higher than the reclassification procedure based on the maximum probability vector. The results presented in the summary table (Table 5.1) indicate that 98.6 % of all grid nodes fall within -0.5 and 0.5 units. The difference map of 3 ka shows an increase in the number of points giving different estimates (Figure 5.5 a). Most of the over and underestimates are located along the boundaries where the reclassification procedure is partly responsible because of the distinct boundaries established by this approach. Still, only 4.4 % of grid nodes or 148 estimates are greater than +/- 0.5 units. At 6 ka, both approaches give similar results (Figure 5.5 a). Again most over and underestimation mostly occur at boundaries between patterns

(1.2 % of grid nodes or 40 estimates). The map of 9 and 12 ka show that over and underestimations occur more randomly in Europe (Figure 5.5 b). However, the main spatial patterns are evident also for these time periods with less than 1.5 % and 0.5 % of estimates being greater than +/- 0.5 units respectively.

In summary, both approaches have produced almost identical patterns. The main distinction between both approaches resides in the location of boundary limits and unrepresented regions. While the indicator approach produced distinct breaks between regions or patterns due to the reclassification procedure or mutual exclusivity of the categories, the continuous approach yielded more continuous estimates giving rise to discrepancies in those region at those locations. However, the results yielded satisfactory outputs for all time periods under study and enables the use of both approaches to be compared to General Circulation Models outputs (GCMs) in order to infer global hydrological changes through time. The next chapter will discuss such comparisons with GCM's in a paleoclimatological perspective.

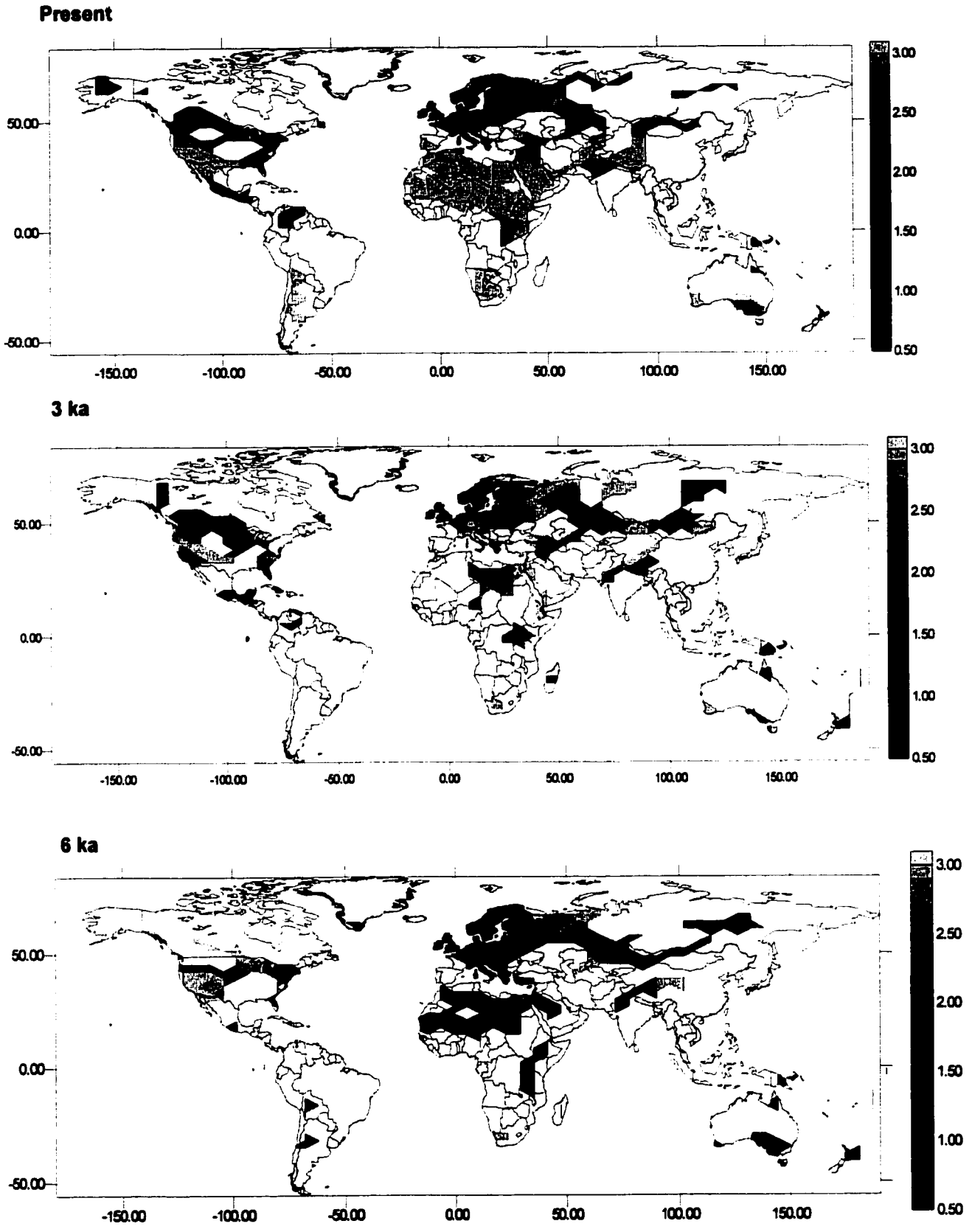

Figure 5.1 a: Lake status maps under climate continuum for present, 3 ka and 6 ka.

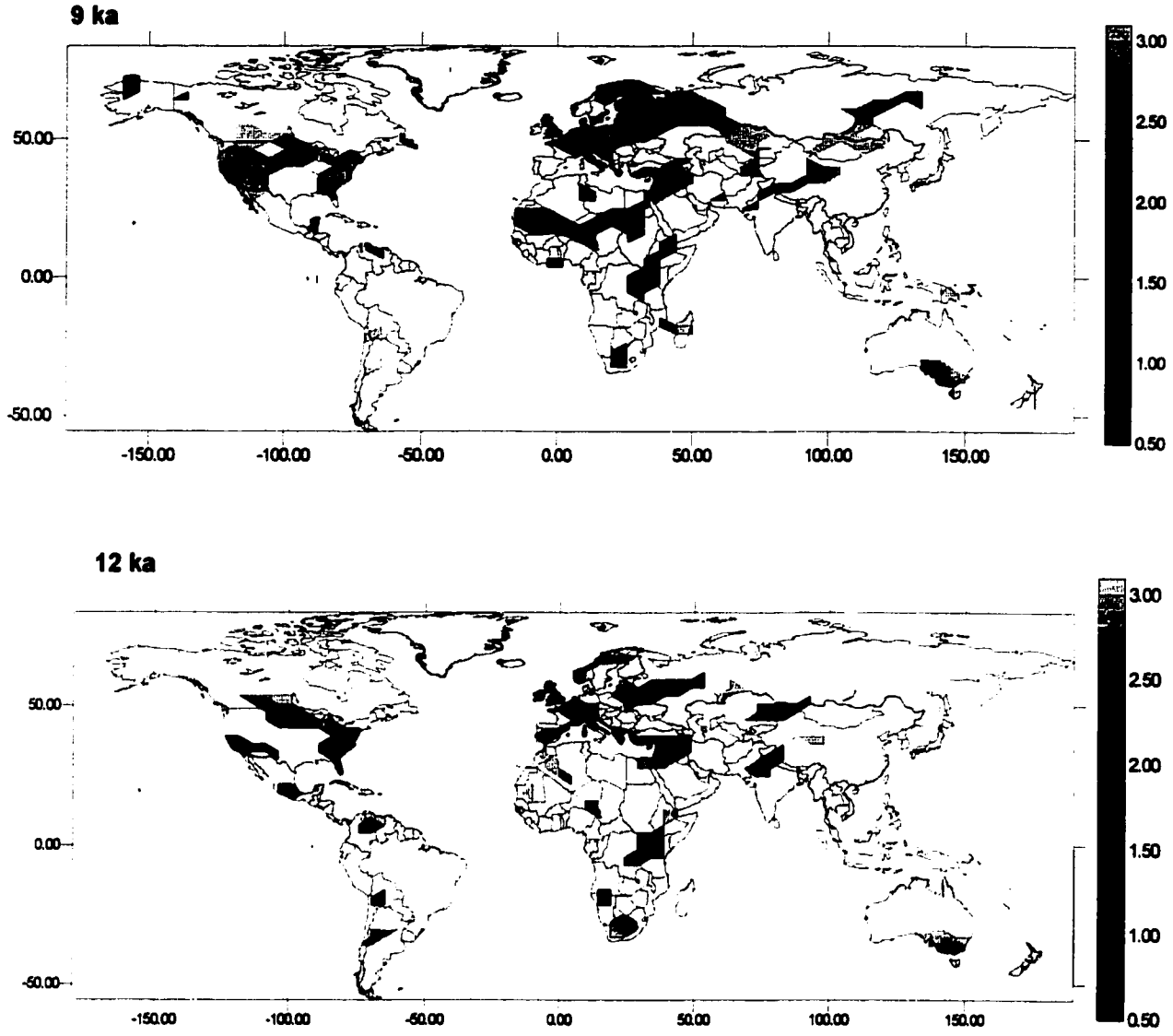

Figure 5.1 b: Lake status maps under climate continuum for 9 ka and 12 ka.

Present

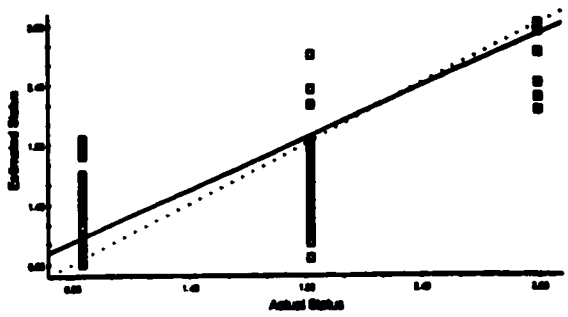

Regression coefficient = .865 (SE = .019 , r2 =.830, y intercept = 0.32)

3 ka

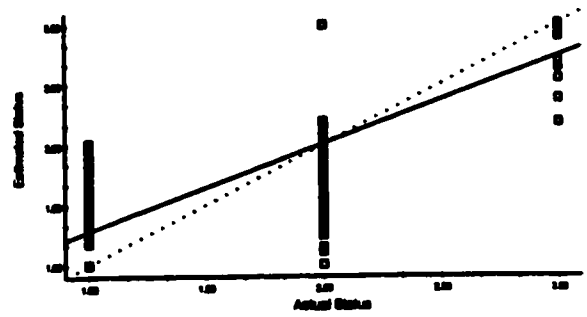

Regression coefficient = .728 (SE = .038 , r2 =.656, y intercept = 0.55)

6 ka

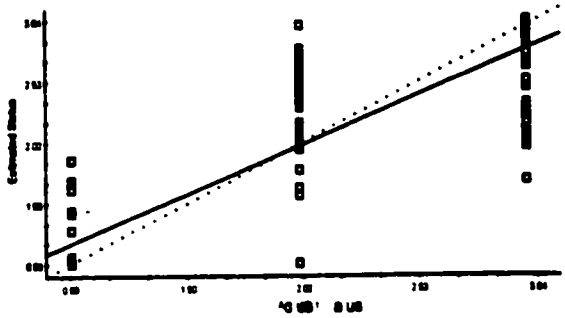

Regression coefficient = .817 (SE = .033 , r2 =.730, y intercept = 0.35)

9 ka

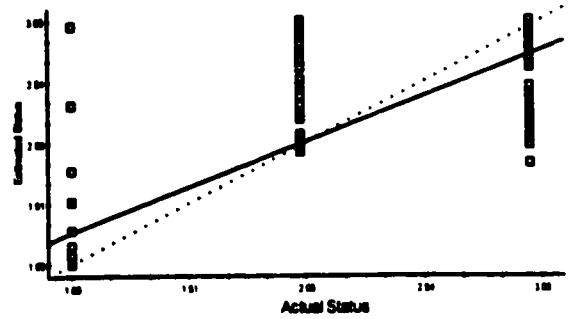

Regression coefficient = .750 (SE = .043 , r2 =.657, y intercept = 0.51)

12 ka

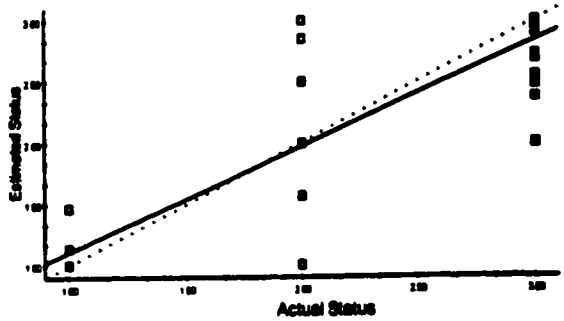

Regression coefficient = .865 (SE = .051 , r2 =.780, y intercept = 0.24)

Figure 5.2: Cross-validation results for present, 3 ka, 6 ka, 9 ka and 12 ka.

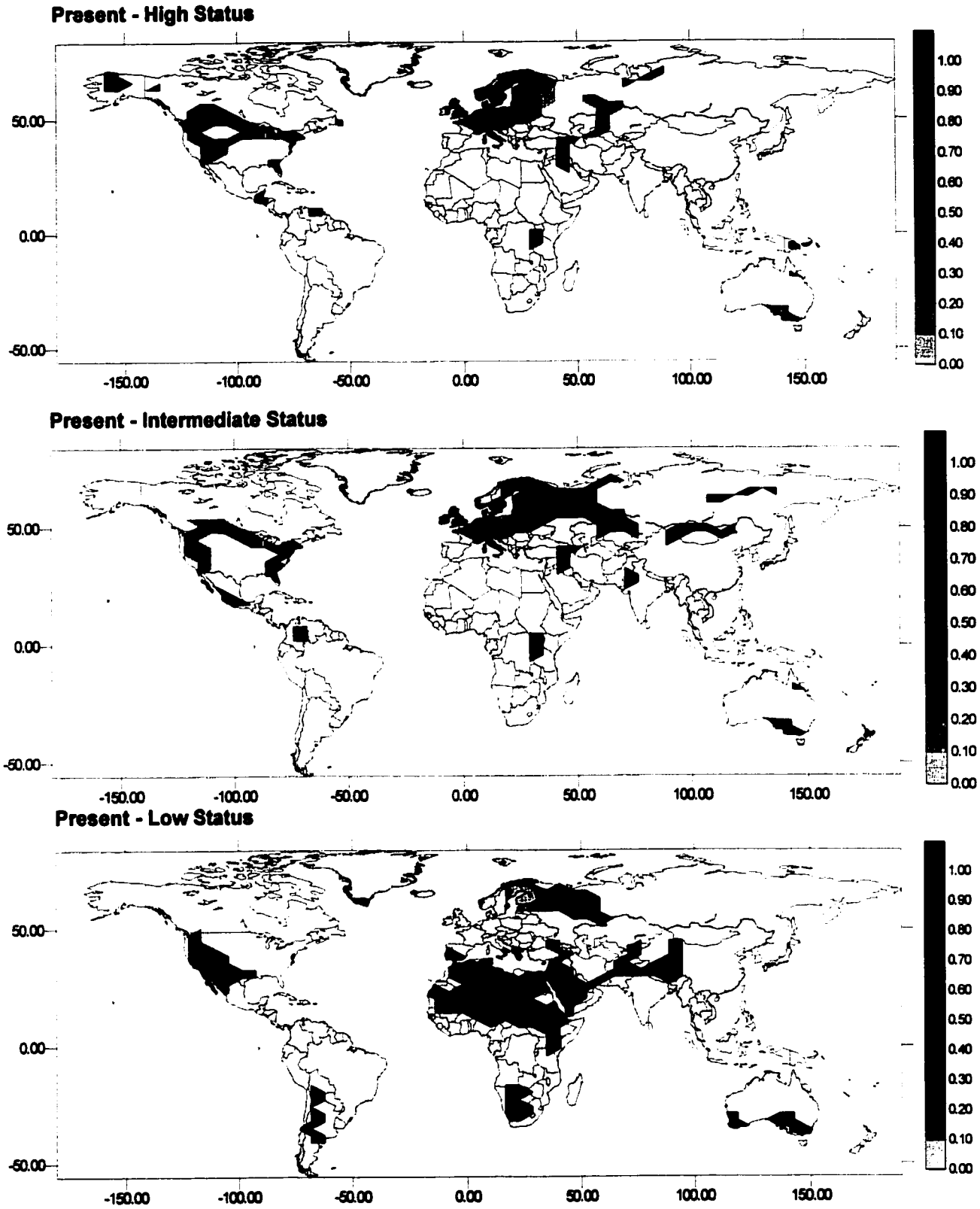

Figure 5.3 a: Indicator estimation of the probability of occurrence for each lake category at 0 ka.

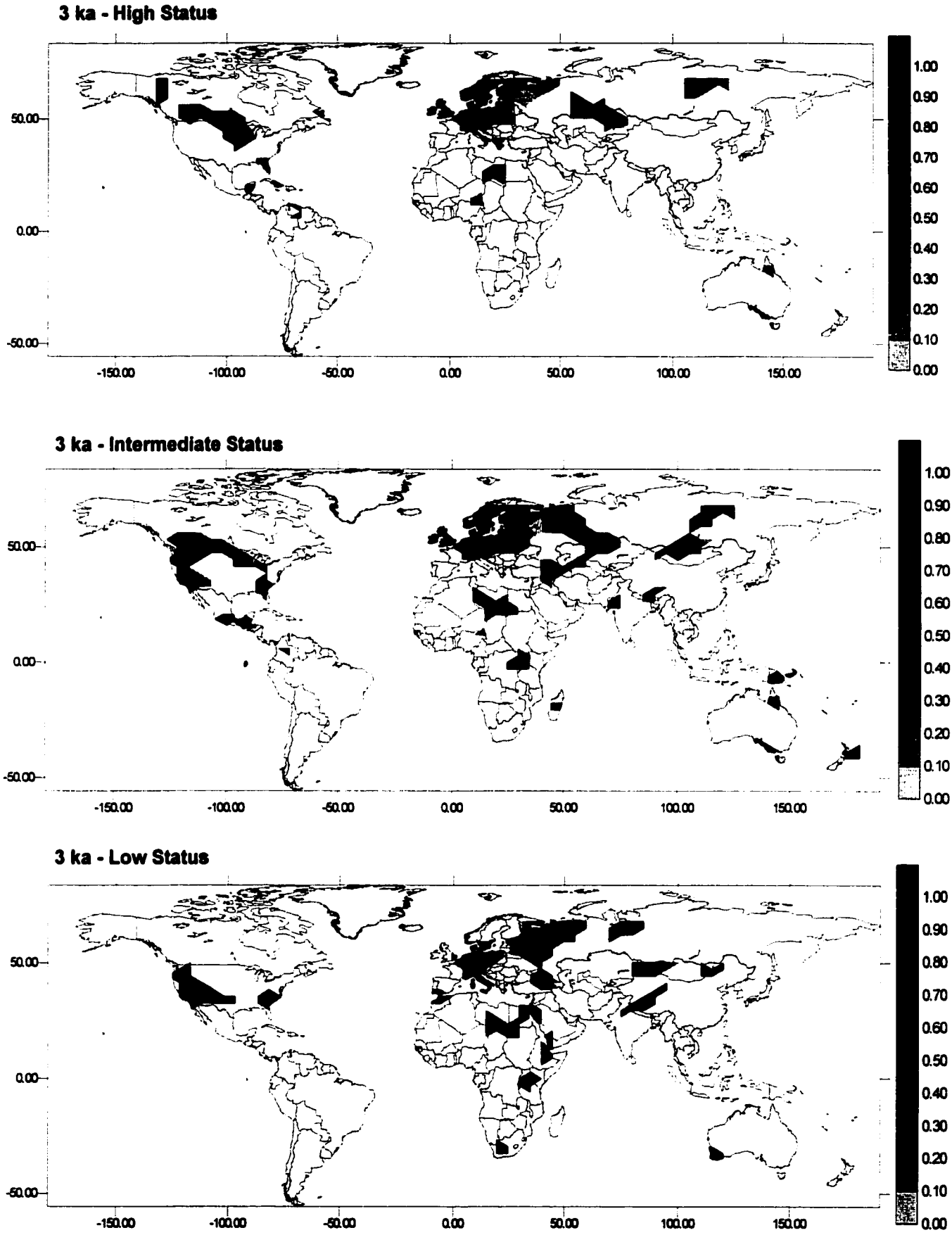

Figure 5.3 b: Indicator estimation of the probability of occurrence for each lake category at 3 ka.

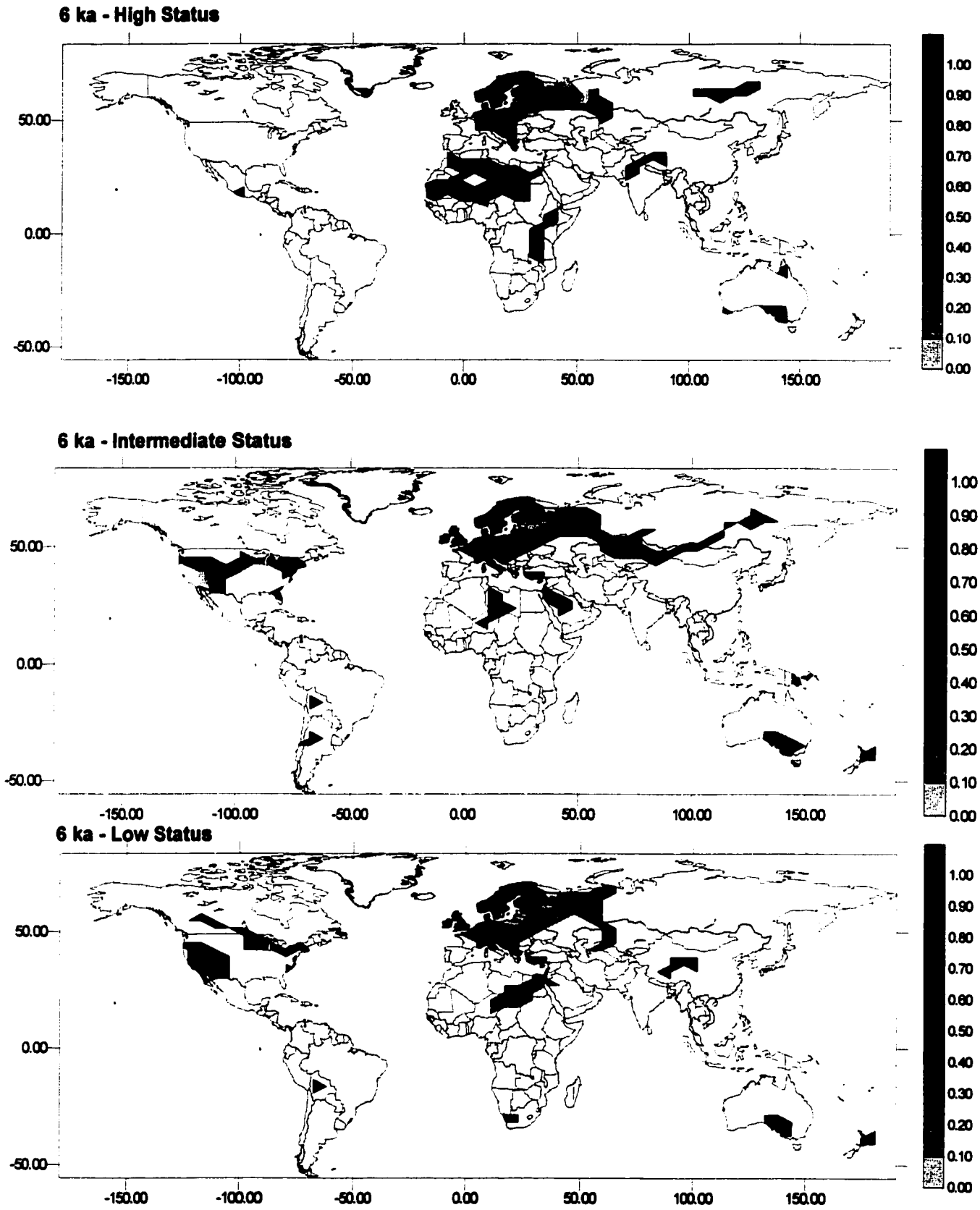

Figure 5.3 c: Indicator estimation of the probability of occurrence for each lake category at 6 ka.

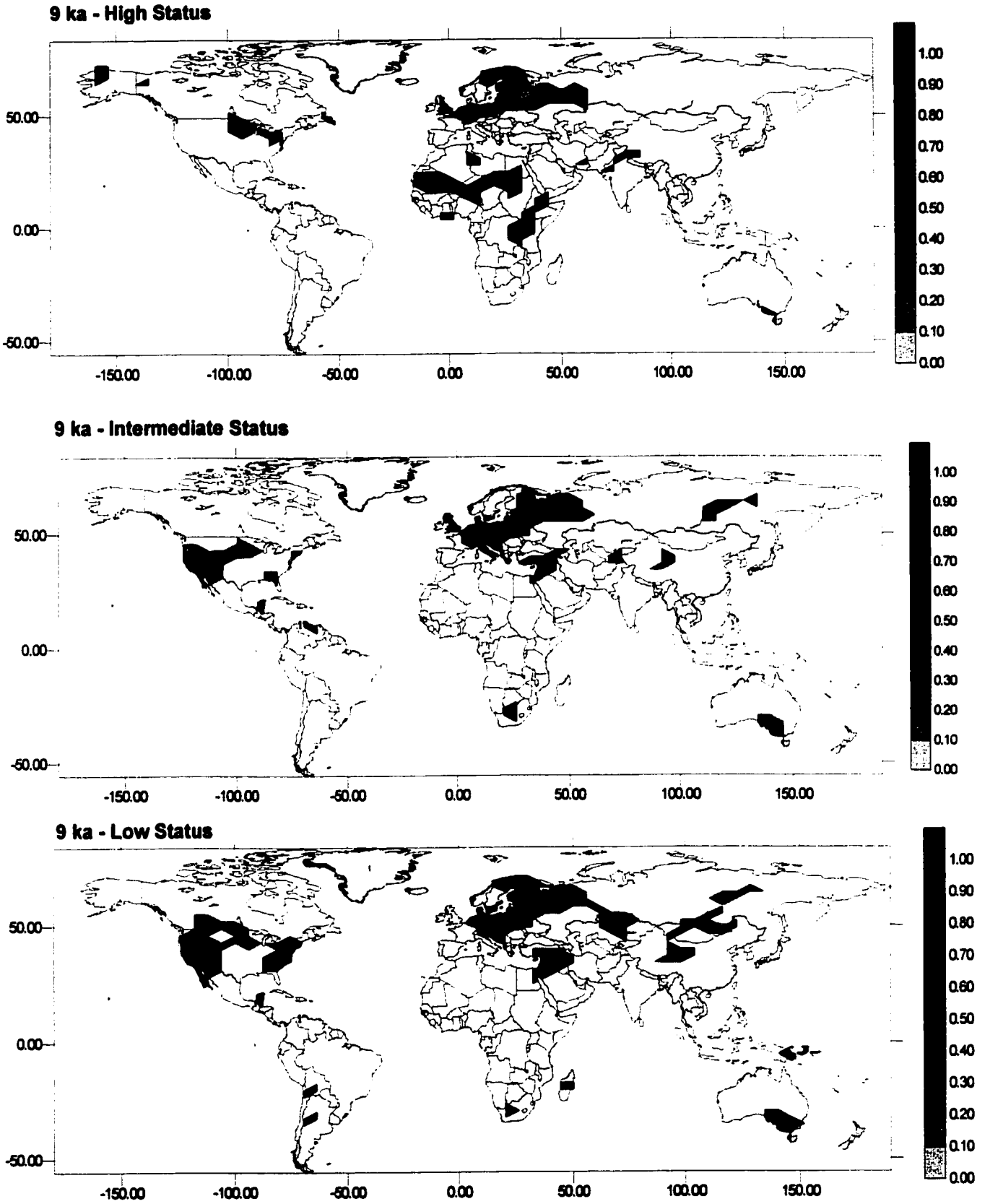

Figure 5.3 d: Indicator estimation of the probability of occurrence for each lake category at 9 ka.

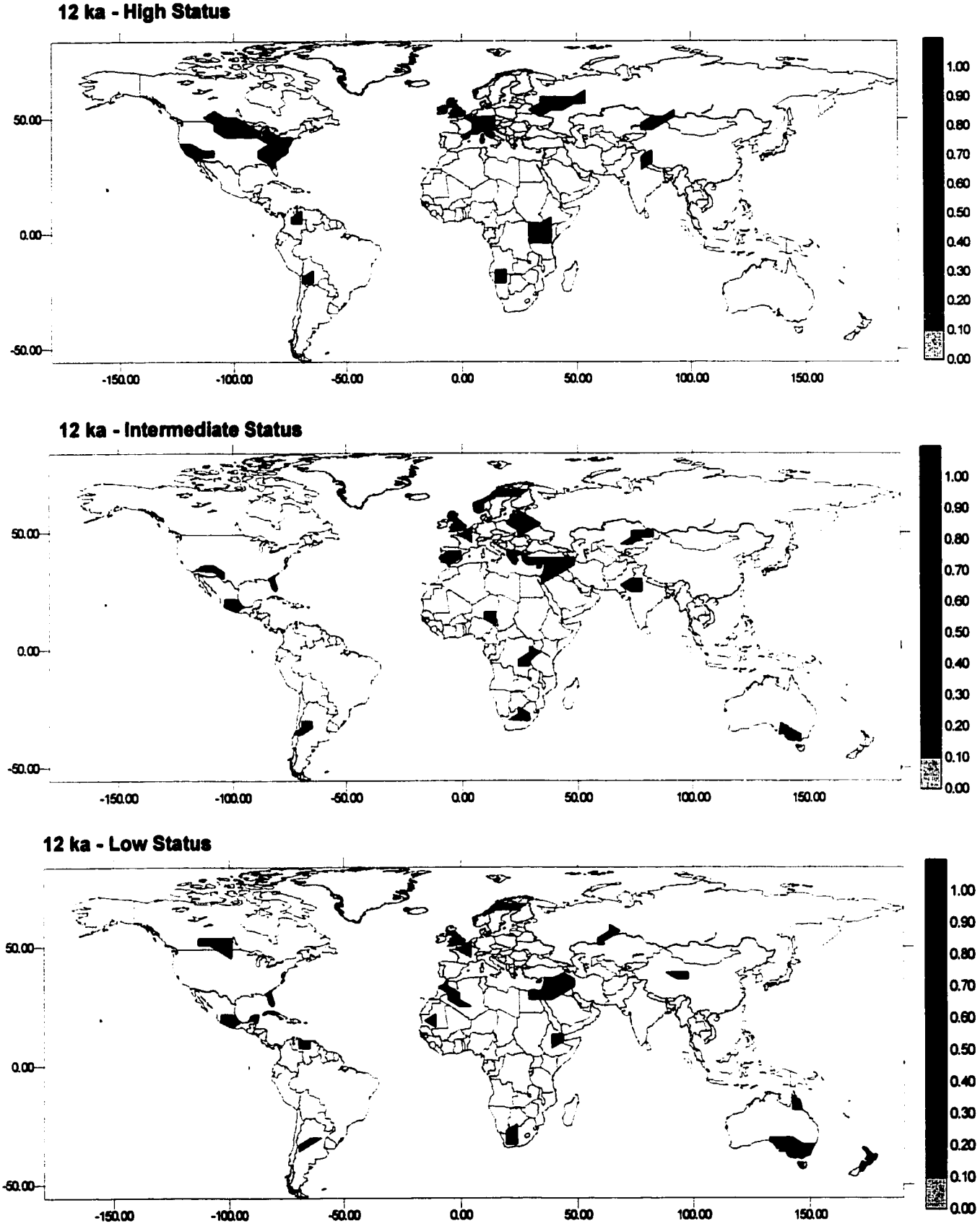

Figure 5.3 e: Indicator estimation of the probability of occurrence for each lake category at 12 ka.

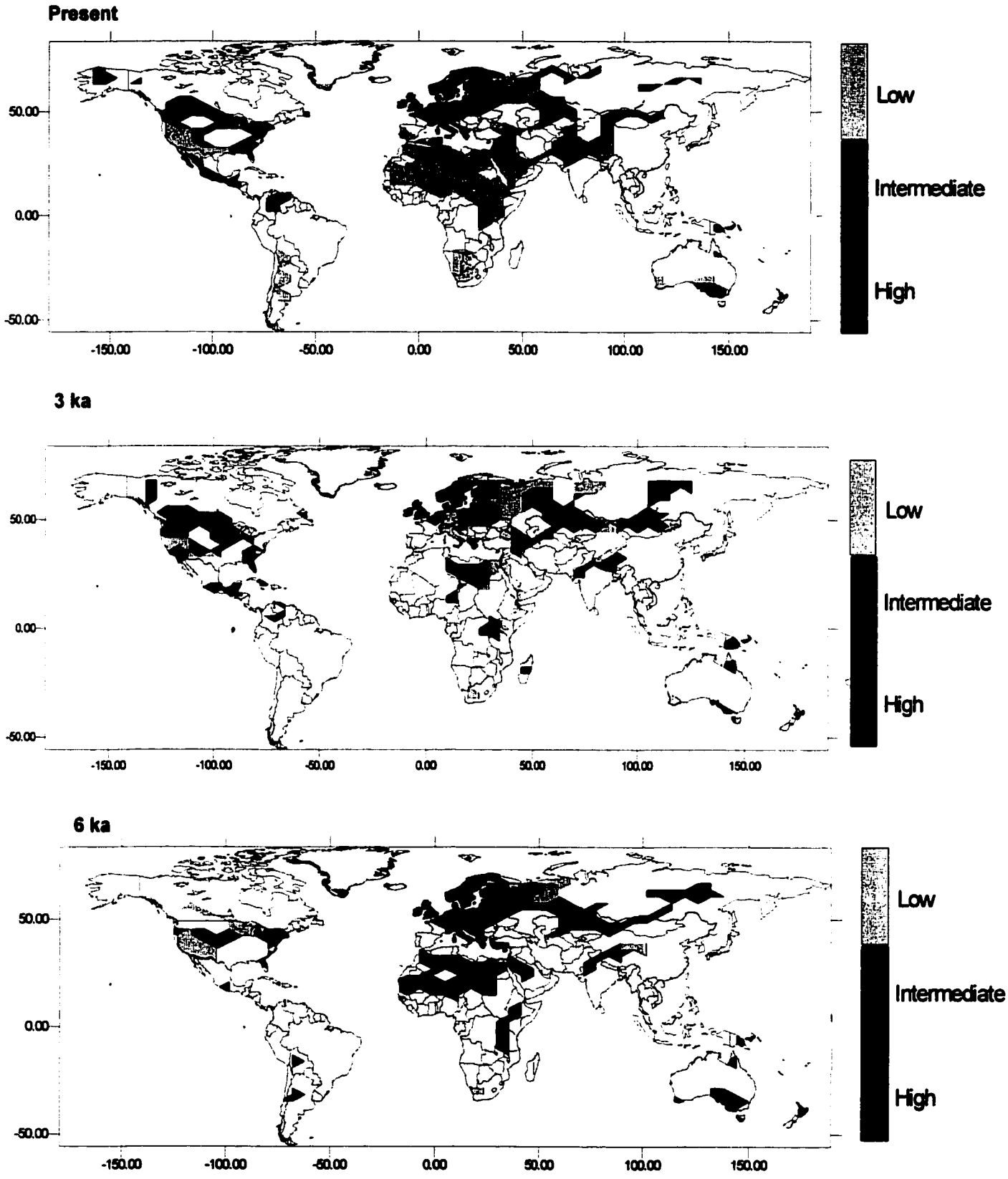

Figure 5.4 a: Indicator maps after reclassification for present, 3 ka and 6 ka.

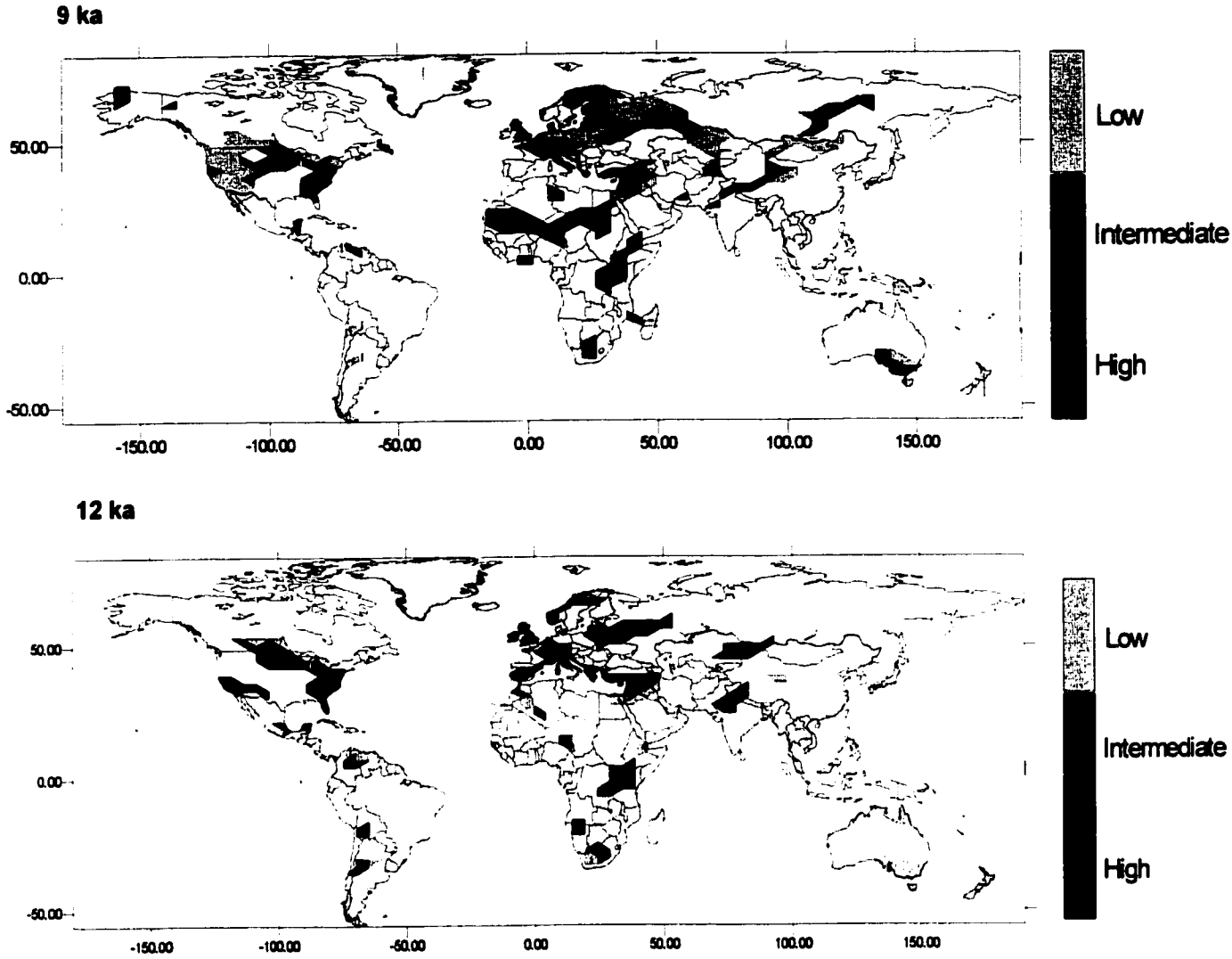

Figure 5.4 b: Indicator maps after reclassification for 9 ka and 12 ka.

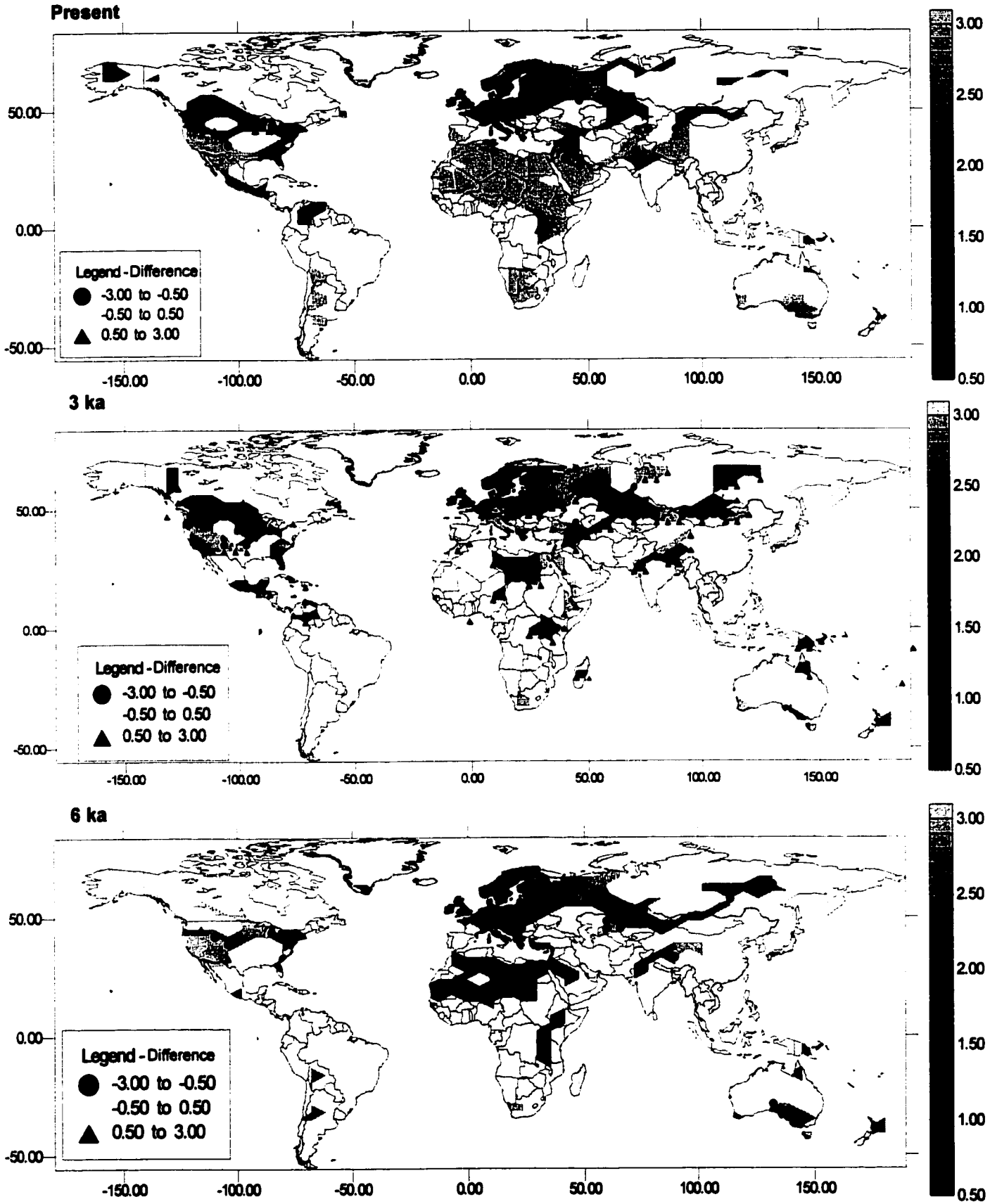

Figure 5.5 a: Difference maps between the two approaches for present, 3 ka and 6 ka.

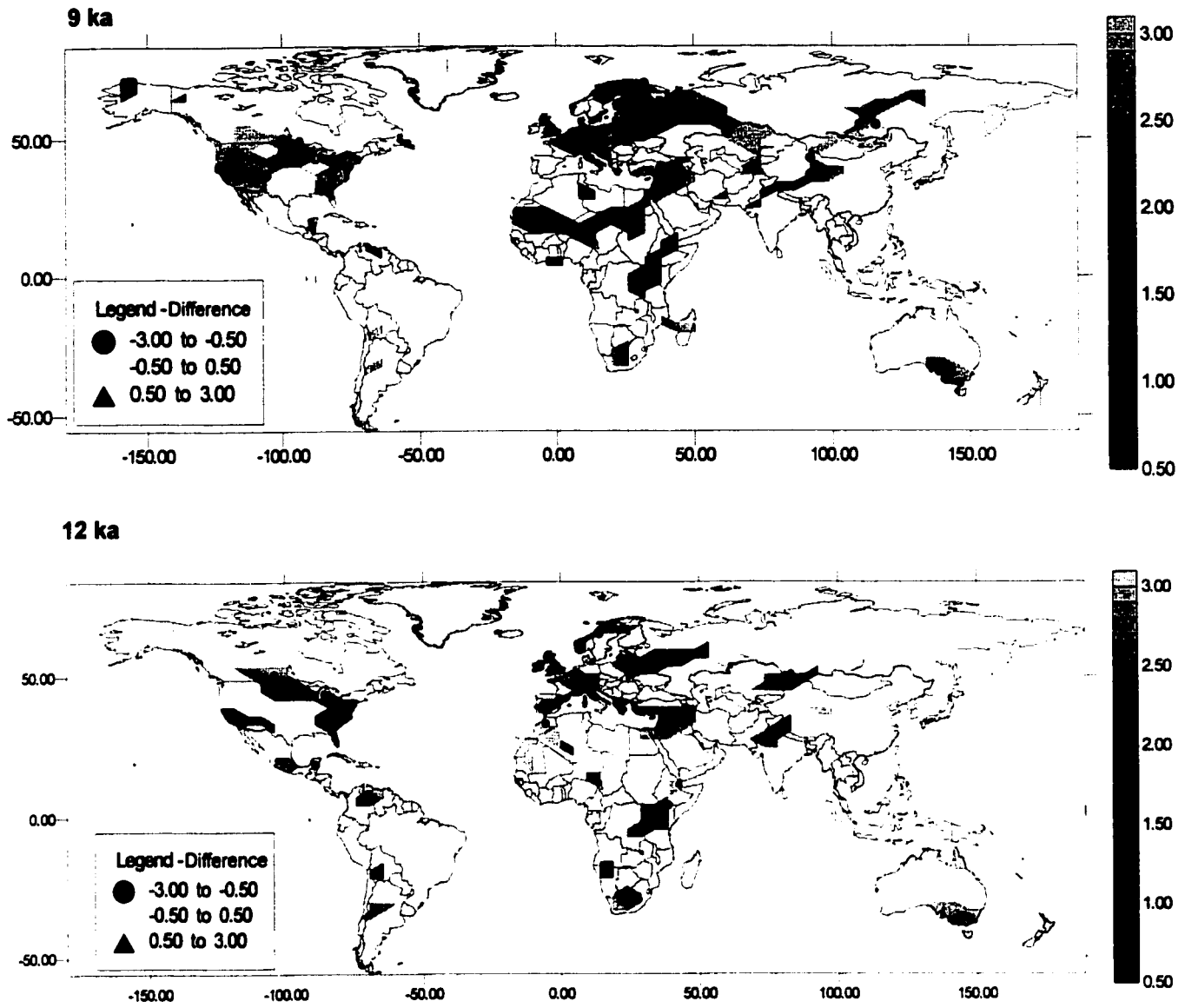

Figure 5.5 b: Difference maps between to the two approaches for 9 ka and 12 ka.

Chapter 6

Lake Level Variations and Global Hydrological Change

6.1 Introduction

Regional climates vary continuously on time scales ranging from years to glacial periods to the age of the earth. This climatic variability is caused in part by forcings (Peixoto and Oort, 1992), comprising, among others, the Milankovitch astronomical parameters (eccentricity of the orbit, axial precession and obliquity of the ecliptic), insolation, the composition of the atmosphere, oceanic circulation and temperature, the presence of ice sheets and long-term tectonic factors (ie. continental drift, mountain building). Understanding the relative importance of these, or other factors, on the climate of any scale is the fundamental goal of paleoclimate research.

Atmospheric general circulation models (AGCMs) are used to simulate broad-scale patterns in atmospheric circulation. Numerous time periods throughout the Earth's history have been simulated using AGCMs, however the Quaternary has received the most attention because the boundary conditions are better known, and because there are large amounts of data available for this period for validation. Some example of modelling experiment studies are CLIMAP project (1976), Kutzbach (1981), Boer *et al.* (1984), Kutzbach and Guetter (1986), COHMAP members (1988), Rind *et al.* (1989), Schultz *et al.* (1992), Marshall *et al.* (1997), Hewitt and Mitchell (1997), Texier *et al.* (1997), and Vettoretti *et al.* (1998). These modelling experiments are used to simulate particular climate processes, or to test hypotheses of forcing mechanisms. Output from these models need to be tested against maps of paleoclimate data. Data-model comparisons can thus make significant

contributions to paleoclimate research in that they determine to what extent these climate models accurately simulate the past and which of the various models are the best estimators of climate. However, to properly test the model output, the paleoclimate data need to be (a) spatial, and cover as large a part of the globe as possible and (b) objectively derived independently of the model output.

One source of information about past climate are lake level variations. Lakes respond to the hydrological balance over its surface and catchment over many time and space scales (Street-Perrott and Harrison, 1985). Lake depth and areal extent are controlled by several factors, including local non-climatic, as well as climatic ones, and any individual lake integrates all these factors in its record of lake levels. However, when a majority array of lakes in a region fluctuate in a similar way, then it can only be climatically controlled (Harrison *et al.*, 1991).

Lake level fluctuations leave traces in the shores, including drowned beaches. Changes in the area and depth influence the biotic and abiotic processes of the lake and its catchment, and these leave a record in lake sediments so that sediment-stratigraphic analyses can also be used to reconstruct past lake level fluctuations (Harrison *et al.*, 1991). Variations in lake area and depth have been reconstructed using multiple geomorphic, geological and biostratigraphic evidences as indicators (Street-Perrott and Harrison, 1985).

Lake level data, available from throughout the globe, have been extensively used in paleoclimate research as an indicator of past regional climate (Street and Grove, 1976,79, Street-Perrott and Harrison, 1985; Harrison and Metcalfe, 1985 a,b; Harrison, 1989; Guiot *et al.*, 1993; Yu and Harrison, 1995, a,b; Cheddadi *et al.*, 1997). However, little has been done to objectively study these spatial patterns. An objective study of the lake-level data can isolate the regional patterns in any of

the many sources of variability in the data. For example, some sites may not be ideal or sensitive enough for regional climate reconstructions, or in some cores the stratigraphic record may be incomplete. The available evidence of lake level change may have alternative interpretation or may suffer from poor radiocarbon dating. However, lake levels sites that are primarily controlled by regional climatic variations should be spatially coherent within different regions (Harrison *et al.*, 1991). The identification of these spatial patterns in lake levels variations, and this is true for any proxy climate data, is the first step in the study of the mechanisms that govern climate change using terrestrial observations.

Previous data-model verification studies using lake-level data have been qualitative visual comparisons of the observations in lake status change (Street and Grove, 1979; Harrison and Metcalfe, 1985; Harrison *et al.*, 1991; Yu and Harrison, 1996) or semi-quantitative using regional averages of lake data (Kutzbach and Street-Perrott, 1985; Harrison, 1989; Webb *et al.*, 1993). More recently was an attempt at a quantitative comparison using only the lake data which had a continuous record for 0 and 6 ka (Qin *et al.*, 1998). This is limited due to the lack of objectivity in the comparison and the difficulty in determining the regional signal in point maps exhibiting considerable fine-scale variability.

In this paper, lake-level data are objectively analysed to identify regional climatically controlled spatial patterns. These gridded lake status data are then compared to model simulations. To objectively identify the climatically-induced lake status spatial patterns requires the analysis of spatial dependence between sites at different spatial scales. In this study, the geostatistical approach is used to measure the spatial autocorrelation between sites over different spatial scales for several time periods, in order to extract the regional climate signals at the global scale. Once patterns are identified, the gridding of these spatial patterns requires a model. Geostatistical models

enable estimation of unknown locations between sites where the lake status is measured. Estimations will enable mapping of the spatially coherent patterns in an objective way. The mapping is here done under two assumptions. First, lake-level status is analysed under the assumption of climate continuum. It is assumed that a region of high lake status will decrease in status towards a low region through a transitional or intermediate region. Therefore, the lake data is assumed to be spatially continuous interval data. Next, the data is examined assuming mutual exclusivity or independence between regions. A region of high lake status is independent from a low or intermediate adjacent one. Therefore, the data is assumed to be spatial categorical data with mutually exclusive classes.

We then use the gridded regional lake status dataset to compare with four simulations of the climate at 6 ka in order to quantify the degree of agreement between estimated lake status regional patterns and simulated regional moisture balance. We compare the gridded lake status change at 6 ka with two versions of the Canadian Centre for Climate Modelling and Analysis (CCCMA GCMII), and two versions of the National Centre for Atmospheric Research (NCAR) Community Climate Model (CCM0 and CCM1).

6.2 Lake Level Data

A global lake level database was assembled using three available lake status datasets in order to maximize geographical coverage. The Oxford Lake-level Database (Street-Perrott *et al.*, 1989), which emphasizes closed-basin lakes, is the largest. This database is global in extent and covers the last 30,000 ka years estimated at 1,000 year intervals. However, geographical coverage is unequally distributed. The European Lake Status Database (Yu and Harrison, 1995 a) contains records from 118 sites across Europe spanning 30,000 ka years B.P. estimated at 500-yr intervals,

in which temperate or overflowing lakes are also included. The Former Soviet Union (FSU) and Mongolia Lake Status Database (Tarasov *et al.*, 1994) comprises 98 basins for the FSU and 5 basins from Mongolia and covers the last 15,000 ka years at 500-yr intervals, where Western Russia is particularly well represented.

The Global Lake Level Database used in this study thus consists of records of paleolake level reconstructions at 1,000 ka year intervals for 579 lake sites spanning the last 30,000 ka years and global in extent. However, the geographical distribution is irregular, and some regions of the world are still unrepresented or poorly represented. In addition, geographical coverage decreases through time (see Chapter 2; Figure 2.4) Each of the datasets included was verified for consistency using the available documentation. Inconsistencies, such as reversed coding and duplicate coordinate sites, were addressed and made consistent with the Oxford Lake Level Database. The Global Lake Level Database contains continuous and discontinuous chronological sequences; sites that have no record for a particular time interval are given a 0 code for "no status". Chronologies are provided either by ^{14}C dating or correlation with a well established ^{14}C regional stratigraphy. Lake sites where water-level change appears to have been influenced by non climatic factors, such as tectonism, glacier fluctuations or human impact, have been excluded (Street-Perrott and Harrison, 1985; Yu and Harrison, 1995a and Tarasov *et al.*, 1994). Dating control for all sites are based on the COHMAP dating control scheme (see Webb, 1985).

Coding of the lake status (or relative water depth) for each sites have been standardized into three categories, with an overall frequency of occurrence in the datasets, in order to render all basins comparable, regardless of size (Street-Perrott and Harrison, 1985). In the case of the Oxford Lake Level Database, the categorisation is based on absolute altitudinal range of fluctuation, where low lake status is assigned to 0-15% of the total range of fluctuation, including dry lakes; intermediate

status to 15-70% of the total range and high status to 70-100% of the total range of fluctuation, including overflowing lakes. The lower and upper boundaries between lake status classes in the European and FSU databases, which contain temperate lakes, are not based on absolute altitudinal range, rather they are defined so as to obtain a broadly similar frequency of occurrence of each lake status category (Harrison *et al.*, 1993).

6.3 Model simulations

Four sets of climate simulations for 6 ka and modern were used in this study. These model outputs correspond to two versions of the NCAR Community Climate Model (CCM0 and CCM1) and two versions of the Canadian Centre for Climate Modelling and Analysis (CCCMA) General Atmospheric Circulation Model (AGCM).

The NCAR CCM0 and CCM1 models have a resolution grid size of ca 4.5° latitude by 7.5° longitude corresponding to an R15 spectral truncation run. The CCM0 simulation (Kutzbach and Guetter, 1986; COHMAP Members, 1988) was run in 'perpetual' January and July mode with prescribed effective soil moisture. Sea surface temperatures (SSTs) and sea-ice distribution at 6 ka were prescribed to be the same as in the control. CO_2 was set to 330 ppmv in both 6 ka and control experiments. The computed annual P-E averages (mm/yr) were calculated following the Qin *et al.*, (1998) scheme, using the January and July averages weighted accordingly to the length of the summer and winter half-year. The CCM1 simulation (Kutzbach and Guetter, 1986) was run with a full-seasonal cycle. Interactive soil moisture was calculated using a one-layer soil with a field capacity of 15 cm. There was a 50 m mixed-layer ocean allowing SSTs and sea-ice distribution to be calculated. CO_2 was set to a 'pre-industrial' level of 267 ppmv in both 6 ka and control simulations. In this case, the computed annual P-E (mm/yr) averages were calculated using the

monthly averages and weighted according to the length of each month (Qin *et al.*,1998).

The two set of experiments from the CCCMA represent a second generation AGCM (GCMII). Both model simulation outputs used in this paper have a *ca* 3.75° latitude by 3.75° longitude grid size corresponding to an T32 spectral triangular truncation run (Vettoretti *et al.*, 1998). The first model simulations (hereafter: CCCfix) were run for 12 annual cycles where the last 10 annual cycles were used to compute monthly, seasonal and annual climatology averages. The CCCfix simulation uses prescribed SSTs and sea-ice for both 6 ka and control experiments. CO_2 concentrations were set to 'modern' levels of 345 ppmv for the control simulation while a 'pre-industrial' CO_2 level of 280 ppmv was prescribed for the 6 ka simulation. The second set of simulations (hereafter: CCCcal) calculates SSTs and sea-ice using a mixed layer ocean and sea-ice module as described in McFarlane *et al.*, 1992. CO_2 is set to a 'pre-industrial' level of 280 ppmv for both the control and 6 k simulations. The CCCcal control simulation was run for 50 annual cycles, where the last 10 annual cycles were averaged to produce monthly, seasonal and annual modern climatologies. The CCCcal simulation for 6 ka was run for 40 annual cycles, where the last 10 annual cycles were averaged to produce the 6 ka climatologies. In both sets of simulations, annual P-E averages (mm/yr) were computed using the annual P-E (mm/day) weighted according to the length of a year.

6.4 Methods and Results

In this paper, the geostatistical approach is used to describe, measure and grid the dependence between lake sites at different spatial and temporal scales under two assumptions. First, the data is analysed under the assumption of climate continuum where the data are assumed spatial continuous interval data. Next, the data are analysed under the assumption that they are spatial categorical data with mutually exclusive classes. We assume that a region of high lake status is

independent of an adjacent intermediate or low lake status region. The results of the application of these approaches include (a) the identification of large-scale patterns in the lake status data, (b) the identification of small-scale variability or influential outliers, and (c) the modelling of the underlying spatial structure. These will permit robust estimates of regional lake status at 3,000 ka years interval covering the last 12,000 years B.P.

6.4.1 Exploratory spatial data analysis (ESDA)

The initial step in any geostatistical study is exploratory spatial data analysis. Distinct spatial patterns in many spatial data may be difficult to identify because of fine-scale variability (Isaaks and Srivastava, 1989). A detailed visual analysis using symbol maps was conducted to analyse the spatial distribution of lake status sites, and aid in the identification of distinct spatial patterns for all time periods under investigation (see Chapter 3, section 3.2,3.3). While some regions of the world are well represented such as Europe and Northern Africa, others are left unrepresented, for example, most of Eastern Asia and South America. There is also a decrease in site density through time.

Fine-scale variability is present in most regions for all time periods studied especially at 3 and 9 ka (see Chapter 3; figures 3.3 a-e). In spite of this variability in different regions of the world at 0 ka, distinct spatial patterns in lake status can be visually identified, especially over North Africa and North America (Figure 3.4 a). Due the heightened fine-scale variability that characterises 3 ka in most regions of the world, the patterns are not as obvious as 0 ka. In addition, certain regions, for example Northern Africa, have declined significantly in the number of available sites (Figure 3.4 b). Contrary to the situation at 3 ka, lake status at 6 ka visually exhibit more coherent patterns. Fine-

scale variability across most of the regions is still present but to a lesser degree than at 3 ka. However, there remain many regions where both high and low lake status are found in close proximity (Figure 3.4 c). An increase in fine-scale spatial variability is evident at 9 ka and is comparable to that of 3 ka which suggest a possible transition phase in the global hydrological cycle. Africa is the only region that exhibits low spatial variability (Figure 3.4 d). Lake status at 12 ka display a decrease in fine-scale variability in most regions of the world due in part to the decreased geographical coverage (Figure 3.4 e). Although there are exceptions, such as southwestern Europe and North America. The fine-scale variability identified at this stage is global in extent for all time periods under study. This suggests that the lake status database may contain potential interpretation errors and/or sites that may not be representative of the large-scale climate patterns within a given region.

An investigation into fine-scale variability identified potential interpretations errors that may be present in the lake data. This investigation involved a region of Europe where a majority of lakes are low at 3 ka (Figure 3.5). Within this region of low lake status is Lac de Chalain which is coded high. Using the available documentation, it was identified that Lac de Chalain which is close in proximity to the surrounding low lakes may have been misinterpreted due in part to poor radiocarbon dating and stratigraphic analysis. Although this investigation illustrates potential errors in developing a large database, some investigation into fine-scale variability may confirm the validity of the coding. Two lakes close in proximity could presumably exhibit very different lake status due to local factors influencing the hydrological balance. Since this study deals with a large amount of sites, checking every site for validity in coding would require an enormous amount of time and may prove to be a futile effort. In this case, the analysis points to poor temporal control, but in other areas, it may not be as clear.

The variogram or indicator variogram ($\gamma(H)$) and correlogram functions ($\rho(H)$) are spatial statistics used to describe the extent or range of spatial autocorrelation at different spatial and temporal scales. These statistics describe the spatial continuity as a function of distance between pairs of sample sites (Isaaks and Srivastava, 1989, Deutsch and Journel, 1992). These two statistics are sensitive to outliers, as is true for many statistics. Thus, one approach is to remove outliers from the data. However, this is often arbritary, as some values may have been truly representative of the spatial continuity of the phenomenon under investigation (Isaaks and Srivastava, 1989). Alternatively, the statistic can be estimated using all points, hoping that the underlying structure will still be appropriately estimated. Unfortunately, this may not be possible if the outlier data are too influential.

In general, spatial continuity or autocorrelation is present at 0 ka and to a lesser extent at 12 ka. However, the periods of 3,6 and 9 ka suggest a lack of spatial autocorrelation at all distances investigated. Indeed, the findings reveal that there are large amount of samples that exhibit high variance within relatively small distances (lower lag distances), thus creating a high nugget effect (see Chapter 4, section 4.1). This high nugget effect results in variogram and correlogram structures that suggests a lack of spatial autocorrelation. The large number of samples exhibiting high variance at the lower lags distances suggests a high ratio of fine-scale variability and/or potential interpretation errors present in the datasets. One conclusion of this study is therefore that the lake data contain significant numbers of samples that may not necessarily reflect large-scale climate patterns. Although 0 ka revealed a clearly interpretable variogram and correlogram structure under the first assumption, 3,6 and 9 ka did not. These same results were also confirmed under the second assumptions using the indicator transforms.

If we hypothesize that only large-scale patterns are climatically meaningful, then a climatically-caused spatial scale can be objectively determined from the lake data. Spatial autocorrelation tests whether one site is independent of neighbouring localities. A more appropriate approach to deal with influential points is to focus on local patterns of spatial autocorrelation (Getis and Ord, 1992). The use of local indicators of spatial association (LISA) (Anselin, 1995) has two important uses: the identification of local correlated patterns and the identification of local areas which displays fine-scale variability or negative spatial autocorrelation within specific distances.

The LISA statistics indicate that maximum geographical coverage can be obtained at 500 km distances with less than 10% of sites left with no neighbours in all time periods except for 12 ka (14%) (see Chapter 4 section 4.2). In this study, 500 km is also chosen as the optimal scale of study because the ratio between negative and positive autocorrelation increases with distance. The ratio between positive and negative spatial autocorrelation is high for most time periods and at all lag distances examined (see Chapter 4, section 4.2). These results provide further evidence that the lake data contain a large amount of sites which exhibit fine-scale variability, especially over relatively small distances. The resulting scale was prescribed at 500 km which is consistent for all time periods under study. Samples sites that exhibited negative spatial autocorrelation within this scale were excluded from this study objectively, and this is true for Lac de Chalain at 3 ka. This filtering exercise permitted the extraction of the large-scale climate signal present in the lake data under a consistent scale of study.

In this study LISA is used as an alternative to error-checking, arbitrarily removing outlier samples and other data-cleaning exercises such as including only sites with continuous records (Harrison, 1989, Harrison et al., 1993), quality dating control schemes (Guiot et al., 1993, Cheddadi et al, 1997 and Qin et al., 1998), and qualitative exclusion (Street-Perrott and Harrison, 1984, Harrison and

Metcalfe, 1985 a,b). This resulted in analyses using only a fraction of the sites. This study differs only in that the exclusion is done objectively by deciding on the scale of study. Therefore, LISA enables the filtering of the data to include only the large-scale signal at a consistent scale. The variograms of 3,6 and 9 ka became more clearly interpretable as the filtering exercise resulted in lowering fine-scale variability (see Chapter 4 section 4.3). It is important to note that the initial spatial structures were retained from the original data where the only difference being a lowered fine-scale. The results of both approaches reveal that spatial continuity is present for all time periods and could be modelled with some success (see Chapter 4 section 4.4). LISA is also used to optimize the spatial scale of study in order to maximize global coverage while retaining maximum spatial resolution.

6.4.2 Gridding

Gridding requires a model for estimating values in areas that have not been sampled. One of the advantages of geostatistical estimation techniques is that estimates are based on a clearly stated model (Isaaks and Srivastava, 1989). Geostatistical models were fitted to the clearest interpretable variograms and indicator variograms using best-fit statistics such as r2 and RSS (Reduced Sum of Squares) (see modelling section in Chapter 4). Gridding was performed using both ordinary and indicator kriging with a search radius as prescribed previously of 500 km in order to ensure neighbouring data on which to estimate with confidence. While ordinary kriging yields more continuous estimates between lake status regions, indicator kriging provides a value of uncertainty or probability of occurrence for the binary transformed data of each independent lake status category, rather than an estimate of the value (Deutsch and Journel, 1992, Goovearts, 1997). Indicator kriging involves three distinct steps: (a) the binary transformation of each observation into a binary indicator vector corresponding to the three lake status categories (ie. High = 1,0,0), (b)

indicator variogram analysis and modelling of each independent category, and (c) reclassification of each estimated probability of occurrence into a corresponding lake status based on the maximum probability vector (Goovearts, 1997).

In this study, we use local estimation rather than global estimation to take into account the variability, clustering and scale effect present in the data which may not be representative of the whole world. The choice of a search strategy that restricts the samples included in the local estimation process is important as it allows local rescaling as in the case of variability present in the lake data. Both methods discussed above involve weighted linear combinations where weights assigned by local estimation should account for both the distance and possible redundancy between sample sites (Isaaks and Srivastava, 1989) as in the case of clustering.

The resulting grids under both approaches correspond to a (30x60) or 3° latitude by 6° longitude grid size (see chapter 5; Figures 5.1a,b and Figures 5.3 a,b). After the reclassification of the indicator transforms, both kriging estimates of lake status for all time periods reveal more distinct interpretable patterns, thus resulting in gridded large-scale patterns in lake status. Note that the main spatial patterns are retained from the original data. For example, regions of low variability versus high variability are retained such as North Africa and Europe respectively. Regions where no data were present were restricted by the 500 km search radius so that little extrapolation was undertaken, except in border region where no neighbours are found within the 500 km search. Moreover, both approaches yielded grids which are almost identical, thus suggesting a robust estimation of the large-scale lake status patterns.

The resulting grids produced under both assumption were then compared in order to evaluate the agreement and discrepancies between both kriging methods. Difference maps were constructed

to aid in the evaluation, as indicator kriging estimates minus ordinary kriging estimates. With the ordinary kriging estimates being plotted in the background, only the discrepancies between the two grids are plotted. A leeway of +/- 0.5 units was allocated in order to take into account the continuous characteristic of the ordinary kriging estimates, so that only the over and under estimates that exhibit greater differences are plotted on the foreground. The main discrepancies occur in the proximity of boundaries between regions. This is caused in part by the estimation technique where the indicator kriging approach gave rise to distinct breaks between region , the continuous estimates gave more continuous estimates thus resulting in discrepancies between boundary regions. However, the main spatial patterns in lake status are almost identical.

6.4.3 Holocene lake status change and data-model comparison application

The Holocene lake status change at 3,000 ka years interval are presented as maps to illustrate the spatial patterns of change in regional water balance using the gridded lake status. The maps are produced by computing the anomalies in lake status change (ie. 3-0 ka, 6-0 ka, 9-0 ka and 12-0 ka) using both the indicator and ordinary kriging lake status grids. The lake status anomalies result in five classes, where in the case of indicator kriging +2 means an increase of 2 status classes, +1 an increase of 1 status class, etc. In the case of ordinary kriging estimates, the lake status anomalies result in essentially the same scheme except an +/-0.5 unit is allocated to each class except for the extreme values in order to take into account the continuous aspect of the estimates.

The anomalies in lake status using the lake status grids under both assumption are generally in agreement with the description of Street-Perrott et al.(1989). At 12 ka, the ice sheets were retreating rapidly associated with an orbitally-induced change in insolation. Due to a northward migration of the jet stream, most of North America and Europe was distinctly wetter, except for the

southern Canadian prairies (Figure 6.1 a,b). Higher lake levels were also evident in many regions of Africa associated with enhanced Afro-Asian summer monsoons and land-sea temperature contrasts (Kutzbach and Street-Perrott, 1985). While the ice-sheets margins stood at almost modern positions in most of Europe and Asia and sea surface temperatures were close to modern values by 9ka, the orbitally-induced seasonal insolation were becoming increasingly marked in different regions of the world. In North America, the seasonal increase in insolation and the northward migration of the storm tracks were the main factors contributing to the decrease in lake levels over most of the regions (COHMAP Members, 1988; Harrison, 1989). This is also evident in southern Eurasia resulting from high rates of evaporation in areas beyond the reach of the enhanced tropical monsoons (Street-Perrott, 1986). High lake-levels are evident over much of Northern Africa, northern India and southern Tibet in agreement with a strengthening of the Afro-Asian monsoons. By 6 ka, the ice sheets had disappeared, although the Laurentide ice sheet had remained longer than the Eurasian ice sheets. Although the orbitally-induced seasonal insolation was reached, the remnants of the Laurentide ice sheet still influenced the circulation and caused a widespread persistence of low lake-levels over much of North America (Street-Perrott *et al.*, 1989). The high lake-levels over much of North Africa, Arabia and northern India are in good agreement with a persistent Afro-Asian monsoon circulation. By 3 ka, the seasonal insolation had decreased almost to modern levels as lake status in North America were rising to present levels. A decrease in the westerly transport of moisture caused a fall in lake levels in the Mediterranean regions and interior Eurasia. (Street-Perrott *et al.*, 1989). The weakening Afro-Asian monsoons were responsible for a dramatic fall in lake levels over North Africa, Arabia and South Asia. Almost all lake-levels changes that occurred from 3 ka to modern point to the continuation of trends in lake status patterns observed today (see figure 5.1 a).

To illustrate this potential and versatility of the gridded lake status data in more objective data-model

comparisons we use essentially the same data-model comparison scheme used by Qin *et al.*, (1998). The lake status grids under both assumptions are used to compare the changes in water balance simulated by two versions of the CCCMA (CCCfix and CCCcal) and two versions of the NCAR (CCM0 and CCM1). The anomaly lake status grids at 6 ka (lake status at 6 ka minus lake status at 0 ka: ΔS) compared with model simulated 6 ka anomalies in precipitation minus evaporation (P-E at 6 ka minus control: Δ(P-E) on a grid to grid basis. The gridded lake status data are not only grid estimates but represent homogenous regions of change. The simulated P-E value from each model output is interpolated to the estimated lake status change grid nodes. The difference in lake status at 6ka (ΔS) of each estimated grid node is then compared with the interpolated Δ(P-E) at 6 ka using a modified version of Qin *et al.*, (1998) agreement index scheme; where 1 means an agreement and 0 a disagreement between ΔS and simulated Δ(P-E) at 6 ka. Where no evident lake status change occurs (ΔS = 0), a potential agreement value of 0.5 is assigned, however, it is not compared to other model simulations that generates the smaller Δ(P-E) value as in Qin *et al.*, (1998) (Table 6.1). The latter is done in order to emphasize the agreement between data and different resolution models. We then compute the number of grid nodes that are in agreement or potential agreement, and disagreement expressed in percentages of agreement between data and model output (Appendix I).

Lake status (6-0k)	P-E (6-0k)	Agreement / Disagreement		Kriging technique
IF $\Delta S > 0.5$	*and $\Delta P\text{-}E < 0$*	*1*	*0*	*Ordinary*
IF $\Delta S > 0$	*and $\Delta P\text{-}E < 0$*	*1*	*0*	*Indicator*
IF $\Delta S < -0.5$	*and $\Delta P\text{-}E > 0$*	*1*	*0*	*Ordinary*
IF $\Delta S < 0$	*and $\Delta P\text{-}E > 0$*	*1*	*0*	*Indicator*
IF $\Delta S < 0.5$ and > -0.5		*0.5*		*Ordinary*
IF $\Delta S = 0$		*0.5*		*Indicator*

Table 6.1: Data-model agreement criteria scheme

The persistence of low lake-levels over much of North America seen in lake-level data at 6 ka is not in agreement with CCCcal, except for an area of low lake lakes over the Cordilleran region in western Canada and north-western United States (Figure 6.2 a,b). The CCCfix also does not capture this trend in drier conditions over most regions of North America. CCM0 captures the broad-scale patterns in lake status over much of North America while CCM1 is in agreement with a deficit in moisture over much of North America. Lake status over much of Europe reveals little or no change in conditions, and therefore, is difficult to assess the data-model agreements. The widespread high lake levels over much of North Africa, Arabia and Northern India are not captured by CCCcal, however, the annual P-E signal is known to be weak (Vettoretti *et al.*, 1998). The CCCfix simulation is in better agreement over North Africa. CCM0 fails to capture the northward extension of the Afro-Asian monsoonal belt over North Africa, while CCM1 reveals better agreement over this region, except for the northwestern region.

All four models (CCM1, CCM0, CCCfix) are all approximately comparable with 68%, 66%, 67% of estimated grid cells in agreement respectively (Figure 6.5 (a). The poorest result are obtained using the CCCcal model simulation with 59% agreements for the continuous assumption and 61% under the indicator approach (Figure 6.3 b,c). While CCM1 yielded the best overall performance in this exercise in data-model comparison, the CCM simulations are coarser resolution models than the CCCMA. Indeed, CCM1 and CCM0 simulate broader-scale patterns resulting in an increase in grid cell agreements between the lake status grids for homogenous moisture balance (ΔP-E) regions.

6.5 Discussion

The exploratory spatial data analysis undertaken in this study revealed distinct spatial patterns in lake behaviour at all time periods under study. However, there are still many regions in the world

left poorly represented or unrepresented both spatially and temporally. In addition, dependence between sample sites in space and time is not so obvious as large numbers of sites, close in proximity, exhibit negative spatial autocorrelation thus suggesting potential interpretation errors and/or fine-scale variability over most regions of the world.

The use of the variogram and correlogram functions confirms this variability at small distances, especially at 3, 6 and 9 ka. The variograms of 3,6 and 9 ka revealed a structure close to a pure nugget effect model which is caused by a complete lack of spatial correlation (Isaaks and Srivastava, 1989).This fine-scale variability was consistent over almost all separation distances covered in this study. The lake status data contains this variability for several reasons including, among others, site sensitivity to climate change, quality dating control schemes, coding, and different sampling schemes. Recommendations from this study include (a) going back to the original data to explore the spatio-temporal dependence on a site by site basis and, (b) the coding scheme need to be enhanced, perhaps into a larger number of classes in order to differentiate the intermediate class, as it has been suggested in the past (ie. Much drier to much wetter) (Cheddadi *et al.*, 1997). This would result in more accurate spatio-temporal analysis using the lake data.

The use of local indicators of spatial association (LISA) permitted the identification of local highly correlated patterns from variable ones and, aided in the identification of problematic sites at specific distances. The LISA results further provided evidences of fine-scale variability present in the lake data at several distances spanning 500 km in radius. This analysis enabled the extraction of locally correlated patterns at a consistent scale of study in order to maximize global coverage. The filtering exercise resulted in the exclusion of sites exhibiting negative spatial autocorrelation at a consistent scale. Moreover, it yielded more clearly interpretable variograms on which to estimate the underlying spatial structures for all time periods under both assumptions.

Although both approaches resulted in almost identical grids, there remains methodological questions concerning the estimations, such as anisotropy, which was not explored since different anisotropy can co-exist at the global scale. Non-parametric validation of the models could also be attempted, such as by the use of stochastic simulations. Estimation of unknown locations using irregularly spaced data remains problematic where some regions are more represented than others. Estimation of a more variable region will always suffer in relation to regions that more homogenous. Clustering and redundancy in the data is another problem which will affect the estimates (Isaaks and Srivastava, 1989). In addition, the exclusion of data samples is another consideration to take into account where some samples may have been truly representative of the spatial phenomenon under investigation. The restriction of a 500 km search to ensure neighbouring sample on which to estimate may partly be responsible for the agreement between both sets of grids.

The methodology illustrated here demonstrates that the data contain large-scale patterns that can be objectively determined at a consistent scale of study. The advantage of gridding has the potential of objectively eliminating finer-scale variability in a dataset so that large-scale patterns can be extracted from local noise. The methodology established in this study also recognizes the potential of different spatial and temporal application in order to determine the climate signal present in the lake data at different spatial and temporal scales. It also recognizes that some data samples may be useful at different spatial scales while being unrepresentative at others. The grids also have the potential for data-model comparisons in a more objective way. Objectively determining homogenous spatial patterns, whether at the global or subcontinental scales, results in better resolution in grid to grid comparisons. It is therefore important to establish spatial dependence in the original data.

Finally, the methodology illustrated in this study can be applied to other paleoclimate research fields, such as pollen analysis. Its ability to identify the climate signal from other noises in space and time results in better reconstructions and interpretations using proxy climate data. In the case of lake level variations, the analysis of the spatio-temporal dependence between sites can lead to a better understanding of climate change mechanisms and, hence global hydrological change, as geographical coverage increases in the future.

6.6 Acknowledgments

This paper is a contribution to the Climate System History and Dynamics Programme that is jointly sponsored by the Natural Sciences and Engineering Research Council of Canada and the Atmospheric Environment Service of Canada. A special thanks to M. Sawada of the LPC group of the University of Ottawa. Results of the lake level study have been standardized into a regular Cartesian grid (30x120) 3°x3° form and can be accessed through the Laboratory for Paleoclimatology and Climatology (LPC) web page at http://aix1.uottawa.ca/academic/arts/geographie/lpcweb/.

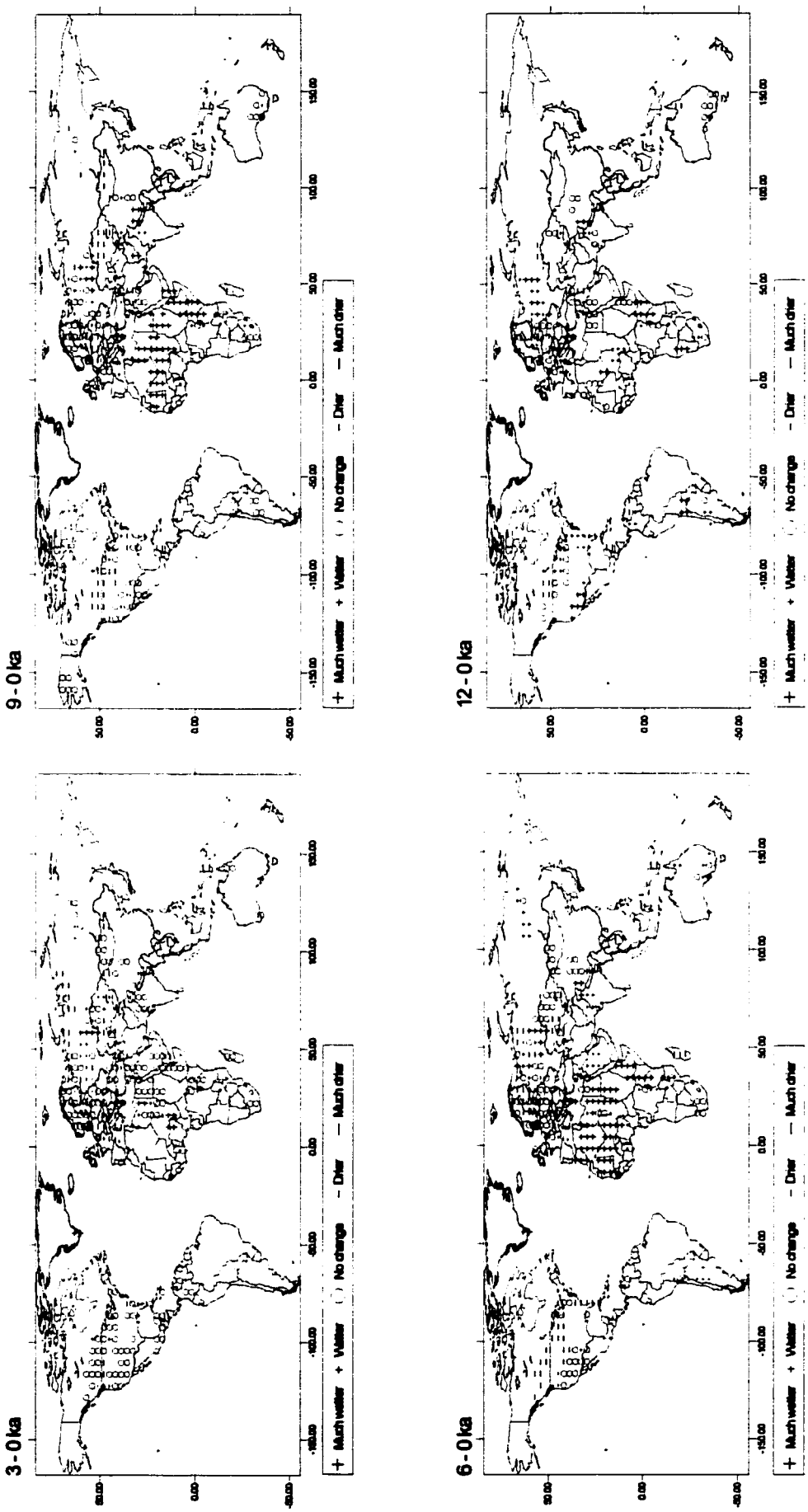

Figure 6.1 a: Anomaly maps under continuous assumption.

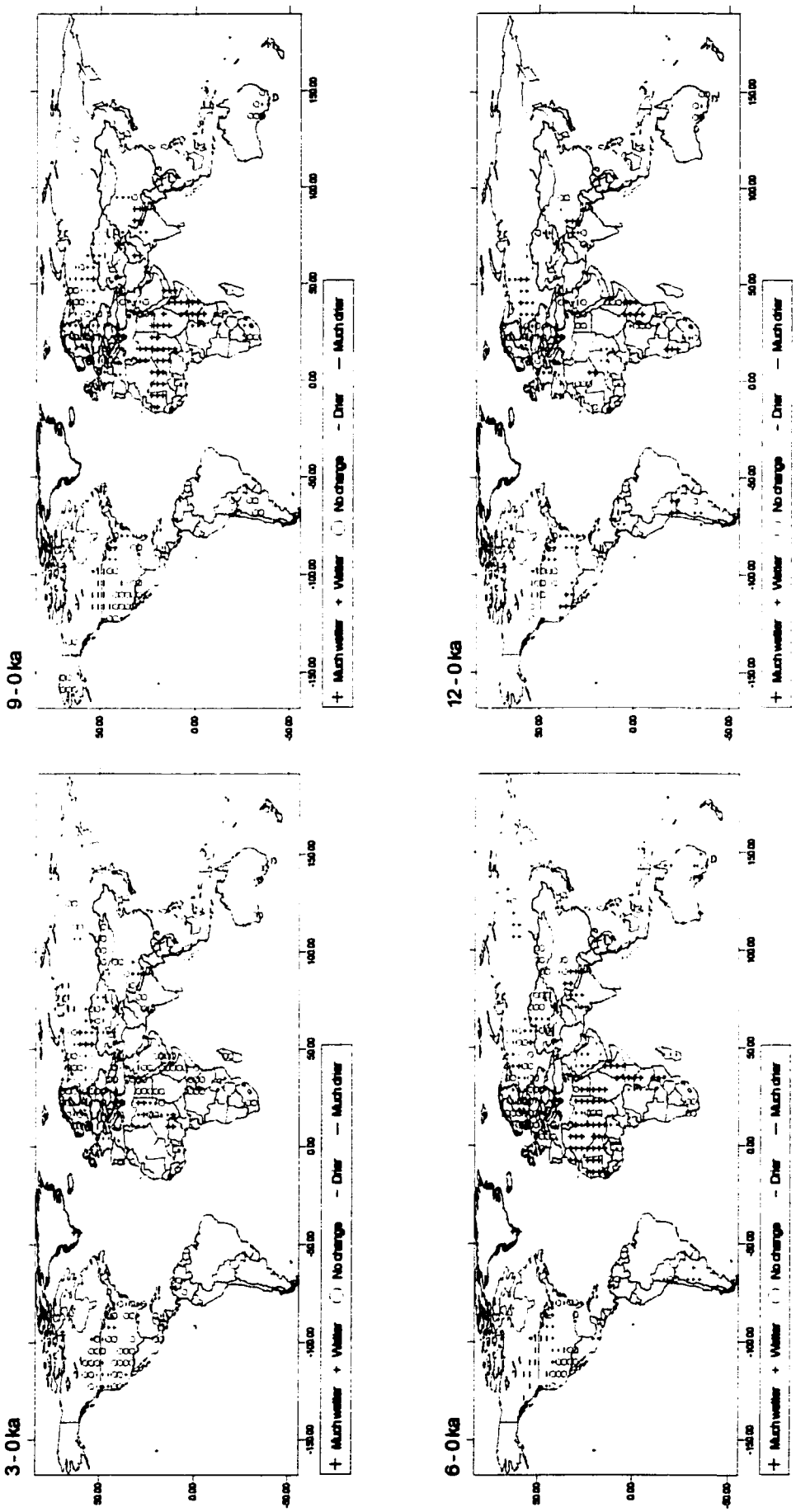

Figure 6.1b: Anomaly maps under indicator approach.

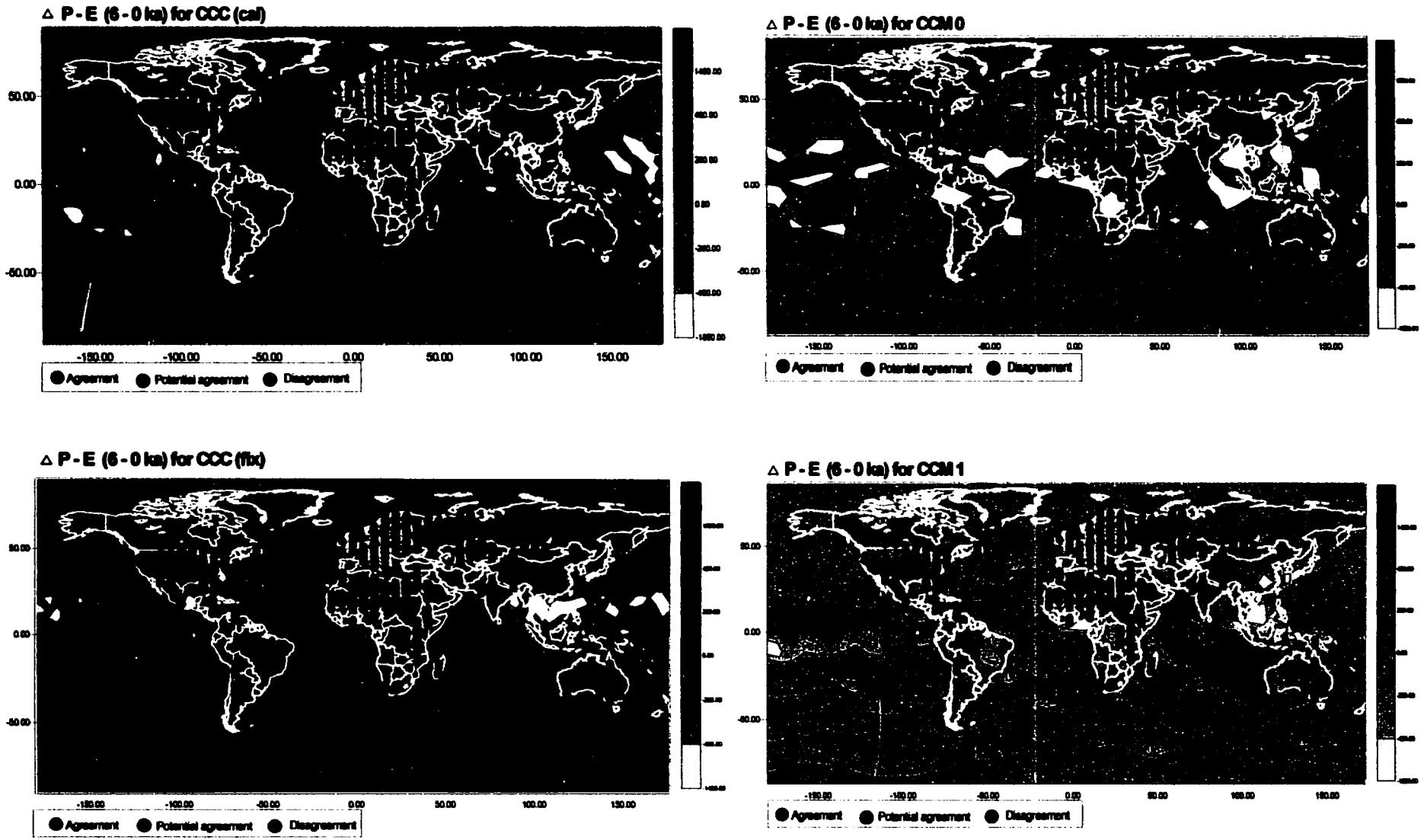

Figure 6.2a: Distribution of agreements between model and gridded lake levels under continuous assumption.

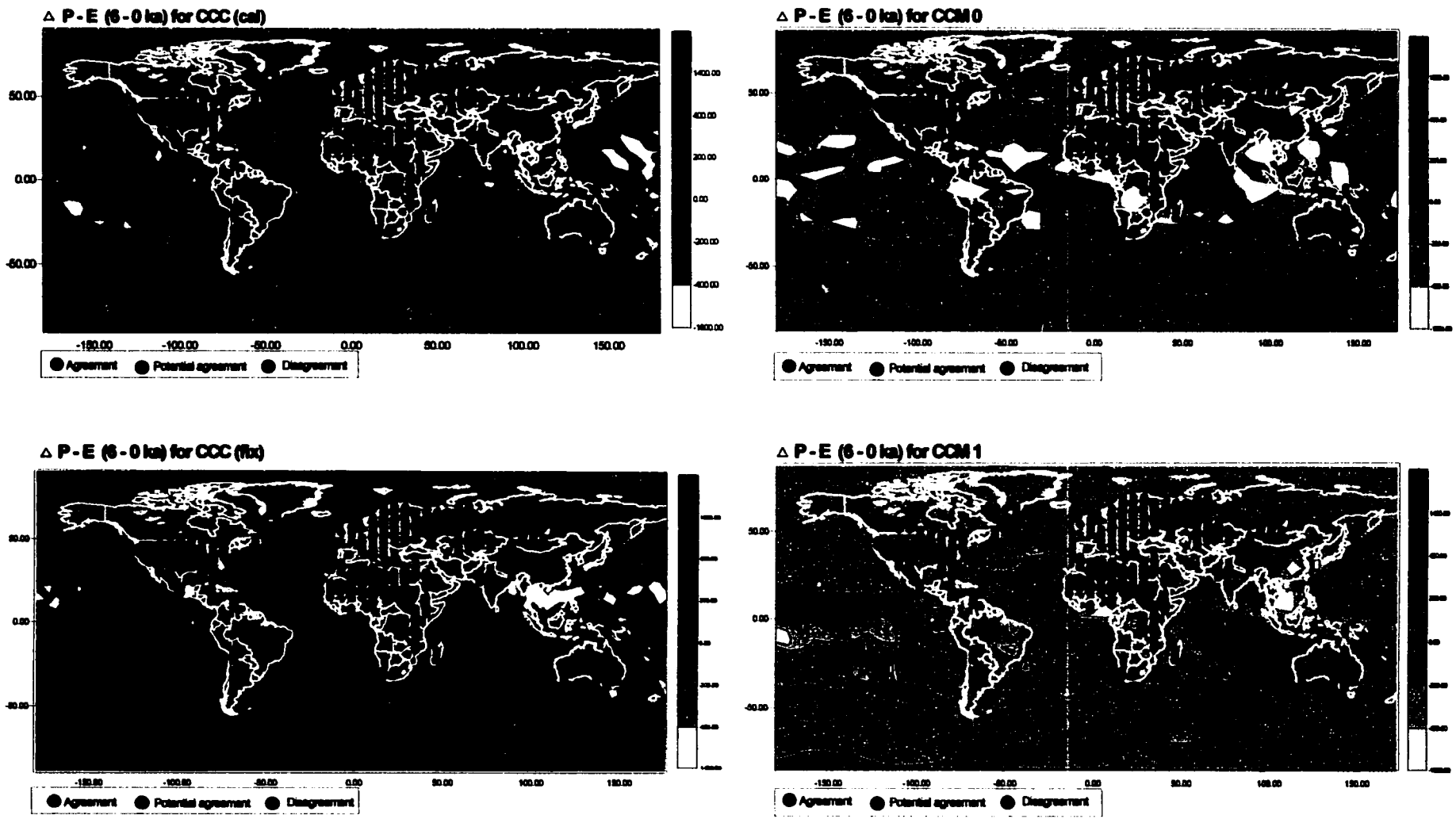

Figure 6.2b: Agreements between models and gridded lake levels under indicator approach.

(a)

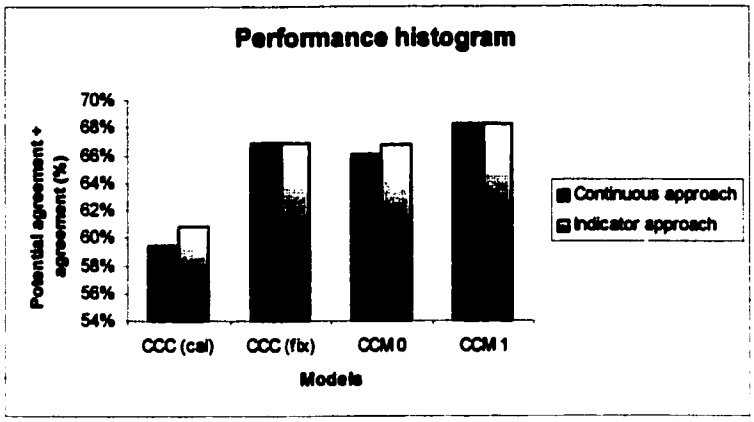

(b)

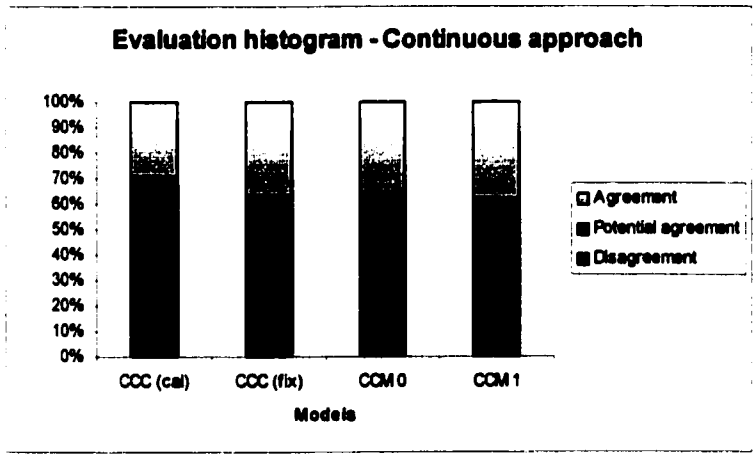

(c)

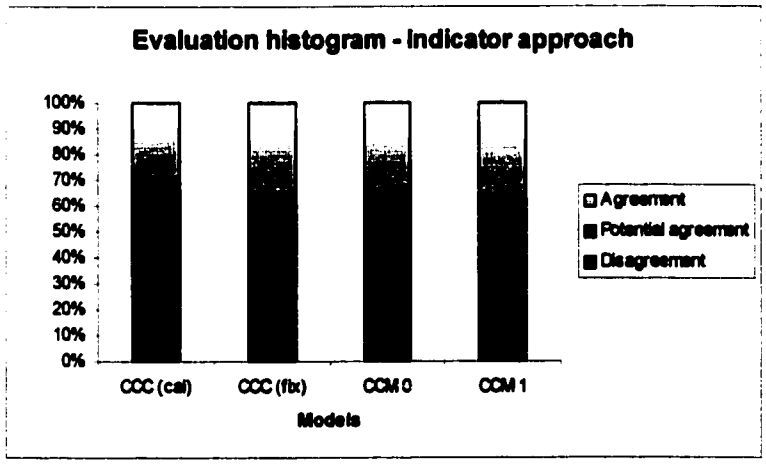

Figure 6.3: (a) Performance evaluation of the model-data comparison under both approaches, (b) Evaluation of the data-model comparison by category under continuous approach and (c) indicator approach.

Chapter 7

Summary and conclusion

"Climate has influenced human activities. Two great developments emerged at about the time of major environmental change between 12 and 10 ka- the earliest appearance of agriculture in the Old World, and the cultural changes accompanying extinction of the Pleistocene megafauna in the New World. Both developments may have been caused at least indirectly by the types of climatic change examined here. Now we may be faced with the reverse: human modification of climate and of related aspects of the physical environment. Application of a well-tested climate model is at present the only method for predicting these climatic and environmental changes and can help in planning a response to them"

COHMAP Members, 1988.

The hypothesis tested in this thesis was that changes in closed basin as well as temperate lake-levels exhibit spatial autocorrelation that is primarily controlled by large-scale climate patterns. As we have seen, there is an enormous amount of literature suggesting that this hypothesis is verified. However, most of these studies were based on visual identification of spatial patterns in lake-level variations. As we have also seen in the literature, the climatic inferences using lake-level variations have been used at different spatial and temporal scales. The history of the use of lake-level variations in climate reconstruction as proxy to precipitation and temperature or moisture balance (P-E) is an important consideration in that the initial studies were restricted to closed basin lakes in arid to semi-arid regions of the world. The inclusion of temperate or overflowing lakes in recent years and the use of a different scheme in determining long-term lake-level changes may or may not have increased noise in the database. When trying to develop a large database, sorting out inconsistencies between the different datasets becomes crucial. The use of lake-level variations in climate research must take into account the continuous characteristic of climate, so that regions reflect this continuity in space and time. Observations, such as lake-level variations, can only be used in climate research by initially determining the spatially coherent patterns from other noises.

In Chapter 3, we explored the distribution of the lake-level data at the global scale as part of the

identification of spatially coherent patterns from variable ones. This initial step revealed a significant amount of fine-scale variability in the lake-data at different spatial and temporal scales. Indeed, the fine-scale variability identified at this stage was global in extent and present in most regions of the world. Furthermore, the identification of potential errors in interpretation resulted in the conclusion that this fine-scale variability could be caused in part by interpretation errors.

In Chapter 4, we pursued the investigation into fine-scale variability using spatial autocorrelation techniques. The variogram and correlogram functions were used to analyse the spatial dependence between sites at different spatial and temporal scales under two assumptions. The results objectively suggested further evidence of fine-scale variability, especially over small distances where a lack of spatial autocorrelation was found at 3,6 and 9 ka. Geostatistics offer techniques of removing outliers to yield better spatial structures in variogram analysis in order to capture the underlying spatial characteristics in the data. However, this is often arbitrary as some sample may be truly representative of the spatial phenomenon under investigation. To pursue the analysis of spatial dependence between sample sites, we used the LISA statistics as a more appropriate tool. The LISA statistic enables an analysis of the data for spatial autocorrelation within local regions on a site by site basis. This permitted the identification of local negatively correlated sites that influenced greatly the variogram structures. The goal of the LISA analysis was to maximize global coverage while retaining the original spatial structure inherent in the data. The results of the analysis revealed yet more evidence of fine-scale variability present within several distances spanning 500 km. However, it identified local spatially correlated patterns at a consistent scale of study. After removing objectively the negatively correlated sites at a consistent scale from the database, we now had a dataset that reflected the continuous characteristic of climate on which to rely for estimation of the patterns. Indeed, using the filtered lake data revealed more clearly interpretable variogram structures. Models were then successfully fitted to the variograms under both assumptions in order to estimate and grid the spatially coherent patterns in respect to climate change.

In Chapter 5, we used the models imposed on the filtered data to estimate location between sites. Local estimation was preferred to global estimation because of clustering, redundancy and the irregular distribution of the data. This resulted in estimates in location where neighbours were available within the prescribed 500 km scale of study. Both kriging approaches yielded almost identical estimates, thus suggesting a robust estimation of the climate patterns in lake-level data. The main differences resulting in location of boundary regions between both kriging approaches.

In Chapter 6, we used the lake status grids to reconstruct global hydrological change. The gridded lake status results are in good agreement with known boundary conditions and other paleoclimatic reconstructions, such as the enhanced Afro-Asian monsoon circulation and orbitally-induced changes in insolation during the Holocene. The lake status grids were also used in data-model comparisons in a more objective way to illustrate its versatility in paleoclimatic research.

While the main contribution of this thesis is a clearly stated methodology of identifying the climate signal from local noise in lake data, there remain unsolved questions. Anisotropy or the tendency for data values to favour a particular direction was not explored. In addition, validation of the models imposed on the data remains an open research question in geostatistics. Some possibilities include non-parametric stochastic simulations.

Do lake-levels exhibit spatial autocorrelation? To answer this initial question requires a thorough understanding of the limitations associated with lake-level reconstructions. If we hypothesize that only large-scale patterns in lake-level variations are climatically meaningful, then the lake data do exhibit spatial autocorrelation and the hypothesis is verified. However, there remains the question of fine-scale variability present in the original data. As stated in the previous chapter, possible recommendations include (a) going back to the original data to investigate the spatio-temporal dependence on a site-by-site basis, and (b) enhancing the coding scheme into a larger number of

classes in order to differentiate the intermediate class.

If lake-level variations exhibit spatial autocorrelation, can it be modelled? What are the limitations of these models imposed on the data and what are the implications of imposing these models on the data? The methodology illustrated in this thesis confirms that the lake data can be modelled with some success. However, the models imposed on the lake data are not deterministic models, as the processes underlying lake-level variations and climate change are not fully understood. Imposing a model on the data always involves a choice of distances that is usually based on the researcher's knowledge of the data. Another consideration to take into account in spatial modelling of the lake data is the non-continuous aspect of lake distribution where some estimates of unsampled locations may not have any lakes on which to validate the model.

Can these modelled patterns be used in paleoclimate reconstructions and aid in the validation of global climate model (GCMs) simulations? This thesis illustrated that by extracting the climate signal from local noise in the lake data and modelling it gave more clearly interpretable spatial patterns at a consistent scale. As the grids now represent spatial continuity within regions in respect to climate, more objective paleoclimate reconstructions and climate data-model comparisons can be achieved.

In conclusion, the methodology established in this thesis recognises its ability to identify lake-level variations that are primarily controlled by large-scale climate patterns. Its versatility in both space and time can only lead to a better understanding of the mechanisms that control climate change and the global hydrological cycle as geographical coverage increases in the future.

References

Anselin, L., 1995. Local indicators of spatial association - LISA. Geographical Analysis, 27(2):93.

Boer, G.J., MacFarlane, N.A., Laprise, R., Henderson, J.D., Blanchet, J.P., 1984. The Canadian Climate Centre spectral atmospheric general circulation model. Atmosphere and Ocean. Vol.22, p.397-429.

Bourdier, F., 1962. Le basin du Rhone au Quaternaire. Éditions du C.R.N.S., Paris, 364 pp.

Brackenridge, G.R., 1978. Evidence for a cold, dry full-glacial climate in the American southwest. Quaternary Research. Vol. 9, p. 22-40.

Bradley, R.S., 1985. Quaternary Paleoclimatology: Methods of Plaeoclimatic Reconstruction. Boston, Allen & Unwin. London. 472 pp.

Butzer, K.W., Isaac, G.L., Richardson, J.L., Washbourn-Kamau, C., 1972. Radiocarbon dating of East African lake-levels. Science, 175, 1069-76.

Cheddadi, R., Yu, G., Guiot, J., Harrison, S.P., Prentice, I.C., 1997. The climate of Europe 6000 years ago. Climate Dynamics. Vol. 13, p. 1-9.

CLIMAP Project Members, 1976. The surface of the ice-age earth. Science 191, p.1138-1144.

COHMAP Members, 1988. Climatic changes of the last 18,000 years: Observations and model simulations. Science 241, p. 1043-1052.

Delibrias, G., Guiller, M-T., Labeyrie, J., 1986. Gif natural radiocarbon measurements X. Radiocarbon 28: 9-68.

Deutsch, C.V., Journel, A.G., 1992. GSLIB Geostatistical Software Library and User's Guide. Oxford University Press, NY. 340 pp.

Duret, J-J., Martini, J., 1965. Un niveau de cendres volcaniques dans la craie lacustre du lac de Chalain (Jura francais). Arch. Sc. Soc. Phys. Hist. Nat. Genève 18: 679-686.

Evin, J., Marien, G., Pachiaudi, Ch., 1973. Lyon natural radiocarbon measurements III. Radiocarbon 15: 134-155.

Evin, J., Marechal, J., Marien, G., 1983. Lyon natural radiocarbon measurements IX. Radiocarbon 25: 59-128.

Fang, Jin-qi, 1991. Lake evolution during the past 30,000 years in China, and its implications for environmental change. Quaternary Research, 36, 37-60.

Gaillard, M.-J., 1985. Postglacial paleoclimatic changes in Scandinavia and Central Europe: A tentative correlation based on studies of lake-level fluctuations. Ecologia Mediterranea. Vol 11, p. 159-175.

Galloway, R.W., 1965. Late Quaternary climates in Australia. Journal of Geology. Vol. 73, p. 603-618.

Galloway, R.W., 1970. The full-glacial climate in Soouth-western United States. Annals of the Association of American Geographers. Vol. 60, p. 245-256.

Getis, A., Ord, J.K., 1992. The analysis of spatial association by use of distance statistics. Geographical Analysis, 24(3):189-206.

Goodchild, M.F. 1987. Spatial Autocorrelation. CATMOG 47.

Goovearts, P., 1997. Geostatistics for natural ressources evaluation. Oxford University Press - New York, 483 pp.

Guiot, J., Harrison, S.P., Prentice, I.C., 1993. Reconstruction of Holocene precipitation patterns in Europe using pollen and lake-level data. Quaternary Research. Vol. 40, p. 139-149.

Halley, E., 1715. On the cause of the saltness of the ocean, and of the several lakes that emit no rivers; with a proposal, by help thereof, to discover the age of the world. Philos. Trans. R. Soc. London. Vol. 29, p. 296-300.

Harrison, S.P., Metcalfe, S.E., 1985a. Spatial variations in lake levels since the last Glacial Maximum in the Americas north of the Equator. Zeitschift für Gletscherkunde und Glazialgeologie. Vol. 21, p. 1-15.

Harrison, S.P., Metcalfe, S.E., 1985b. Variations in lake levels during the Holocene in North America: An indicator of changes in atmospheric circulation patters. Géographie physique et Quaternaire. Vol. 39, p. 141-150.

Harrison, S.P., 1988. Reconstructing climate from lake level changes. Ph.D Thesis. LUNDQUA, Lund University, Lund. Vol. 21.

Harrison, S.P., Saarse, L., Digerfeldt, G., 1991. Holocene changes in lake levels as climate proxy data in Europe. Paläoklimaforschung. Vol. 6, p. 159-179.

Harrison, S.P., Dodson, J., 1992. Climates of Australia and New Guinea since 18,000 yr BP. In: Wright H.E. Jr, Kutzbach J.E., Webb, T. III, Street-Perrott, F.A, Ruddiman, W.F., Bartlein, P.J., (Eds.) Global climates since the last Glacial Maximum. University of Minnesota Press, Minneapolis.

Harrison, S.P., Digerfeldt, G., 1993. European lakes as palaeohydrological and palaeoclimatic indicators. Quaternary Science Review. Vol. 12, p. 233-248.

Harrison, S.P., Yu, G., 1995. Lake Status Records from Europe: Data Base Documentation. Paleoclimatology Publication Series Report No. 3. World Data Center - A For Paleoclimatology. NOAA Paleoclimatology Program. Boulder, Colorado, USA. 451 pp.

Harrison, S.P., Prentice, I.C., Guiot, J., 1993. Climatic controls on Holocene lake-level changes in Europe. Climate Dynamics. Vol. 8, p. 189-200.

Harrison, S.P., 1989. Lake levels and climatic change in eastern North America. Climate Dynamics. Vol. 3, p. 157-167.

Harrsison, S.P., Clymo, R.S., Southall, H., 1988. Order Amid Sparse Data: the pattern of lake level changes in North America during the Late Quaternary. Mathematical Geology.

Hassko, B., Guillet, B., Jaegy, R., Coppens, R., 1974. Nancy natural radiocarbon measurements III. Radiocarbon 16: 118-130.

Hetch, A.D., 1985. Paleoclimate Analysis and Modelling. John Wiley & Sons. 445 pp.

Hewitt, C.D., Mitchell, J.F.B., 1997. Radiative forcing and response of a GCM to ice age boundary conditions: cloud feedback and climate sensitivity. Climate Dynamics. Vol. 13, p.821-834.

Isaaks, E.H., Srivastava, R.H., 1989. An introduction to Applied Geostatistics. Oxford University Press. NY. 561 pp.

Kutzbach, J.E., Street-Perrott, F.A., 1985. Milankovitch forcing of fluctuations in the level of tropical lakes from 18 to 0 kyr BP. Nature, 317, 130-134.

Kutzbach, J.E. and Guetter, P.J., 1986. The influence of changing orbital parameters and surface boundary conditions on climatic simulations for the past 18,000 years. Journal of Atmospheric Science. Vol.43, p.1726-1759.

Kutzbach, J.E., 1981. Monsoon climate of the early Holocene: Climate experiment with the Earth"s orbital parameters for 9,000 years ago. Science. Vol.214, p.59-61.

Kutzbach, J.E., Guetter, P.J., Behling, P.J., Selin, R., 1993. Simulated climatic changes: results of the COHMAP climate-model experiments. In: Wright H.E. Jr, Kutzbach J.E., Webb, T. III, Street-Perrott, F.A, Ruddiman, W.F., Bartlein, P.J., (Eds.) Global climates since the last Glacial Maximum. University of Minnesota Press, Minneapolis.

Kutzbach, J.E., Gallimore, R., Harrison, S.P., Behling, P., Selin, R., Laarif, F., 1998. Climate and biomes simulations for the past 21,000 years. Quaternary Science Reviews, 17, 473-506.

Lambert, G., Petrequin, P., Richard, H., 1983. Périodicité de l'habitat lacustre néolithique et rythmes agricoles. L'Anthropologie (Paris) 87: 393-411.

Magny, M., Richard, H., Evin, J., 1988. Nouvelle contribution à l'histoire holocène des lacs de Jura francais: recherches sédimentologiques et palynologiques sur les lacs de Chalain, de Clairvaux et d' Abbaye. Revue de Paléobiologie 7: 11-23.

Marshall, S., Roads, J.O., Oglesby, R.J., 1997. Effects of resolution and physics on precipitation in the NCAR Community Climate Model. Journal of Geophysical Research. Vol. 102, No. D16, p. 19529-19541.

McFarlane, N.A., Boer, G.J., Blanchet, J-P., Lazare, M., 1992. The Canadian Climate Centre second-generation general circulation model and its equilibrium climate. Journal of Climate, 5: 1013-1044.

Pannetier, Y., 1994. Variowin - Software for Spatial Data Analysis in 2D. Springer-Verlag New York. 91 pp.

Peixoto, J.P., Oort, A.H., 1992. Physics of Climate. American Institute of Physics. New York.

Prentice, I.C., Guiot, J., Huntley, B., Jolly, D., Cheddadi, R., 1996. Reconstructing biomes from paleoecological data: a general method and its application to European pollen data at 0 and 6 ka. Climate Dynamics. Vol. 12, p. 185-194.

Qin, B., Harrison, S.P., Kutzbach, J.E., 1998. Evaluation of modelled regional water balance using lake status data: A comparison of 6 ka simulations with the NCAR CCM. Quaternary Science Review, Vol. 17, pp. 535-548.

Rind, D., Peteet, D., Kukla, G., 1989. Can Milankovitch orbital variations imitate the growth of Ice Sheets in a general circulation model. Journal of Geophysical Research. Vol.94, p.12854-12871.

Schultz, P. Barron, E.J., Sloan, J.L.II, 1992. Assessment of NCAR General Circulation Model precipitation in comparaison with observation. Palaeogeography, Palaeoclimatology, Palaeoecology. Vol.197, p.269-310.

Sears, P. B., 1964. The goals of paleoclimatological reconstruction. In The reconstruction of past environments, J. H. Hester and J. Schoenwetter (ed), 4-5, Fort Burgwin Research Center Publication No. 3. Fort Burgwin, New Mexico: Fort Burgwin Research Center.

Sokal, R.R. and Oden, N.L. 1978a. Spatial autocorrelation in biology 1. Methodology. Biological Journal of the Linnean Society, 10:199

Sokal, R.R. and Oden, N.L. 1978b. Spatial autocorrelation in biology 2. Some biological implications and four applications of evolutionary and ecological interest. Biological Journal of the Linnean Society, 10:229

Smith, G.I., Street-Perrott, F.A., 1983. Pluvial lakes of the Western United States. In: Porter, S.C. (Ed.): Late Quaternary Environments of the United States, Volume 1, The late Pleistocene. University of Minnesota Press, Minneapolis, p. 190-212.

Street, F. A., Grove, A. T., 1979. Global maps of lake-level fluctuations since 30,000 BP. Quaternary Research. Vol. 12, p. 83-118.

Street, F.A., Grove, A. T., 1976. Environmental and climatic implications of Late-Quaternary lake-level fluctuations in Africa. Nature. Vol. 261, p. 385-390.

Street-Perrott, F.A., Roberts, N., 1983. Fluctuations in closed lakes as an indicator of past atmospheric circulation patterns. In: Street-Perrott, F.A., Beran, M., and Ratcliffe, R.A.S. (Eds.), Variations in the Global Water Budget: D. Reidel, Dordrecht, p. 331-345.

Street-Perrott, F.A., 1986. The response of lake levels to climatic change- Implications for the future. In: Climate-Vegetation Interactions (C" Rozenweig and R. Dickinson, Eds.), pp. 77-80. Report OIES-2 University Corporation for Atmospheric Research, Office of Interdisciplinary Earth Sciences, Boulder, Colo.

Street-Perrott, F.A., and Harrison, S.P., 1985. Lake levels and climate reconstructions. In: Hetch, A.D. (ed.), Paleoclimate Analysis and Modelling, pp291-340. Wiley, New York.

Street-Perrott, F.A., Harrison, S.P., 1984. Temporal variations in lake levels since 30,000 yr BP - an index of the global hydrological cycle. In: Hansen, J.E. and Takahashi, T. (Eds.), Climate Processes and Climate Sensitivity: American Geophysical Union, Geophysical Monograph 29, Maurice Ewing Series, v. 5, p. 118-129.

Street-Perrott, F.A., Marchand, D.S., Roberts, N., Harrison, S.P., 1989. Global lake-level variations from 18,000 to 0 years ago: a paleoclimatic analysis US DOE/ER/60304-H1 TR-046, US Department of Energy, Technical Report, 101 pp.

Tarasov, P.E., Harrison, S.P., Saarse, L., Ya Pushenko, M., Andreev, A.A., Aleshinskaya, Z.V., Davydova, N.N., Dorofeyuk, N.I., Efremov, Yu.V., Khomutova, V.I., Sevastyanov, D.V., Tamosaitis, J., Uspenskaya, O.N., Yakushko, O.F., Tarasova, I.V., 1994. Lake Status Records from the Former Soviet Union and Mongolia: Data Base Documentation. Paleoclimatology Publications Series Report No. 2. World Data Center- A dor Paleoclimatology. NOAA Paleoclimatology Program. Boulder, Colorado, USA. 274 pp.

Texier, D., de Noblet, N., Harrison, S.P., Haxeltine, A., Jolly, D., Joussaume, S., Laarif, F., Prentice, I.C., Tarasov, P., 1997. Quantifying the role of biosphere-atmosphere feedbacks in climate change: coupled model simulations for 6000 years BP and comparaison with paleodata for northern Eurasia and northern Africa. Climate Dynamics. Vol. 13, p.865-882.

Tricart, J., 1956. Tentative de corrélation des périodes pluviales africaines et des périodes glaciaires. Compte rendus sommaires de la Société géologique de France. Vol. 9-10, p.164-167.

Vettoretti, G., Peltier, W.R., McFarlane, N.A., 1998. Simulations of Mid-Holocene climate using an atmospheric general circulation model. Journal of Climate. 11: 2607-2627.

Webb, T. III, 1985. A global paleoclimatic data base for 6000 yr BP. U.S. Department of Energy, Technical Report, 18, 1-155.

Webb, T. III, Bartlein, P.J., Harrison, S.P., Anderson, K.H., 1993. Vegetation, lake levels and climate in eastern North America for the past 18,000 years. In: Wright, H.E., Kutzbach, J.E., Webb, T. III, Ruddiman, W.F., Street-Perrott, F.A. and Bartlein, P.J. (eds), Global Climates since the last Glacial Maximum, pp. 415-467, University of Minnesota Press, Minneapolis.

Winkler, M., Swain, A. M., Kutzbach, J.E., 1986. Middle Holocene dry period in the northern midwestern United States: Lake levels and pollen stratigraphy. Quaternary Reserch. Vol. 25, p. 235-250.

Wright, H.E. Jr., Kutzbach, J.E., Webb, T., III, Ruddiman, W., Street-Perrott, F.A., Bartlein, P.J., (Eds.), 1993. Global Climates since the last glacial maximum. University of Minnesota Press. Minneapolis

Yu, G., Harrison, S.P., 1995a. Lake status records from Europe: Data Base Documentation. NOAA Paleoclimatology Publications Series Report 3. 451 pp.

Yu, G., Harrison, S.P., 1995b. Lake status changes in northern Europe during the Holocene. Boreas. Vol. 24, p. 260-268.

Yu, G., Harrison, S.P., 1996. An evaluation of the simulated water balnce of Eurasia and northern Africa at 6000 y BP using lake status data. Climate Dynamics. Vol 12, p. 723-735.

Appendix A: The Oxford Lake Level Data Bank

Id	Basin	Longitude	Latitude	Altitude (m)	0 ka	3 ka	6 ka	9 ka	12 ka
1	ABHE, ETHIOPIA/DJIBOUTI	42	11.25	240	3	3	1	1	3
2	ABU BALLAS, EGYPT	27.42	24.23	508	3	0	2	2	0
3	ABU TARTUR, EGYPT	29.3	25.5	145	3	0	1	1	1
4	ADOBE, CALIFORNIA, U.S.A.	-118.6	37.91	1951	3	2	3	2	0
5	ADRAR BOUS, NIGER	9.03	20.3	700	3	0	0	0	0
6	AFRERA, ETHIOPIA	40.83	13.42	-62	3	3	1	1	0
7	AGADEM, NIGER	13.33	16.83	360	3	2	2	2	0
8	AHNET-MOUYDIR, ALGERIA	0.8	23.58	360	3	0	0	0	0
9	AL-HASA, SAUDI ARABIA	48.5	25.4	80	3	0	0	0	0
10	AL-LUHY, SAUDI ARABIA	46.6	24.43	1119	3	0	0	0	0
11	ALBACUTYA, VICTORIA, AUSTRALIA	141.97	-35.75	220	3	0	0	0	0
12	ALEXANDERSFONTEIN, S.AFRICA	24.8	-28.83	800	3	3	2	2	2
13	ALSACIA, COLOMBIA	-73.85	3.9	3100	0	2	1	2	2
14	AN-NAFUD, SAUDI ARABIA	40.93	28.03	700	3	3	2	0	0
15	ANNIE, FLORIDA, U.S.A	-81.4	27.3	36	1	1	2	2	2
16	AOZERKAT, NIGER	5.39	16.2	425	3	0	0	0	0
17	ARCH, NEW MEXICO, U.S.A.	-103.13	34.06	1174	3	0	0	0	0
18	ARD EL AKHDAR, EGYPT	26.03	23.18	860	3	2	2	2	0
19	ASAL, DJIBOUTI	42.5	11.6	-155	3	2	1	1	3
20	AZAWAGH, NIGER	4.67	17.65	360	3	0	0	0	0
21	AZEFAL, MAURITANIA	-16	19.9	150	3	0	0	0	0
22	BADR, SAUDI ARABIA	43.68	17.62	400	3	0	0	0	0
23	BAHARIYA, EGYPT	27	28	155	3	0	0	0	0
24	BALATON, HUNGARY	17.5	46.8	-105	1	2	2	0	0
25	BANCANNIA, N.S.W., AUSTRALIA	141.93	-30.62	107	3	2	3	3	3
26	BARINGO, KENYA	36	0.5	997	2	0	0	0	1
27	BEATTIES, TASMANIA, AUSTRALIA	146.63	-42.67	980	1	1	1	3	0
28	BEBEDERO, ARGENTINA	-66.75	-33.33	380	3	2	2	3	3
29	BEGOUR, CHAD	16.25	21.32	1400	3	0	0	0	0
30	BEHAR BELAMA, EGYPT	21.25	27.47	180	3	1	1	0	0
31	BEN CHORA, ALGERIA	-0.93	28.23	250	3	0	0	0	0
32	BESAKA, ETHIOPIA	39.97	8.66	1000	3	3	0	1	0
33	BEYSEHIR, TURKEY	31.5	37.75	1120	2	2	2	2	3
34	BILMA, NIGER	13	18.75	310	3	2	1	2	3
35	BIR TARFAWI - BIR SAHARA, EGYPT	28.66	22.8	275	3	3	0	0	0
36	BIRKET RAM, ISRAEL/JORDAN	35.25	33.25	940	2	2	2	2	2
37	BOGORIA, KENYA	36.1	0.3	980	2	1	1	1	2
38	BONNEVILLE, UTAH, U.S.A.	-113	40.5	1280	3	3	3	3	2
39	BOSUMTWI, GHANA	-1.42	6.5	100	2	1	1	1	1
40	BOU ALI, ALGERIA	-0.25	27.17	380	3	2	1	0	0
41	BOU BERNOUS, ALGERIA	-3.07	27.33	200	3	0	1	0	0
42	BOUGDOUMA, NIGER	11.7	13.3	320	3	1	2	1	2
43	BOULOUM GANA, NIGER	10.62	15.02	340	3	0	0	1	0
44	BREADALBANE, N.S.W., AUSTRALIA	149.48	-34.78	697	3	1	2	3	0
45	BREEK BEEN KOLK, SOUTH AFRICA	20.1	-30.6	800	3	3	3	3	3
46	BROMFIELD, QUEENSLAND, AUSTRALIA	145.55	-17.38	756	2	2	1	1	0
47	BROWN'S, OHIO, U.S.A.	-82.07	40.68	340	0	0	0	0	1
48	BUENOS AIRES, COLOMBIA	-75.5	4.85	3660	0	0	0	0	0
49	BULLENMERRI, VICTORIA, AUSTRALIA	143.12	-38.25	148	1	3	1	2	3
50	BURDUR, TURKEY	30.1	37.6	864	0	0	0	0	1

51	BUSHMAN'S FOUNTAIN, SOUTH AFRICA	24.17	-28.58	980	3	0	0	0	0
52	CAHABA, ALABAMA, U.S.A.	-86.53	33.5	210	2	2	3	3	1
53	CARI LAUFQUEN GRANDE, ARGENTINA	-68.57	-41.4	860	3	0	0	0	0
54	CARP, WASHINGTON, U.S.A.	-122.08	46.92	714	1	2	2	3	3
55	CHAD, NIGERIA/NIGER	14	13	282	2	2	2	1	2
56	CHALBI, KENYA	37.5	3	370	3	0	0	0	0
57	CHALMER'S, ALBERTA, CANADA	-114.48	50.64	1370	3	0	0	1	1
58	CHATYRKEL, KIRGIZ, U.S.S.R.	76.3	40.6	3530	3	3	2	0	0
59	CHEMCHANE-ADERG, MAURITANIA	-12.12	21	280	3	3	1	1	3
60	CHENCO, XIZANG, CHINA	90.7	29	4000	3	2	1	0	0
61	CHESHI-MWERU WANTIPA, ZAMBIA	29.08	-8.67	928	2	2	1	1	3
62	CHEW BAHIR, ETHIOPIA-KENYA	37	4.76	800	3	0	1	0	0
63	CHEWAUCAN, OREGON, U.S.A.	-120.5	42.67	1296	3	3	3	0	0
64	CHICHANCANAB, MEXICO	-89.75	19.5	36	3	1	3	3	3
65	CHICONAHUAPAN, MEXICO	-89.67	19.13	2575	2	2	2	2	0
66	CHILWA, MALAWI	35.5	-15.5	622	3	0	2	2	0
67	CHIU-CHIU, CHILE	-68.65	-22.4	2520	3	0	0	0	0
68	CIEGA, COLOMBIA	-72.3	6.5	4000	0	0	0	0	0
69	CLARK, CALIFORNIA, U.S.A.	-116.3	33.33	199	3	0	0	0	0
70	CLEVELAND, IDAHO, U.S.A.	-114.5	42.5	2519	1	3	1	3	1
71	CLOVIS, NEW MEXICO, U.S.A.	-103.33	34.25	1250	3	3	3	2	0
72	COBRICO, VICTORIA, AUSTRALIA	143.03	-36.3	80	1	1	1	3	0
73	COCHISE, ARIZONA, U.S.A.	-109.85	32.13	1290	3	3	3	3	3
74	COLONGULAC, VICTORIA, AUSTRALIA	143.45	-36.25	85	2	0	0	0	0
75	COMARUM SO, GREENLAND	-45.53	61.13	125	3	1	1	0	0
76	CORANGAMITE, VICTORIA, AUSTRALIA	143.5	-38.25	117	2	2	0	0	0
77	CROWN, TASMANIA, AUSTRALIA	147.63	-42.28	375	2	2	0	0	0
78	DA QAIDAM, QINGHAI, CHINA	95.2	38	2900	3	3	3	2	3
79	DAIET EL MELAH, ALGERIA	1.24	31.13	995	3	0	2	0	0
80	DAMASCUS, SYRIA	36.52	33.62	600	3	0	0	2	0
81	DAWASIR, SAUDI ARABIA	45	20.35	600	3	0	0	1	0
82	DAYET AAOUA, MOROCCO	-6.03	33.35	1180	3	0	1	0	0
83	DE AGUA SUCIA, COLOMBIA	-73.47	3.4	280	1	1	0	0	0
84	DEELPAN, SOUTH AFRICA	25.78	-29.17	1278	3	0	0	0	0
85	DEEP SPRING, CALIFORNIA, U.S.A.	-118.03	37.28	1499	3	3	3	3	0
86	DEVIL'S, NORTH DAKOTA, U.S.A.	-98.95	48.02	430	2	2	3	0	0
87	DHAR TICHITT, MAURITANIA	-9.2	18.35	375	3	2	0	0	0
88	DIAMOND, OREGON, U.S.A.	-118.78	43.09	1341	2	1	3	0	0
89	DIBELLA, NIGER	13.14	17.54	360	3	0	0	0	0
90	DIDWANA, INDIA	74.58	27.33	360	2	2	1	2	2
91	DIXIE, NEVADA, U.S.A.	-118	39.91	1027	3	0	0	0	1
92	DOBI-HANLE, ETHIOPIA	42	11.5	120	3	2	1	1	0
93	DUCK, MASSACHUSETTS, U.S.A.	-70	41.93	3	2	2	3	2	2
94	E.I., ALBERTA, CANADA	-112.85	53.63	724	1	2	0	0	0
95	EAGLE, TASMANIA, AUSTRALIA	146.5	-42.67	1033	1	1	2	1	3
96	EL ABRA, COLOMBIA	-74	5	2870	3	3	3	3	1
97	EL BAKHT, EGYPT	28.31	23.22	850	3	0	1	2	0
98	EL GOBERNADOR, COLOMBIA	-74.35	3.85	3815	3	2	2	2	0
99	EL JAFR, JORDAN	36.33	30.28	847	3	0	0	0	0
100	EL JUNCO, ECUADOR	-89.45	-0.97	650	1	2	2	2	3
101	EL RHARSA, TUNISIA	7.76	34.61	10	3	0	0	0	0
102	EL'ATRUN, SUDAN	28.63	18.17	510	3	0	1	1	0
103	ELEGANTE CRATER, MEXICO	-113.52	31.8	1190	3	0	0	0	0
104	ELK, MINNESOTA, U.S.A.	-95.21	47.21	463	1	1	3	1	0
105	EN NAHUD, SUDAN	28.4	12.6	700	3	0	0	0	0
106	ENNERI BARDAGUE, CHAD	17	21.5	1025	3	3	3	1	2
107	ENNERI YEBBIGUE, CHAD	18.1	20.95	1000	3	0	0	0	0
108	ERG INE SAKANE 20, MALI	-0.63	20.63	320	3	0	1	0	0

109	ERG INE SAKANE 48-50, MALI	-0.7	20.8	320	3	0	1	0	0
110	ERG INE SAKANE 67-19, MALI	-0.53	20.96	320	3	0	2	0	0
111	ERG INE SAKANE, MALI	-0.75	21.08	310	3	0	0	0	0
112	ERG JMEYA, MALI	-3.81	20.6	350	3	0	0	0	0
113	ESTANCIA, NEW MEXICO, U.S.A.	-105.6	34.6	1842	3	0	0	0	0
114	ETOSHA, NAMIBIA	16.5	-19	900	3	0	0	0	1
115	EURAMOO, QUEENSLAND, AUSTRALIA	146.83	-17.17	730	2	2	1	3	0
116	EYASI, TANZANIA	35	-3.5	1200	3	0	0	0	0
117	EYRE, S. AUSTRALIA, AUSTRALIA	137.25	-28.5	-15	3	0	0	0	0
118	FACHI, NIGER	11.67	18.12	275	3	2	1	2	0
119	FDERICK(FORT-GOURAUD), MAURITANIA	-12.7	22.67	350	3	0	0	1	0
120	FESHFESH, SUDAN	25.06	18.75	1200	3	0	1	0	0
121	FIDDLER'S, B.C., CANADA	-120.75	56.25	630	1	1	3	0	0
122	FORT ROCK, OREGON, U.S.A.	-120.75	43.17	1311	3	2	3	3	1
123	FROME, SOUTH AUSTRALIA, AUSTRALIA	139.83	-30.75	-2	2	2	3	2	1
124	FUCINO,ITALY	13.56	42	650	2	3	2	3	2
125	FUQUENE, COLOMBIA	-73.75	5.5	2580	1	1	1	1	1
126	GAWANE, NIGER	5.93	16.46	500	3	0	0	0	0
127	GEBEL MAGHARA, SINAI	33.4	30.75	400	3	3	3	3	3
128	GEORGE, N.S.W., AUSTRALIA	149.42	-35.08	673	3	3	1	3	3
129	GEORGE, NEW YORK, U.S.A.	-73.65	43.52	86	1	1	2	3	1
130	GEORGE, UGANDA	30.3	0.2	900	2	2	0	0	0
131	GHADAMES, LIBYA	10.1	30.17	300	3	2	0	1	0
132	GNOTUK, VICTORIA, AUSTRALIA	143.1	-38.22	102	2	2	1	3	3
133	GOBABEB, NAMIBIA	14.98	-23.55	850	3	0	0	0	0
134	GOSHEN, ALABAMA, U.S.A.	-86.13	31.72	105	2	2	1	2	0
135	GRACE, WEST. AUSTRALIA, AUSTRALIA	118.4	-33.3	200	3	3	0	0	0
136	GRIQUALAND, SOUTH AFRICA	23.5	-28.3	1250	3	0	0	0	0
137	GUTHRIE, TEXAS, U.S.A.	-101.8	33.08	914	3	0	0	0	0
138	HAASKRAAL, SOUTH AFRICA	24.37	-31.42	1800	2	0	0	0	0
139	HAIJAD, MALI	-3.56	22.57	175	3	0	1	0	0
140	HARNEY-MALHEUR, OREGON, U.S.A.	-119.1	43.2	1246	3	0	0	2	0
141	HASSEI GABOUN, MAURITANIA	-15.82	16.3	150	3	0	1	0	0
142	HASSI CHEIKH, ALGERIA	1.8	31.13	500	3	2	0	0	0
143	HASSI EL ABIOD, MALI	-3.83	19.17	400	3	0	1	0	0
144	HASSI EL MEJNA, ALGERIA	2.3	31.5	500	3	2	1	2	0
145	HASSI MESSOUAD, ALGERIA	5.85	32	470	3	0	1	0	0
146	HASTINGS, ALBERTA, CANADA	-112.66	53.42	736	1	1	0	0	0
147	HAY, ARIZONA,U.S.A.	-109.5	34	2780	1	1	1	1	2
148	HERRERA, COLOMBIA	-74.26	4.7	2550	2	1	0	0	0
149	HIRAFOK, ALGERIA	5.67	23.65	90	3	0	0	0	0
150	HOOK, WISCONSIN, U.S.A.	-89.33	42.95	280	2	2	3	2	1
151	HORA, ETHIOPIA	41.95	9.43	1800	3	0	0	0	0
152	HOWAR, SUDAN	28.5	17.58	400	3	0	1	1	0
153	HUSSEIN, SUDAN	26.52	16.33	1150	3	0	0	1	0
154	ICHOURAD, MALI	-1.13	20.5	300	3	0	2	1	0
155	IMURUK, ALASKA, U.S.A.	-163.25	66.58	340	1	0	0	1	0
156	IN ARIDAL, NIGER	4.31	17.68	380	3	0	0	0	0
157	INE KOUSAMENE, MALI	-0.58	20.67	330	3	0	1	1	0
158	IOANNINA,GREECE	20.86	39.67	469	2	0	0	0	0
159	IRZERZOU, ALGERIA	5.56	22.73	100	3	0	0	0	1
160	ISLE, ALBERTA, CANADA	-114.43	52.62	700	1	1	3	3	0
161	ISSYK-KUL, KIRGIZ, U.S.S.R.	77.3	42.5	1609	3	0	0	0	0
162	JACOB, ARIZONA, U.S.A.	-110.83	34.42	2295	2	2	3	3	2
163	JEBEL AULIA, SUDAN	32.3	15.33	400	3	0	0	0	0
164	JEBEL MARRA(DERIBA LAKE), SUDAN	24.23	13	2000	3	0	0	0	0
165	JEBEL QUOQUIN, LIBYA	19.17	25.67	180	3	0	0	0	0
166	KADDA, ALGERIA	-0.68	28.2	250	3	0	1	0	0

167	KAFRA/ACHEGOUR, NIGER	12	18	460	3	2	0	0	0
168	KANDAHAR, AFGHANISTAN	66.14	31.36	1000	3	0	0	0	0
169	KATWE, UGANDA	29.88	-0.13	1800	3	0	0	0	0
170	KEILAMBETE, VICTORIA, AUSTRALIA	142.87	-36.04	95	2	2	1	2	3
171	KEPA, POLAND	22	49.4	320	3	2	0	0	0
172	KETTLE HOLE, IOWA, U.S.A.	-95	43	360	3	3	2	3	1
173	KHARGA, EGYPT	30.53	25.45	20	3	2	0	0	0
174	KHAT, MAURITANIA	-12.5	19.17	100	3	3	3	1	0
175	KHOTA, BOLIVIA	-68	-21.6	3000	3	0	0	0	1
176	KING, W. AUSTRALIA, AUSTRALIA	119.53	-33.08	360	3	0	0	0	0
177	KIRCHNER, MINNESOTA, U.S.A.	-92.77	44.83	275	2	2	3	2	1
178	KIVU, RWANDA/BURUNDI/ZAIRE	29	-2	1462	1	2	1	1	2
179	KLEIN AWAS, SOUTH AFRICA	20.48	-28.57	800	3	0	0	0	0
180	KOICHAB, NAMIBIA	16.5	-28.25	460	3	0	0	0	0
181	KONYA, TURKEY	33	37.5	980	3	3	3	3	2
182	KOW, VICTORIA, AUSTRALIA	144.3	-36.2	93	3	3	3	3	2
183	KUFRA, LIBYA	23.3	24.11	420	3	2	0	0	0
184	KUNTEYI, QINGHAI, CHINA	92.3	38.5	2780	3	0	0	0	0
185	LA GUITARRA, COLOMBIA	-74	3.87	3450	3	3	2	1	2
186	LAGUNA SALADA, ARIZONA, U.S.A.	-110.28	34.35	1920	3	0	0	0	0
187	LAHONTAN, NEVADA, U.S.A.	-119.5	40	1054	3	3	3	3	3
188	LEA COUNTY, NEW MEXICO, U.S.A.	-103.16	33.45	1189	3	0	0	0	0
189	LEAKE, S. AUSTRALIA, AUSTRALIA	140.57	-37.62	97	2	1	1	2	3
190	LECONTE, CALIFORNIA, U.S.A.	-116	33.33	-71	3	1	3	3	0
191	LIEBENBERGSPAN, SOUTH AFRICA	25.33	-29.13	1224	3	1	1	0	0
192	LISAN-DEAD SEA, JORDAN/ISRAEL	35.5	31.5	-395	3	3	3	3	3
193	LITTLE SALT, FLORIDA, U.S.A.	-82.17	27	5	1	1	2	1	3
194	LONGSWAMP, PENNSYLVANIA, U.S.A.	-75.67	40.48	192	2	0	0	3	1
195	LOP NOR, XINJIANG, CHINA	90.5	40.5	780	3	0	0	0	0
196	LUBBOCK, TEXAS, U.S.A.	-101.9	33.63	975	2	2	1	1	0
197	LUNKARANSAR, INDIA	73.75	28.5	200	2	0	1	1	0
198	LYNCH'S CRATER, QUEENSLAND, AUST.	145.7	-17.37	760	1	1	2	1	3
199	MAGAD, TANZANIA	35.53	-3.18	617	3	0	0	0	0
200	MAGADI-NATRON, KENYA/TANZANIA	36.04	-2.12	600	3	3	3	1	1
201	MAINE-SOROA, NIGER	12	13.12	315	3	1	2	2	0
202	MAKGADIKGADI, BOTSWANA	24.42	-20.67	880	3	0	0	0	2
203	MANAPOURI, NEW ZEALAND	167.5	-45.5	178	2	1	1	0	0
204	MANIX, CALIFORNIA, U.S.A.	-116.7	35.05	130	3	0	0	0	0
205	MANLY, CALIFORNIA, U.S.A.	-116.8	36	-86	3	0	0	0	1
206	MANYARA, TANZANIA	35.82	-3.62	945	3	3	2	1	3
207	MARSHES, S. AUSTRALIA, AUSTRALIA	140.53	-37.62	80	2	2	1	3	0
208	MELLALA, ALGERIA	4.24	32.3	700	3	0	0	0	0
209	MENDOTA, WISCONSIN, U.S.A.	-89.42	43.1	258	2	2	3	1	2
210	MENTES, NIGER	4.3	17	360	3	0	0	0	0
211	MERGA, SUDAN	26.34	19	760	3	0	0	0	0
212	MEXICO, MEXICO	-99	19.5	2240	2	2	1	2	2
213	MISSION CROSS, NEVADA, U.S.A.	-115.5	41.75	2424	1	1	1	3	0
214	MOBUTU SESE SEKO, UGANDA/ZAIRE	31	1.5	619	2	2	1	1	1
215	MOJAVE, CALIFORNIA, U.S.A.	-116.13	35.37	276	3	3	0	1	1
216	MONAHANS DUNES, TEXAS, U.S.A.	-102.77	31.62	823	3	0	0	0	0
217	MOORE, ALBERTA, CANADA	-110.5	53	600	1	1	3	3	3
218	MOUND, TEXAS, U.S.A.	-102.08	33.08	980	3	0	0	0	0
219	MOUSKORBE, CHAD	18.53	21.37	2800	3	0	0	1	0
220	MUNDAFAN,RUB'AL KHALI, S.ARABIA	45.42	18.53	670	3	3	0	2	3
221	MURZUK (ACHELOUMA), NIGER	12.68	22.33	900	3	0	0	0	0
222	MURZUK (ANAI), LIBYA	11.5	24.32	480	3	0	0	0	0
223	MURZUK (EL-GATRUN), LIBYA	14.67	24.36	300	3	3	0	0	0
224	MYALUP, W. AUSTRALIA, AUSTRALIA	115.72	-33.12	6	3	3	1	0	0

225	NABTA, EGYPT	31	23	250	3	3	1	1	3
226	NADQUAN, SAUDI ARABIA	50.23	23.26	180	3	0	0	0	0
227	NAIVASHA, KENYA	36.33	-0.88	1890	2	3	1	1	2
228	NAKURU-ELMENTEITA, KENYA	36.17	-0.42	1780	2	3	1	1	2
229	NEFUD AS-SIRR, SAUDI ARABIA	44.32	28.17	700	3	0	0	0	0
230	NEFUD URAYQ, SAUDI ARABIA	42.66	25.6	900	3	0	2	0	0
231	NGAMI-MABABE, BOTSWANA	23.53	-19.86	919	2	0	0	0	1
232	OKOBOJI, IOWA, U.S.A.	-95.2	43.33	425	1	1	3	2	1
233	OUKEDHERT, MALI	-0.75	20.67	320	3	0	2	1	0
234	OUM AROUABA, MAURITANIA	-12.67	20.67	150	3	0	1	0	0
235	OUNIANGA KEBIR, CHAD	20.5	19.05	310	3	0	1	0	0
236	OYO, SUDAN	26.18	19.27	510	3	3	2	0	0
237	PALMYRA, SYRIA	38.17	34.5	370	3	0	0	0	0
238	PANAMINT, CALIFORNIA, U.S.A.	-117.3	36.3	317	3	0	0	0	0
239	PATZCUARO, MEXICO	-101.58	19.58	2044	2	2	2	1	3
240	PHAIR, BRITISH COLUMBIA, CANADA	-122.05	50.57	716	1	2	3	0	0
241	PICKEREL, SOUTH DAKOTA, U.S.A.	-97.33	43.5	396	1	1	3	3	0
242	PITYOULISH, SCOTLAND	-3.76	57.2	210	1	1	1	0	0
243	PORTALES VALLEY,NEW MEXICO,U.S.A.	-103.83	34.44	1177	3	0	0	0	0
244	POUKAWA, NEW ZEALAND	176.73	-39.77	21	2	2	3	0	0
245	PULBEENA, TASMANIA, AUSTRALIA	145.12	-40.99	30	2	2	2	1	3
246	QAIDAM, QINGHAI, CHINA	94.5	37.5	2700	3	3	3	3	3
247	QARAT EL HOWEIT, EGYPT	27	29	100	3	0	0	0	0
248	QINGHAI, QINGHAI, CHINA	100.5	36.6	3286	2	0	3	3	0
249	QUEXIL, GUATEMALA	-90.12	16.93	110	1	2	1	2	0
250	QUINCAN, QUEENSLAND, AUSTRALIA	145.58	-17.3	790	2	2	2	0	0
251	RHIZ, MAURITANIA	-16.5	16.83	50	0	0	0	0	0
252	RICH, TEXAS, U.S.A.	-102.2	33.28	1008	3	0	0	0	0
253	ROCK BASIN, N.W.T., CANADA	-76.74	78.49	295	0	0	2	3	0
254	ROSEBUD, NEBRASKA, U.S.A.	-101	43	360	3	0	0	0	1
255	ROTORUA, NEW ZEALAND	176.3	-38.1	280	2	2	2	3	3
256	RUB'AL KHALI, SAUDI ARABIA, S. 3	48.08	17.5	500	3	0	0	0	0
257	RUB'AL KHALI, SAUDI ARABIA, S. 6	48.63	17.63	150	3	0	0	0	1
258	RUB'AL KHALI, SAUDI ARABIA,S. 15	48.43	20.42	600	3	0	0	0	0
259	RUB'AL KHALI, SAUDI ARABIA,S. A	47	20.33	210	3	0	2	0	0
260	RUB'AL KHALI, SAUDI ARABIA,S. B	45.61	18.28	660	3	0	0	0	0
261	RUB'AL KHALI, SAUDI ARABIA,S. C	46	18.08	600	3	0	0	0	0
262	RUB'AL KHALI, SAUDI ARABIA,S. D	46.22	19.05	650	3	0	0	0	0
263	RUB'AL KHALI, SAUDI ARABIA,S. E	46.47	18.03	500	3	0	0	0	0
264	RUB'AL KHALI, SAUDI ARABIA,S. F	45.48	18.34	500	3	0	0	0	0
265	RUB'AL KHALI, SAUDI ARABIA,S.12	48.67	19.42	600	3	0	0	0	0
266	RUB'AL KHALI, SAUDI ARABIA,S.16	48.62	20.48	500	3	0	1	0	0
267	RUB'AL KHALI,SAUDI ARABIA,S. 18	47.71	21.69	550	3	0	0	0	0
268	RUB'AL KHALI,SAUDI ARABIA,S. 19	51.02	21.73	600	3	0	0	0	0
269	RUB'AL KHALI,SAUDI ARABIA,SITE U	47.84	18.17	600	3	0	0	0	0
270	RUBY, NEVADA, U.S.A.	-115.33	40.58	1918	2	2	3	1	0
271	RUKWA, TANZANIA	32.5	-8	783	3	3	1	1	1
272	RUSSELL, CALIFORNIA, U.S.A.	-119.77	36.05	1961	3	2	3	2	1
273	RUTZ, MINNESOTA, U.S.A.	-93.67	44.67	314	2	2	3	2	1
274	SALPETEN, GUATEMALA	-89.67	17	104	1	0	0	0	0
275	SALT, NEW SOUTH WALES, AUSTRALIA	142.18	-30.06	78	3	0	0	0	0
276	SAMBHAR, INDIA	75	27	360	2	0	1	1	0
277	SAN AGUSTIN, NEW MEXICO, U.S.A.	-108.17	33.83	1842	3	3	2	2	2
278	SAN BARTOLO, MEXICO	-111.95	28.05	5	3	0	0	0	0
279	SAOURA, ALGERIA	-2	30	400	3	3	1	1	3
280	SBEITA, MALI	-4.2	22.83	220	3	0	0	1	0
281	SEARLES, CALIFORNIA, U.S.A.	-117.7	35.8	463	3	2	3	3	2
282	SEGUEDINE, NIGER	12.8	20.4	570	3	3	3	0	0

283	SEISTAN, AFGHANISTAN	61.91	30.85	500	3	0	0	1	0
284	SELIMA, SUDAN	29.34	21.32	200	3	2	2	1	0
285	SERIR, LIBYA	17.47	29.52	250	3	0	0	1	0
286	SEVAN, ARMENIA, U.S.S.R.	45.3	40.3	1902	2	3	1	0	0
287	SHATI, LIBYA	14	27.5	270	3	0	2	0	0
288	SHAW-SAHIL, SUDAN	27.5	20.5	470	3	3	0	0	0
289	SIETE CABEZAS, COLOMBIA	-75.15	4.9	3700	0	3	0	0	0
290	SMALLBOY, ALBERTA, CANADA	-114.13	53.58	762	1	1	3	0	0
291	STOREY'S, W. AUSTRALIA, AUSTRALIA	118.03	-31.52	300	3	0	0	0	0
292	SUGUTA, KENYA	36.46	1.91	900	3	0	0	1	0
293	SWAN, NEBRASKA, U.S.A.	-102.5	41.72	1300	1	1	2	2	0
294	SWARTKOLKVLOER, SOUTH AFRICA	20.09	-30.75	918	3	0	0	0	0
295	SZABO, NEW JERSEY, U.S.A.	-74.48	40.4	152	1	0	0	0	1
296	TABUK, SAUDI ARABIA	36.5	28.33	900	3	0	0	0	0
297	TAGERU, SUDAN	28.86	17	700	3	0	0	1	0
298	TAGNOUT-CHAGGARET, MALI	-0.75	21.03	310	3	0	1	0	0
299	TAGUA TAGUA, CHILE	-71.17	-34.5	900	3	3	2	3	2
300	TAHOE, CALIFORNIA/NEVADA, U.S.A.	-120.07	39.03	1897	2	2	0	0	0
301	TAMAYA MELLET, NIGER	5.44	17.8	360	3	0	1	0	0
302	TANGANYIKA, BURUN/TANZ/ZAM/ZAIRE	29.53	-6.03	773	2	2	1	1	2
303	TAOUDENNI, MALI	-4	22.5	120	0	0	1	0	0
304	TARADA, NIGER	4.85	15.68	400	3	0	0	1	0
305	TARSO YEGA, CHAD	17.38	20.67	2000	3	0	0	0	0
306	TASSARA, NIGER	5.7	16.89	450	3	0	0	0	0
307	TAUCA, BOLIVIA	-68	-19.5	3860	3	3	3	3	1
308	TEEL, NEVADA, U.S.A.	-118.34	38.21	1495	3	0	0	0	0
309	TERMIT OUEST-KANDEL BOUZOU,NIGER	11.25	16.08	300	3	3	1	1	0
310	TIBERIAS, TASMANIA, AUSTRALIA	147.37	-42.37	442	2	2	2	2	3
311	TIGALMAMINE, MOROCCO	-5.35	32.9	1626	0	2	1	2	3
312	TIGUENT, MAURITANIA	-16.22	20.7	50	3	1	0	0	0
313	TIN GUETTAI, MALI	-3.54	19.27	350	3	0	1	1	0
314	TIRERSIOUM, MAURITANIA	-16.68	21.37	100	3	2	1	0	0
315	TITICACA, BOLIVIA/PERU	-69.25	-16.13	3810	1	2	2	0	0
316	TRITRIVAKELY, MADAGASCAR	46.92	-19.78	1800	2	2	3	3	0
317	TROU AU NATRON, CHAD	15.52	20.97	2300	3	0	0	0	1
318	TSONDAB, NAMIBIA	15.25	-24	840	3	0	0	0	0
319	TULARE, CALIFORNIA, U.S.A.	-119.67	36	57	3	0	0	1	1
320	TURKANA, KENYA	36	5	375	3	1	1	1	0
321	TYOTJARVI, FINLAND	26.47	60.66	143	3	1	1	3	0
322	TYRRELL, VICTORIA, AUSTRALIA	142.76	-35.33	42	2	1	1	2	3
323	TYSON'S, N.S.W., AUSTRALIA	149.83	-33.85	350	3	0	0	0	0
324	URMIA, IRAN	45.5	37.63	1284	1	1	1	2	2
325	URVI, BOTSWANA	20.45	-23.05	200	3	0	0	0	0
326	VALENCIA, VENEZUELA	-67.75	10.1	402	1	1	1	2	3
327	VALLEY, SOUTH AUSTRALIA, AUSTRALIA	140.77	-37.85	100	1	1	1	0	0
328	VAN, TURKEY	43	38.5	1648	2	0	0	0	0
329	VERA, TASMANIA, AUSTRALIA	146.87	-42.27	880	1	1	3	1	3
330	VICTORIA, N.S.W., AUSTRALIA	141.28	-34	200	3	0	2	0	0
331	VICTORIA, UGANDA/TANZANIA/KENYA	33	-1	1134	1	1	1	1	1
332	WABAMUN, ALBERTA, CANADA	-114.25	53.5	732	2	2	3	1	0
333	WALDSEA, SASKATCHEWAN, CANADA	-105.2	52.28	530	1	1	0	0	0
334	WALKER, ARIZONA, U.S.A.	-111.67	36.5	2700	2	2	3	2	2
335	WALLYWASH, JAMAICA	-77.8	17.95	7	1	1	1	3	3
336	WANUM, PAPUA NEW GUINEA	146.78	-6.63	36	1	2	2	3	0
337	WARNER VALLEY, OREGON, U.S.A.	-119.83	42.45	1341	0	0	0	0	0
338	WASHBURN, WISCONSIN, U.S.A.	-90.95	43.53	248	2	2	3	1	0
339	WEBER, MINNESOTA, U.S.A.	-91.85	47.47	559	1	3	3	2	0
340	WEDGE, ALBERTA, CANADA	-115.17	50.87	1800	1	1	1	3	0

341	WEERANGANUK, VICTORIA, AUSTRALIA	143.46	-36.25	85	2	0	0	0	0
342	WELD, W. AUSTRALIA, AUSTRALIA	116.51	-34.86	0	3	0	0	0	0
343	WHITE, SOUTH CAROLINA, U.S.A.	-80.76	34.16	90	2	3	3	3	1
344	WHITE, TEXAS, U.S.A.	-102.73	33.97	1156	3	0	0	0	0
345	WHITNEY'S GULCH, QUEBEC, CANADA	-57.3	51.52	98	1	1	3	1	0
346	WIELKE GACNO, POLAND	17.2	53.73	130	1	2	2	3	0
347	WILLANDRA, N.S.W., AUSTRALIA	143	-33.5	200	3	3	3	3	3
348	WINTERGREEN, MICHIGAN, U.S.A.	-85.38	42.4	271	2	3	2	2	1
349	WONCHI,ETHIOPIA	37.92	8.8	2040	3	0	0	0	0
350	WYRIE, SOUTH AUSTRALIA, AUSTRALIA	140.3	-37.65	100	0	0	0	1	3
351	XIAO QAIDAM, QINGHAI, CHINA	95.4	37.4	2800	3	0	0	0	0
352	ZAWIYAH, LIBYA	12.73	32.87	102	3	0	0	0	0
353	ZERIBAR, IRAN	46.12	35.53	1300	1	2	2	3	3
354	ZHANGZANG CHAKA, XIZANG, CHINA	82.33	32.5	6000	3	3	1	1	1
355	ZHARINANMUCO, XIZANG, CHINA	85.55	31.08	4613	3	0	0	0	0
356	ZIWAY-SHALA, ETHIOPIA	38.67	7.75	1658	3	3	1	1	3
357	ZOO BABA, NIGER	13.08	18.22	385	3	0	0	0	0
358	ZUNI, NEW MEXICO, U.S.A.	-108.77	34.45	1935	3	0	0	0	0

```
/*****************************************************/
/*                                                   */
/*   COHMAPL1.SAS to read the COHMAP(1994) lake       */
/*   level information databases, include RC info    */
/*                                                   */
/*   This read in station names, lat, long, BNN,     */
/*   Time period, and lake status, trend and # of    */
/*   radio-carbon dates that went into each time     */
/*   period level.  Output is one line per time      */
/*   period with all station data repeated each      */
/*   line.  Identical Text file and SAS DS           */
/*   generated.                                      */
/*                                                   */
/*   JULY  7, 1997                                   */
/*   D.E. Atkinson.                                  */
/*                                                   */
/*                                                   */
/*   Modified for Windows use                        */
/*   Sept. 29, 1997                                  */
/*   A.E. Viau                                       */
/*****************************************************/

LIBNAME LAKE 'c:\users\viau\lake';

DATA lake.lakedata;
        INFILE 'c:\users\viau\lakeleve\lakedata.dat' MISSOVER;
        INPUT  @1 CHK $ 1  @  ;
        ATTRIB STN      LENGTH=$35;
        ATTRIB LAT      FORMAT=6.2;
        ATTRIB LONG     FORMAT=7.2;
        ATTRIB BMN      FORMAT=4. ;
        ATTRIB TP       FORMAT=2. ;
        ATTRIB STATUS   FORMAT=1. ;
        ATTRIB TREND    FORMAT=1. ;
        ATTRIB RCDTOT   FORMAT=2. ;
        ATTRIB RCDATE   FORMAT=5. ;
        ATTRIB SDPOS    FORMAT=5. ;
        ATTRIB SDNEG    FORMAT=5. ;
        ATTRIB REFS     FORMAT=2. ;
        ATTRIB LABNO    LENGTH=$10;
        ATTRIB MATLINFO LENGTH=$116;
        IF _N_=1 OR _N_=2 THEN RETURN;

        IF (CHK GE 'A' AND CHK LE 'z') THEN DO;

           INPUT     STN   $ 1-35
                 @37 LAT     6.
                 @46 LONG    7.
                 @55 BMN     4.
                 /////
                 @1  TP      2.
```

```
        @4  STATUS  1.
        @6  TREND   1.
        @10 RCDTOT  2.;
    IF RCDTOT=0 THEN DO;
       RCDATE=' ';SDPOS=' ';SDNEG=' ';REFS=' ';LABNO=' ';MATLINFO=' ';
       OUTPUT;
       FILE 'c:\users\viau\sasfiles\lakeout.txt';
       PUT    @1  STN
              @37 LAT   6.2
              @46 LONG  7.2
              @55 BMN
              @60 TP
              @64 STATUS
              @66 TREND
              @68 RCDTOT
              @71 RCDATE
              @77 SDPOS
              @82 SDNEG
              @87 REFS
              @90 LABNO
              @102 MATLINFO
              ;
       END;

    DO I=1 TO RCDTOT;
       INPUT @6  RCDATE  5.
             @16 SDPOS   5.
             @26 SDNEG   5.
            /
             @4  REFS    2.
                 LABNO $ 6-15
                 MATLINFO & $ 16-132;
        OUTPUT;
        FILE 'c:\users\viau\sasfiles\lakeout.txt';
        PUT    @1  STN
               @37 LAT   6.2
               @46 LONG  7.2
               @55 BMN
               @60 TP
               @64 STATUS
               @66 TREND
               @68 RCDTOT
               @71 RCDATE
               @77 SDPOS
               @82 SDNEG
               @87 REFS
               @90 LABNO
               @102 MATLINFO
               ;
        END;
    RETURN;
```

```
      END;

      RETAIN STN LAT LONG BMN TP STATUS TREND RCDTOT
             RCDATE SDPOS SDNEG REFS LABNO MATLINFO;

   ELSE DO;
      DROP CHK CHK2 I J;
      INPUT  CHK2 $ 1-2 @;
      IF CHK2 = '  ' THEN RETURN;
      INPUT @1 TP 2. @4 STATUS 1. @6 TREND 1. @10 RCDTOT 2.;
      IF (TP=80 OR TP=90) THEN RETURN;
      IF RCDTOT=0 THEN DO;
        RCDATE=' ';SDPOS=' ';SDNEG=' ';REFS=' ';LABNO=' ';
MATLINFO=' ';
        OUTPUT;
         FILE 'c:\users\viau\sasfiles\lakeout.txt';
         PUT    @1  STN
                @37 LAT   6.2
                @46 LONG  7.2
                @55 BMN
                @60 TP
                @64 STATUS
                @66 TREND
                @68 RCDTOT
                @71 RCDATE
                @77 SDPOS
                @82 SDNEG
                @87 REFS
                @90 LABNO
                @102 MATLINFO
                ;
         END;

      DO J=1 TO RCDTOT;

        INPUT @6  RCDATE  5.
              @16 SDPOS   5.
              @26 SDNEG   5.
              /
              @4  REFS    2.
                  LABNO $ 6-15
                  MATLINFO & $ 16-132;

      OUTPUT;

       FILE 'c:\users\viau\sasfiles\lakeout.txt';
       PUT    @1  STN
              @37 LAT   6.2
              @46 LONG  7.2
              @55 BMN
              @60 TP
```

```
                    @64 STATUS
                    @66 TREND
                    @68 RCDTOT
                    @71 RCDATE
                    @77 SDPOS
                    @82 SDNEG
                    @87 REFS
                    @90 LABNO
                    @102 MATLINFO
                    ;

               END;
            END;

   LABEL STN='Station Name' LAT='Lat.' LONG='Long.' BMN='Brown Master Number'
         TP='Time Period' STATUS='Lake Status' TREND='Lake Trend'
         RCDTOT='No. supporting RC dates';

RUN;
QUIT;
```

```
*************************************************************************
*                                                                       *
* This program enables extraction of lake level data by area            *
* (latitude/Longitude) from the output file of the main program         *
* cohmap.sas.                                                           *
*                                                                       *
* A.E. Viau (LPC) Nov. 97                                               *
*                                                                       *
* The lakex data step reads in lakeout.txt file created in              *
* cohmap.sas program and then based on the area needed extract          *
* the data and write it to an output file (lakena.txt)                  *
*                                                                       *
* Modification needed: path in LIBNAME; Latitude/Longitude;             *
*                      path of output file.                             *
*                                                                       *
*************************************************************************
LIBNAME lake 'c:\users\viau\lake';
DATA lakex;
        INFILE 'c:\users\viau\sasfiles\lakeout.txt'  MISSOVER;
        INPUT           STN     $ 1-35
                @37     LAT     6.2
                @46     LONG    7.2
                @55     BMN     4.
                @60     TP      2.
                @64     STATUS  1.
                @66     TREND   1.
                @68     RCDTOT  2.
                @71     RCDATE  5.
                @77     SDPOS   5.
                @82     SDNEG   5.
                @87     REFS    2.
                @90     LABNO   $10.
                @102    MATLINFO $116.
                ;

        IF LAT > 20.00 AND LAT < 90.00 THEN
                IF LONG < -50.00 AND LONG > -170.00 THEN
                DO;
                OUTPUT;
                  FILE 'c:\users\viau\sasfiles\lakena.txt';
                  PUT   @1      STN     $ 1-35
                        @37     LAT     6.2
                        @46     LONG    7.2
                        @55     BMN
                        @60     TP
                        @64     STATUS
                        @66     TREND
                        @68     RCDTOT
                        @71     RCDATE
                        @77     SDPOS
                        @82     SDNEG
                        @87     REFS
                        @90     LABNO
                        @102    MATLINFO;
                END;RUN;QUIT;
```

```
*************************************************************************
*                                                                       *
* This program enables extraction of lake level data by                 *
* the closest radiocarbon date within an interval of time               *
* search from the output files of the main program or LAKENA.sas        *
*                                                                       *
* A.E. Viau (LPC) Nov. 97                                               *
*                                                                       *
* The destin1 destin2 data step reads in the output file under          *
* investigation and based on the radiocarbon date interval that         *
* is needed will separate the interval in two equal working files       *
* (ie: if rc=3000 +- 500 years, the destin1 will contain the data       *
* for 2500-3000 rc date and destin2 will contain 3001-3500 years        *
*                                                                       *
* Modification needed: path in LIBNAME; RCDATE(s); interval             *
* for this step.                                                        *
*                                                                       *
*************************************************************************
LIBNAME LAKE 'c:\users\viau\lake';

DATA DESTIN1 DESTIN2;
        INFILE 'c:\users\viau\sasfiles\lakena.txt' MISSOVER;
        INPUT           STN     $ 1-35
                @37     LAT     6.2
                @46     LONG    7.2
                @55     BMN     4.
                @60     TP      2.
                @64     STATUS  1.
                @66     TREND   1:
                @68     RCDTOT  2.
                @71     RCDATE  5.
                @77     SDPOS   5.
                @82     SDNEG   5.
                @87     REFS    2.
                @90     LABNO   $10.
                @102    MATLINFO $116.
                ;

        IF RCDATE>=2500 AND RCDATE<=3000 THEN output DESTIN1; ELSE
        IF RCDATE > 3000 AND RCDATE <= 3500 THEN  output DESTIN2;
RUN;
*************************************************************************
*                                                                       *
* This step sorts the output of destin1,destin2 by stn and rcdate       *
* in ascending order                                                    *
*                                                                       *
* Modification optional: sorting keys                                   *
*                                                                       *
*************************************************************************
PROC SORT DATA=DESTIN1; BY STN RCDATE; RUN;
PROC SORT DATA=DESTIN2; BY STN RCDATE; RUN;
```

```
*************************************************************************
* This step extract  the closest date to the search date from          *
* destin1 and outputs it into working dataset res1a                    *
*                                                                       *
* Modification optional: set key (BY)                                  *
*                                                                       *
*************************************************************************
DATA RES1 RES1A;
        SET DESTIN1;
        BY STN;
        IF LAST.STN THEN output RES1A;
RUN;
*************************************************************************
* This step extract  the closest date to the search date from          *
* destin2 and outputs it into working dataset res2a                    *
*                                                                       *
* Modification optional: set key (BY)                                  *
*                                                                       *
*************************************************************************
DATA RES2 RES2A;
        SET DESTIN2;
        BY STN;
        IF FIRST.STN THEN output RES2A;
RUN;
*************************************************************************
*                                                                       *
* This step sorts the output of res1a,res2a by stn and rcdate          *
* in ascending order                                                   *
*                                                                       *
* Modification optional: sorting keys                                  *
*                                                                       *
*************************************************************************
PROC SORT DATA=RES1A;BY STN RCDATE; RUN;
PROC SORT DATA=RES2A;BY STN RCDATE; RUN;

*************************************************************************
*                                                                       *
* The result data step consists of mergin both res1a and res2a         *
* and extracting the closest date to the search date whether it be*
* less or plus from the expected date. The closest date and            *
* associated fields are then output to a text file.                    *
*                                                                       *
* Modification optional: set keys; search date; output file name       *
*                                                                       *
*************************************************************************
DATA RESULT;
        SET RES1A RES2A;
        BY STN RCDATE;

        IF (FIRST.STN AND (RCDATE-3000)) <= (LAST.STN AND (3000-RCDATE)) THEN
         DO;
```

```
        OUTPUT;
        FILE 'c:\users\viau\sasfiles\lake3000.txt';
             PUT     @1      STN
                     @37     LAT     6.2
                     @46     LONG    7.2
                     @55     BMN
                     @60     TP
                     @64     STATUS
                     @66     TREND
                     @68     RCDTOT
                     @71     RCDATE
                     @77     SDPOS
                     @82     SDNEG
                     @87     REFS
                     @90     LABNO
                     @102    MATLINFO;
    END;

    ELSE
            IF  LAST.STN THEN

              DO;
                OUTPUT;
                FILE 'c:\users\viau\sasfiles\lake3000.txt';
                    PUT     @1      STN
                            @37     LAT     6.2
                            @46     LONG    7.2
                            @55     BMN
                            @60     TP
                            @64     STATUS
                            @66     TREND
                            @68     RCDTOT
                            @71     RCDATE
                            @77     SDPOS
                            @82     SDNEG
                            @87     REFS
                            @90     LABNO
                            @102    MATLINFO;
              END;
RUN;
QUIT;
```

Appendix B: The European Lake Level Database

Id	Basin	Longitude	Latitude	Altitude	0 ka	3 ka	6 ka	9 ka	12 ka
1	Attersee	13.53	47.86	469	2	3	1	0	0
2	Mondsee	13.37	47.83	475	2	3	1	0	0
3	Schwemm	12.17	47.58	664	0	0	2	2	2
4	Aapalampi	28.53	66.6	204	0	0	1	1	0
5	Ahvenainen	25.11	61.03	122.2	2	2	1	2	0
6	Hakojärvi	25.2	61.25	145.6	2	2	1	1	0
7	Isohattu	23.6	68.6	386	2	2	3	1	0
8	Jierstivaara	23.63	68.6	456	2	2	3	1	0
9	Kaunispää	27.42	68.42	300	0	0	0	2	0
10	Kissalammi	24.35	61.28	90.4	2	3	1	0	0
11	Kyrösjärvi	23.17	61.75	83	1	2	2	0	0
12	Lampellonjärvi-Lamminjarvi	29.07	62.07	108.6	2	2	1	3	0
13	Lovojärvi	25.03	61.08	108.2	1	3	1	1	0
14	Pieni Majaslampi	24.58	60.31	97.3	1	1	2	3	0
15	Sarkkilanjärvi	23.1	61.75	87	1	1	1	0	0
16	Tankavaara	27.23	68.18	335	0	0	2	3	0
17	Työtjärvi	25.47	60.98	142.8	2	1	1	2	0
18	Vanhalampi	29.58	66.37	205	1	1	3	2	0
19	Abbaye	5.87	46.67	871	2	0	0	0	0
20	Chalain	5.77	46.68	488	2	1	1	1	0
21	Clairvaux	5.75	46.57	526	2	3	3	0	0
22	Hières-sur-Amby	5.28	45.79	212	0	0	2	2	1
23	Issarlès	4.07	44.8	997	2	2	2	3	0
24	Landos	3.8	44.83	1000	2	2	2	2	1
25	Le Grand Lemps	5.42	45.47	456	3	3	1	1	2
26	Paladru	5.5	45.42	492	1	2	0	0	0
27	Pelléautier	6.18	44.52	975	2	3	3	2	1
28	Pluvis	5.63	45.63	215	1	3	1	2	0
29	Rousses	5.2	46.8	1058	2	3	2	1	0
30	Saint-Julien-de-Ratz	5.62	45.35	650	0	0	0	1	2
31	Federsee	9.58	48.17	501	2	3	2	3	1
32	Großer Plöner See	10.42	54.17	578	1	2	2	1	0
33	Schleinsee	9.5	47.75	40	2	2	1	3	3
34	Seeburger See	10.17	51.5	474	1	2	2	3	0
35	Sewensee	6.87	47.82	156	2	3	2	2	0
36	Tegeler See	13.25	52.58	35	3	2	1	2	3
37	Ioannina	20.88	39.66	469	3	3	2	2	2
38	Kastoria	21.32	40.55	650	3	1	0	0	0
39	Khimaditis	21.57	40.6	560	3	1	1	3	2
40	Vegoritis	21.75	40.75	570	2	3	1	0	0
41	Xinias	22.26	39.07	500	2	1	1	1	2
42	Balaton	17.5	46.8	105	1	1	3	3	0
43	Hafratjörn	-20.1	65.83	97	2	3	1	0	0
44	Lomatjörn	-20.33	64.33	100	3	2	2	0	0

45	Belle Lake	-7.03	52.18	33	0	0	2	2	2
46	Cannons Lough	-6.58	54.92	30	0	0	0	3	1
47	Coolteen	-6.6	52.35	50	0	0	0	3	1
48	Cregganmore	-9.6	54.25	60	2	2	1	2	2
49	Sheeauns	-10.05	53.55	18	2	2	2	1	0
50	Castiglione	12.76	41.89	44	1	3	3	1	1
51	Fucino	13.55	42	667	2	3	2	3	2
52	Lago di Ganna	8.83	45.87	452	3	3	3	1	1
53	Ellasjöen	19.01	74.38	20.6	3	2	2	3	0
54	Endletvatn	19.08	69.73	35	2	2	2	1	2
55	Lerstadvatn	6.5	62.5	44	1	1	1	1	2
56	Nedre Æråsvstn	19.07	69.75	35	0	0	0	0	2
57	Øvre Æråsvstn	19.05	69.73	44	2	0	0	0	3
58	Pølsa	16.93	74.5	14	3	3	1	3	0
59	Saudedalsmyra	6.4	62.4	30	0	0	0	2	0
60	Skinkevatna	16.81	74.48	19.3	3	2	1	3	0
61	Torvlømyra	6.5	62.4	35	0	0	0	2	0
62	Goplo	18.31	52.6	77	1	2	1	0	0
63	Kepa	22	49.4	320	3	3	3	3	0
64	Kolno	23.01	53.77	121	1	2	2	0	0
65	Kruklin	21.87	54.07	127	2	3	1	0	0
66	Lukcze	23	51.5	170	2	2	2	1	3
67	Steklin	19	52.95	73.3	1	1	2	1	0
68	Wielkie Gacno	17.2	53.73	130	1	1	2	1	1
69	Lagoa Comprida	-8	39.75	1600	3	2	1	1	0
70	L. de las Madres	-6.85	37.17	20	3	3	0	0	0
71	Padul	-4.63	37.03	785	3	3	2	2	1
72	Sanguijuelas	-6.73	42.1	1050	2	3	2	2	2
73	Ageröds mosse	13.43	55.93	55	1	1	2	3	0
74	Bjäresjö	13.75	55.45	48	1	0	0	0	0
75	Bysjön	13.53	55.67	22	1	2	2	3	0
76	Juokojauratj	19.27	66.6	400	1	2	2	0	0
77	Krageholmssjön	13.73	55.5	43	1	2	1	3	0
78	Kroktjärnen	20.85	66.23	58	1	1	0	0	0
79	Lilla Gloppsjön	14.62	59.81	198	1	1	3	1	0
80	Ljustjärnen	14.48	59.76	183	1	2	3	1	0
81	Lyngsjö	12.55	56.98	55	0	0	0	3	0
82	Ranviken	14.3	56.27	81	1	3	1	3	0
83	Sandsjön	13.42	56.75	157.8	1	2	1	2	0
84	Torreberga	13.14	55.37	8	1	3	1	3	0
85	Trummen	14.75	56.87	161	1	3	1	3	0
86	Växjösjön	14.75	56.87	161	1	2	3	3	0
87	Vielången	13.17	56.19	93	1	3	1	3	0
88	Bielersee	7.1	47.1	429	1	2	3	3	2
89	Hobschensee	8.01	46.25	2017	2	2	2	3	1
90	Léman	7.25	46.91	373	2	3	2	2	1
91	Lobsigensee	7.3	47.03	514.4	2	3	2	2	2
92	Nussbaumersee	8.45	47.85	434	1	2	3	2	1
93	Rotsee	8.31	47.15	419	2	3	3	1	0

94	a'Chnuic	-3.58	57.2	310	0	0	2	0	0
95	a'Mhuillinn	-5.27	55.7	25	1	3	2	1	0
96	Berrington Pool	-2.12	52.63	40	1	0	0	0	0
97	Black Lock	-3.17	56.25	90	2	2	2	2	2
98	Borralan	-4.9	58.05	139	2	2	3	2	3
99	Cam	-5	58.08	123.5	2	2	2	2	2
100	Crose Mere	-2.83	52.83	87	1	2	2	3	2
101	Diss Mere	1.1	52.37	26	2	1	2	1	3
102	Dubh Lochan	-4.6	56.15	75	2	2	1	1	0
103	Ellesmere Mere	-2.9	52.9	80	1	0	0	0	0
104	Garten	-3.7	57.22	220	1	1	1	0	0
105	Hockham Mere	0.83	52.5	33	2	2	3	2	3
106	Hornsea Old Mere	-0.1	53.83	1	0	3	2	2	0
107	Linton Loch	-2.63	55.67	91.5	2	1	3	2	0
108	Llangorse Lake	-3.25	51.95	155	1	2	3	1	0
109	Llyn Clyd	-4.17	53.08	746.8	2	1	3	0	0
110	Melynllyn	-4.12	53.12	632.5	2	1	2	1	0
111	Old Buckenham Mere	1.02	52.5	35	1	3	3	2	0
112	Pityoulish	-3.8	57.2	210	1	1	2	3	0
113	Roos	0.07	53.67	5	0	0	2	2	1
114	Saham Mere	0.8	52.57	38	0	0	1	1	2
115	Sea Mere	1	52.57	38	1	2	2	2	3
116	Traeth Mawr	-3.5	51.92	330	0	0	0	3	1
117	Malo Jezero	17.35	42.78	0	0	2	2	0	0
118	Palu	13.7	45.01	0	0	2	1	0	0

Appendix C: The FSU and Mongolia Lake Level Database

Id	Basin	Longitude	Latitude	Altitude (m)	0 ka	3 ka	6 ka	9 ka	12 ka
1	Antu Sinijärv	26.33	59.13	94.6	2	1	2	1	0
2	Kaali	22.67	58.37	13.5	1	2	0	0	0
3	Kalina	27.42	59.37	50	2	2	2	1	0
4	Kirikumäe	27.25	57.67	183	2	1	1	1	0
5	Päidre	25.5	58.27	50.6	2	2	2	3	0
6	Punso	27.25	57.68	183.2	1	1	2	3	0
7	Raigastvere	26.73	58.6	51.8	1	1	3	3	0
8	Saviku	27.24	58.42	31	3	3	1	0	0
9	Tuuljärv	27.14	57.69	257	3	3	1	0	0
10	Vaharu	24.37	58.34	45	3	3	2	1	0
11	Lubanas	26.92	56.77	90.8	2	2	1	1	0
12	Rudushskoe	27.55	56.5	150	2	2	2	0	0
13	Vorkalu	27.5	56.33	154.3	1	2	2	0	0
14	Bebrukas	24.55	54.12	160	2	1	2	3	0
15	Cepkeliu	24.52	54.02	129.5	2	2	3	1	0
16	Shventoji	21.25	55	5	3	2	0	0	0
17	Chervonoe	28	52.38	136	2	2	2	2	0
18	Glubelka	26.41	54.95	165.8	1	3	1	3	0
19	Krivoe	29.07	55.14	131	2	2	1	3	0
20	Naroch	26.85	54.85	120	1	3	2	1	2
21	Oltush	23.96	51.7	158.3	2	2	2	3	0
22	Peschanoe	25.48	51.98	139.3	2	2	2	2	0
23	Richi	26.72	55.68	146.2	2	1	2	3	0
24	Sporovskoe	25.33	52.33	142	2	1	3	1	0
25	Sudoble	28.1	54.03	165	3	2	3	1	0
26	Svitjaz	23.87	51.5	163	1	2	0	0	0
27	Tur	24.3	51.67	155	2	1	2	3	0
28	Kanent'yavr	34.3	68.8	182.9	2	1	1	3	0
29	Kovdor	30.88	67.65	160	3	2	2	1	0
30	Pasmlambina	35.45	66.7	122	3	2	2	3	0
31	Bezdonnoe	32.5	62	123	3	3	1	2	0
32	Chechkino	34	62.25	55	2	2	1	3	0
33	Dlinnoe	33.65	62.32	66	2	2	2	3	0
34	Gotnavolok	33.75	62.17	68	2	3	1	3	0
35	Moshkarnoe	34.25	62.25	58	3	3	1	1	0
36	Nosuo	30.58	64.58	165	2	2	2	3	0
37	Paanayarvi	29.95	66.26	136.6	3	2	3	1	0
38	Razlomnoe	34.53	62.24	53	2	2	1	3	0
39	Rugozero	32.52	64.08	130	2	2	2	1	0
40	Michurinskoe	29.98	60.52	94	3	2	2	2	0
41	Uzomoe	29.97	60.58	55	1	3	1	0	0
42	Vishnevskoe	29.52	60.5	15	2	2	1	0	0
43	Il'men	31.23	58.3	18	2	3	2	2	0
44	Tesovo-Netyl'skoe	30.9	58.92	58.5	2	2	2	1	0

45	Valdaiskoe	33.27	57.98	192.5	2	2	2	3	2
46	Mutnoe	31.78	55.5	180	1	3	2	2	0
47	Zaozer'e	31.92	55.02	175	2	1	2	3	0
48	Beloe	39	62.33	135	3	3	3	3	0
49	Lacha	37.67	62.58	118	2	3	2	1	0
50	Laksa	40.58	62.6	109	3	3	1	1	0
51	Mitrofanovskoe	59	67.83	116.8	2	3	3	0	0
52	Rodnichnoe	43.17	64.93	100	3	3	2	2	0
53	Schukozero	39.83	62.35	165	2	1	2	3	0
54	Kubenskoe	39.5	59.7	110	0	0	0	3	2
55	Vozhe	39.08	60.43	121	2	2	3	1	0
56	Melekhovo	38.5	56.83	150	3	3	3	1	0
57	Nero	39.48	57.17	93	2	3	2	1	2
58	Somino .	38.8	56.6	134.4	3	2	2	1	0
59	Beloe-Chernoe	37.35	55.72	145	2	3	2	1	1
60	Chistoe	38.32	55.78	160	2	2	2	1	1
61	Dolgoe	37.32	56.07	200	2	1	3	3	0
62	Nerskoe	37.39	56.08	165	2	2	2	3	1
63	Trostenskoe	36.48	55.66	195	2	2	1	0	0
64	Galichskoe	42.28	58.4	101.2	2	3	1	0	0
65	Luganskoe	40.68	43.72	2425	3	3	0	0	0
66	Rybnoe	41.17	43.58	2151	3	0	0	0	0
67	Melent'evskoe	48.57	63.93	90	0	0	0	3	0
68	Sindorskoe	52	60.77	130	2	2	3	2	1
69	Krasnokamsk	55.7	58.05	90	3	2	2	1	0
70	Osintsevo	57.63	57.37	149	3	3	1	1	0
71	Argayash	60.89	55.58	250	2	1	2	3	0
72	Bol'shoi Kisegach	60.38	55.04	317	2	1	1	2	0
73	Uvil'dy	62.37	55.53	273.4	1	1	2	1	3
74	Jamylimujaganto	78	66.42	10.3	1	3	0	0	0
75	Chany	77.5	54.75	106.1	3	2	2	1	1
76	Boguda	123.25	63.67	117	2	2	1	2	0
77	Chabada	129.37	61.98	245	3	3	2	2	0
78	Khomustakh	121.62	63.62	120	2	2	2	3	0
79	Madjagara	120.97	64.83	160	2	1	1	0	0
80	Nuochaga	129.55	61.3	250	1	2	0	0	0
81	Kotokol	108.17	52.83	460	2	2	2	3	0
82	Sevan	45.42	40.5	1898	2	2	3	2	1
83	Borovoe	70.27	53.08	321	2	2	2	3	2
84	Karas'e	70.22	53.03	435	2	2	1	3	0
85	Maybalyc	70.13	53.15	306	3	3	3	0	0
86	Mokhovoe	64.25	53.77	178	2	1	2	0	0
87	Pashennoe	75.4	49.37	871	2	1	2	3	2
88	Schuch'ye	70.17	52.98	398	2	0	0	0	0
89	Shalkar	68.42	53.18	309.7	2	0	0	0	0
90	Aral	60	45	53	1	2	3	0	0
91	Issyk-Kul	77.3	42.5	1607	2	2	0	0	0
92	Sonkel	75.15	41.82	3016	3	2	0	0	0
93	Rangkul-Shorkul	74.2	38.52	3779	3	2	1	2	0

94	Achit-Nur	90.6	49.5	1435	2	2	2	3	1
95	Buir-Nur	117.7	47.75	583	2	3	0	3	0
96	Daba-Nur	98.8	48.2	2465	2	3	1	3	0
97	Dood-Nur	99.38	51.33	1538	3	2	2	1	2
98	Gun-Nur	106.6	50.25	600	2	2	1	3	0
99	Hara-Nur	93.12	47.97	1132	2	0	0	0	0
100	Hara-Us-Nur	92	47.92	1156	2	3	0	0	0
101	Hoton-Nur	88.3	48.67	2063	3	3	2	1	1
102	Hubsugul	100.17	50.53	1645	2	1	3	0	0
103	Terkhiin-Tsagan-Nur	99.7	48.15	2060	2	2	3	0	0

Appendix D: Projection and summary spatial statistic procedures.

Presented below are two procedures used in the transformation of Lat/Long Plate Carré to Hammer-Aitoff Equal Area Projection, the latter being used for the summary spatial statistics.

Procedure 1: Steps for converting Mapviewer v2.13 maps (.gsb) into Hammer-Aitoff projection.

1- Import .gsb file from Mapviewer v2.13 into Surfer v 6.0

2- Export .gsb file from Surfer v 6.0 in .dxf format

3- Import .dxf file into IDRISI v. 5.0 using FILE IMPORT - DXFIDRIS option

4- Conversion of projection using PROJECT option into Hammer-Aitoff projection (clabsha)

5- Export IDRISI v. 5.0 vector file in .dxf format using EXPORT - DXFIDRIS option

Procedure 2: Steps for converting data points (.dat) into Hammer-Aitoff projection.

1- Import .dat or .txt files into Microsoft Excel 97

2- Save files as .csv (comma delimited) files

3- Open .csv file into an editor (ie: Wordpad) and replace commas for blanks to give a true space delimited format (eg: Microsoft Excel has problems doing this task and IDRISI v 5.0 only takes spaced-delimited data files as input).

4- Rename .csv files with an extension of .dat if you wish

5- Import .dat files into IDRIS v. 5.0 using XYZIDRIS option to create point vector files (.vec and .dvc)

6- Make necessary projection conversion using PROJECT option (ie: clabsha)

7- Export IDRISI v. 5.0 vector file to Surfer v. 6.0 using EXPORT - SRFIDRIS option

8- Now the .dat files contain the coordinate system of Hammer-Aitoff projection and can be used to compute distances in kilometers.

```
*************************************************************************
*
* This S-Plus program calculates the mean distance between sample sites in
* kilometers, the median distance, minimum distance, maximum distance, first and third
* quartiles for irregularly spaced data
*
* Written by M. Sawada - LPC
* University of Ottawa, June 1998
*
*************************************************************************
meandistance
function(datafile, dist = 2)
{
        easting <- vector("numeric")
        northing <- vector("numeric")
        easting <- 1
        northing <- 2
        output <- list("numeric")
        mindst <- vector("numeric")
        firstquart <- vector("numeric")
        meandist <- vector("numeric")
        mediandist <- vector("numeric")
        thirdquart <- vector("numeric")
        maxdist <- vector("numeric")
        toloop <- ncol(datafile)/2
        for(i in 1:toloop) {
                place <- cbind(na.omit(datafile[, easting]), na.omit(datafile[, northing]))
                quad <- quad.tree(place)
                nhbr <- find.neighbor(x = place, quadtree = quad, k = dist)
                nhbr <- nhbr[nhbr[, 1] != nhbr[, 2], ]
                nhbr[, 3] <- ifelse(nhbr[, 3] == 0, 0, nhbr[, 3])
                nhbr <- spatial.neighbor(row.id = nhbr[, 1], col.id = nhbr[, 2], weights = nhbr[, 3])
                nhbr <- summary(nhbr[, 3])
                easting <- easting + 2
                northing <- northing + 2
                mindst <- c(mindst, nhbr[1])
                firstquart <- c(firstquart, nhbr[2])
                mediandist <- c(mediandist, nhbr[3])
                meandist <- c(meandist, nhbr[4])
                thirdquart <- c(thirdquart, nhbr[5])
                maxdist <- c(maxdist, nhbr[6])
        }
        mindst <- unlist(mindst, recursive = T, use.names = F)
        firstquart <- unlist(firstquart, recursive = T, use.names = F)
        mediandist <- unlist(mediandist, recursive = T, use.names = F)
        meandist <- unlist(meandist, recursive = T, use.names = F)
        thirdquart <- unlist(thirdquart, recursive = T, use.names = F)
        maxdist <- unlist(maxdist, recursive = T, use.names = F)
        output <- cbind(min = mindst, FirstQuart = firstquart, median = mediandist, mean = meandist, ThirdQuart =
thirdquart, max = maxdist)
        output }
```

Appendix E: Lake sites excluded from study.

0 ka

Id	Basin	Longitude	Latitude	Altitude	Present
17	Työjärvi	25.47	60.88	142.8	2
25	Le Grand Lemps	5.42	45.47	456	3
36	Tegeler See	13.25	52.58	35	3
40	Vegortis	21.75	40.75	870	2
41	Xinias	22.28	39.07	500	2
42	Balaton	17.5	46.8	105	1
43	Hafratjörn	-20.1	65.83	97	2
44	Lomatjörn	-20.33	64.33	100	3
52	Lago di Ganna	8.83	45.87	452	3
63	Kepe	22	49.4	320	3
72	Sanguijuelas	-6.73	42.1	1050	2
86	Växjösjön	14.75	56.87	161	1
126	Saviku	27.24	58.42	31	3
127	Tuujärv	27.14	57.69	257	3
128	Veharu	24.37	58.34	45	3
134	Shventoji	21.25	55	5	3
143	Sudobie	28.1	54.03	165	3
146	Kanent'yevr	34.3	68.8	182.9	2
147	Kovdor	30.88	67.65	160	3
148	Pasmiambina	35.45	68.7	122	3
149	Bezdonnoe	32.5	62	123	3
153	Moshkarnoe	34.25	62.25	58	3
155	Paanayarvi	29.95	66.28	136.6	3
158	Michurinskoe	29.98	60.52	94	3
166	Beloe	39	62.33	135	3
171	Schukozero	39.83	62.35	165	2
174	Malakhovo	38.5	58.83	150	3
176	Somino	38.8	58.6	134.4	3
177	Beloe-Chernoe	37.35	56.72	145	2
180	Norskoe	37.38	58.08	165	2
186	Sindorskoe	52	60.77	130	2
188	Osintsevo	57.83	57.37	149	3
190	Bol'shoi Kisegach	60.38	55.04	317	2
193	Chany	77.5	54.75	108.1	3
195	Chebada	129.37	61.98	245	3
196	Nuochaga	129.55	61.3	250	1
199	Kotokol	108.17	52.83	460	2
201	Borovoe	70.27	53.08	321	2
202	Karas'e	70.22	53.03	435	2
203	Maybalyc	70.13	53.15	308	3
206	Schuch'ye	70.17	52.98	368	2

209	Issyk-Kul	77.3	42.5	1607	2
212	Achit-Nur	90.6	49.5	1435	2
215	Dood-Nur	99.36	51.33	1536	3
218	Hara-Us-Nur	92	47.92	1156	2
219	Hoton-Nur	88.3	48.67	2083	3
232	ALBACUTYA, VICTORIA, AUSTRALIA	141.67	-35.75	220	3
245	BALATON, HUNGARY	17.5	46.8	-106	1
247	BARINGO, KENYA	36	0.5	987	2
254	BEYSEHIR, TURKEY	31.5	37.75	1120	2
257	BIRKET RAM, ISRAEL/JORDAN	35.25	33.25	940	2
258	BOGORIA, KENYA	36.1	0.3	980	2
259	BONNEVILLE, UTAH, U.S.A.	-113	40.5	1280	3
276	CHAD, NIGERIA/NIGER	14	13	282	2
278	CHALMER'S, ALBERTA, CANADA	-114.46	50.64	1370	3
282	CHESHI-MWERU WANTIPA, ZAMBIA	29.66	-8.87	928	2
285	CHICHANCANAB, MEXICO	-88.75	19.5	38	3
304	DE AGUA SUCIA, COLOMBIA	-73.47	3.4	280	1
317	EL ABRA, COLOMBIA	-74	5	2570	3
319	EL GOBERNADOR, COLOMBIA	-74.35	3.85	3815	3
336	EURAMOO, QUEENSLAND, AUSTRALIA	145.63	-17.17	730	2
343	FORT ROCK, OREGON, U.S.A.	-120.75	43.17	1311	3
344	FROME, SOUTH AUSTRALIA, AUSTRALIA	139.83	-30.75	-2	2
345	FUCINO,ITALY	13.55	42	650	2
346	FUQUENE, COLOMBIA	-73.75	5.5	2580	1
359	HAASKRAAL, SOUTH AFRICA	24.37	-31.42	1900	2
361	HARNEY-MALHEUR, OREGON, U.S.A.	-119.1	43.2	1246	3
363	HASSI CHEIKH, ALGERIA	1.8	31.13	500	3
368	HAY, ARIZONA,U.S.A.	-109.5	34	2780	1
379	IOANNINA,GREECE	20.85	39.67	469	2
382	ISSYK-KUL, KIRGIZ, U.S.S.R.	77.3	42.5	1608	3
383	JACOB, ARIZONA, U.S.A	-110.83	34.42	2285	2
390	KATWE, UGANDA	29.88	-0.13	1900	3
392	KEPA, POLAND	22	49.4	320	3
393	KETTLE HOLE, IOWA, U.S.A.	-96	43	350	3
402	KONYA, TURKEY	33	37.5	990	3
403	KOW, VICTORIA, AUSTRALIA	144.3	-38.2	83	3
406	LA GUITARRA, COLOMBIA	-74	3.67	3450	3
417	LUBBOCK, TEXAS, U.S.A.	-101.9	33.63	975	2
420	MAGAD, TANZANIA	35.53	-3.18	617	3
427	MANYARA, TANZANIA	35.82	-3.62	945	3
434	MISSION CROSS, NEVADA, U.S.A.	-115.5	41.75	2424	1
448	NAIVASHA, KENYA	36.33	-0.68	1890	2
449	NAKURU-ELMENTEITA, KENYA	36.17	-0.42	1750	2
452	NGAMI-MABABE, BOTSWANA	23.53	-19.86	919	2
468	QARAT EL HOWEIT, EGYPT	27	28	100	3
469	QINGHAI, QINGHAI, CHINA	100.5	36.8	3286	2

475	ROSEBUD, NEBRASKA, U.S.A.	-101	43	360	3
491	RUBY, NEVADA, U.S.A.	-115.33	40.58	1818	2
492	RUKWA, TANZANIA	32.5	-8	783	3
514	SWAN, NEBRASKA, U.S.A.	-102.5	41.72	1300	1
521	TAHOE, CALIFORNIA/NEVADA, U.S.A.	-120.07	39.03	1897	2
536	TITICACA, BOLIVIA/PERU	-69.25	-16.13	3810	1
542	TYOTJARVI, FINLAND	25.47	60.96	143	3
552	VICTORIA, UGANDA/TANZANIA/KENYA	33	-1	1134	1
555	WALKER, ARIZONA, U.S.A.	-111.67	38.5	2700	2
567	WIELKE GACNO, POLAND	17.2	53.73	130	1

3 ka

Id	Basin	Longitude	Latitude	Altitude	3 ka
10	Kisselammi	24.35	61.28	90.4	3
13	Lovojärvi	25.03	61.08	106.2	3
17	Työtjärvi	25.47	60.96	142.8	1
20	Chelein	5.77	46.66	486	1
23	Issarlès	4.07	44.6	997	2
24	Landos	3.8	44.83	1000	2
26	Paladru	5.5	45.42	492	2
32	Großer Plöner See	10.42	54.17	578	2
33	Schleinsee	9.5	47.75	40	2
34	Seeburger See	10.17	51.5	474	2
36	Tegeler See	13.25	52.58	35	2
37	Ioannina	20.88	39.66	469	3
40	Vegoritis	21.75	40.75	570	3
42	Balaton	17.5	46.8	105	1
43	Hafratjörn	-20.1	65.83	97	3
44	Lomatjörn	-20.33	64.33	100	2
53	Elisejön	19.01	74.38	20.8	2
58	Paise	18.83	74.5	14	3
60	Skinkavatna	18.81	74.48	19.3	2
63	Kepa	22	49.4	320	3
65	Kruklin	21.87	54.07	127	3
68	Wielkie Gacno	17.2	53.73	130	1
69	Lagoa Comprida	-8	39.75	1800	2
72	Sanguijuelas	-6.73	42.1	1060	3
79	Lilla Gloppsjön	14.62	58.81	186	1
80	Ljustjärnen	14.48	58.76	183	2
82	Ranviken	14.3	58.27	61	3
83	Sandsjön	13.42	58.75	157.8	2
84	Tarreberga	13.14	55.37	8	3
85	Trummen	14.75	56.67	161	3
86	Vättsjön	14.75	58.67	161	2

87	Vielängen	13.17	58.19	93	3
88	Bielersee	7.1	47.1	429	2
89	Hobschensee	8.01	46.25	2017	2
92	Nussbaumersee	8.45	47.05	434	2
95	a'Mhuillinn	-6.27	56.7	25	3
108	Hornsea Old Mere	-0.1	53.93	1	3
111	Old Buckenham Mere	1.02	52.5	35	3
117	Malo Jezero	17.35	42.78	0	2
118	Palu	13.7	45.01	0	2
121	Kalina	27.42	59.37	50	2
122	Kirikumäe	27.25	57.97	183	1
124	Puruo	27.25	57.88	183.2	1
126	Saviku	27.24	58.42	31	3
127	Tuuljärv	27.14	57.99	257	3
128	Vaharu	24.37	59.34	45	3
136	Glubelka	26.41	54.95	165.8	3
138	Naroch	26.85	54.85	120	3
148	Pasmiambina	35.45	56.7	122	2
150	Chechkino	34	62.25	55	2
151	Dlinnoe	33.85	62.32	66	2
156	Raziomnoe	34.53	62.24	53	2
157	Rugozero	32.52	64.06	130	2
159	Uzomoe	29.97	60.58	55	3
162	Tesovo-Netyl'skoe	30.9	58.92	58.5	2
163	Valdaiskoe	33.27	57.96	192.5	2
164	Mutnoe	31.78	55.5	180	3
165	Zaozer'e	31.92	55.02	175	1
171	Schukozero	39.83	62.35	165	1
173	Vozhe	39.08	60.43	121	2
176	Somino	38.8	56.6	134.4	2
178	Chiatoe	38.32	55.78	160	2
179	Dolgoe	37.32	56.07	200	1
180	Nerskoe	37.38	56.08	165	2
181	Trostenskoe	36.48	55.86	195	2
187	Krasnokamsk	56.7	58.05	90	2
188	Osintsevo	57.83	57.37	149	3
190	Bol'shoi Kisegach	60.36	55.04	317	1
193	Chany	77.5	54.75	108.1	2
195	Chebada	129.37	61.98	245	3
196	Nuochega	129.56	61.3	250	2
203	Maybalyc	70.13	53.15	308	3
209	Issyk-Kul	77.3	42.5	1607	2
210	Sonkul	75.15	41.82	3016	2
211	Rangkul-Shortul	74.2	38.52	3778	2
212	Achit-Nur	90.6	49.5	1436	2
214	Dabe-Nur	88.8	49.2	2465	3

215	Dood-Nur	99.38	51.33	1638	2
220	Hubsugul	100.17	50.53	1645	1
225	ADOBE, CALIFORNIA, U.S.A.	-118.6	37.91	1951	2
233	ALEXANDERSFONTEIN, S.AFRICA	24.8	-28.83	500	3
239	ARD EL AKHDAR, EGYPT	28.03	23.18	950	2
240	ASAL, DJIBOUTI	42.5	11.6	-155	2
245	BALATON, HUNGARY	17.5	46.8	-105	2
246	BANCANNIA, N.S.W., AUSTRALIA	141.93	-30.82	107	2
249	BEBEDERO, ARGENTINA	-66.75	-33.33	380	2
254	BEYSEHIR, TURKEY	31.5	37.75	1120	2
255	BILMA, NIGER	13	18.75	310	2
257	BIRKET RAM, ISRAEL/JORDAN	35.25	33.25	940	2
258	BOGORIA, KENYA	36.1	0.3	990	1
259	BONNEVILLE, UTAH, U.S.A.	-113	40.5	1280	3
261	BOU ALI, ALGERIA	-0.25	27.17	350	2
265	BREADALBANE, N.S.W., AUSTRALIA	149.48	-34.78	697	1
270	BULLENMERRI, VICTORIA, AUSTRALIA	143.12	-38.25	146	3
279	CHATYRKEL, KIRGIZ, U.S.S.R.	75.3	40.6	3530	3
280	CHEMCHANE-ADERG, MAURITANIA	-12.12	21	260	3
282	CHESHI-MWERU WANTIPA, ZAMBIA	29.68	-8.87	928	2
291	CLEVELAND, IDAHO, U.S.A.	-114.5	42.5	2519	3
294	COCHISE, ARIZONA, U.S.A.	-109.85	32.13	1280	3
304	DE AGUA SUCIA, COLOMBIA	-73.47	3.4	280	1
308	DHAR TICHITT, MAURITANIA	-9.2	18.35	375	2
309	DIAMOND, OREGON, U.S.A.	-118.78	43.08	1341	1
313	DOBI-HANLE, ETHIOPIA	42	11.5	120	2
317	EL ABRA, COLOMBIA	-74	5	2570	3
325	ELK, MINNESOTA, U.S.A.	-95.21	47.21	453	1
339	FACHI, NIGER	11.67	18.12	275	2
343	FORT ROCK, OREGON, U.S.A.	-120.75	43.17	1311	2
344	FROME, SOUTH AUSTRALIA, AUSTRALIA	139.83	-30.75	-2	2
345	FUCINO,ITALY	13.56	42	650	3
346	FUQUENE, COLOMBIA	-73.75	5.5	2580	1
349	GEORGE, N.S.W., AUSTRALIA	149.42	-35.08	673	3
363	HASSI CHEIKH, ALGERIA	1.6	31.13	500	2
365	HASSI EL MEJNA, ALGERIA	2.3	31.5	500	2
368	HAY, ARIZONA,U.S.A.	-109.5	34	2780	1
369	HERRERA, COLOMBIA	-74.28	4.7	2560	1
371	HOOK, WISCONSIN, U.S.A.	-88.33	42.95	280	2
383	JACOB, ARIZONA, U.S.A	-110.83	34.42	2285	2
386	KAFRA/ACHEGOUR, NIGER	12	19	450	2
392	KEPA, POLAND	22	49.4	320	2
393	KETTLE HOLE, IOWA, U.S.A.	-95	43	350	3
394	KHARGA, EGYPT	30.53	25.45	20	2
396	KHAT, MAURITANIA	-12.5	18.17	100	3
402	KONYA, TURKEY	33	37.5	980	3

403	KOW, VICTORIA, AUSTRALIA	144.3	-38.2	83	3
408	LA GUITARRA, COLOMBIA	-74	3.87	3450	3
411	LECONTE, CALIFORNIA, U.S.A.	-116	33.33	-71	1
412	LIEBENBERGSPAN, SOUTH AFRICA	25.33	-29.13	1224	1
417	LUBBOCK, TEXAS, U.S.A.	-101.9	33.63	975	2
430	MENDOTA, WISCONSIN, U.S.A.	-89.42	43.1	259	2
434	MISSION CROSS, NEVADA, U.S.A.	-115.5	41.75	2424	1
491	RUBY, NEVADA, U.S.A.	-115.33	40.58	1818	2
492	RUKWA, TANZANIA	32.5	-8	783	3
493	RUSSELL, CALIFORNIA, U.S.A.	-118.77	38.05	1951	2
500	SAOURA, ALGERIA	-2	30	400	3
505	SELIMA, SUDAN	29.34	21.32	200	2
507	SEVAN, ARMENIA, U.S.S.R.	45.3	40.3	1902	3
510	SIETE CABEZAS, COLOMBIA	-75.15	4.8	3700	3
520	TAGUA TAGUA, CHILE	-71.17	-34.5	890	3
521	TAHOE, CALIFORNIA/NEVADA, U.S.A.	-120.07	38.93	1897	2
523	TANGANYIKA, BURUN/TANZ/ZAM/ZAIRE	29.53	-6.03	773	2
528	TAUCA, BOLIVIA	-68	-19.5	3660	3
530	TERMIT OUEST-KANDEL BOUZOU,NIGER	11.25	16.08	300	3
532	TIGALMAMINE, MOROCCO	-5.35	32.9	1626	2
533	TIGUENT, MAURITANIA	-16.22	20.7	50	1
535	TIRERSIOUM, MAURITANIA	-16.68	21.37	100	2
536	TITICACA, BOLIVIA/PERU	-69.25	-16.13	3810	2
541	TURKANA, KENYA	36	5	375	1
542	TYOTJARVI, FINLAND	25.47	60.98	143	1
543	TYRRELL, VICTORIA, AUSTRALIA	142.78	-35.33	42	1
545	URMIA, IRAN	45.5	37.83	1284	1
552	VICTORIA, UGANDA/TANZANIA/KENYA	33	-1	1134	1
555	WALKER, ARIZONA, U.S.A	-111.67	35.5	2700	2
560	WEBER, MINNESOTA, U.S.A.	-91.65	47.47	559	3
567	WIELKE GACNO, POLAND	17.2	53.73	130	2
568	WILLANDRA, N.S.W., AUSTRALIA	143	-33.5	200	3
569	WINTERGREEN, MICHIGAN, U.S.A.	-86.38	42.4	271	3
577	ZIWAY-SHALA, ETHIOPIA	38.67	7.75	1558	3

6 ka

Id	Basin	Longitude	Latitude	Altitude	6 ka
1	Attersee	13.53	47.88	469	1
2	Mondsee	13.37	47.83	475	1
4	Aapalampi	28.53	68.6	204	1
11	Kyrösjärvi	23.17	61.75	83	2
14	Pieni Majasiampi	24.58	60.31	97.3	2
20	Chalain	5.77	46.68	488	1
25	Le Grand Lemps	5.42	45.47	458	1

28	Pluvis	5.83	45.83	215	1
32	Großer Plöner See	10.42	54.17	576	2
33	Schleinsee	9.5	47.75	40	1
34	Seeburger See	10.17	51.5	474	2
37	Ioannina	20.66	39.66	466	2
42	Balaton	17.5	46.8	105	3
43	Hafnarfjörn	-20.1	65.63	97	1
44	Lonsfjörn	-20.33	64.33	100	2
48	Creggannmore	-9.6	54.25	60	1
50	Castiglione	12.76	41.89	44	3
53	Ellasjön	19.01	74.36	20.8	2
65	Krutlin	21.87	54.07	127	1
67	Stetlin	19	52.96	73.3	2
68	Wielkie Gacno	17.2	53.73	130	2
69	Lagoa Comprida	-8	38.75	1600	1
71	Padul	-4.63	37.03	785	2
72	Sanguljuslas	-6.73	42.1	1050	2
73	Ageröds mosse	13.43	55.63	55	2
75	Bysjön	13.53	55.67	22	2
79	Lilla Gloppsjön	14.62	58.81	196	3
80	Ljustjärnen	14.48	58.76	183	3
85	Trummen	14.75	56.67	161	1
86	Växjösjön	14.75	56.67	161	3
98	Borralan	-4.9	58.05	139	3
102	Dubh Lochan	-4.6	56.15	75	1
104	Garten	-3.7	57.22	220	1
114	Saham Mere	0.8	52.57	38	1
117	Malo Jezero	17.35	42.78	0	2
118	Palu	13.7	45.01	0	1
119	Antu Sinijärv	29.33	58.13	94.6	2
121	Kalina	27.42	58.37	50	2
123	Päidre	25.5	58.27	50.6	2
124	Puruo	27.25	57.68	183.2	2
125	Raigastvere	26.73	58.6	51.8	3
128	Vaharu	24.37	58.34	45	2
130	Rudushskoe	27.55	58.5	150	2
131	Vorkalu	27.5	58.33	154.3	2
133	Cepkelu	24.52	54.02	129.5	3
136	Glubelka	26.41	54.86	165.8	1
137	Krivoe	29.07	56.14	131	1
146	Kanentyew	34.3	68.6	182.9	1
148	Pesmiambina	35.45	66.7	122	2
151	Dimnoe	33.85	62.52	66	2
154	Noeuo	30.58	64.58	165	2
157	Rugozero	32.52	64.08	130	2
158	Michurinskoe	29.98	60.52	94	2

161	Il'men	31.23	58.3	18	2
162	Teseve-Nelyl'skoe	30.9	56.92	68.5	2
163	Valdaiskoe	33.27	57.98	192.5	2
164	Mutnoe	31.76	55.5	180	2
166	Beloe	38	62.33	136	3
167	Lacha	37.67	62.59	118	2
171	Schukozero	38.83	62.36	165	2
173	Vozhe	38.08	60.43	121	3
181	Trostenskoe	38.48	55.88	195	1
182	Galichskoe	42.28	58.4	101.2	1
189	Argayash	60.89	55.58	250	2
191	Uvil'dy	62.37	56.53	273.4	2
196	Khomustakh	121.62	63.62	120	2
200	Seven	45.42	40.5	1868	3
202	Karas'e	70.22	53.03	435	1
203	Maybalyc	70.13	53.15	308	3
204	Mokhovoe	64.25	53.77	178	2
211	Rangkul-Shorkul	74.2	38.52	3779	1
214	Dabe-Nur	98.8	48.2	2485	1
216	Gun-Nur	106.6	50.25	600	1
220	Hubsugul	100.17	50.53	1645	3
221	Terkhiin-Tsagan-Nur	99.7	48.15	2060	3
223	ABU BALLAS, EGYPT	27.42	24.23	508	2
228	AGADEM, NIGER	13.33	16.83	350	2
233	ALEXANDERSFONTEIN, S.AFRICA	24.6	-28.83	500	2
234	ALSACIA, COLOMBIA	-73.86	3.9	3100	1
239	ARD EL AKHDAR, EGYPT	28.03	23.18	950	2
245	BALATON, HUNGARY	17.5	46.8	-105	2
248	BEATTIES, TASMANIA, AUSTRALIA	146.63	-42.67	980	1
273	CAHABA, ALABAMA, U.S.A.	-86.53	33.5	210	3
276	CHAD, NIGERIA/NIGER	14	13	282	2
279	CHATYRKEL, KIRGIZ, U.S.S.R.	75.3	40.6	3530	2
285	CHICHANCANAB, MEXICO	-88.75	19.5	38	3
286	CHICONAHUAPAN, MEXICO	-98.67	19.13	2575	2
291	CLEVELAND, IDAHO, U.S.A.	-114.5	42.5	2519	1
292	CLOVIS, NEW MEXICO, U.S.A.	-103.33	34.25	1250	3
300	DAIET EL MELAH, ALGERIA	1.24	31.13	695	2
317	EL ABRA, COLOMBIA	-74	5	2570	3
331	ERG INE SAKANE 57-19, MALI	-0.53	20.95	320	2
345	FUCINO,ITALY	13.55	42	650	2
346	FUQUENE, COLOMBIA	-73.75	5.5	2580	1
349	GEORGE, N.S.W., AUSTRALIA	149.42	-35.09	673	1
355	GOSHEN, ALABAMA, U.S.A.	-86.13	31.72	105	1
368	HAY, ARIZONA,U.S.A.	-109.5	34	2780	1
375	ICHOURAD, MALI	-1.13	20.5	300	2
395	IOHAT, MAURITANIA	-12.5	19.17	100	3

403	KOW, VICTORIA, AUSTRALIA	144.3	-38.2	83	3
406	LA GUITARRA, COLOMBIA	-74	3.87	3450	2
412	LIEBENBERGSPAN, SOUTH AFRICA	25.33	-28.13	1224	1
417	LUBBOCK, TEXAS, U.S.A.	-101.9	33.63	975	1
419	LYNCH'S CRATER, QUEENSLAND, AUST.	145.7	-17.37	760	2
421	MAGADI-NATRON, KENYA/TANZANIA	36.04	-2.12	600	3
422	MAINE-SORÒA, NIGER	12	13.12	315	2
427	MANYARA, TANZANIA	36.82	-3.62	945	2
434	MISSION CROSS, NEVADA, U.S.A.	-118.5	41.75	2424	1
454	OUKECHERT, MALI	-0.75	20.67	320	2
456	OUNIANGA KEBIR, CHAD	20.5	19.08	310	1
457	OYO, SUDAN	28.18	19.27	510	2
460	PATZCUARO, MEXICO	-101.58	19.58	2044	2
461	PHAIR, BRITISH COLUMBIA, CANADA	-122.05	50.57	716	3
463	PITYOULISH, SCOTLAND	-3.78	57.2	210	1
466	PULBEENA, TASMANIA, AUSTRALIA	145.12	-40.89	30	2
470	QUEXIL, GUATEMALA	-90.12	16.93	110	1
471	QUINCAN, QUEENSLAND, AUSTRALIA	145.58	-17.3	760	2
480	RUB'AL KHALI, SAUDI ARABIA,S. A	47	20.33	210	2
487	RUB'AL KHALI, SAUDI ARABIA,S.16	48.62	20.48	500	1
503	SEGUEDINE, NIGER	12.8	20.4	570	3
505	SELIMA, SUDAN	29.34	21.32	200	2
507	SEVAN, ARMENIA, U.S.S.R.	45.3	40.3	1902	1
542	TYOTJARVI, FINLAND	25.47	60.96	143	1
545	URMIA, IRAN	45.5	37.63	1284	1
550	VERA, TASMANIA, AUSTRALIA	145.87	-42.27	580	3
561	WEDGE, ALBERTA, CANADA	-115.17	50.67	1500	1
567	WIELKE GACNO, POLAND	17.2	53.73	130	2
574	ZERIBAR, IRAN	46.12	35.53	1300	2

9 ka

Id	Basin	Longitude	Latitude	Altitude	9 ka
4	Aapalampi	28.53	66.6	204	1
5	Ahvenainen	25.11	61.03	122.2	2
9	Kauniopää	27.42	66.42	300	2
12	Lampelanjärvi-Lammijarvi	29.07	62.07	108.6	3
14	Pieni Majaslampi	24.58	60.31	97.3	3
16	Tankavaara	27.23	68.18	335	3
17	Tydöjärvi	25.47	60.98	142.8	2
18	Vanhalampi	29.58	66.37	205	2
20	Chalain	5.77	46.66	486	1
22	Hières-sur-Amby	5.29	45.79	212	2
23	Issarlès	4.07	44.8	997	3
24	Landes	3.8	44.83	1000	2

25	Le Grand Lemps	5.42	45.47	456	1
27	Petiéautier	6.18	44.52	875	2
28	Pluvis	5.63	45.83	215	2
29	Rousses	5.2	46.8	1058	1
30	Saint-Julien-de-Ratz	5.62	45.35	650	1
31	Federsee	9.58	48.17	501	3
32	Großer Plöner See	10.42	54.17	578	1
33	Schleisee	9.5	47.75	40	3
39	Khimaditis	21.57	40.6	580	3
41	Xinias	22.26	39.07	500	1
45	Belle Lake	-7.03	52.18	33	2
46	Cannone Lough	-8.58	54.92	30	3
47	Cooltsen	-8.6	52.35	50	3
48	Creggannmore	-9.6	54.25	60	2
49	Sheesuns	-10.05	53.55	18	1
50	Castiglione	12.76	41.89	44	1
51	Fucino	13.55	42	667	3
52	Lago di Ganna	8.83	45.87	452	1
54	Endletvatn	19.06	69.73	35	1
55	Lerstadvatn	6.5	62.5	44	1
59	Saudadalsmyra	6.4	62.4	30	2
61	Torvismyra	6.5	62.4	35	2
66	Lukcze	23	51.5	170	1
67	Steklin	19	52.95	73.3	1
68	Wielkie Gacno	17.2	53.73	130	1
69	Lagoa Comprida	-8	39.75	1600	1
71	Padul	-4.63	37.03	785	2
72	Sanguijuelas	-6.73	42.1	1050	2
79	Lilla Gloppsjön	14.62	59.81	198	1
80	Ljustjärnen	14.48	59.76	183	1
86	Vikasjön	14.75	56.87	161	3
88	Bielersee	7.1	47.1	429	3
89	Hobechensee	8.01	46.25	2017	3
93	Rotsee	8.31	47.15	419	1
95	sMhuillinn	-5.27	55.7	25	1
97	Black Lock	-3.17	58.25	90	2
98	Sorralan	-4.9	58.05	139	2
100	Cross Mare	-2.83	52.83	87	3
102	Dubh Lochan	-4.6	58.15	75	1
105	Hockham Mere	0.83	52.5	33	2
106	Hornsea Old Mere	-0.1	53.83	1	2
107	Linton Loch	-2.63	55.67	91.5	2
110	Melynllyn	-4.12	53.12	632.5	1
111	Old Buckenham Mere	1.02	52.5	35	2
112	Pityoulish	-3.8	57.2	210	3
113	Rose	0.07	53.67	5	2

115	Sea Mare	1	62.57	38	2
116	Traeth Mawr	-3.5	51.62	330	3
119	Antu Sinijärv	26.33	59.13	94.6	1
121	Kaline	27.42	58.37	50	1
122	Kirikumäe	27.25	57.67	183	1
123	Päidre	25.5	58.27	50.6	3
125	Raigastvere	26.73	58.6	51.6	3
129	Lubanas	26.92	56.77	80.8	1
133	Cepkeliu	24.52	54.02	129.5	1
136	Glubelka	26.41	54.95	165.8	3
138	Naroch	26.85	54.85	120	1
142	Sporovskoe	25.33	52.33	142	1
143	Sudobie	28.1	54.03	185	1
146	Kanent'yavr	34.3	68.8	182.9	3
153	Moshkamoe	34.25	62.25	58	1
155	Paanajarvi	29.95	66.26	136.6	1
157	Rugozero	32.52	64.08	130	1
163	Valdaiskoe	33.27	57.98	192.5	3
165	Zaozer'e	31.92	55.02	175	3
167	Lacha	37.67	62.58	118	1
168	Laksa	40.58	62.8	109	1
173	Vozhe	39.08	60.43	121	1
174	Melekhovo	38.5	58.83	150	1
176	Somino	38.8	56.6	134.4	1
177	Beloe-Chernoe	37.35	55.72	145	1
178	Chistoe	38.32	55.78	160	1
179	Dolgoe	37.32	56.07	200	3
180	Nerskoe	37.39	56.08	165	3
189	Argayash	60.69	55.58	250	3
190	Bol'shoi Kisegach	60.38	55.04	317	2
191	Uvil'dy	62.37	55.53	273.4	1
193	Chany	77.5	54.75	108.1	1
212	Achit-Nur	90.6	49.5	1435	3
215	Dood-Nur	99.38	51.33	1538	1
219	Hoton-Nur	88.3	48.67	2083	1
223	ABU BALLAS, EGYPT	27.42	24.23	506	2
228	AGADEM, NIGER	13.33	16.83	350	2
234	ALSACIA, COLOMBIA	-73.85	3.9	3100	2
236	ANNIE, FLORIDA, U.S.A	-81.4	27.3	38	2
239	ARD EL AKHDAR, EGYPT	28.03	23.18	860	2
248	BEATTIES, TASMANIA, AUSTRALIA	146.63	-42.67	980	3
255	BILMA, NIGER	13	18.75	310	2
267	BROMFIELD, QUEENSLAND, AUSTRALIA	145.55	-17.38	755	1
276	CHALMER'S, ALBERTA, CANADA	-114.48	50.84	1370	1
285	CHICHANCANAB, MEXICO	-88.75	19.5	36	3
286	CHICONAHUAPAN, MEXICO	-98.67	19.13	2575	2

282	CLOVIS, NEW MEXICO, U.S.A.	-103.33	34.25	1250	2
302	DAWASIR, SAUDI ARABIA	46	20.35	600	1
311	DIDWANA, INDIA	74.58	27.33	360	2
317	EL ABRA, COLOMBIA	-74	5	2570	3
318	EL BAKHT, EGYPT	28.31	23.22	850	2
319	EL GOBERNADOR, COLOMBIA	-74.35	3.85	3815	2
336	EURAMOO, QUEENSLAND, AUSTRALIA	145.63	-17.17	730	3
339	FACHI, NIGER	11.67	18.12	275	2
345	FUCINO,ITALY	13.55	42	650	3
346	FUQUENE, COLOMBIA	-73.75	5.5	2580	1
365	HASSI EL MEJNA, ALGERIA	2.3	31.5	500	2
368	HAY, ARIZONA,U.S.A.	-109.5	34	2780	1
371	HOOK, WISCONSIN, U.S.A.	-89.33	42.95	280	2
393	KETTLE HOLE, IOWA, U.S.A.	-95	43	350	3
396	KIRCHNER, MINNESOTA, U.S.A.	-92.77	44.83	275	2
406	LA GUITARRA, COLOMBIA	-74	3.67	3450	1
414	LITTLE SALT, FLORIDA, U.S.A.	-82.17	27	5	1
417	LUBBOCK, TEXAS, U.S.A.	-101.9	33.63	975	1
419	LYNCH'S CRATER, QUEENSLAND, AUST.	145.7	-17.37	760	1
422	MAINE-SOROA, NIGER	12	13.12	315	2
430	MENDOTA, WISCONSIN, U.S.A.	-89.42	43.1	259	1
433	MEXICO, MEXICO	-99	19.5	2240	2
436	MOJAVE, CALIFORNIA, U.S.A.	-118.13	35.37	276	1
441	MUNDAFAN,RUB'AL KHALI, S.ARABIA	45.42	18.53	870	2
460	PATZCUARO, MEXICO	-101.58	19.58	2044	1
466	PULBEENA, TASMANIA, AUSTRALIA	145.12	-40.89	30	1
491	RUBY, NEVADA, U.S.A.	-115.33	40.58	1818	1
494	RUTZ, MINNESOTA, U.S.A.	-93.87	44.87	314	2
498	SAN AGUSTIN, NEW MEXICO, U.S.A.	-108.17	33.83	1842	2
531	TIBERIAS, TASMANIA, AUSTRALIA	147.37	-42.37	442	2
532	TIGALMAMINE, MOROCCO	-5.35	32.9	1626	2
540	TULARE, CALIFORNIA, U.S.A.	-119.67	36	57	1
542	TYOTJARVI, FINLAND	25.47	60.98	143	3
553	WABAMUN, ALBERTA, CANADA	-114.25	53.5	732	1
560	WEBER, MINNESOTA, U.S.A.	-91.65	47.47	559	2
567	WIELKE GACNO, POLAND	17.2	53.73	130	3
569	WINTERGREEN, MICHIGAN, U.S.A.	-86.38	42.4	271	2
571	WYRIE, SOUTH AUSTRALIA, AUSTRALIA	140.3	-37.85	100	1

12 ka

Id	Basin	Longitude	Latitude	Altitude	12 ka
3	Schwemm	12.17	47.58	684	2
25	Le Grand Lemps	5.42	45.47	456	2
30	Saint-Julien-de-Ratz	5.62	45.35	660	2

33	Schleinsee	9.5	47.75	40	3
36	Tegeler See	13.25	52.58	35	3
45	Belle Lake	-7.03	52.18	33	2
48	Creggenmore	-9.6	54.25	60	2
50	Castiglone	12.76	41.89	44	1
51	Fucino	13.55	42	667	2
66	Lukcze	23	51.5	170	3
68	Wielkie Gacno	17.2	53.73	130	1
71	Padul	-4.63	37.03	785	1
80	Bielersee	7.1	47.1	429	2
91	Labelgensee	7.3	47.03	514.4	2
96	Borralan	-4.9	58.05	139	3
99	Cam	-5	58.08	123.5	2
100	Cross Mere	-2.83	52.83	87	2
113	Rose	0.07	53.67	5	1
116	Traeth Mawr	-3.5	51.92	330	1
163	Valdaiskoe	33.27	57.98	192.5	2
172	Kubenskoe	39.5	59.7	110	2
175	Nero	39.48	57.17	93	2
193	Chany	77.5	54.75	106.1	1
200	Sevan	45.42	40.5	1898	1
201	Borovoe	70.27	53.08	321	2
215	Dood-Nur	99.38	51.33	1538	2
224	ABU TARTUR, EGYPT	29.3	25.5	145	1
234	ALSACIA, COLOMBIA	-73.85	3.9	3100	2
254	BEYSEHIR, TURKEY	31.5	37.75	1120	3
255	BILMA, NIGER	13	18.75	310	3
258	BOGORIA, KENYA	36.1	0.3	990	2
259	BONNEVILLE, UTAH, U.S.A.	-113	40.5	1280	2
271	BURDUR, TURKEY	30.1	37.6	854	1
275	CARP, WASHINGTON, U.S.A.	-122.88	45.92	714	3
282	CHESHI-MWERU WANTIPA, ZAMBIA	29.68	-8.67	928	3
291	CLEVELAND, IDAHO, U.S.A.	-114.5	42.5	2519	1
294	COCHISE, ARIZONA, U.S.A.	-109.85	32.13	1280	3
312	DIXIE, NEVADA, U.S.A.	-118	38.91	1027	1
314	DUCK, MASSACHUSETTS, U.S.A.	-70	41.93	3	2
327	ENNERI BARDAGUE, CHAD	17	21.5	1025	2
343	FORT ROCK, OREGON, U.S.A.	-120.75	43.17	1311	1
344	FROME, SOUTH AUSTRALIA, AUSTRALIA	139.83	-30.75	-2	1
345	FUCINO,ITALY	13.55	42	650	2
350	GEORGE, NEW YORK, U.S.A.	-73.85	43.52	98	1
368	HAY, ARIZONA,U.S.A.	-109.5	34	2780	2
383	JACOB, ARIZONA, U.S.A	-110.83	34.42	2295	2
399	KIVU, RWANDA/BURUNDI/ZAIRE	29	-2	1462	2
406	LA GUITARRA, COLOMBIA	-74	3.67	3450	2
408	LAHONTAN, NEVADA, U.S.A.	-119.5	40	1054	3

423	MAKGADIKGADI, BOTSWANA	24.42	-20.67	960	2
427	MANYARA, TANZANIA	35.82	-3.62	945	3
430	MENDOTA, WISCONSIN, U.S.A.	-89.42	43.1	259	2
441	MUNDAFAN,RUB'AL KHALI, S.ARABIA	45.42	18.53	870	3
446	NASTA, EGYPT	31	23	250	3
448	NAIVASHA, KENYA	36.33	-0.68	1890	2
449	NAKURU-ELMENTEITA, KENYA	36.17	-0.42	1750	2
452	NGAMI-MABABE, BOTSWANA	23.53	-19.86	919	1
478	RUB'AL KHALI, SAUDI ARABIA, S. 6	46.63	17.63	150	1
492	RUKWA, TANZANIA	32.5	-8	793	1
502	SEARLES, CALIFORNIA, U.S.A.	-117.7	35.6	493	2
538	TROU AU NATRON, CHAD	15.52	20.67	2300	1
555	WALKER, ARIZONA, U.S.A	-111.67	38.5	2700	2

Appendix F: Procedure for transforming the data into a binary vector format.

```
'*************************************************
'
' This subroutine (Macro - VBA, Excel v 7.0) was written
' for transforming the original lake status into a
' binary vector; where 1 if present and 0 otherwise for the
' three lake categories. Ex: High was coded (1,0,0); intermediate
' was coded (0,1,0) and low coded as (0,0,1)
'
' Written by A.E. Viau and M. Sawada (LPC)
' June 1998
'
' Execution via Excel v 7.0
' Fields required: Id;easting;northing;original lake status
' row 1 contains field titles
'
'*************************************************************


Attribute VB_Name = "Module1"
Sub vector()

Dim arrayif1(2)
arrayif1(0) = 1
arrayif1(1) = 0
arrayif1(2) = 0

Dim arrayif2(2)
arrayif2(0) = 0
arrayif2(1) = 1
arrayif2(2) = 0

Dim arrayif3(2)
arrayif3(0) = 0
arrayif3(1) = 0
arrayif3(2) = 1

Dim arrayif0(2)
arrayif0(0) = 0
arrayif0(1) = 0
arrayif0(2) = 0

Range("A1").Select
While ActiveCell.Value <> ""
numrows = numrows + 1
ActiveCell.Offset(1, 0).Range("A1").Select
Wend

Range("D2").Select

For i = 1 To numrows - 1
    testvalue = ActiveCell.Value
    For j = 0 To 2
        If testvalue = 0 Then
            ActiveCell.Value = arrayif0(j)
        ElseIf testvalue = 1 Then
            ActiveCell.Value = arrayif1(j)
        ElseIf testvalue = 2 Then
            ActiveCell.Value = arrayif2(j)
        Else
            ActiveCell.Value = arrayif3(j)
```

```
        End If
        ActiveCell.Offset(0, 1).Range("a1").Select
    Next 'j
    ActiveCell.Offset(1, -3).Range("a1").Select
Next 'i
End Sub
```

Appendix G: Procedure for reprojection from Hammer-Aitoff to Latlong.

Presented below is the procedure followed in the reprojection of the data into Plate Carré projection

Procedure:

1) import Surfer v 6.0 grid files into Idrisi v 5.0 (module SRFIDRIS)

2) raster/vector conversion ofthe grid files using module POINTVEC

3) reprojection of Hammer-Aitoff to Latlong using module PROJECT

4) conversion of vector file to binary format (CONVERT)

5) EXPORT vector file using module SRFIDRIS

6) once in Surfer v 6.0 grid vector data file (XYZ for Idrisi) using nearest neighbour gridding technique using a smaller search distance than actual interpoint distance to keep the original data values intact.

Appendix H: Reclassification procedure

```
'*************************************************************************************
'
' This program (VBA) enables the reclassification of the indicator grid files based on the
' maximum probability vector. After the indicator kriging of each individual statuses has been
' performed, each separate grid file was then imported into Excel v 7.0, file lakgrid.xls for
' reclassification computations. The final results is a single grid file containing the
' reclassification categories (1,2,3; mutual exclusivity) for each grid node.
'
' Written by A.E. Viau and M. Sawada - LPC - University of Ottawa
' May 1998
'
' Input required:  maxrows and maxcol
'
'*************************************************************************************

Sub Lake()
'
' Macro1 Macro
' Macro recorded 5/1/98
'
Dim holdarray(3)

Application.ScreenUpdating = False
Sheets("final").Select
Range("A6").Select
Sheets("1").Select
Range("A6").Select
Sheets("2").Select
Range("A6").Select
Sheets("3").Select
Range("A6").Select

For k = 1 To 400
offsetvalue = 0
   For i = 1 To 10

          ActiveCell.Select
          Sheets("3").Select
          ActiveCell.Offset(0, offsetvalue).Range("A1").Select
             holdarray(3) = ActiveCell.Value
          Sheets("2").Select
          ActiveCell.Offset(0, offsetvalue).Range("A1").Select
             holdarray(2) = ActiveCell.Value
          Sheets("1").Select
          ActiveCell.Offset(0, offsetvalue).Range("A1").Select
             holdarray(1) = ActiveCell.Value

          testvalue = -99999
            For Sort = 1 To 3
               If holdarray(Sort) > testvalue Then
                  testvalue = holdarray(Sort)
                  pos = Sort
               Else
               End If
            Next

          If holdarray(pos) = Empty Then
             pos = ""
          ElseIf holdarray(pos) = -99 Then
             pos = -99
         Else
         End If

          Sheets("final").Select
```

```
        ActiveCell.Offset(0, offsetvalue).Range("A1").Select
        ActiveCell.Value = pos

      offsetvalue = 1

  Next 'i

  Sheets("final").Select
     Range("A6").Select
     ActiveCell.Offset(k, 0).Range("A1").Select
     Sheets("1").Select
     Range("A6").Select
     ActiveCell.Offset(k, 0).Range("A1").Select
     Sheets("2").Select
     Range("A6").Select
     ActiveCell.Offset(k, 0).Range("A1").Select
     Sheets("3").Select
     Range("A6").Select
     ActiveCell.Offset(k, 0).Range("A1").Select

Next 'k

Application.ScreenUpdating = True
End Sub
```

Reclassification procedure

1) Use convert module in Surfer v.6.0 to convert indicator grid files to ascii grid files

2) Import grid files into Excel v 7.0 (file c:\users\viau\excel\lakgrid.xls)

3) copy\paste indicator grid files into proper sheet (1-High, 2-Intermediate, 3-Low)

4) run VBA macro (lake) to get resulting reclassification grid (final)

5) import "final sheet" into a single Excel v 7.0 worksheet

6) save worksheet as .csv (comma delimited) file

7) import file into an editor (wordpad) and find\replace "," for " "

8) save file (text) with the extension .grd (for use in Surfer v 6.0)

Appendix I: Agreement procedures

The following two VBA programs are used to (a) test for afreement on a grid to grid basis between data and model and (b) to ensure only common grids nodes that have values for both time periods in question are used in the comparisons.

```
**********************************************************************************************
*
* This VBA routine checks on a grid to grid node that have values (not -99) and assigns a 1 value
* if conditions are satisfied as per criteria scheme in data-model comparison, 0 if not and 0.5 if
* potential agrement is satsfied (ie: no lake status change)
*
* Written by: A. E. Viau and M. Sawada (LPC)
* Jan. 1999
*
* input required: delta lake status (6-0k) and delta P-E (interpolated to lake grid 6-0k) of model
* output.
*
**********************************************************************************************
Sub agreement()
Application.ScreenUpdating = False

Dim DELTA()
Dim condition1(), condition1rows
Dim condition2(), condition2rows2
Dim nrows As Long
Dim ncols As Long
Dim vectorarray()
Dim DeltArrayPermuted()
Dim DeltaArray()
Dim distribution()
Dim total
total = 0
ncols = 2
nrows = 0
condition1rows = 0


Range("a1").Select
While ActiveCell.Value <> ""
nrows = nrows + 1
ActiveCell.Offset(1, 0).Range("a1").Select
Wend


'Range("d1").Select
'ReDim DELTA(2, nrows)
'
'For i = 1 To nrows
'  For j = 1 To ncols
'  DELTA(j, i) = ActiveCell.Value
'     If j = 1 Then
'     Position = 5
```

```
'     Else
'     Position = -5
'     End If
'   ActiveCell.Offset(0, Position).Range("a1").Select
'   Next 'j
'   ActiveCell.Offset(1, 0).Range("a1").Select
'Next 'i

Range("e1").Select
ReDim DELTA(2, nrows)
ReDim DeltaArray(nrows)

For i = 1 To nrows
   For j = 1 To ncols
   DELTA(j, i) = ActiveCell.Value
      If j = 1 Then
      Position = 4
      DeltaArray(i) = ActiveCell.Value
      Else
      Position = -4
      End If
   ActiveCell.Offset(0, Position).Range("a1").Select
   Next 'j
   ActiveCell.Offset(1, 0).Range("a1").Select
Next 'i

'For i = 1 To nrows
'   If DELTA(1, i) < -0.5 And DELTA(2, i) > 0 Then
'   . condition1rows = condition1rows + 1
'      ReDim Preserve condition1(condition1rows)
'      condition1(condition1rows) = DELTA(2, i)
'   ElseIf DELTA(1, i) > 0.5 And DELTA(2, i) < 0 Then
'      condition2rows2 = condition2rows2 + 1
'      ReDim Preserve condition2(condition2rows2)
'      condition2(condition2rows2) = DELTA(2, i)
'   End If
'Next

'get min of condition1 array
'minofcondition1 = condition1(1)
'For i = 1 To UBound(condition1)
'If (minofcondition1 > condition1(i)) Then
'   minofcondition1 = condition1(i)
'End If
'Next
'
"get max of condition2 array
'maxofcondition2 = condition2(1)
'For i = 1 To UBound(condition2)
'If (maxofcondition2 < condition2(i)) Then
'   maxofcondition2 = condition2(i)
'End If
'Next
'Range("J1").Select

'For i = 1 To nrows
'   If DELTA(1, i) >= 0.5 And DELTA(2, i) <= maxofcondition2 Then
'   ActiveCell.Value = 1
```

```
'   Elself DELTA(1, i) <= -0.5 And DELTA(2, i) >= minofcondition1 Then
'   ActiveCell.Value = 1
'   Elself (DELTA(1, i) > -0.5 And DELTA(1, i) < 0.5) And (DELTA(2, i) > maxofcondition2 And DELTA(2, i) <
minofcondition1) Then
'   ActiveCell.Value = 0.5
'   Else
'   ActiveCell.Value = 0
'   End If
'ActiveCell.Offset(1, 0).Range("a1").Select
'Next

Range("j1").Select
For i = 1 To nrows
   If DELTA(1, i) >= 0.5 And DELTA(2, i) < 0 Then
   ActiveCell.Value = 1
   total = total + 1
   Elself DELTA(1, i) <= -0.5 And DELTA(2, i) > 0 Then
   ActiveCell.Value = 1
   total = total + 1
   Elself DELTA(1, i) > -0.5 And DELTA(1, i) < 0.5 Then
   ActiveCell.Value = 0.5
   total = total + 1
   Else
   ActiveCell.Value = 0
   End If
ActiveCell.Offset(1, 0).Range("a1").Select
Next

Position = 1
npermutes = 500
ReDim distribution(npermutes + 1)

distribution(1) = total / nrows

For k = 1 To npermutes
total = 0

Position = Position + 1
'put permute here
          ReDim DeltArrayPermuted(nrows)
          ReDim vectorarray(nrows)

            Randomize
            r = Int((((nrows)) * Rnd) + 1)
              For i = 1 To nrows
                  While vectorarray(r) = 1
                  r = Int((((nrows)) * Rnd) + 1)
                  Wend
               DeltArrayPermuted(i) = DeltaArray(r) 'permr should have your delta whateever and permi
               'is what you will use in the program after permutation
               vectorarray(r) = 1
              Next
'           '"DELETE
'           Range("k1").Select
'           'offsetvalue = offsetvalue + 1
'           ActiveCell.Offset(0, k).Range("a1").Select
'           For i = 1 To nrows
'           ActiveCell.Value = DeltArrayPermuted(i)
```

```
'             ActiveCell.Offset(1, 0).Range("a1").Select
'             Next


'put program code here
For i = 1 To nrows
  If DeltArrayPermuted(i) >= 0.5 And DELTA(2, i) < 0 Then
  total = total + 1
  ElseIf DeltArrayPermuted(i) <= -0.5 And DELTA(2, i) > 0 Then
  total = total + 1
  ElseIf DeltArrayPermuted(i) > -0.5 And DeltArrayPermuted(i) < 0.5 Then
  total = total + 1
  Else
  'nothing
  End If
Next

distribution(Position) = total / nrows

Next

Worksheets.Add
Range("a1").Select
For i = 1 To UBound(distribution)
  ActiveCell.Value = distribution(i)
  ActiveCell.Offset(1, 0).Range("a1").Select
Next

Application.ScreenUpdating = True

End Sub


*****************************************************************************************
* This VBA routine is used to determine the common grid nodes in lake status for
* for both time periods (ie: 6 and 0 ka). In the event of one lake grid estimate is only valid for
* 0 ka and not for 6 ka , it is excluded from the file. This results in a file with calculated deltas
* in lake status common between the trwo lake grids used in data-model comparisons.
*
* Written by: A. E. Viau and M. Sawada (LPC)
* Jan. 1999
*
* input required: Lake status grids for both time periods in XYZ format
*
*****************************************************************************************


Sub Macro1()
'
' Macro1 Macro
' Macro recorded 12/23/98 by K. Gajewski
'

Range("c1").Select

While (ActiveCell.Value <> "") ' Or ActiveCell.Value <> 0) '  i = 1 To 50
```

```
   If ActiveCell.Value = -99 Then
   ActiveCell.EntireRow.Select
   Selection.Delete Shift:=xlUp
   ActiveCell.Offset(0, 2).Range("a1").Select
   GoTo dds:
   Else
   ActiveCell.Offset(1, 0).Range("a1").Select
   End If
dds:
Wend

Range("d1").Select

While (ActiveCell.Value <> "") ' Or ActiveCell.Value <> 0) '  i = 1 To 50

   If ActiveCell.Value >= 50 Then
   ActiveCell.EntireRow.Select
   Selection.Delete Shift:=xlUp
   ActiveCell.Offset(0, 3).Range("a1").Select
   GoTo ddsa:
   Else
   ActiveCell.Offset(1, 0).Range("a1").Select
   End If
ddsa:
Wend

End Sub
```